Soil erosion and fluxes of sediment within landscapes of the Canadian Prairies

By

Ehsan Zarrinabadi

A thesis submitted to the Faculty of Graduate Studies of

The University of Manitoba

in partial fulfillment of the requirements for the degree of

Doctor of Philosophy

Department of Soil Science

University of Manitoba

Winnipeg, Manitoba, Canada

Abstract

Maintaining the future sustainability of agriculture and ensuring soil security is of primary concern across Canada. Understanding the state of soil erosion and determining the vulnerable areas are essential measures in combatting future soil erosion and avoiding soil degradation. Therefore, the general goal of this thesis was to quantify soil erosion rates and develop an improved understanding of erosion processes within the Canadian Prairies. To fulfill the aim of the research project, typical agricultural and native prairie landscapes of the region were studied within three watersheds including the Red River Valley and the Broughton's Creek watershed in Manitoba, and the Bigstone Creek watershed in Alberta.

Initially, passive uni-directional wind erosion sediment samplers were employed to assess wind-eroded soil movement in agricultural lands of the Red River Valley. Cesium-137 (^{137}Cs) measurements were conducted to quantify total soil loss and deposition rates within the wetland landscapes in the Broughton's Creek and Bigstone Creek watersheds. In addition, soil and sediment properties were characterized to understand tillage-, water- and wind-induced sediment transport dynamics and distinguish between eroded and depositional zones. Landform classification maps of the studied wetland catchments were also created to assist developing sediment budgets of soil loss and accumulation, and quantify sediment flux rates from agricultural fields to wetland environments. Furthermore, soil erosion models were used to characterize spatial patterns of soil loss by tillage, water, and wind erosion and assess relative contribution of these processes towards total soil erosion.

This study found that: i) Measured soil loss and sedimentation caused by wind erosion are very small in the Red River Valley. Moreover, abrasion of crops by wind-transported sediment was not observed in this study; ii) Using the measurements of ^{137}Cs, average annual soil losses in cultivated

fields were estimated at about 1.2 kg m^{-2} yr^{-1} and 0.9 kg m^{-2} yr^{-1} in Manitoba and Alberta, respectively, with approximately 70% of cultivated field being classified as eroded zone in both provinces; and iii) On the knoll of hummocky landscapes, tillage erosion dominates the pattern of total soil erosion and the effects of water erosion and wind erosion are minor.

Acknowledgments

First and foremost, I would like to acknowledge my supervisor Dr. David Lobb for his guidance, encouragements, and support throughout these five years. You helped me champion my ideas and I am very grateful for this invaluable journey and experience.

Thanks are also extended to my Advisory Committee members Dr. Yvonne Lawley, Dr. Alexander Koiter and Dr. Pascal Badiou, who always provided supportive ideas during all stages of the research and their invaluable insight and feedback to improve the quality of this thesis. As well, a big thank you to Irena Creed for her contributions in this research.

This project would not have been possible without the help of the Landscape Dynamics Laboratory group and others in the Department of Soil Science. It is important that I acknowledge support from Brendan Brooks, Amber Aligawesa, Gabrielle Lint, Adriana Avila and Hannah Ziegler-Blair, Dr. Hamid Abedi and Dr. Masoud Goharrokhi for help with field works, and from Anthony Buckley for assistance with laboratory analyses. I also wish to extend my gratitude to all my friends. Being far from home is not always easy, but you have been part of my family and provided an essential support system over the last few years.

And above all, a loving thank you to my parents, Jalil Zarrinabadi and Nahid Nazari, for their endless love, support and encouragement over the past 33 years. Thank you both for giving me strength to follow my dreams. My sister, Elham, and little niece, Nika, deserve my wholehearted thanks as well.

This project received funding from the Natural Sciences and Engineering Research Council of Canada (NSERC) Strategic Partnership Grant to IFC and DAL (STPGP 506809). Furthermore, I am grateful to scholarship funding provided by the Manitoba Zero Tillage Research Association

(MZTRA), University of Manitoba Graduate Fellowship (UMGF) and Graduate Enhancement of the Tri-Council Stipends (GETS).

Table of Contents

Abstract ... 2

Acknowledgments ... 4

Contributions of Authors ... 18

Copyright notices and journal papers information ... 19

Chapter 1 ... 20

Introduction and literature review ... 20

1.1. Soil erosion and degradation ... 21

1.1.1. Soil erosion in the Canadian Prairie provinces ... 23

1.1.2 Potential impacts of sedimentation on wetland health and function ... 25

1.2. Soil erosion processes ... 27

1.2.1. Water erosion ... 27

1.2.2. Wind erosion ... 28

1.2.3. Tillage erosion ... 29

1.3. Soil erosion modelling ... 30

1.4. Aims and objectives of the thesis ... 32

1.5. Thesis structure ... 34

1.6. References ... 37

Chapter 2 ... 47

Assessment of the effects of land rolling on wind erosion and crop growth in soybean production in the Red River Valley, Canada 47

2.1. Abstract 48

2.2. Introduction 49

2.3. Materials and methods 54

2.3.1. Study area 54

2.3.2. Experimental design 57

2.3.3. Soybean crop management 57

2.3.4. Design and fabrication of uni-directional sediment sampler 60

2.3.5. Measurements 61

2.3.6. Statistical analysis 66

2.4. Results and discussion 66

2.4.1. Impact of land rolling on soil properties 66

2.4.2. Impact of land rolling on wind-transported sediment 69

2.4.3. Impact of land rolling on soybean yield and growth characteristics 76

2.5. Conclusions 78

2.6. References 79

Chapter 3 92

Agricultural activities lead to sediment infilling of wetlandscapes in the Canadian Prairies: Assessment of soil erosion and sedimentation fluxes 92

3.1. Abstract 93

3.2. Introduction 93

3.3. Materials and methods 98

3.3.1. Study area 98

3.3.2. Soil sampling 100

3.3.2.1. Soil and sediment core collection and processing 101

3.3.2.2. Measurement of radionuclide activity 104

3.3.3. ^{137}Cs reference sites selection 105

3.3.4. Total sedimentation and soil erosion estimation using ^{137}Cs measurements 106

3.3.4.1. Estimation of point-based soil erosion and sedimentation rates 108

3.3.4.2. Development of soil loss and accumulation budgets 109

3.3.5. Characterization of landform elements and sedimentary features 110

3.3.6. Data treatment and statistical analysis 113

3.4. Results and discussion 113

3.4.1. ^{137}Cs reference data 113

3.4.2. ^{137}Cs transect data 115

3.4.3. Soil erosion and sedimentation rates 124

3.4.4. Soil loss and accumulation budgets 125

3.4.5. Sedimentary features 130

3.4.6. Potential error sources in discrimination of sedimentary features using LiDAR DEM 132

3.5. Conclusions 133

3.6. References 134

Chapter 4 151

Agricultural activities lead to sediment infilling of wetlandscapes in the Canadian Prairies: Assessment of contributions by tillage, water and wind erosion 151

4.1. Abstract 152

4.2. Introduction 153

4.3. Materials and methods 158

4.3.1. Description of the study area 158

4.3.2. Soil sampling and laboratory analysis 162

4.3.3. Total soil erosion estimated from ^{137}Cs Measurements 167

4.3.4. Modelling tillage, water, and wind erosion 169

4.3.4.1 Tillage erosion- TillEM 169

4.3.4.2 Water erosion- RUSLE2 170

4.3.4.3 Wind erosion- SWEEP 172

4.3.5. Landscape segmentation 175

4.3.6. Statistical analysis 176

4.4. Results and discussion 177

4.4.1. Patterns and magnitudes of predicted tillage, water, and wind erosion 177

4.4.1.1. TillEM 177

4.4.1.2. RUSLE2 180

4.4.1.3. SWEEP 180

4.4.2. Discrimination of sources of soil erosion 182

4.4.2.1. Soil redistribution and spatial patterns of ^{137}Cs 182

4.4.2.2. Principal Component Analysis (PCA) 184

4.4.2.3. Spatial pattern of soil and sediment properties 186

4.4.3. Uncertainties associated with the soil erosion models 191

4.4.5. Discrepancies between the model-predicted and ^{137}Cs-estimated soil erosion 193

4.5. Conclusions 194

4.6. References 196

Chapter 5 211

Summary and Conclusions 211

5.1. Context of thesis research 212

5.2. Major Findings 213

5.2.1. Assessment of the impacts of farming practices on wind erosion 213

5.2.2. Assessment of total soil loss and accumulation rates using ^{137}Cs 213

5.2.3. Improved understanding of soil erosion processes 215

5.3. Implications 216

5.4. Suggested field- and laboratory- based method improvements 217

5.5. Recommendation and further research direction 218

Appendices 222

Appendix A 223

Supplementary materials for Chapter 3 223

Appendix B 237

Supplementary materials for Chapter 4 237

List of Tables

Table 2. 1. The location, tillage history, soybean variety and management practices for study fields 59

Table 2. 2. Effect of management practices on soybean yield and growth characteristics........... 76

Table 3. 1. Descriptive statistics for the ^{137}Cs inventories documented for the sampling points along the transects within wetland catchments with different land uses in Manitoba and Alberta. 116

Table 3. 2. Point soil loss and deposition rates within the wetland catchments using ^{137}Cs reference value estimated from individual local stable sites. 125

Table 3. 3. Point soil loss and deposition rates within the wetland catchments using catchment-level ^{137}Cs reference value. 126

Table 4. 1. Average Point soil loss and deposition rates within the individual wetland catchments using ^{137}Cs and soil erosion models. 177

List of Figures

Fig. 1. 1. Schematic of the thesis structure linking the chapters to the objectives 36

Fig. 2. 1. Location of the study area within Manitoba, Canada. Circles are the location of fields included in the study. 55

Fig. 2. 2. Average annual wind speed and direction for the study area over the study period (2018-2019). 56

Fig. 2. 3. (a) the sampler with inlet height at 5-cm, and (b) the sampler with inlet height at 20-cm. [A sealed solid concrete block, fiberglass filter and coarse mesh on the inlet and outlet not shown]. 60

Fig. 2. 4. Location of wind erosion samplers within strip trial fields. The strips ranged from 200- to 500-m in length and 10-m in width. Fields are replicates in the experimental design. Direction of wind-eroded sediment movement is shown with arrows. Wind erosion samplers were located centrally within each strip and oriented based on the direction of soybean rows. Inlets of wind erosion samplers were faced to each other within each treatment. [Inlet shown with black rectangle].. 64

Fig. 2. 5. Impact of land rolling on soil moisture measured in September, 2018 and biweekly from May to September in 2019. * denotes a significant difference (P-value < 0.05) at the 0-10 cm soil depth. The circle and triangle symbols show observations for non-rolled and rolled treatments, respectively. 67

Fig. 2. 6. Impact of land rolling on soil surface roughness (2018-2019). There is a significant difference (P-value < 0.05) between the RMSH values on non-rolled and rolled trials. 69

Fig. 2. 7. (a) Impact of land rolling on soil movement by wind, and (b) wind-transported sediment collected by samplers with different collection opening heights. * denotes a significant difference

(*P*-value < 0.05) between collected wind-transported sediment by samplers with different collection opening heights (5-cm and 20-cm). 71

Fig. 2. 8. Particle size composition of wind-transported sediment trapped at heights of 5-cm and 20-cm in rolled and non-rolled treatments. Particle size composition is represented by the clay (≤ 0.002 mm), silt (0.002-0.063 mm) and sand (0.063-2 mm) content of collected wind-transported sediment. 72

Fig. 2. 9. (a) ^{137}Cs activities (Bq kg^{-1}) and (b) organic matter (%) of wind-transported sediment captured in sediment samplers with collection opening at two heights above the soil surface. * denotes a significant difference (*P*-value < 0.05) between the ^{137}Cs activity and organic matter values of wind-transported sediment captured by samplers. 74

Fig. 2. 10. The mean spectral reflectance for wind-transported sediment collected by samplers with different collection opening heights (5-cm and 20-cm).. 75

Fig. 3. 1. Geographic location of the studied catchments in Prairie provinces of Manitoba and Alberta, Canada. Light brown area shows the Canadian portion of the Prairie Pothole Region and dark gray areas are Broughton's Creek watershed, Manitoba and Bigstone Creek watershed, Alberta... 100

Fig. 3. 2. Photographs of collected cores in Broughton's Creek watershed, Manitoba, which are retrieved from riparian areas of (a) wetland surrounded by cropland (wetlandA-T1), (b) wetland surrounded by cropland (WetlandJ-T3) and (c) wetland surrounded by native prairie. The cores show the same characteristic pattern with a black organic-rich layer overlaying homogenous parent materials. 104

Fig. 3. 3. Three-dimensional (3D) view illustrating the landscape classification in Broughton's Creek Watershed, Manitoba (a) and schematic representation of wetland catchment sampling

locations relative to the wetland fringe and boundaries (b). The three studied wetland catchments in a section of land were identified using borderline. 112

Fig. 3. 4. Depth distribution of ^{137}Cs in soil profiles collected from an old rural cemetery at the Broughton's Creek watershed, Manitoba. Two bulk cores were collected from this reference site, which are not shown in the figure, but were used for estimation of average ^{137}Cs reference inventory. 114

Fig. 3. 5. Difference comparison ($P < 0.1$) of the downslope spatial variations in ^{137}Cs inventories along different toposequence positions in wetland catchments surrounding by (a) cultivated land and (b) native prairie. [Yellow, green and blue colours shown upland, riparian and pond center]. 118

Fig. 3. 6. Spatial variation of ^{137}Cs inventories within wetland catchments in Manitoba and Alberta. The red line shows the reference inventories of the study areas in Manitoba and Alberta. 120

Fig. 3. 7. Depth distribution of ^{137}Cs and their variation according to toposequence positions on three transects within one wetland catchment (Wetland K) embedded in cultivated land in Manitoba. The points are showing analyzed depth of each core. ^{137}Cs activity was measured down to 80-cm depth in some cores, but are not shown in the figure. The dashed line shows the approximate depth of tillage that is the zone of frequent mixing in the cultivated land............ 122

Fig. 3. 8. Soil redistribution assessment estimated from ^{137}Cs measurement along transects using catchment-level reference value and PM in Manitoba (a) and Alberta (b)................................ 128

Fig. 3. 9. Original unsmoothed 1-m DEM of one wetland catchment: (a) three-dimensional (3D) view of the catchment, (b) colour relief view of the catchment and (c) geometrical characteristics of the sedimentary features for the shown transect in the colour relief view. 131

Fig. 4. 1. Geographic location of (a) the Prairie Pothole Region (PPR) in North America and (b) the studied wetland catchments in Prairie provinces of Manitoba and Alberta, Canada. 160

Fig. 4. 2. Historical distribution of wind speeds and directions for each season in the Broughton's Creek (Manitoba) and Bigstone Creek (Alberta) watersheds, measured at ECCC stations (ID: 5010480, Brandon, Manitoba and ID: 3011240, Camrose, Alberta). Historical wind data for the months that soil surface is not fully protected are presented as well. 162

Fig. 4. 3. Three-dimensional (3D) view illustrating the landscape classification of (a) one section of land and (b) one individual wetland landscape (WetlandA) located within the section of land in Broughton's Creek Watershed, Manitoba. Sampling points on three individual transects extending from upper slope position to the central area of wetland are shown. 164

Fig. 4. 4. Average soil redistribution estimated by ^{137}Cs and soil erosion models along transect using a linear model and catchment-level reference value (on-site values) in Manitoba (a) and Alberta (b). Soil erosion models only applied to the field portion of wetland landscapes. 183

Fig. 4. 5. Three-dimension Principal Components Analysis biplot of the measured and modelled data. Field-measured variables (~20-cm depth) including ^{137}Cs estimated soil erosion (E_{Cs}), hue, saturation, value, sand, silt and clay, and model-estimated variables including tillage erosion (E_{Till}), water erosion (Ewat) and total erosion (E_{all}, tillage- + water- + wind-erosion). Eigenvalues for the first, second and third axis are 3.0, 2.7 and 1.5, respectively, which are standardized to 1.000 and the cumulative percentage variance of each axis is shown in the following bracket. Two-dimension Principal Components Analysis projection using PC1 and PC2 was shown in red and each vector was labelled. 186

Fig. 4. 6. Average particle size composition of collected soil and sediment samples from different toposequence positions on three transects within one wetland catchment (WetlandA) in

Broughton's Creek watershed, Manitoba. Particle size composition is represented by the clay (≤0.002 mm), silt (0.002–0.063 mm) and sand (0.063–2 mm) content of collected samples. 188

Fig. 4. 7. Colour coefficients properties of soil and sediment collected (~20-cm depth) at different toposequence positions (U1; upper slope position, U2; middle slope position, U3; lower slope position, R; riparian areas, W; water body (central area)) in the studied agricultural catchments. Points are the average across studied wetland catchments. 189

Fig. 4. 8. Depth characterization of HSV colour attributes of hue (e.g., colour itself), saturation (e.g., colour brilliance) and value (e.g., lightness/darkness) for different toposequence position within one wetland catchment (WetlandA) in Broughton's Creek, Manitoba. HSV colour attributes have been used for quantitative descriptions of soil colour. 191

Contributions of Authors

The outline of this thesis follows the "grouped manuscript style" whose guidelines are appointed by the Faculty of Graduate Studies at University of Manitoba. In accordance with the regulations, the present thesis consists of a collection of manuscripts of which the candidate is the first author. The candidate was fully responsible for the development and implementation of the field-based research studies, supervising research assistants, analysis of data, writing of the manuscripts, submitting the manuscripts, and responding to reviewer's comments, and re-submitting the revisions.

Chapter 1 contains an introduction about the study area, research objectives, and thesis contributions; Chapters 2, 3 and 4 are manuscripts, each containing an abstract, introduction, methods, results, discussion, and conclusions; Chapter 5 provides the final synthesis and general conclusions of this research and recommendations for future research.

Chapters 2, 3 and 4 are co-authored by the candidate's supervisor Dr. David Lobb from University of Manitoba, Dr. Alexander Koiter from Brandon University, Dr. Pascal Badiou from Ducks Unlimited Canada, Winnipeg, Manitoba, Dr. Irena Creed from University of Toronto, Dr. Sheng Li from Agriculture and Agri-food Canada, Fredericton, New Brunswick, and Dr. Eric Enanga from University of Manitoba. Chapter 2 was published in 2022 in the Journal of Soil and Tillage Research. Chapter 3 and 4 have were published in 2023 in the Journal of Geoderma.

Copyright notices and journal papers information

Zarrinabadi, E., Lobb, D.A., Koiter, A.J., Goharrokhi, M., 2022. Assessment of the effects of land rolling on wind erosion and crop growth in soybean production in the Red River Valley, Canada. Soil Tillage Res. 222, 105439. https://doi.org/10.1016/j.still.2022.105439

Zarrinabadi, E., Lobb, D.A., Enanga, E., Badiou, P., Creed, I.F., 2023. Agricultural activities lead to sediment infilling of wetlandscapes in the Canadian Prairies: Assessment of soil erosion and sedimentation fluxes. Geoderma. 436, 116525. https://doi.org/10.1016/j.geoderma.2023.116525

Zarrinabadi, E., Lobb, D.A., Li, S., Koiter, A.J., Badiou, P., 2023. Agricultural activities lead to sediment infilling of wetlandscapes in the Canadian Prairies: Assessment of contributions by tillage, water and wind erosion. Geoderma. 438, 116621. https://doi.org/10.1016/j.geoderma.2023.116621

Chapter 1

Introduction and literature review

1.1. Soil erosion and degradation

The introduction of agriculture to the Canadian Prairie Pothole Region by European settlers in the late 1800s and early 1900s brought about many dramatic changes in the natural landscape. Soil erosion is a naturally occurring phenomenon and is part of soil and landscape formation; however, anthropogenic activities and interventions have considerably exacerbated this process through the removal of native vegetation cover, expansion of farming onto marginal lands and overgrazing (Borrelli et al., 2017). According to the Food and Agriculture Organization of the United Nations (FAO), soil erosion is considered the major threat to the sustainability of soil management (FAO, 2019). Soil erosion is of global environmental concern due to its direct and indirect negative impact on ecosystem services, agricultural productivity, and soil security. Soil erosion processes result in the removal of fertile topsoil and its deposition elsewhere in the surrounding environment, which further degrades soil fertility and ecosystem functions. On a larger scale, soil erosion can lead to contamination of aquatic environments (e.g., wetlands) through nutrient loss and other agro-chemicals, and delivery to waterways and water bodies (Blanco-Canqui and Lal, 2008a).

Soil erosion and sedimentation are a widespread form of lateral soil redistribution (Lal, 2019). The redistribution of soil within landscapes due to erosion processes modifies soil physical, chemical, and biological characteristics. The loss of topsoil and exposure of subsoil on upper slopes amplifies the variability in soil properties, which has major impacts on crop production, biophysical processes and greenhouse gas emissions. Unproductive subsoil that is exposed on eroded is then hilltops is dragged down by erosive agents the hillslope and buries productive topsoil at the lower part of the hillslope, which creates an “inverted” soil profile (Lobb, 2011). Accelerated soil erosion also sets-in-motion a process, which can impact the soil carbon budget through breakdown of aggregates and exposure of soil organic carbon to climatic elements and microbial enzymes (Lal, 2019).

Additionally, changes in climate conditions directly affect soil erosion risk. With drier weather conditions, Canadian Prairies are currently experiencing a reduction in soil vegetation cover and an increase in the number of extreme erosional events (Leys et al., 2018). For example, 2019 was a record-breaking year for extreme environmental conditions around the globe (World Meteorological Organisation, 2019). As a result, in Canada, low ground cover, dry conditions and strong wind gusts in spring can lead to increased frequencies of dust storms across the Prairie Pothole Region. Furthermore, long-term climate trends in low rainfall regime areas can also cause aeolian processes to be more dominant than fluvial ones, leading to extreme wind erosion risk (Field et al., 2011).

Water and wind erosion were assumed to be the major forms of soil erosion on cultivated landscape. According to Meyer and Moldenhauer (1985), the first scientific investigation of water erosion was conducted by the German soil physicist, Ewald Wollny, who was a pioneer in soil and water conservation research in the late 19th Century. However, the soil loss caused by wind did not gain attention until the early 20th Century when it was studied by Edward E. Free (Free, 1911). In North America, the major water and wind erosion research effort began in 1930s, with the establishments of Universal Soil Loss Equation (USLE) (Wischmeier and Smith, 1965) and Wind Erosion eQuation (WEQ) (Woodruff and Siddoway, 1965) as the respective milestones. The movement of soil downslope due to the mechanization of agriculture, referred to as tillage erosion, was recognized as an important factor that influenced soil erodibility as early as the 1920s, but primarily in a qualitative manner. However, the systematic studies on tillage translocation and erosion were conducted in the late 20th Century (Lindstrom et al., 1992). Recent studies have demonstrated that the direct movement of soil by tillage implements is a significant erosive process, distinct from wind and water erosion (Lobb et al., 1995; Li et al., 2007; Tiessen et al., 2009).

1.1.1. Soil erosion in the Canadian Prairie provinces

Soil loss by erosion processes has been identified as a major threat to sustainability of food production in Canada (McConkey et al., 2010) and still remains a concern within the various agro-ecosystems across Canada, specifically in the western Prairie provinces. Soil surveys in the Prairie provinces started in 1935, where drought and soil erosion presented the main problems (McKeague and Stobbe, 1978). Although there is substantial qualitative evidence of serious wind and water erosion in the Canadian Prairies, but few studies were conducted under natural conditions to assess the magnitude and spatial distribution of erosion on the Canadian Prairies prior to the 1980s (de Jong et al., 1983). Toogood (1963) conduced a long-term study (1950 to 1960) in Alberta on water erosion and reported the maximum soil loss of 4.5 t ha^{-1} yr^{-1} on summer fallow lands. Nicholaichuk and Read (1978) estimated annual water erosion of 2 t ha^{-1} yr^{-1} from fall-fertilized summer fallow lands in southwest Saskatchewan. In Manitoba, Shaw (1980) predicted soil loss ranging from 12.6 to 16.6 t ha^{-1} yr^{-1} and from 66.7 to 86.7 t ha^{-1} yr^{-1} under continuous fallow and crop rotation of small grains, respectively, using USLE.

Quantitative assessment of soil erosion using ^{137}Cs technique in the Canadian Prairies began in the early 1980s. de Jong et al. (1983) estimated soil loss using ^{137}Cs technique and documented that upper slope positions lost between 10 and 30 t ha^{-1} yr^{-1}; whereas, the lower slopes gained between -12 and -40 t ha^{-1} yr^{-1} over the period of 20 years in Saskatchewan. In 1984, Jenkins et al. quantified soil erosion in southern Manitoba using ^{137}Cs in which they reported severe soil loss from knoll position and soil accumulation on the mid-slope and depressional positions of the landscape.

Gregorich and Anderson (1985) documented soil erosion rates ranging from 6 to 44 t ha^{-1} yr^{-1} using ^{137}Cs on three hillslopes in the Black soil zone along the Saskatchewan/Alberta border. In one study in Saskatchewan, Martz and de Jong, (1987) reported soil losses as high as 57 t ha^{-1} yr^{-1}, which were observed over 60% of the basin with 90 % of the total soil accumulation occurring in less 3% of the basin. Southerland and de Jong (1990) in another study in Saskatchewan estimated maximum net sediment flux ranging from 37.5 t ha^{-1} yr^{-1} to -46.5 t ha^{-1} yr^{-1} during a period of 30 to 35 years, resulting in net sediment output of 1.5 t ha^{-1} yr^{-1} from cultivated land. These studies have identified water erosion as a serious problem in the Canadian Prairie Pothole Region and indicated severe soil loss mostly from crest, upper slope, and middle slope positions. It is clear that on- and off-site effects associated with water erosion have been in scientific and political focus. Consequently, other soil erosion drivers like wind and tillage were somewhat out of the scope of most studies. Sparrow (1984) reported that more than one-half of the total annual soil loss due to wind and water is ascribed to wind erosion in Canada. The use of ^{137}Cs in wind erosion studies is less common in Canada, but Sutherland et al. (1991) estimated soil redistribution on near level landscape using ^{137}Cs in Saskatchewan and documented mean net sediment output ranging from 0.8 to 38 to ha^{-1} yr^{-1}. Larney et al., (1995) have quantified soil loss by wind, for the first time in Canada, using wind erosion samplers and the total wind erosion of 144.4 t ha^{-1} (ranging from 0.3 to 30.4 t ha^{-1}) was documented on summer fallow lands of Alberta for a period of 2 years (April 1990 to May 1992).

Tillage erosion was a mostly ignored soil erosion process; however, substantially contributes to on-sites effects on soil properties and productivity. It was only in the early 1990s that systematic studies of tillage translocation and erosion were made (Lobb et al., 1995). Thereby, with the knowledge that tillage erosion is a major erosive agent, recent studies were performed to assess soil redistribution by tillage erosion in Canada (Lobb and Kachanoski 1999; Li et al., 2007; Li et al., 2008; Tiessen et al., 2009). For example, Li et al., 2007 determined that their tillage erosion model accounted for most of the soil lost from the convex upper slope positions (as estimated by ^{137}Cs) from a field site located in southern Manitoba, suggesting that tillage erosion was the dominant soil redistribution process in that region. In general, these studies have documented that the patterns of tillage and water erosion within the landscape are primarily dependent on topographic complexity, with water erosion dominating on steep mid-slopes and upper lower slopes where the water flow converges, while tillage erosion dominates on convex landscape positions. The Prairie Pothole agroecosystem (e.g., wetland catchments) are characterized by complex landscape structures, generating high local variability in terms of erosion processes. Thus, due to such spatial heterogeneity, we still face a lack of knowledge to decipher dominant soil erosion processes in that region. Since the spatial patterns of soil loss by tillage, water and wind erosion are fundamentally different, it is possible to model their relative contributions towards combined tillage, water and wind erosion, hereinafter referred to as total soil erosion, within a cultivated landscape.

1.1.2 Potential impacts of sedimentation on wetland health and function

The rise in worldwide crop production has primarily been achieved through intensive farming activities (e.g., Monoculture cropping, fertilizers and pesticide application, drainage systems, tillage methods, and livestock intensification) (Watmough and Schmoll, 2007), which play an undeniable role in causing widespread pollution, leading to environmental concerns (i.e., excessive sediment loadings in floodplains and depressional wetlands). The majority of the depressional wetlands in the Prairie Pothole Region of Canada are embedded within an agricultural landscape, making them vulnerable to different levels of sediment accumulation (Gleason and Euliss, 1998;

Preston et al., 2013). The farming of uplands surrounding these depressional wetlands can exacerbate downslope translocation of soil and associated constituents into wetland ecosystems (i.e., riparian area and waterbody), leading to increased rates of soil erosion through terrestrial fluxes and atmospheric deposition of sediment originating from the local and regional sources (Gleason and Euliss, 1998; Santhi et al., 2006). On watershed scales, depressional wetlands physically control runoff by increasing surface storage and reducing effective contributing areas, while at the individual wetland catchment scales, the ponds and associated riparian vegetation physically slow the movement of runoff causing sedimentation (Blann et al., 2009; Baulch et al., 2019).

Depressional wetlands are especially fragile and there has been a gradual increase in the drastic degradation of such natural systems over the past century due to sediment accumulation. The most significant impacts of soil erosion arises when sediment accumulation fills the central area of wetlands (i.e., waterbody) to the extent that they no longer hold water, causing a loss of their primary natural functions (e.g., production of aquatic macrophytes and algae) through reducing water clarity. Furthermore, increased sedimentation in wetlands surrounded by agricultural landscapes can lead to degradation of wetland invertebrate egg and seed banks, through sediment burial, which can limit emergence of invertebrates from egg banks. Moreover, the impact of sedimentation on wetland wildlife is likely indirect through alteration of composition of vegetation, vegetation cover, and aquatic invertebrate communities (Gleason and Euliss, 1998; Gleason et al., 2003). In addition, sedimentation can cause notable changes in riparian areas surrounding wetlands, altering their composition, structure, and functionality as transitional zones between the aquatic and terrestrial areas of a landscape.

1.2. Soil erosion processes

More than 70 years ago, Ellison characterized soil erosion as "a process of detachment and transportation of soil constituents by erosive agents" (Ellison, 1948). The development of soil erosion processes has a detrimental effect on soil quality for agricultural production because it degrades soil functions for crop growth. Soil erosion is a complex process because of the many factors affecting the rate of erosion, including topography, soil erodibility, vegetation cover, weather conditions and soil management practices (Blanco-Canqui and Lal, 2008a). Soil management methods (e.g., farming operation) is a key component to the success of site-specific soil erosion control. Additionally, this factor is important in seedbed preparation (e.g., land rolling) and sustainable production within an individual field (Carter and Johannsen, 2017). This assumption is particularly accurate for regions with higher soil erosion risk, especially in early growing season, such as Prairie provinces. Hence the study of soil erosion in such areas represents a great interest for the farming community as well as governmental agencies.

1.2.1. Water erosion

Soil loss due to water erosion is the removal of soil from one location and its movement to another, usually downhill, by the action of rainfall or snowmelt and surface runoff. Water erosion processes have been classified into five classes including rain splash erosion, sheet erosion, rill erosion, gully erosion and stream bank erosion. At the initial stage, soil particles are detached from aggregates by the impact of falling raindrops (splash erosion) or overland flow (sheet-inter-rill erosion). The concentration of water as it flows over the surface cuts into the soil, detaching even more soil, forms small, well-defined channels (rill erosion). The detached soil particles are deposited when the velocity and depth of the flow decreases. These eroded channels can later grow and develop into ephemeral and permanent gullies from repeated runoff cycles (Vrieling, 2006; Kothyari, 2008;

Blanco and Lal, 2008b). Rills are differentiated from gullies by the fact that they are small enough to be erased easily with normal tillage practices (Kothyari 2008). Water erosion and runoff remove fertile topsoil leading to a decline in nutrients and soil organic carbon. These nutrients can either be deposited in nearby fields, thus enrich them, or be carried away until they reach waterways and, ultimately, water bodies (e.g., wetlands), where they can lead to eutrophication. Siltation (sediment accumulation) of water bodies can also be a significant off-site consequence of water erosion, leading to a reduction of storage capacity and an increase in the expenses related to cleaning up the affected area (Nearing et al., 2017). Additionally, in cold winter climates (e.g., Canadian Prairie provinces) freeze-thaw processes and snowmelt over frozen soils influence the structure of soil; thereby, increasing soil erodibility to erosion by runoff (Liu et al., 2014).

1.2.2. Wind erosion

Wind erosion is the loss and movement of coarse and fine soil particles by airflow across a landscape at various heights above the soil surface. The wind-eroded sediment moves along the soil surface via three mechanisms: creep, saltation, and suspension (Lyles, 1988). Particles moving by creep roll over the ground for a few centimeters to a few meters within a localized area, and they have a diameter of 0.05 to 2 mm. Particles moving by saltation have a diameter of 0.1 to 0.5 mm, and can be lifted into and bounce in the airflow at heights generally below 1 m, and be transported many meters before they come to rest. The suspended particles (e.g., very fine silt and clay particles and organic matter) have diameters of less than 0.1 mm and are subject to long-range (regional) transport, with some material being transported across continents and even around the globe (Fryrear et al., 1991). Wind-eroded sediment transport is omnidirectional as airborne material can be conveyed in all wind directions but follows prevailing winds. The on-site and off-site effects of wind eroded particles released into the environment depends on the composition and size of the particles as well as the distance transported (Goossens and Riksen, 2004). Wind erosion can lead to a reduction of agricultural productivity by depleting soil nutrients content. As well, saltating coarse particles can injure plants by abrasion and desiccation due to infection and sparse and/or short plant canopies during early growing season (Bennell et al., 2007). Dust storms can also adversely affect visibility and air quality, negatively impacting human health (e.g., irritation of eyes and skin).

1.2.3. Tillage erosion

Tillage erosion is the soil redistribution that occurs within a landscape, whenever soil is moved or translocated as a direct result of tillage. Tillage disturbs the soil vertically and throws soil in the tillage direction mostly. Soil displacement by tillage implements occurs at rates varying according to the local slope gradient, as a primary factor, and operational factors, including: implement type and size; tillage depth, speed, and orientation relative to the slope; and soil condition before tillage. Typically, tillage results in the progressive downslope movement of soil over time, causing severe soil loss on convexities and the upslope field boundaries, and causing soil accumulation in concavities and downslope field boundaries. In topographically complex landscapes, composed of convexities and concavities, soil losses by tillage erosion are most severe near convexities (e.g., hilltops, knolls and on upslope field areas), while soil accumulation occurs at slope concavities and hill bottoms (Lindstrom et al., 1992; Govers et al., 1999, Lobb et al., 1999; Papiernik et al., 2005). Tillage erosion has been reported as an important soil degradation process and a major contributor to the total soil erosion in cultivated fields (Li et al., 2007).

Soil erosion studies are generally carried out through field observation, tracer studies, experimental plots, and soil erosion modelling (Walling and Quine, 1990; Li et al., 2007; Wainwright and Mulligan, 2013). It is important to carry out field measurements of fallout radionuclides (e.g., ^{137}Cs) and employ soil erosion models to differentiate patterns of tillage erosion from water and wind erosion within a landscape (Li et al., 2010).

1.3. Soil erosion modelling

Modelling can be considered as quantitative representation of complex environmental systems. Environmental models are not an alternative to field-measurements but, under certain circumstances, can be a powerful tool in understanding environmental processes and in developing and testing various scenarios (e.g., characterizing driving forces of change across landscape, under a wide range of conditions). Most of the environmental models used in soil erosion research are classified as the empirical "grey-box" type model, which are based on characterizing the most important factors and, through the use of observation, measurement, experiment and statistical techniques, relating them to soil loss. Environmental models employed in soil erosion and conservation studies can assist to fulfill three primary purposes including: (a) to understand the scope of the problem over a landscape and to quantitatively track soil erosion changes over time, and (b) to help policy-makers choose sustainable agricultural practices (Morgan, 2010; Braizer, 2013).

For decades, research on water erosion was by far the most studied process using the soil erosion models worldwide. Most of these global studies performed water erosion predictions using (R)USLE family models (Borelli et al., 2021). The USLE is an empirical model derived from a correlation between soil erosion measured on experimental plots and environmental parameters (e.g., topography, climate, soil properties and land use). The USLE was later improved, Revised USLE, to account for more modern farming practices and make use of computer technologies (Renard et al., 1997). Furthermore, the most commonly used spatially distributed, process-based model is Water Erosion Prediction Project (WEPP), which was designed by USDA to improve the empirically-based USLE to provide a continuous simulation of soil erosion predictions (sheet-inter-rill erosion) from distributed parameters (Nearing et al., 1989; Borelli et al., 2021).

Although the Dust Bowl of 1930 proved to be a low point in North American environmental history, wind erosion modelling has not been as common as water erosion modelling. The most applied wind erosion models are Wind Erosion eQuation ((R)WEQ), the Single-event Wind Erosion Evaluation Program (SWEEP) and the Wind Erosion Prediction System (WEPS) (Borelli et al., 2021). The WEQ and RWEQ are empirical models with a similar structure to the USLE, while SWEEP and WEPS are process-based models that can produce daily and sub-hourly simulation of wind erosion at a field scale (Tatarko et al., 2016). One of the main limitations of the models mentioned above is that these models can only be applied to field scale and a large amount of detailed input parameters are required for modelling. However, up scaling wind erosion models from the plot- to regional-scale is time-consuming, expensive, and difficult to calibrate and validate over a large region (Youssef et al., 2012).

Development of tillage erosion models started in early 1990s by a growing awareness of tillage as another important deriver of soil redistribution within agricultural field; however, tillage erosion modelling is still understudied compared to water and wind erosion modelling. Lindstorm et al. (1992) developed the first tillage erosion model as a statistical relationship between soil displacement and slope gradient and documented that tillage translocation distances are inversely proportional to slope gradient. This led the introduction of a diffusion-type approach that simulates tillage erosion as a function of local slope and a tillage transport coefficient (Govers et al., 1994), which resulted in the development of Water and Tillage Erosion Model (WaTEM) by Van Oost et al. (2000). While these previous models focused primarily on the effect of slope gradient on tillage translocation, researchers in Canada have also documented that slope curvature can significantly influence tillage erosion within topographically complex landscapes (Lobb et al., 1995; Lobb and Kachanoski, 1999a); therefore, these researchers recommended that slope curvature be included as a second topographic variable in development of tillage erosion models. In response, researchers in Canada developed Tillage Erosion Model (TillEM, Lobb and Kachanoski, 1999b; Li et al., 2007), Tillage Translocation Model (TillTM, Li et al., 2008), The Directional Tillage Erosion Model (DirTillEM, Li et al., 2009) and Soil Constituent Redistribution by Erosion Model (SCREM, Li et al., 2010). There are more complex models of tillage erosion exist (Tillage Erosion Prediction model (TEP, Lindstrom et al., 2000), Soil Redistribution by Tillage (SORET, De Alba et al., 2004), TILDA: Quine and Zhang, 2004, Cellular Automata model for Tillage Translocation (CATT, Vanwalleghem et al., 2010), (Tillage Erosion and Landscape Evolution Model (TELEM, Vieira and Dabney, 2009; 2011)), which additionally require more input parameters such as tillage direction, the interaction between complex topography and soil translocation, opertational settings, on-field objects or complex field boundary effects. These models provide excellent tools to assess the effectiveness of different management strategies to combat soil erosion.

1.4. Aims and objectives of the thesis

The overarching aim of this study is to quantify the atmospheric and terrestrial fluxes of soil mass and associated constituents from agricultural fields into wetlands and their surrounding riparian areas, and demonstrate the benefit of tillage, water, and wind erosion modelling approaches to identify the spatio-temporal variability of soil erosion and sedimentation within the Canadian Prairies. The information gained by assessing wind erosion under conditions that are considered highly prone to wind erosion (Objective 1) provided critical background for assessing soil erosion and sedimentation under the conditions of the wetland landscapes (Objectives 2 and 3), where constraining the upper limits to what should be expected for soil erosion, especially wind erosion.

In developing this thesis research, the study consisted of two projects, which was mainly focused on three main sets of specific objectives to meet the overall aim:

1. To assess the impact of land rolling on soil properties, soybean yields and growth characteristics, and on the detachment and transport of wind-eroded sediment using passive uni-directional samplers;
2. To assess the severity and variability of soil loss and deposition, and develop sediment budgets within wetland landscapes using ^{137}Cs; and
3. To assess contributions of tillage, water and wind erosion to total soil erosion within wetland landscapes, and soil and sediment properties (e.g., ultimate particle size distribution and spectral reflectance).

The objectives were met throughout the chapters using different approaches (i.e., experimental, observational, and modelling). Each approach answers a specific research question, which can be related to the objectives as follow:

1. How soil management impacts crop yield and wind erosion potential through changing transitory properties of soil? (objective 1)
2. What is the state of soil erosion within wetland catchments of agricultural landscape? (objective 2)
3. Can sediment budgets be used to constrain uncertainties associated with assessment of soil erosion? (objective 2)
4. Can erosional and sedimentary features (patterns) be identified and used to improve assessment of soil erosion? (objective 2)
5. What are the relative contributions of tillage, water and wind erosion to soil movement and flux within the cultivated wetland catchment? (objective 3)

6. What is the relative contribution of runoff transfers (i.e., sediment) to the total quantity stored in wetlands and their surrounding riparian areas? (objective 3)

1.5. Thesis structure

This thesis is composed of five chapters that address the research aims (Fig. 1.1).

This chapter, **Chapter 1,** presents a general introduction to soil erosion processes and the diverse modelling approaches applied to study this phenomenon as well as the motivations behind the research. This chapter also presents the research objectives and the outline of the thesis. This chapter is followed by three chapters written in the form of scientific journal manuscripts.

Chapter 2 describes the field experiments conducted to assess the effects of land rolling on transport of soil particles by wind and crop growth in soybean production in the Red River Valley, Manitoba. This chapter seeks to understand the impact of soil management on wind erosion potential. The development and fabrication of a wind erosion sampler is discussed in this chapter as well. Chapter 2 was published in a peer-reviewed journal.

Expanding on the work in Chapter 2, the next two chapters consider soil loss and sedimentation by tillage, water and wind within the Prairie Pothole Region of Manitoba and Alberta.

Chapter 3 evaluates the magnitude of soil loss and sedimentation within wetland catchments using ^{137}Cs. The developed budget of soil losses and accumulations is also discussed in this chapter. Using the soil erosion measurements described in Chapter 3 and established tillage, water and wind erosion models, the **fourth chapter** improves our understanding of the relative contributions of tillage, water and wind erosion within Prairie Pothole Region. Additionally, this chapter defines the adaptations of each model to local conditions and describes the interaction between each erosional process and their influencing factors. Chapters 3 and 4 have been submitted for publication in a peer-reviewed journal; Chapter 3 is undergoing its second review, and Chapter 4 its first review. Finally, **Chapter 5** summarizes the key findings of this study, limitations and broader implication of the research and the recommendations for further exploration in the field.

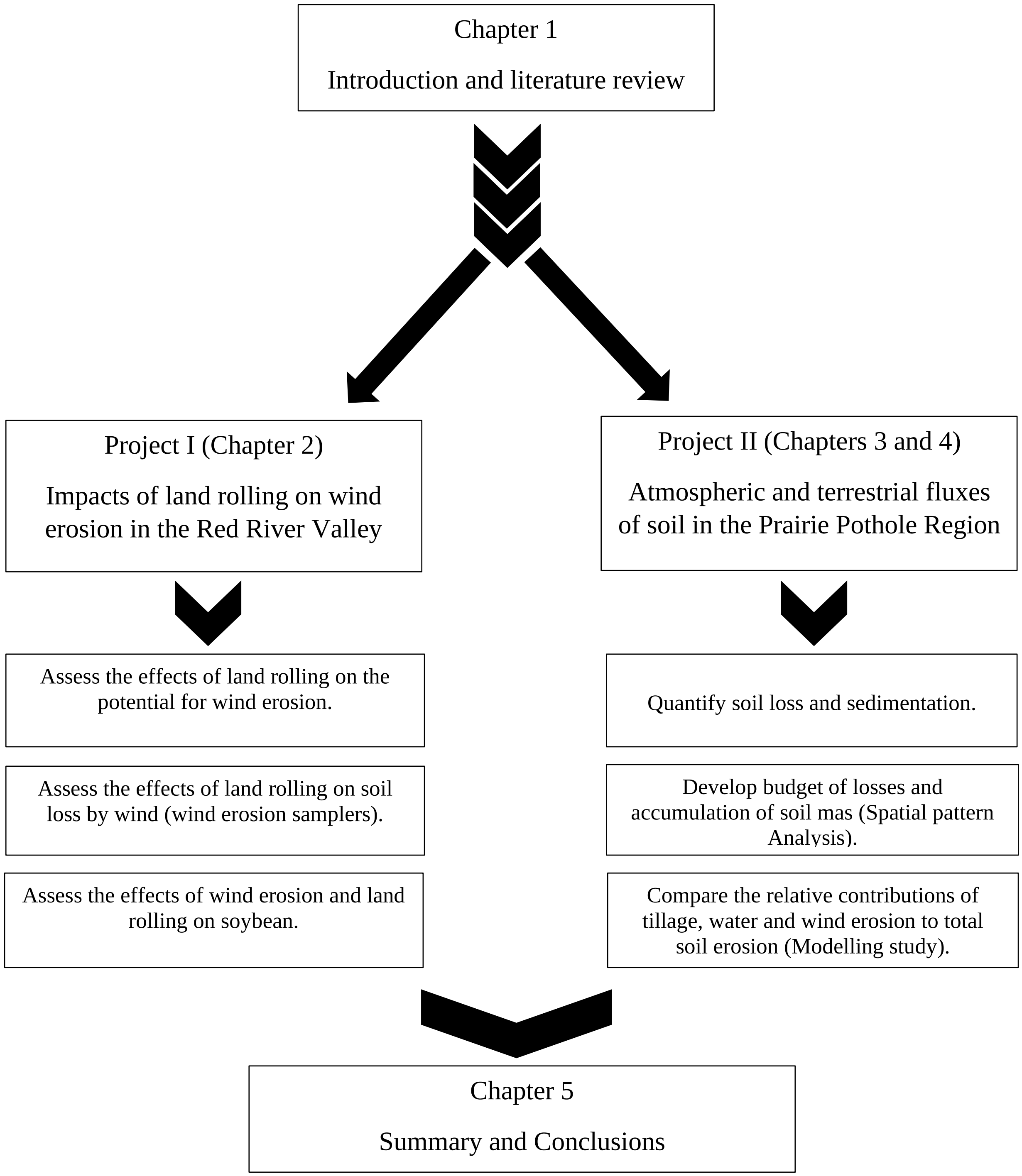

Fig. 1. 1. Schematic of the thesis structure linking the chapters to the objectives

1.6. References

Baulch, H.M., Elliott, J.A., Cordeiro, M.R.C., Flaten, D.N., Lobb, D.A., Wilson, H.F., 2019. Soil and water management: Opportunities to mitigate nutrient losses to surface waters in the northern great plains. Environ. Rev. 27, 447–477. https://doi.org/10.1139/er-2018-0101

Bennell, M.R., Leys, J.F., Cleugh, H.A., 2007. Sandblasting damage of narrow-leaf lupin (Lupinus angustifolius L.): A field wind tunnel simulation. Aust. J. Soil Res. 45, 119–128. https://doi.org/10.1071/SR06066

Blanco-Canqui, H., Lal, R., 2008a. Soil and Water Conservation, in: Blanco-Canqui, H., Lal, R. (Eds.), Principles of Soil Conservation and Management. Springer Netherlands, Dordrecht, pp. 1–19. https://doi.org/10.1007/978-1-4020-8709-7_1

Blanco-Canqui, H., Lal, R., 2008b. Water Erosion, in: Blanco-Canqui, H., Lal, R. (Eds.), Principles of Soil Conservation and Management, Springer Netherlands, Dordrecht, pp. 21–53. https://doi.org/10.1007/978-1-4020-8709-7_2

Blann, K.L., Anderson, J.L., Sands, G.R., Vondracek, B., 2009. Effects of agricultural drainage on aquatic ecosystems: A review. Crit. Rev. Environ. Sci. Technol. 39, 909–1001. https://doi.org/10.1080/10643380801977966

Borrelli, P., Alewell, C., Alvarez, P., Anache, J.A.A., Baartman, J., Ballabio, C., Bezak, N., Biddoccu, M., Cerdà, A., Chalise, D., Chen, S., Chen, W., De Girolamo, A.M., Gessesse, G.D., Deumlich, D., Diodato, N., Efthimiou, N., Erpul, G., Fiener, P., Freppaz, M., Gentile, F., Gericke, A., Haregeweyn, N., Hu, B., Jeanneau, A., Kaffas, K., Kiani-Harchegani, M., Villuendas, I.L., Li, C., Lombardo, L., López-Vicente, M., Lucas-Borja, M.E., Märker, M., Matthews, F., Miao, C., Mikoš, M., Modugno, S., Möller, M., Naipal, V., Nearing, M., Owusu, S., Panday, D., Patault, E., Patriche, C.V., Poggio, L., Portes, R., Quijano, L., Rahdari, M.R., Renima, M., Ricci, G.F., Rodrigo-Comino, J., Saia, S., Samani, A.N., Schillaci, C., Syrris, V., Kim, H.S., Spinola, D.N., Oliveira, P.T., Teng, H., Thapa, R., Vantas, K., Vieira, D., Yang, J.E., Yin, S., Zema, D.A., Zhao, G., Panagos, P., 2021. Soil erosion modelling: A global review and statistical analysis. Sci. Total Environ. 780. https://doi.org/10.1016/j.scitotenv.2021.146494

Borrelli, P., Lugato, E., Montanarella, L., Panagos, P., 2017. A new assessment of soil loss due to wind erosion in european agricultural soils using a quantitative spatially distributed modelling approach. L. Degrad. Dev. 28, 335–344. https://doi.org/10.1002/ldr.2588

Brazier, R.E., 2013. Erosion and Sediment Transport: Finding Simplicity in a Complicated Erosion Model, in: Wainwright, J., Mulligan, M. (Eds.), Environmental Modelling: Finding Simplicity in Complexity, pp. 253–266. https://doi.org/https://doi.org/10.1002/9781118351475.ch15

Carter, P.G., Johannsen, C.J., 2017. Site-specific soil management. Ref. Modul. Earth Syst. Environ. Sci. https://doi.org/https://doi.org/10.1016/B978-0-12-409548-9.10497-X

De Alba, S., Lindstrom, M., Schumacher, T.E., Malo, D.D., 2004. Soil landscape evolution due to soil redistribution by tillage: A new conceptual model of soil catena evolution in agricultural landscapes. Catena 58, 77–100. https://doi.org/10.1016/j.catena.2003.12.004

de Jong, E., Begg, C.B.M., Kachanoski, R.G., 1983. Estimates of soil erosion and deposition for some Saskatchewan soils. Can. J. Soil Sci. 63, 607–617. https://doi.org/10.4141/cjss83-061

Ellison, W.D., 1948. Soil detachment by water in erosion processes. Eos, Trans. Am. Geophys. Union 29, 499–502. https://doi.org/https://doi.org/10.1029/TR029i004p00499

FAO, 2019. "Soil Erosion: The Greatest Challenge to Sustainable Soil Management." Rome, pp. 100. Licence: CC BY-NC-SA 3.0 IGO. http://www.fao.org/3/ca4395en/ca4395en.pdf.

(accessed 10.13.2022)

Free, E.E., 1911. Studies in soil physics. I. The physical condition of soils. The Plant World, 14(2), 29–39. http://www.jstor.org/stable/43476841

Field, J.P., Breshears, D.D., Whicker, J.J., Zou, C.B., 2011. On the ratio of wind- to water-driven sediment transport: Conserving soil under global-change-type extreme events. J. Soil Water Conserv. 66, 51–56. https://doi.org/10.2489/jswc.66.2.51A

Fryrear, D.W., Stout, J.E., Hagen, L.J., Vories, E.D., 1991. Wind erosion: field measurement and analysis. Trans. Am. Soc. Agric. Eng. 34, 155–160. https://doi.org/10.13031/2013.31638

Gleason, R.A., Euliss, N.H., Hubbard, D.E., Duffy, W.G., 2003 Effects of sediment load on emergence of aquatic invertebrates and plants from wetland soil egg and seed banks. Wetlands. 23, 26-34. https://doi-org.uml.idm.oclc.org/10.1672/0277-5212(2003)023[0026:EOSLOE]2.0.CO;2

Gleason, R.A., Euliss, N.H.J., 1998. Sedimentation of prairie wetlands. Gt. Plains Res. 8, 97–112. http://www.jstor.org/stable/24156336

Goossens, D., Riksen, M.J.P.M., 2004. Wind erosion and dust dynamics at the commencement of the 21st century. Preface. In: Goossens, D., Riksen, M.J.P.M. (Eds.), Wind Erosion and Dust Dynamics: Observations, Simulations, Modelling. Wageningen University, Wageningen, pp. 7-14.

Govers, G., Lobb, D.A., Quine, T.A., 1999. Tillage erosion and translocation: emergence of a new paradigm in soil erosion research. Soil Tillage Res. Vol.51 (3/4), 167-174

Govers, G., Vandaele, K., Desmet, P., Poesen, J., Bunte, K., 1994. The role of tillage in soil redistribution on hillslopes. Eur. J. Soil Sci. 45, 469–478. https://doi.org/10.1111/j.1365-2389.1994.tb00532.x

Gregorich, E.G., Anderson, D.W., 1985. Effects of cultivation and erosion on soils of four toposequences in the Canadian prairies. Geoderma 36, 343–354. https://doi.org/10.1016/0016-7061(85)90012-6

Jenkins, C. Shaykewich, C.F. and de Jong, E., 1984. Potential for the use of Cesium-137 as a tracer for soil erosion in Manitoba. 27th Manitoba Soil Science Society Meeting, Winnipeg, Manitoba, 181-187.

Kothyari, U.C., 2008. Soil erosion and sediment yield modelling. ISH J. Hydraul. Eng. 14, 84–103. https://doi.org/10.1080/09715010.2008.10514895

Lal, R., 2019. Accelerated Soil erosion as a source of atmospheric CO_2. Soil Tillage Res. 188, 35–40. https://doi.org/10.1016/j.still.2018.02.001

Larney, F.J., Bullock, M.S., McGinn, S.M., Fryrear, D.W., 1995. Quantifying wind erosion on summer fallow in southern Alberta. J. Soil Water Conserv. 50, 91–95.

Leys, J., Strong, C., Heidenreich, S., Koen, T., 2018. Where she blows! a ten year dust climatology of western New South Wales Australia. Geosci. 8, 1–15. https://doi.org/10.3390/geosciences8070232

Li, S., Lobb, D.A., Lindstrom, M.J., 2007. Tillage translocation and tillage erosion in cereal-based production in Manitoba, Canada. Soil Tillage Res. 94, 164–182. https://doi.org/10.1016/j.still.2006.07.019

Li, S., Lobb, D.A., Lindstrom, M.J., Farenhorst, A., 2008. Patterns of water and tillage erosion on topographically complex landscapes in the North American Great Plains. J. Soil Water Conserv. 63, 37–46. https://doi.org/10.2489/63.1.37

Li, S., Lobb, D.A., Tiessen, K.H.D., 2009. Modeling tillage-induced morphological features in cultivated landscapes. Soil Tillage Res. 103, 33–45.

https://doi.org/10.1016/j.still.2008.09.005

Li, S., Lobb, D.A., Tiessen, K.H.D., McConkey, B.G., 2010. Selecting and applying cesium-137 conversion models to estimate soil erosion rates in cultivated fields. J. Environ. Qual. 39, 204–219. https://doi.org/10.2134/jeq2009.0144

Lindstrom, M.J., Nelson, W.W., Schumacher, T.E., 1992. Quantifying tillage erosion rates due to moldboard plowing. Soil Tillage Res. 24, 243–255. https://doi.org/10.1016/0167-1987(92)90090-X

Lindstrom, M.J., Schumacher, J.A., Schumacher, T.E., 2000. TEP: A Tillage Erosion Prediction model to calculate soil translocation rates from tillage. J. soil water Conserv. 55, 105–108

Liu, K., Elliott, J.A., Lobb, D.A., Flaten, D.N., Yarotski, J., 2014. Nutrient and sediment losses in snowmelt runoff from perennial forage and annual cropland in the Canadian Prairies. J. Environ. Qual. 43, 1644–1655. https://doi.org/10.2134/jeq2014.01.0040

Lobb, D.A., 2011. Understanding and managing the causes of soil variability. J. Soil Water Conserv. 66, 175–179. https://doi.org/10.2489/jswc.66.6.175A

Lobb, D.A., Kachanoski, R.G., 1999a. Modelling tillage erosion in the topographically complex landscapes of southwestern Ontario, Canada, Paper presented at International Symposium on Tillage Translocation and Tillage Erosion held in conjunction with the 52nd Annual Conference of the Soil and Water Conservation Society. Soil Tillage Res. 51, 261–277. https://doi.org/https://doi.org/10.1016/S0167-1987(99)00042-2

Lobb, D.A., Kachanoski, R.G., 1999b. Modelling tillage translocation using step, linear-plateau and exponential functions1Paper presented at International Symposium on Tillage Translocation and Tillage Erosion held in conjunction with the 52nd Annual Conference of the Soil and Water Conservation Society. Soil Tillage Res. 51, 317–330.

https://doi.org/https://doi.org/10.1016/S0167-1987(99)00045-8

Lobb, D.A., Kachanoski, R.G., Miller, M.H., 1999. Tillage translocation and tillage erosion in the complex upland landscapes of southwestern Ontario, Canada. Soil Tillage Res. 51, 189–209. https://doi.org/10.1016/S0167-1987(99)00037-9

Lobb, D.A., Kachanoski, R.G., Miller, M.H., 1995. Tillage translocation and tillage erosion on shoulder slope landscape positions measured using ^{137}Cs as a tracer. Can. J. Soil Sci. 75, 211–218. https://doi.org/10.4141/cjss95-029

Lyles, L., 1988. Basic wind erosion processes. Agric. Ecosyst. Environ. 22–23, 91–101. https://doi.org/https://doi.org/10.1016/0167-8809(88)90010-2

Martz, L.W., de Jong, E., 1987. Using cesium-137 to assess the variability of net soil erosion and its association with topography in a Canadian Prairie landscape. Catena 14, 439–451. https://doi.org/10.1016/0341-8162(87)90014-2

McConkey, B.G., Lobb, D.A., Li, S., Black, J.M.W., Krug, P.M., 2010. Soil erosion on cropland: introduction and trends for Canada. Canadian Biodiversity: Ecosystem Status and Trends 2010, Technical Thematic Report No. 16. Canadian Councils of Resource Ministers. Ottawa, ON. URL https://publications.gc.ca/site/eng/9.696092/publication.html (accessed 12.12.2022)

McKeague, J.A., Stobbe, P., 1978. History of Soil Survey in Canada (1914-1975). Soil Res. Inst. Canada Dep. Agric. 1, 32.

Meyer, L.D., Moldenhauer, W. C., 1985. Soil Erosion by Water: The Research Experience. Agricultural History, 59(2), 192–204. http://www.jstor.org/stable/3742384

Morgan, R.P.C., 2010. Model Development: A User's Perspective, in: Morgan, R. P. C., Nearing M. A., (Eds.), Handbook of Erosion Modelling. pp. 7–32.

https://doi.org/https://doi.org/10.1002/9781444328455.ch2

Nearing, M.A., Foster, G.R., Lane, L.J., Finkner, S.C., 1989. A process-based soil erosion model for USDA-Water Erosion Prediction Project technology. Trans. ASAE 32, 1587–1593. https://doi.org/https://doi.org/10.13031/2013.31195

Nearing, M.A., Lane, L.J., Lopes, V.L., 2017. Modeling soil erosion, in: Lal, R. (Eds.), Soil Erosion Research Methods. Routledge, pp. 127–158

Nicholaichuk, W., Read, D.W.L., 1978. Nutrient runoff from fertilized and unfertilized fields in western Canada. J. Environ. Qual. 7, 542–544. https://doi.org/https://doi.org/10.2134/jeq1978.00472425000700040015x

Papiernik, S.K., Lindstrom, M.J., Schumacher, J.A., Farenhorst, A., Stephens, K.D., Schumacher, T.E., Lobb, D.A., 2005. Variation in soil properties and crop yield across an eroded prairie landscape. J. Soil Water Conserv. 60, 388–395.

Preston, T.M., Sojda, R.S., Gleason, R.A., 2013. Sediment accretion rates and sediment composition in Prairie Pothole wetlands under varying land use practices, Montana, United States. J. Soil Water Conserv. 68, 199 LP - 211. https://doi.org/10.2489/jswc.68.3.199

Quine, T.A., Zhang, Y., 2004. Re-defining tillage erosion: quantifying intensity–direction relationships for complex terrain. Soil Use Manag. 20, 124–132. https://doi.org/https://doi.org/10.1111/j.1475-2743.2004.tb00347.x

Renard, K.G., Foster, G.R., Weesies, G.A., McCool, D.K., Yoder, D.C., 1997. Predicting soil erosion by water: A guide to conservation planning with the Revised Universal Soil Loss Equation (RUSLE). U.S. Department of Agriculture. Agriculture Handbook.

Santhi, C., Srinivasan, R., Arnold, J.G., Williams, J.R., 2006. A modeling approach to evaluate the impacts of water quality management plans implemented in a watershed in Texas.

Environ. Model. Softw. 21, 1141–1157. https://doi.org/10.1016/j.envsoft.2005.05.013

Shaw, G.A. 1980. Predicted soil erosion by water for various soil types in Manitoba. 24th Manitoba Soil Science Society Meeting, Winnipeg, Manitoba. pp. 63-70

Sparrow, H.O., 1984. Soil at Risk, Canada's Eroding Future, A report on soil conservation by the standing committee on agriculture, Fisheries and Forestry to the Senate of Canada, Senate of Canada, Ottawa.

Sutherland, R.A., de Jong, E., 1990. Estimation of sediment redistribution within agricultural fields using caesium-137, Crystal Springs, Saskatchewan, Canada. Appl. Geogr. 10, 205–221. https://doi.org/https://doi.org/10.1016/0143-6228(90)90022-H

Sutherland, R.A., Kowalchuk, T., de Jong, E., 1991. Cesium-137 estimates of sediment-redistribution by wind. Soil Sci. 151, 387-396.

Tatarko, J., van Donk, S.J., Ascough, J.C., Walker, D.G., 2016. Application of the WEPS and SWEEP models to non-agricultural disturbed lands. Heliyon 2, e00215. https://doi.org/10.1016/j.heliyon.2016.e00215

Tiessen, K.H.D., Li, S., Lobb, D.A., Mehuys, G.R., Rees, H.W., Chow, T.L., 2009. Using repeated measurements of ^{137}Cs and modelling to identify spatial patterns of tillage and water erosion within potato production in Atlantic Canada. Geoderma 153, 104–118. https://doi.org/10.1016/j.geoderma.2009.07.013

Toogood, J.A. 1963. Water erosion in Alberta. J. Soil Water Conserv. 6: 238-240.

Van Oost, K., Govers, G., Desmet, P., 2000. Evaluating the effects of changes in landscape structure on soil erosion by water and tillage. Landsc. Ecol. 15, 577–589. https://doi.org/10.1023/A:1008198215674

Vanwalleghem, T., Jiménez-Hornero, F.J., Giráldez, J. V, Laguna, A., 2010. Simulation of long-term soil redistribution by tillage using a cellular automata model. Earth Surf. Process. Landforms 35, 761–770. https://doi.org/https://doi.org/10.1002/esp.1923

Vieira, D.A.N., Dabney, S.M., 2011. Modeling edge effects of tillage erosion. Soil Tillage Res. 111, 197–207. https://doi.org/10.1016/j.still.2010.10.007

Vieira, D.A.N., Dabney, S.M., 2009. Modeling Landscape Evolution Due to Tillage: Model Development. Trans. ASABE 52, 1505–1522. https://doi.org/https://doi.org/10.13031/2013.29139

Vrieling, A., 2006. Satellite remote sensing for water erosion assessment: A review. Catena 65, 2–18. https://doi.org/10.1016/j.catena.2005.10.005

Wischmeier, W.H., Smith, D.D., 1965. Predicting rainfall-erosion losses from cropland east of the Rocky Mountains. Guide for selection of practices for soil and water conservation. Agric. Handbook, 282. US Gov. Print. Office, Washington, DC.

Woodruff, N.P., Siddoway, F.H., 1965. A wind erosion equation. Soil Sci. Soc. Am. J. 29, 602–608. https://doi.org/https://doi.org/10.2136/sssaj1965.03615995002900050035x

World Meteorological Organisation, 2019. United in science. Science Advisory Group of the UN Climate Action Summit 2019. https://public.wmo.int/en/resources/united_in_science (accessed 10/13/2022)

Youssef, F., Visser, S., Karssenberg, D., Bruggeman, A., Erpul, G., 2012. Calibration of RWEQ in a patchy landscape; a first step towards a regional scale wind erosion model. Aeolian Res. 3, 467–476. https://doi.org/10.1016/j.aeolia.2011.03.009

Chapter 2

Assessment of the effects of land rolling on wind erosion and crop growth in soybean production in the Red River Valley, Canada

2.1. Abstract

Land rolling has become a popular practice in soybean and pulse production in the Northern Great Plains. The practice of land rolling is simply pulling a large-scale cylindrical roller over a cultivated field to push down stones and improve seed-to-soil contact. Many soybean farms in Manitoba are routinely rolled either immediately after seeding or at the very early stages of crop development. There has been considerable concern regarding the potential effects of land rolling on wind-induced soil loss, soil properties, and plant growth in soybean production. To address this concern, an on-farm research project was conducted at eight different field sites in the Red River Valley of southern Manitoba, Canada, in 2018 and 2019. Trials were established with rolled and non-rolled treatments arranged using a randomized complete block design. To examine the environmental and agronomic impacts of land rolling, data was collected to characterize wind-transported sediment (passive uni-directional samplers), soil properties (e.g., surface roughness and moisture content), yield, and plant growth parameters. Despite the land rolling reducing surface roughness the results showed no significant difference in the amount of collected wind-transported sediment between the two treatments. In addition, the particle size of the wind-transported sediment ranged between 0.002-0.1 mm suggesting that this size fraction was the most susceptible to wind erosion. Furthermore, there was a small, but significant, increase in soybean yield in the non-rolled treatment, despite having significantly lower volumetric soil moisture content (~ 30 cm soil depth). Overall, while land rolling reduced soil surface roughness and increased the wind erosion risk, it did not result in an increase in the amount of wind-transported soil loss. Lastly, within the Red River Valley the practice of land rolling to support higher soybean yield was not supported; however, the exact reasons for the small yield reduction is not fully understood.

2.2. Introduction

Soybeans (*Glycine max* L Merril) are a valuable food source and are an important agricultural commodity globally. Soybean production in Manitoba, Canada, has increased substantially over the past few decades, and contributes to the growing significance of the Prairie Region in Canada's soybean production. In 2020, the province of Manitoba produced about 20% of the total annual production in Canada (Soy Canada 2020). Seeded area of soybean production in Manitoba increased from 20,200 ha in 2001 to 465,200 ha in 2020 (Soy Canada, 2020), representing < 1% and ~ 6.5% of the province's annual cropland (~ 7,137,698 ha), respectively (Statistics Canada, 2016; 2020). This increase is primarily driven by the development of short growing season varieties, and the continued development of varieties will likely result in further expansion of the soybean crop and will demand advances in soil and crop management practices to ensure sustainable production.

The sustainability of soybean productivity depends on many interacting factors including soil quality, agricultural management practices, and local climatic conditions (Faé et al., 2020). Soil quality decline through human activity can lead to reduced health and productivity of natural ecosystems and agro-ecosystems, which impacts global socio-economic systems (Lal, 2009). Bai et al. (2008) reported that around 24% of agricultural land globally was affected by various types of land degradation (e.g., soil erosion, nutrient loss, salinity, soil physical problems, and chemical contamination). Conversion from native grassland to annual crop production in the Canadian Prairie provinces of Manitoba, Saskatchewan, and Alberta has resulted in a cumulative loss of native grasslands from pre-colonial levels by 99.9%, 81.3% and 61%, respectively (Samson and Knopf, 1994). This has resulted in extensive areas being exposed to increased risk of soil erosion.

Soil erosion due to land conversion and intensive farming operations, therefore, represents a great threat to soil health and productivity (Thangavel and Sridevi, 2017).

Farming operations, such as rolling (e.g., smooth, notched and coil drums), cultipacker (e.g., smooth and notched wheels), planking, and press-wheels are practiced to improve seedling emergence by achieving optimal seed-to-soil contact and seedbed firmness according to field conditions and management requirements (e.g., soil texture, stoniness, planting depth, preceding crop, and climate) (Couture et al., 2004; Barker et al., 2012). Rolling improves the initial consolidation and increases capillary moisture movement, especially in a dry spring, which is necessary for seed germination (Håkansson et al., 2002; Romaneckas et al., 2010). A study was carried out in Canada (Quebec) by Couture et al. (2004) and demonstrated that rolling of soil prior to seeding on coarse texture soils with a seeding depth of 2 cm can be beneficial for flax fibre production. Similarly, a plot-scale soybean study documented a small yield increase when soybean fields were rolled at the first and second trifoliate stage of plant growth (Bohner, 2018). However, Boyers et al. (2020) reported that land rolling did not influence soybean yield when done before or after emergence (2nd, 3rd, 4th trifoliate stage of plant growth). Although agronomic benefits of land rolling have not been fully studied in a wide variety of crop production and climatic regions, producers practice land rolling to improve harvesting efficiency.

The practice of rolling in pulse and soybean production has become popular in the Prairie Region of Canada over the past couple of decades. This technique was promoted and adopted as a practice to push stones down into the soil and smoothing the ground for harvesting. The coil- and notched-drums leave the soil rougher than the smooth-drum system (Al-Kaisi et al., 2011; DeJong-Hughes et al., 2012), which can reduce the risk of wind erosion. Although land rolling is beneficial where deep tillage may be conducted and the soil surface contains more than 5% of clods bigger than 50 mm (Dürr and Aubertot, 2000), producers recognized that rolling corn root-balls with a coil drums or notch system increases the rate of breakdown by improving soil to plant residue contact (DeJong-Hughes et al., 2012). However, there has been considerable concern regarding the potential effects of land rolling on increasing the risk of soil loss by wind erosion.

Soil erosion by wind is a common phenomenon that occurs in many arid and semi-arid regions, and results in both on- and off-site impacts (Lal, 1998). In the Northern Great Plains Region of North America, the months with the highest risk of wind erosion mostly occur in the spring season, when surface protection by vegetation cover is at a minimum, particularly post seeding (Shao, 2008). Wind erosion is a concern in many areas of Canada, from the sandy soils along the Fraser River in British Columbia to the coastal areas of the Atlantic Provinces. However, it has been a major concern in the Canadian Prairie Region which stretches from southwestern Manitoba to southwestern Alberta and north to central Saskatchewan (Rennie, 1985; Lobb et al., 2017). The risk for wind erosion is the greatest in the more arid south of this region due to lower precipitation and lower crop and crop residue cover (Huffman et al., 2000).

Wind erosion can also cause considerable crop damage, and economic losses associated with increased herbicide, pesticide and fertilizer costs, degraded drainage systems and road ditch cleaning costs (Parry et al., 1988). Physical crop damage has been reported when seedlings suffer from abrasion and/or being buried by sand-sized particles during windstorms. In addition, plants damaged by the scouring effect of creeping and saltating sand particles are more vulnerable to sun burn and diseases which can result in poor crop yields (Bennell et al., 2007; Michels et al., 1995; Riksen and De Graaff, 2001). Soil loss through wind erosion can transport soil-bound herbicides to non-target areas (e.g., field boundary and ditches) as research has shown that risk for removal of surface-applied chemicals by wind erosion is higher than that of soil-incorporated chemicals

(Clay et al., 2001). Off-site physical and economic effects include adverse health impacts caused by dust storms over residential areas (e.g., high fine particulate matter levels), and damage to reservoirs, irrigation, drainage, transportation and communication infrastructure (Riksen and De Graaff, 2001).

Risk of wind erosion on agricultural land can be affected by relatively stable properties including surface soil properties, topography, vegetation cover, climate and land management (e.g., farming operations) (Larney and Bullock, 1994; Shao, 2008). Soil surface properties affecting soil erodibility by wind include relatively stable properties, including texture and organic matter content, as well as more transitory properties (i.e., rapid changes over time) including surface roughness, aggregate size, and crusting. The stable soil properties, land management practices, and their interactions influence the transient soil surface properties, which affect the wind erosion risk (Pi et al., 2021). Both non-oriented soil surface roughness (e.g., random distribution of large soil aggregates) and oriented soil surface roughness formed by active farming operations (e.g., crop rows and tillage furrows) can affect wind erosion (Fryrear, 1984; Zobeck, 1991). Random roughness is associated with soil surface micro-relief, which can impact surface aerodynamic roughness and shear stress (Shao, 2008). Oriented roughness is one of the directional wind erosion control methods, which can control the organic geochemistry of sediment, in addition to the amount of wind-transported sediment (Hou et al., 2021). Aggregate size distribution controls the magnitude of wind erosion because it is directly linked to the entrainment threshold velocity (Kheirabadi et al., 2018; Zobeck, 1991). Beyond the influence of the more stable soil properties, farming operations (e.g., tillage and land rolling practices) are the primary factors influencing the disruption of surface crusts and breakdown of macro aggregates making the soil more vulnerable to wind erosion (Hevia et al., 2007, 2003; Guo et al., 2017).

The physical and biogeochemical characteristics of wind-transported sediment (e.g., particle size distribution, organic matter content, spectral reflectance and ^{137}Cs activity of wind-transported sediment) and the patterns of soil redistribution can facilitate identifying the predominant mechanism(s) of wind erosion in agricultural lands. However, the characteristics of wind-transported sediment have been shown to vary with height. In particular, the concentration and particle size distribution of wind-transported sediment changes with height above the eroding surface as a result of gravitational and drag forces that oppose the upward movement of larger and heavier particles into the atmosphere (Zobeck and Fryrear, 1986; Sharratt, 2011). The wind-transported sediment flux profile is measured to characterize the movement of sediment particles by airflow in different height and trajectories (Dong and Qian, 2007). For example, Van Pelt et al. (2007) demonstrated that in wind-transported sediment, ^{137}Cs activity increased and median particle diameter decreased with height within the first meter above the eroding soil surface.

The impacts of land rolling on crop production, soil properties, and soil susceptibility to wind erosion have been raised as concerns associated with this practice. While changes in the soil surface properties due to land rolling can affect the magnitude of wind erosion, the impact of this practice on wind erosion risk in the Canadian Prairies has not been well studied. As a result, there is still a lack of consensus among agronomists and environmentalists regarding the short- and long-term impacts of land rolling. Given the growing interest in the practice of land rolling in soybean production systems, and the lack of scientific information about its agronomic and environmental impacts in the Canadian Prairies, or in other regions of North America, a study was initiated to provide the information needed to ensure the sustainable production of soybeans in Manitoba. The objectives of this study were to measure the impacts of land rolling on soil properties, soybean yields and growth characteristics, and detachment and transport of wind-eroded sediment. In order to achieve the objectives, the following research hypotheses were tested in this study; (1) land rolling increases the volumetric soil moisture content; (2) land rolling increases transport of wind-eroded sediment when soil surface is not protected; and (3) rolling the land immediately after seeding improves soybean yield.

2.3. Materials and methods

2.3.1. Study area

The study was conducted in the Red River Valley of southern Manitoba (Fig. 2.1). The Red River Valley extends over 17,000 km^2 from northeastern South Dakota through northwestern Minnesota and eastern North Dakota into southern Manitoba, ending at the southern end of Lake Winnipeg. The valley spans from the Manitoba Escarpment (also known as the Pembina Escarpment) in the west to the Canadian Shield in the east (Environment Canada and Manitoba Water Stewardship, 2011).

The Red River Valley is a glacio-lacustrine plain, the remnant of glacial Lake Agassiz. The advance of Pleistocene ice sheets blocked the drainage to the north, leading to the formation of the glacial lake. The soils of the valley are vertisolic, derived from the clay-rich (>60 %) glacio-lacustrine deposits, and chernozemic, typical of the tall-grass prairie ecosystem (Bluemle, 1988; Yates et al., 2014, 2012). Seasonal freezing and thawing, and wetting and drying interact with these clay- and organic-rich soils to form 0.5- to 1.0-mm-sized aggregates that are vulnerable to wind displacement by saltation (Cihacek et al., 1993).

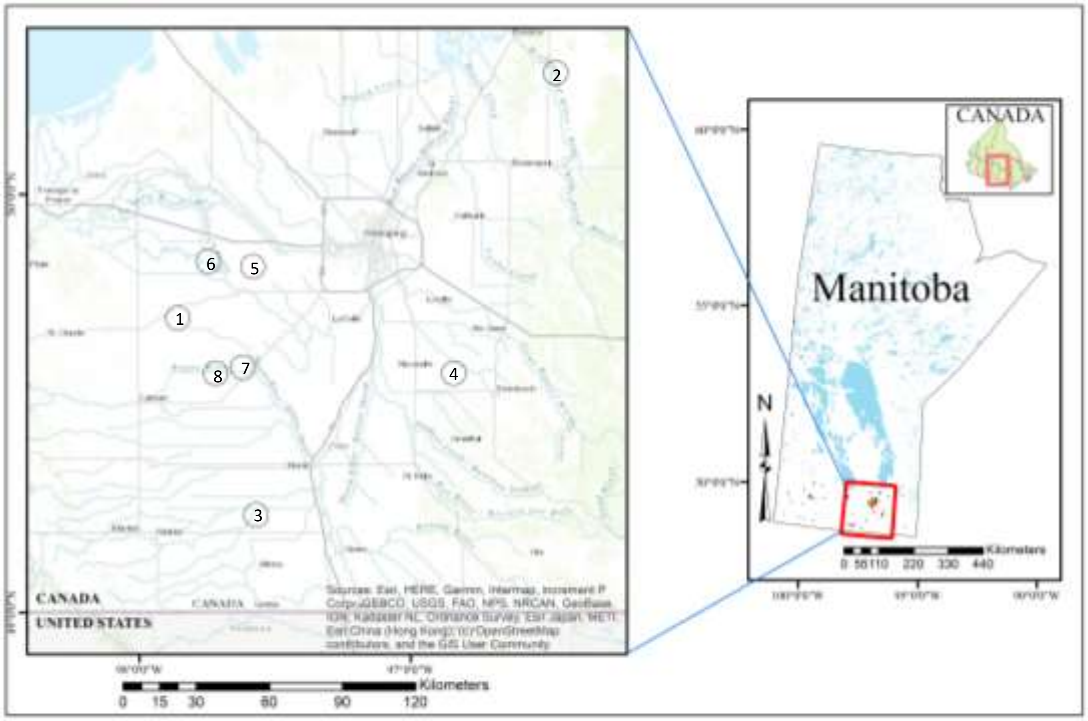

Fig. 2. 1. Location of the study area within Manitoba, Canada. Circles are the location of fields included in the study.

The study area is characterized as mixed prairie agriculture with extensive production of cereals and oilseeds. The growing season is relatively short, ranging from 100 to 140 days, commencing with spring seeding in April/May and fall harvesting in August/September. The region has a sub-humid continental climate with cold and dry winters and warm summers with moderate precipitation falling predominantly during the summer months in the form of intense rainstorms (Bossenmaier and Vogel, 1974; Stoner et al., 1993). Annual precipitation averages 579 mm, with 22% occurring as snow (1980-2010 climate normals for Starbuck, Manitoba, ID: 5022770) (ECCC, 2019).

The wind erosion risk in the Red River Valley is a result of the region's unique combination of geological, climatic, and surface cover conditions (Todhunte and Cihacek, 1999). The minimal aerodynamic roughness provided by the regional low-relief topography creates a wind regime that is generally active and frequently experiences gusty conditions. It has been reported that a wind speed of 6.2 m s^{-1} is required to entrain and displace fine-textured soils (Chepil, 1945). In the study area, mean monthly wind speeds are approximately 5 m s^{-1} and marginally higher during the months of March, April, May (pre- and post-seeding) and October (post-harvest), but do not exceed threshold wind speed that particles motion begin (~ 6.2 m s^{-1}) (1980-2010 climate normals for Winnipeg, Manitoba, ID: 5023222) (ECCC, 2019). However, the average maximum hourly wind speed (~ 22 m s^{-1}) and maximum gust speed (~ 32 m s^{-1}) are far in excess of this threshold value for all months of the year.

The seasonal frequency of wind speed and direction during the experimental period (winter, spring, summer and fall of 2018-2019) for the study area are provided in wind rose diagrams shown (Fig. 2.2) (Winnipeg, Manitoba, ID: 5023222). The wind roses also show the percentage of the total wind speed values that fall within a given category of intensity. The prevailing wind direction in spring within the study area comes from the north, northwest and south reaching a yearly average of 5 m s^{-1}; however, winds also blow from northeast of the study region. A smaller percentage of the wind data (5-10 %) accounts for winds from the west, southwest, southeast and east.

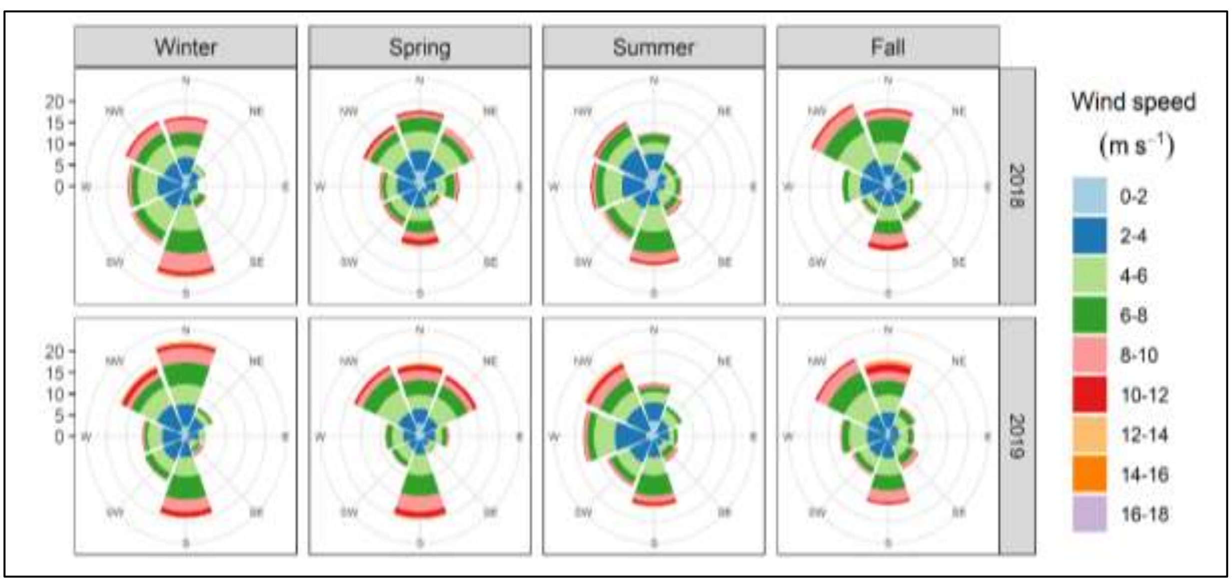

Fig. 2. 2. Average annual wind speed and direction for the study area over the study period (2018-2019).

2.3.2. Experimental design

This research was conducted in 2018 and 2019 on eight farm cooperators' fields. In 2018, four field sites were selected near Dencross, Rosenfeld, Culross, and Randolph. In 2019, two field sites near Macdonald and two field sites near Brunkild were selected for this on-farm study. The sites selection was performed based on their location within the Red River Valley of Manitoba, the availability of land roller equipment, and the farmers' willingness to participate in this study. One field-scale paired strip trials of rolled and non-rolled treatments within each field were established. Strip sizes varied from field to field, depending on field dimension and farmer preference, ranging from 0.2- to 1.5-ha. The experiment was arranged as a randomized complete block design (RCBD) with field as a replicate and located on land with similar conditions. Soils, topography, climate, and crop management conditions were characterized, but were similar by design and not considered as experimental factors. There was a total of eight replicates over the two years of the study.

2.3.3. Soybean crop management

Farm cooperators were responsible for field preparation and performing all tillage, seeding and spraying operations during this on-farm research study. The farmers used their own seeders and equipment, and managed the trials as they normally would their fields. They also chose their own soybean varieties and tillage practices. The diameter of the land rollers used by cooperating producers ranged from 0.91 to 1.1 m with roller length of 15 m. The roller was pulled at the speed ranged between 12.7 and 15.8 km hr^{-1}. The producers planted their soybeans from May 11 through May 14 and rolled their fields within two to three days of planting. The planted soybean varieties were classified as mid-season maturity varieties, falling into maturity group (MG) of 00.5. Each year, the preceding crops in all the fields were different. Farmers applied fertilizers at a rate to match fertility level and target yields within their fields (Table 2.1). The collaborators utilized a post-emergence herbicide and pesticide program to manage weeds, disease and insects followed by best management practices for the region. The soybeans were harvested using producer-owned commercial harvesting equipment from mid- to late-September.

All the selected sites have a history of conventional or minimum tillage management. Conventional tillage management included fall tillage after harvest, followed by additional finishing implements (e.g., disks) in spring prior to seeding, and use of synthetic chemical herbicides and tillage to control weeds. Minimum tillage management included the placement of seed into crop residue that was untilled or moderately tilled (Table 2.1). Minimum tillage usually results in fewer tillage operations than for conventional tillage, which led to reduced soil disturbance and higher crop residue cover. Although the specific operating conditions varied from cooperator to cooperator, they were selected by the funding agency from their on-farm research network and were considered representative of farming conditions used in soybean production in the study area.

Table 2. 1. The location, tillage history, soybean variety and management practices for study fields

Year	Location	Tillage System	Fall Tillage[a]	Spring Tillage[b]	Preceding Crop	Soybean Variety	Treatment Orientation[c]	Seeding Equipment[d]	Fertilizer (N-P-K-S)[e]
2018	Culross (1)	Conventional	High Speed Disc	none	Canola	24-10RY	N-S	1220 Case Planter	none
	Dencross (2)	Conventional	Deep Till	Harrow	Soybean	S006-W5	N-S	Press Drill	11-52-0-0
	Rosenfeld (3)	Conventional	Deep Till	Harrow	Wheat	not-available*	E-W	Air Drill	0-45-0-0
	Randolph (4)	Conventional	High Speed Disc	none	Corn	DKB005-52	E-W	1245 Case Planter	not-available
2019	Macdonald-A (5)	Conventional	High Speed Disc	none	Wheat	WS Syngenta	E-W	Air Drill	12-51-0-0
	Macdonald-B (6)	Conventional	not-available	not-available	not-available	not-available	N-S	not-available	not-available
	Brunkild-A (7)	Minimum	Fertilizer Application	none	Oats	DKB005-52	N-S	Disc Drill	0-30-30-0
	Brunkild-B (8)	Conventional	Heavy Harrow	none	Wheat	24-10RY	E-W	not-available	not-available

* Information is not available.

[a] Deep Till and Heavy Harrow are referred to as Chisel plow.

[b] Harrow is referred to spring-tooth harrow.

[c]N-S and E-W are referred to as North-West and East-West orientations.

[d] 1220 and 1245 Case Planter is equipped with disk opener along with rubber closing wheels.

[e] Fertilizer type required to meet target yield and fertility level based on the agronomic recommendation for the region.

2.3.4. Design and fabrication of uni-directional sediment sampler

Passive, uni-directional sediment samplers, specially designed and fabricated for this study, were used to collect wind-transported sediment moving over the soil surface along the length of each treatment (Fig. 2.3). The samplers were fabricated from cylindrical plastic pails with height and diameter of 368 mm and 286 mm, respectively. Each pail was fitted with a horizontal rectangular collection opening at one of two different heights (5 cm and 20 cm). Sediment-laden air entered through the horizontal, 20-mm high by 100-mm wide (2,000 mm^2 cross-sectional area) collection opening. Air discharged from the pail through an outlet made of large plastic pipe with an inner diameter of 70 mm (3,848 mm^2 cross-sectional area) that was covered with geotextile mesh (150 µm). In order to further reduce the air speed and trap smaller particles, a washable fiberglass filter was placed inside the sampler. Coarse-mesh (1 cm) screens were used to cover the collection opening and the outlet of the sampler to prevent larger pieces of residue and animals from entering. A solid concrete block sealed within a washable plastic bag was placed inside the sampler to stabilize the pail in strong winds.

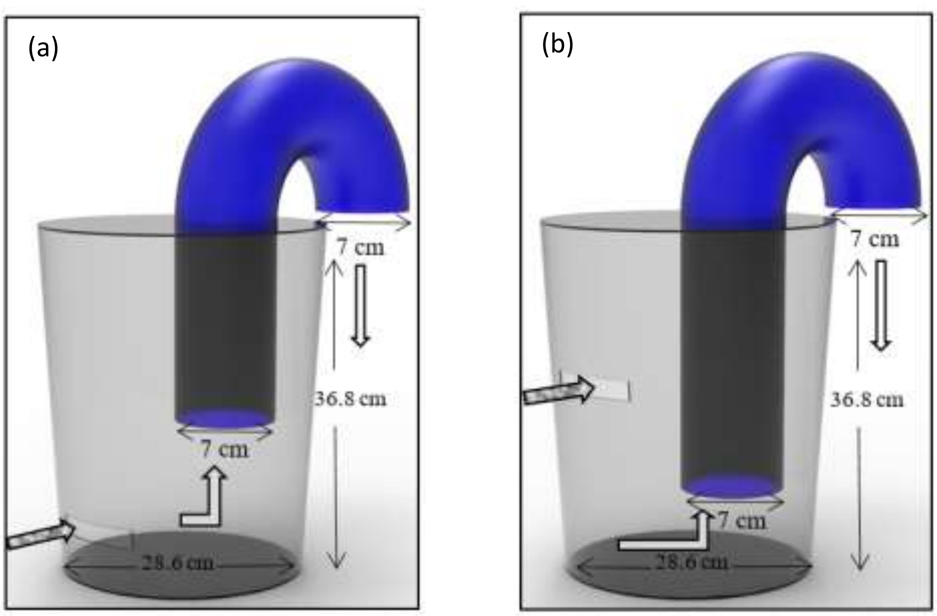

Fig. 2. 3. (a) the sampler with inlet height at 5-cm, and (b) the sampler with inlet height at 20-cm. [A sealed solid concrete block, fiberglass filter and coarse mesh on the inlet and outlet not shown].

Collection efficiency is dependent on design characteristics, wind speed and direction during the measurement process, soil particle size distribution, and other factors (Fryrear, 1984; Dong et al., 2004; Goossens and Offer, 2000). Therefore, detailed consideration focused on the intrinsic spatial and temporal variability of sediment transport associated with collection efficiency (e.g., collected mass), mainly in field conditions. Passive sediment samplers (e.g., Modified Wilson And Cooke (MWAC, Wilson and Cooke, 1980), Leach sand trap (White, 1982), Big Spring Number Eight (BSNE, Fryrear, 1986), and SUspension Sediment TRAp (SUSTRA, Kuntze and Beinhauer, 1989)) with narrow collection openings may not provide a desired sampling of the mass flux, as a result of the variability in air flow pattern that is normally observed in nature (Nickling and McKenna Neuman, 1997; McKenna Neuman and Maxwell, 1999). Rectangular-shaped opening collections ranged from 200 mm^2 to 1000 mm^2, and sediment samplers with circular-shaped opening collection had an inner diameter range from 7.5 mm to 50 mm. Therefore, the collection opening of the developed sediment sampler was adjusted and expanded to 2,000 mm^2 (20 mm × 100 mm) so as to achieve the desired sampling mass and facilitate the efficient trapping of particles. The samplers with collection opening at 5-cm and 20-cm heights above the ground were specifically designed to collect particles that are moving in creep and saltation modes. It has been documented that saltation and creep can make up to 72% and 40% of the transported mass, respectively, and mostly rise less than 30 cm above the soil surface (Chepil, 1945; Zobeck et al., 2003).

2.3.5. Measurements

Gravimetric soil moisture content and soil bulk density were measured biweekly during the growing season from May to September at the soil surface (0-1cm) and at three soil depths (0-10, 10-20 and 20-30 cm). Samples were collected using a foot-operated stainless steel JMC Backsaver soil sampler (with a 45.7-cm-long, 3.17-cm-diameter slotted sampling tube). Sample collection was repeated at four different spots at random to cover the whole length of each treatment. Particular care was taken to select sampling locations representative of the entire trials and avoid sampling areas close to field edges. Samples were weighed, oven-dried at 105°C, and reweighed for measuring gravimetric soil moisture content (Topp et al., 2007). Bulk density was calculated as the weight of oven-dry soil divided by the total soil volume (Blake and Hartge, 1986). The conversion into volumetric soil moisture content was determined by multiplying the gravimetric soil moisture content by the ratio of the bulk density of the samples to the density of water. A high-density terrestrial laser scanner (Trimble Faro TX-5, Trimble Inc., Sunnyvale, CA, USA, at Science and Technology Branch, Agriculture and Agri-Food Canada, Winnipeg, Canada) was used to measure soil surface roughness in this study. Soil roughness data was collected on rolled and non-rolled trials in spring 4-5 days after land rolling, and in fall after harvest. At least five different spots were selected for scanning at random locations within each treatment at all sites.

Measurements of soil surface roughness and data processing were conducted by Agriculture and Agri-Food Canada personnel at the Science and Technology Branch, Winnipeg, Manitoba for two consecutive years (2018 and 2019). The root mean squared height (RMSH) of the surface was characterized for each of the treatments (rolled and non-rolled) using LiDAR point clouds (Bryant et al., 2007; Chabot et al., 2018). Regions of interest were cropped from the point clouds to calculate RMSH. The RMSH is a descriptor of the vertical roughness component. The definition of the RMSH is given by:

$$RMSH = \sqrt{\frac{\sum_{i=1}^{n}(z_i - \overline{z})^2}{n-1}}$$

Where n represents the number of data points, z_i is the elevation of the i^{th} data point and $\overline{z}$ is the mean elevation of all (n) data points.

The wind-transported sediment samplers only collected sediment during the growing season following rolling the land for the comparison of the rolled and non-rolled treatments on the production of wind-eroded sediment. The uni-directional sediment samplers were installed immediately after rolling the sites every year and collected one week before the scheduled time for harvest. In total, four sediment samplers were installed in each treatment (rolled and non-rolled) at all sites. The collection openings of sediment samplers were oriented based on the direction of soybean rows. Two sets of sediment samplers with collection opening at 5-cm and 20-cm height above the ground were placed at each end of the trial to achieve maximum coverage of fetch length. The collection opening of sediment samplers were faced each other in each treatment covering the whole length of the trial to accommodate wind events along the treatment length in both directions. The positions of sediment samplers were identical between rolled and non-rolled treatments allowing side-by-side comparison between treatments (Fig. 2.4). Visual observations of deposited sediment in the roadside ditch at the edge of fields were used to document field-scale wind erosion before and after the growing season.

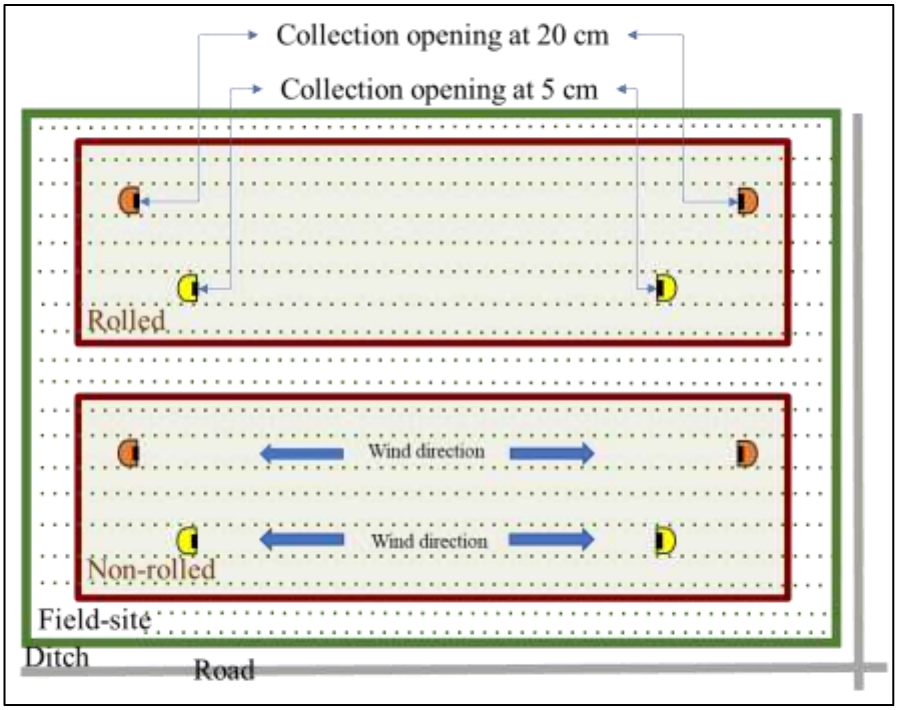

Fig. 2. 4. Location of wind erosion samplers within strip trial fields. The strips ranged from 200- to 500-m in length and 10-m in width. Fields are replicates in the experimental design. Direction of wind-eroded sediment movement is shown with arrows. Wind erosion samplers were located centrally within each strip and oriented based on the direction of soybean rows. Inlets of wind erosion samplers were faced to each other within each treatment. [Inlet shown with black rectangle].

To quantify wind-induced sediment transport dynamics and to characterize the properties of sediment, samples collected from field sites were returned to the lab for analyses, which included measuring mass, particle size distribution, ^{137}Cs activity, spectral reflectance, and organic matter content. The samples were oven dried prior to analysis. The activity of ^{137}Cs in sediment samples was measured by gamma-ray spectrometry, using a high-resolution Small Anode Germanium (SAGe) well detector (Mirion Technologies (Canberra) Inc., Meriden, CT, USA, at the Landscape Dynamics Laboratory, University of Manitoba, Winnipeg, Canada). The samples' ^{137}Cs activity was determined using 661.6 keV gamma emissions and counted for 24 hours (Li et al., 2007). Loss on ignition, a dry combustion method, was used to determine percent organic matter (%OM). Samples were oven dried at 105°C for 24 hours; then, samples were ignited at 400°C for 16 h in a muffle furnace (Thermolyne Largest Tabletop Muffle Furnace, Thermo Fisher Scientific, Waltham, MA, USA, at the Landscape Dynamics Laboratory, University of Manitoba, Winnipeg, Canada) (Nelson and Sommers, 1996). Reflectance spectrometry readings were collected following the procedures described by Barthod et al. (2015), using a spectroradiometer (ASD FieldSpec Pro, Analytical Spectral Device Inc., Boulder, CO, USA, at the Landscape Dynamics Laboratory, University of Manitoba, Winnipeg, Canada). The absolute particle size distribution of samples was obtained after oxidizing organic material with hydrogen peroxide (H_2O_2, 30 %), and using hexametaphosphate as a dispersant (Gray et al., 2010) by laser diffraction in water using a Mastersizer 3000 (Malvern Instruments, Malvern, England, at the Landscape Dynamics Laboratory, University of Manitoba, Winnipeg, Canada).

To evaluate the effects of rolling on grain yield, plant biomass and plant density, plants were counted and harvested by hand in five 1-m lengths of the seeding row with row-spacing ranging from 18 to 76 cm. Hand harvesting was conducted a week before the scheduled harvest time. Leaf abrasion, plant height, number of pods per plant and lowest pod height were monitored and measured on ten randomly selected plants. Leaf abrasion was monitored by sampling soybean leaves from rolled and non-rolled treatments. The collected leaves were photographed using a digital camera (Canon EOS 60D with EF-S18-135mm f3.5-5.36 lens, at the Landscape Dynamics Laboratory, University of Manitoba, Winnipeg, Canada) immediately after returning to the laboratory. The photos were analyzed to identify signs of leaf abrasion (e.g., necrosis of the leaf edge and deformity of leaf shape) for further qualitative analysis. Lowest pod height was assessed by measuring the distance between the bottom of the lowest observed pod and the ground at harvest. The distance from the ground to the lowest pod was chosen as this determines whether the pod can be caught by the combine header. In order to cover the whole length of the trials, all the measurements were repeated in five randomly selected spots within each treatment strip.

2.3.6. Statistical analysis

Analysis of variance was conducted to compare land rolling treatment differences in soybean growth characteristics, soil moisture, and movement of wind-eroded particles using the Proc Glimmix procedure (SAS version 9.4, SAS Institute, Cary, NC). The effect of land rolling was considered fixed, while the site-years were considered as a random effect in the ANOVA. Mean separation between treatments was determined using the Tukey-Kramer test with a probability level for significance of 0.05. Assumptions of ANOVA were tested using the Proc Univariate procedure of SAS to test for normality of the residuals and to see if residuals had homogenous variances. Analysis of soil moisture, soybean population and number of seed pods were conducted with the Proc Glimmix procedure with a Beta and Poisson distribution, respectively.

Colour coefficients of collected sediment were calculated and analyzed using R (version 4.0.1, R Core team, 2020) following the method described by Boudreault et al (2019) and colour analysis scripts (Koiter, 2021), and were compared using a student t-test. Weather data for the weather station (Winnipeg, Manitoba, ID: 5023222), were downloaded from Environment and Climate Change Canada's website using the Weathercan package in R (LaZerte et al., 2018). All figures were created using the ggplot2 package (V3.3.3; Wickham, 2016).

2.4. Results and discussion

2.4.1. Impact of land rolling on soil properties

The effect of land rolling on the volumetric soil moisture content at soil surface (0-1 cm) and subsurface layers (0~30 cm soil depth) was measured over the growing season in 2018 and 2019. Rolled and non-rolled treatments effects on volumetric soil moisture content were not statistically significant at the 0-15 cm depth layer in 2018 (Fig 4). The results indicated that the practice of rolling had greater impacts on soil properties in the surface layers (the top 10 cm). The ANOVA results showed that volumetric soil moisture content at the 0-10 cm depth layer was affected significantly by the rolling treatment in 2019 ($P < 0.05$) (Fig. 2.5). Volumetric soil moisture content of this layer of soil is higher in rolled trials compared to non-rolled trials. However, no statistically significant differences were observed in volumetric soil moisture content at the soil surface (0-1 cm), 10-20, and 20-30 cm soil depth in 2019. Unfortunately, soil moisture content at deeper layers of soil was not measured in 2018; therefore, soil moisture content was analyzed separately for each year.

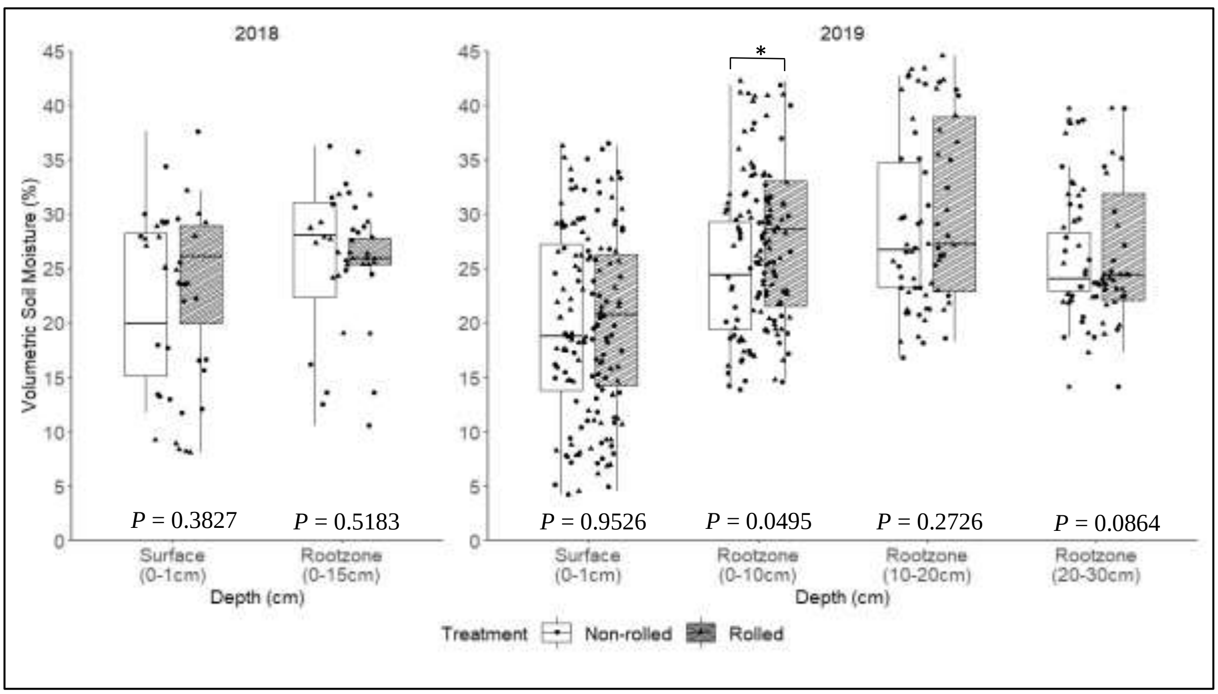

Fig. 2. 5. Impact of land rolling on soil moisture measured in September, 2018 and biweekly from May to September in 2019. * denotes a significant difference (P-value < 0.05) at the 0-10 cm soil depth. The circle and triangle symbols show observations for non-rolled and rolled treatments, respectively.

It seemed reasonable to expect that the significant difference in volumetric soil moisture content at the 0-10 cm soil depth was linked to higher capillary rise that transfers water more efficiently from deeper layers to the surficial layers. The increased capillary moisture movement is likely due to the consolidation of soil (i.e., smaller pore sizes) during land rolling. During the growing season, the volumetric soil moisture content remained almost constant at depths between 10 cm and 30 cm in both treatments and decreased substantially only in the top 10 cm in non-rolled treatment owing to better air exchange and larger surface area for evaporation (i.e., higher absorption of solar radiation), which led to more rapid drying. The whole profile, layers as deep as 30 cm, had lower moisture content in non-rolled treatment, although the drying phenomenon was more considerable in the top 10 cm. Although volumetric soil moisture content at the 0-10 cm soil depth increases with increasing compaction and capillary rise, due to land rolling, the gravimetric soil moisture content remained constant. This suggests that land rolling practice may not have changed the total amount of available water. The results of this study are supported by other studies (e.g., Tong et al., 2015; Gürsoy and Türk, 2019), who reported that soil compaction by land rolling or planking encourages capillary rise of water from subsoil to topsoil. Compaction has long been recognized to increase penetration resistance (Altikat and Celik, 2011; Wen et al., 2016; Gürsoy and Türk, 2019) and reduce infiltration capacity (Rueber and Holmes, 2012). Increased penetration resistance can reduce root growth, which may limit water and nutrient uptake (Halde et al., 2011). It has been also demonstrated that crushing the aggregates on the soil surface by land rolling can result in reduced water infiltration capacity (Al-Kaisi et al., 2011). In addition, soil roughness can affect the infiltration capacity through increasing surface detention capacity and surface sealing (Lal, 1997; Vermang et al., 2015; Zhao et al., 2018). This can be attributed to the fact that rough surfaces (e.g., non-rolled trials) have a larger effective surface area and lower sealing potential. Field surveys were performed to monitor the features of ponding in trials; however, runoff and ponding water were not observed over the course of this study.

RMSH is the most commonly used measure of surface roughness, especially for scattering elevation data such as laser scanning point clouds (Nield and Wiggs, 2011; Hugenholtz et al., 2013). The RMSH values of rolled and non-rolled treatments obtained with the terrestrial laser scanner are shown in Fig. 2.6. The results of the ANOVA test indicated that the practice of land rolling significantly decreased soil surface roughness ($P < 0.05$). The mean RMSH values decreased between the roughest (non-rolled) to the smoothest surface (rolled). Similar to research conducted by Thomsen et al. (2015), data gathered by field-scale terrestrial laser scanners has been demonstrated to be effective in evaluating surface characteristics arising from different soil management practices.

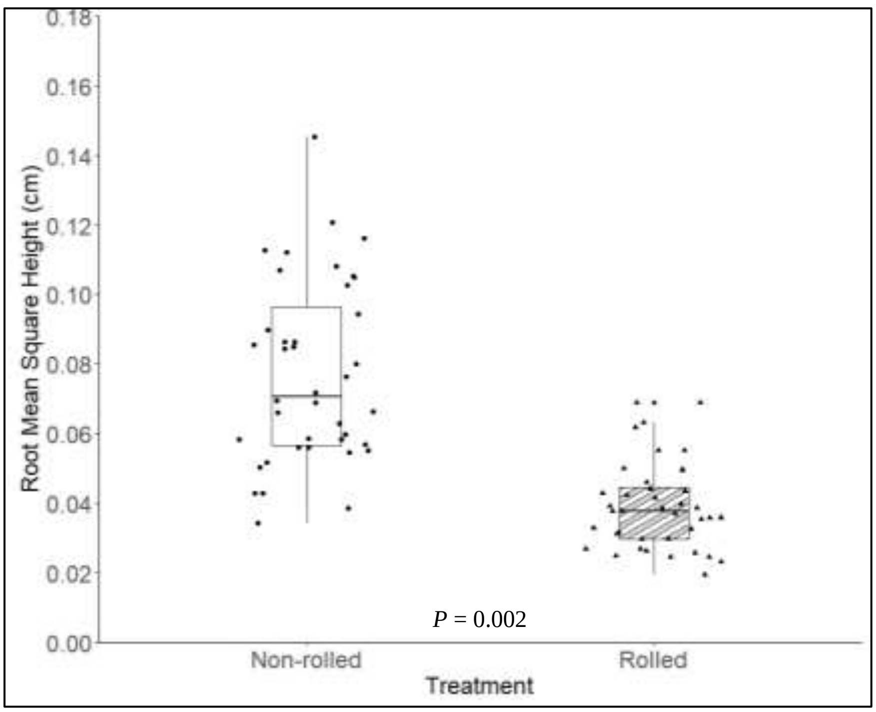

Fig. 2. 6. Impact of land rolling on soil surface roughness (2018-2019). There is a significant difference (*P*-value < 0.05) between the RMSH values on non-rolled and rolled trials.

2.4.2. Impact of land rolling on wind-transported sediment

At the plot scale, transient soil properties (i.e., surface roughness, soil moisture content, aggregate size, crusting) can influence wind-driven soil particle entrainment, transportation, and deposition.

Therefore, evaluation of physicochemical characteristics of wind-transported sediment (e.g., mass, particle size distribution, ^{137}Cs activity, organic matter, and spectral reflectance) can help to determine soil susceptibility to erosion by wind in landscapes affected by the practice of land rolling. The amount of sediment collected by samplers placed in rolled and non-rolled trials over the course of this study ranged between < 1.0 and 9.0 g (Fig. 2.7a and b). The amount of soil movement by wind was lower in non-rolled trials than rolled trials, but the numerical difference is not statistically significant ($P = 0.34$). The influence of soil surface heterogeneity on wind-transported sediment is mainly reflected by the effect of surface roughness elements. It was anticipated that there would be a significant difference in soil movement by wind between rolled and non-rolled trials, as it was reported that the rougher a surface is, the higher the amount of wind-transported sediment is trapped by roughness (Zhang et al., 2004). The findings revealed that rolling the land did not increase soil movement by wind at all, although it can reduce soil surface roughness significantly. The roughness resulting from the tillage may have provided little protection against wind erosion. Moreover, the wind-transported sediment characteristics were not significantly affected by the practice of land rolling. The results of this study are not consistent with the findings of previous studies (e.g., Chepil and Milne, 1941; Armbrust et al., 1964; Labiadh et al., 2013), who found that oriented roughness can reduce wind erosion rates above a relatively flat soil without ridges (e.g., friction velocity).

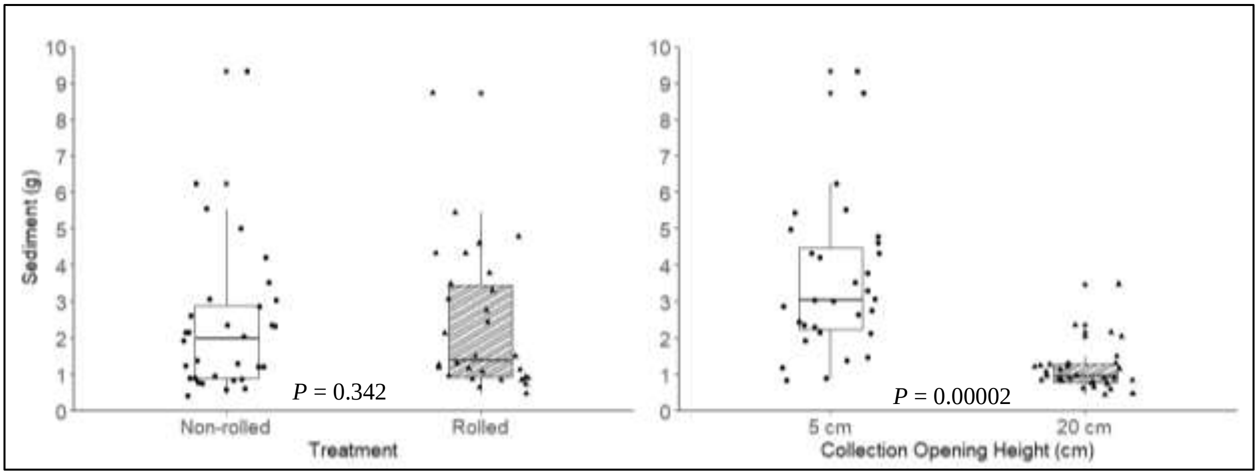

(a) (b)

Fig. 2. 7. (a) Impact of land rolling on soil movement by wind, and (b) wind-transported sediment collected by samplers with different collection opening heights. * denotes a significant difference (*P*-value < 0.05) between collected wind-transported sediment by samplers with different collection opening heights (5-cm and 20-cm).

The ultimate particle size distribution of the wind-transported sediment over the growing season is shown in Fig. 2.8. Wind-transported sediment, at both heights, was largely composed of silt-sized particles (0.002-0.063 mm), as it has been documented that these particles are more erodible and have the lowest threshold velocity in comparison with other size fractions (Basaran et al., 2011; Yan et al., 2018). The median particle size diameter (D_{50}) of wind-transported sediment collected at non-rolled and rolled trials are 22 and 16 µm, respectively. However, we would have expected a difference due to the destruction of coarse aggregates and their transformation into fine aggregates by land rolling. In addition, the results demonstrated that the preferential movement of clay particles by wind is higher on the rolled treatment, but the numerical difference is not statistically significant. It was expected that there would be a significant difference due to the adverse effects of the practice of land rolling in trapping clay particles, in soils with high clay content, by smoothing soil surface roughness.

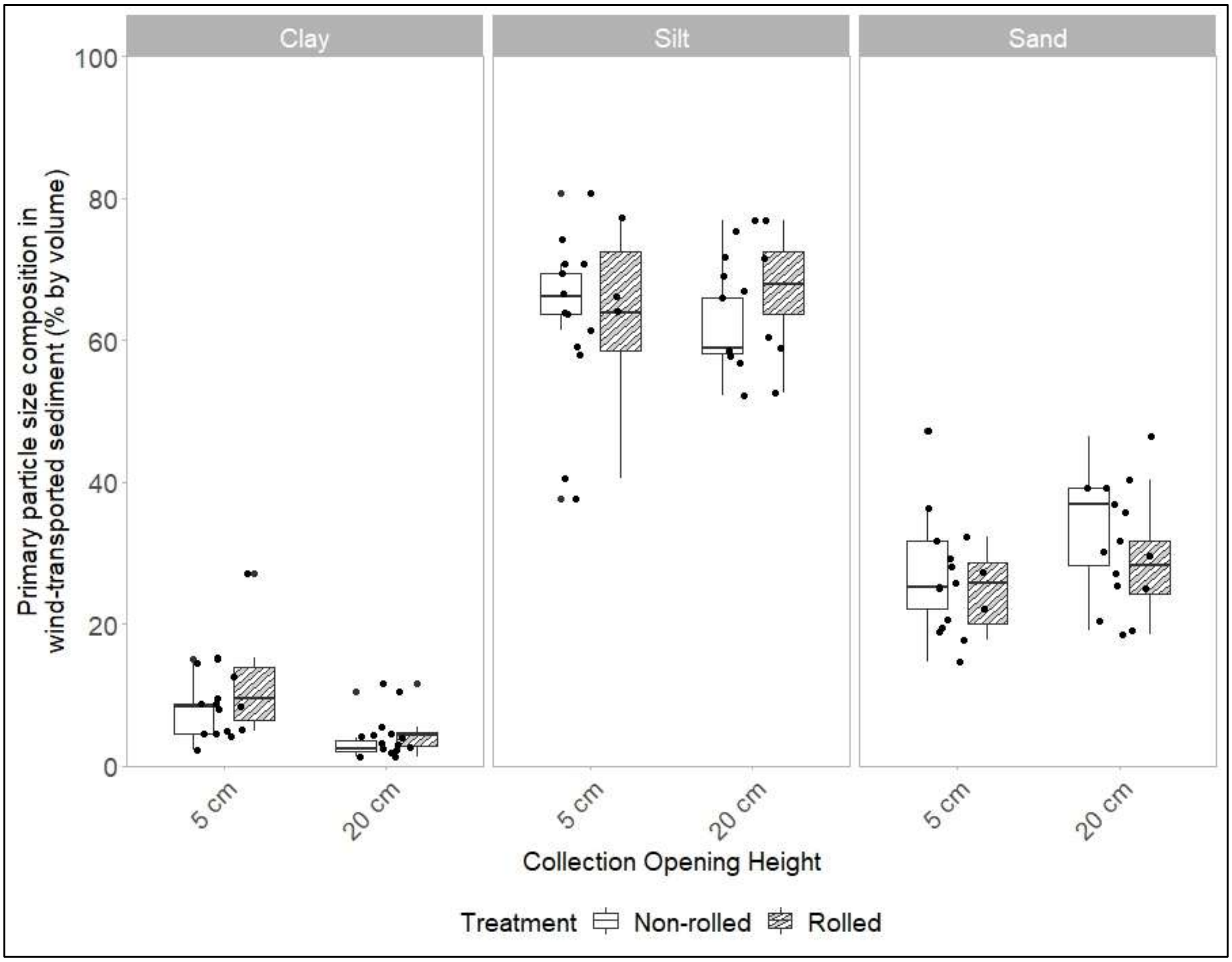

Fig. 2. 8. Particle size composition of wind-transported sediment trapped at heights of 5-cm and 20-cm in rolled and non-rolled treatments. Particle size composition is represented by the clay (≤ 0.002 mm), silt (0.002-0.063 mm) and sand (0.063-2 mm) content of collected wind-transported sediment.

Sediment characteristics can also provide better understanding of wind-induced sediment transport dynamics in agricultural landscapes affected by different soil management practices (e.g., land rolling). The samplers collected a sufficient amount of wind-transported sediment (up to 9.0 g) at each of the two heights (5 cm and 20 cm) during growing seasons to perform chemical analyses (discussed below). This suggests that the performance of samplers in trapping wind-eroded sediment under natural condition was adequate.

The experimental evidence on the amount of wind-transported sediment collected by samplers with collection openings at two different heights is illustrated in Fig. 2.7b. Sediment samplers with a collection opening at 5-cm height above the ground collected significantly ($P < 0.001$) more sediment than samplers with a collection opening at 20-cm height above the ground. This finding suggests that saltation/creep can be considered the dominant modes of transport. The results of this study are supported by other studies (e.g., Chepil, 1945; Lyles, 1988), who reported that the bulk of total transport is by saltation (50-80 %).

Further analysis showed that there is a significant difference between the ^{137}Cs activity and organic matter content of sediment collected at 20-cm height and those of the sediment collected at 5-cm height. The sediment collected by samplers at each of the two heights above the soil surface demonstrates a decrease of ^{137}Cs activity with height (Fig. 2.9a), while the organic matter content of wind-transported sediment increased with height (Fig. 2.9b). The organic matter content of wind-transported sediment from our study sites varied from 9.5 to 27.5% for sediment trapped at the 5-cm height, and from 18.1 to 39.1% in suspended sediment at 20-cm height. The organic matter collected at the higher opening was identified as being plant residue. This is likely related to low density of the organic particles as the smaller and/or less dense particles are transported higher from the soil surface. These findings indicate that the composition of sediments collected at each of the two heights (5 cm and 20 cm) was affected by sorting effects during erosive wind events. This agrees with the preferential transport of low-density organic particles at high height and of minerogenic particles at lower heights. Similarly, Webb et al. (2013) reported that size-selective sorting of soil organic carbon during transport may lead to further enrichment of organic carbon of dust emissions. Iturri et al. (2021) demonstrated that organic and mineral elements are differently distributed in height by the wind. They reported that organic carbon was transported at greater height as they are elements of low-density organic substances like plant debris. In addition, lower ^{137}Cs activity of collected sediment at 20-cm height was contrary to the expectations and suggests that this can be attributed to the dilution action by plant debris, which has no ^{137}Cs activity. This outcome is also contrary to that of Van Pelt et al. (2007) who found an increase of ^{137}Cs activity in collected wind-transported sediment with height from 0.05 to 1.0 m above the eroding soil surface.

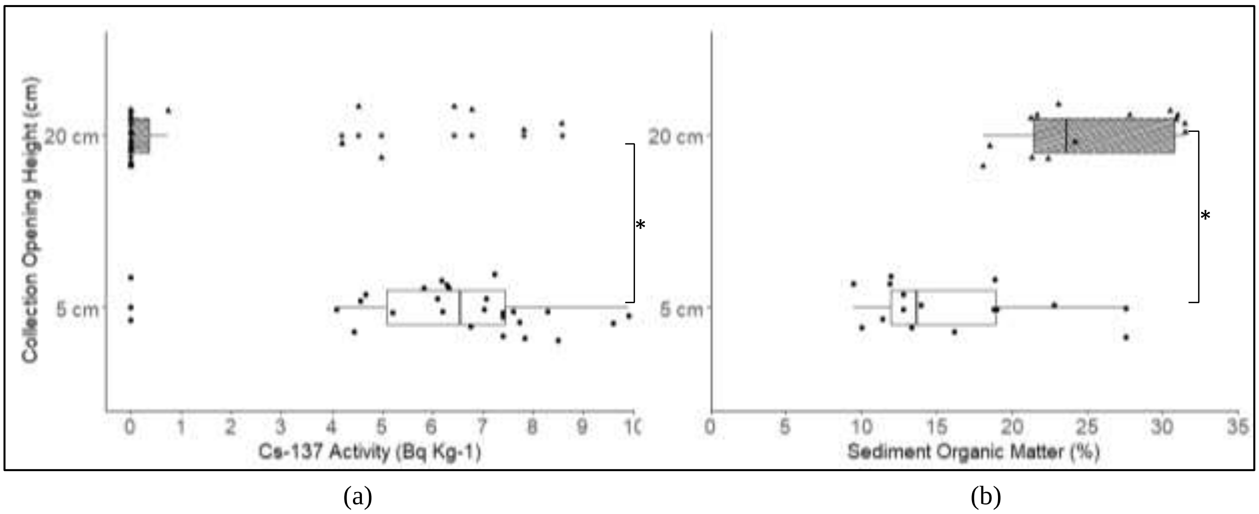

Fig. 2. 9. (a) ^{137}Cs activities (Bq kg^{-1}) and (b) organic matter (%) of wind-transported sediment captured in sediment samplers with collection opening at two heights above the soil surface. * denotes a significant difference (*P*-value < 0.05) between the ^{137}Cs activity and organic matter values of wind-transported sediment captured by samplers.

Spectral signatures of materials can be distinguished by their reflectance, or absorbance, as a function of wavelength (Brown et al., 2006). The reflectance of the collected sediment at 5-cm and 20-cm heights were quite similar in the 350- to 450-nm wavelength range; however, the sediment collected at 20-cm height was enriched with plant residue having slightly higher reflectance than sediment collected at 5-cm height (Fig. 2.10). This means that collected sediment at 20-cm height is brighter or lighter in appearance and confirms the composition of collected sediment. This finding is consistent with that of Gausman et al. (1975), who reported that crop residue littered on the soil had higher reflectance than bare soil. The statistical analyses showed that colour coefficients of collected sediment were significantly different between the two samplers' heights, except for the Z, a and B. The distinct reflectance bands at 660 nm can be attributed to soil organic matter, which can be seen in Fig. 2.10.

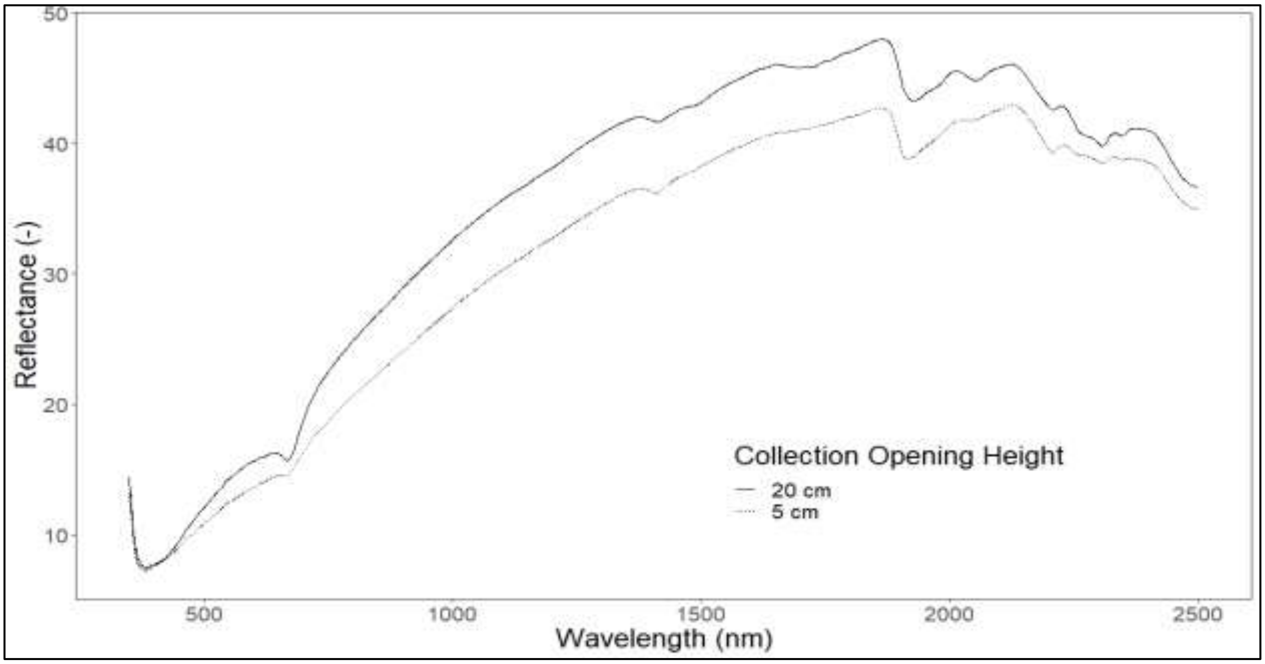

Fig. 2. 10. The mean spectral reflectance for wind-transported sediment collected by samplers with different collection opening heights (5-cm and 20-cm).

Agricultural lands are most susceptible to wind erosion in the spring when the soil has been disturbed (e.g., breakdown of soil structure) by field operations (including seeding) and surface cover is minimal. Ditches adjacent to farms and field edges can be considered a hotspot for the local deposition of wind-eroded sediment. The bottoms of the ditches are about one meter below the surrounding landscape. Thereby, the settling grains can be deposited and resuspended in the lower part of these topographic obstacles where wind velocity and turbulence are reduced is minimal. Surveys were conducted to monitor the features of wind erosion (e.g., deposition of sediment in nearby vegetation cover, abraded plants and buried plants). Field surveys following soybean harvest and land rolling, after wind events, and at the time of seeding the subsequent crop in the following spring revealed very little evidence of sediment blowing off the fields. There were no measurable amounts of sediment found in any of the roadside ditches at any site during the year of the soybean crop, specifically in the spring following soybeans.

2.4.3. Impact of land rolling on soybean yield and growth characteristics

Grain yield and soybean growth characteristics such as plant density, plant biomass, number of seed pods differed significantly between the treatments. However, other growth characteristics such as plant height, lowest pod height and 1,000-kernel weight indicated no significant differences between the treatments (Table 2.2).

Table 2. 2. Effect of management practices on soybean yield and growth characteristics

	Yield	Plant height	Plant population	1,000-kernel weight	Plant biomass	Number of seed pods	Lowest seed pod
Treatment	t ha^{-1}	cm	Plants m^{-1}	g/1000	t ha^{-1}	Per 10 plants	
Management							
Rolled	2.2±0.3b	64±6.11	34±0.1b	100.3±6.5	8±1.5b	26±2.84b	4.7±0.4
Non-Rolled	2.5±0.3a	64±6.11	38±0.1a	100.9±6.5	9±1.5a	34±2.84a	5.0±0.4
ANOVA				***P* value**			
Management	0.0012	0.1159	0.0048	0.7253	0.0019	0.0001	0.2583

Average grain yields for rolled and non-rolled treatments were around 2.2 and 2.5 t ha^{-1}, respectively. Although the rolled treatment had higher volumetric soil moisture content, the grain yield in rolled treatment was lower than non-rolled treatment. Non-rolled treatments had higher plant population, above ground biomass and number of seed pods than rolled treatments. Although land rolling has been shown to increase crop yields in studies in other regions of North America (e.g., Al-Kaisi et al., 2011; DeJong-Hughes et al., 2012; Bohner, 2018), a decrease in yield with land rolling was observed in our study in the northern Red River Valley. Endres and Henson, (2004) evaluated land rolling timing on soybean growth in Carrington, North Dakota, which is in the southern Red River Valley, and indicated that land rolling did not influence soybean yield and plant population. Bohner (2018) carried out a study to assess the influence of land rolling on soybean in Ontario, Canada, and reported that a small soybean yield increase was observed when soybeans were rolled at the first trifoliate stage with weak statistical confidence. A recent study was conducted by Boyers et al. (2020) to study impact of land rolling on soybean in Mason, Michigan. These researchers identified that despite decreasing reproductive nodes and pods on main stems, land rolling did not influence soybean grain yield. Walther (2017) reported that number of seeds per pod and seed weight were important yield components that significantly influence the overall yield response in their study. In a study in Turkey, Gürsoy and Türk, (2019) reported that the chickpea grain yield was influenced by the ground pressures of the land roller, but the effect of the rolling time was not significant.

Plant height and lowest pod height is of great interest to farmers, as low pods result in harvest losses. Plant heights were higher in the non-rolled treatment and the rolled treatment had slightly lower pods compared to non-rolled treatment, 0.3 cm lower. The pod height difference was less than 1 cm and is therefore not of agronomic importance. The abrasion of crops by wind-transported sediment can impose economic impacts; however, we did not observe any evidence of plant abrasion by soil particles during the study.

A power analysis on grain yield and growth characteristics data revealed that the study required a minimum sample of 26 site-years of data to achieve sufficient power with a 95% confidence interval. Therefore, a longer-term study, with same experimental units over a longer period of time, would be necessary to fully assess the potential agronomic and environmental impacts of land rolling. The effects of land rolling on crop performance and soil erosion should be separately investigated during wet and dry years to assess climatic interactions. In addition, the costs associated with the practice of land rolling in soybean production are dealt with in another complementary study (Prairie Agricultural Machinery Institute, Winnipeg, Manitoba, Canada, 2018). These researchers reported that rolling the land did not minimize header loss (grain lost during the harvesting operation), which ranged from 0.09 to 0.26 t ha^{-1} across treatments (rolled and non-rolled) and site-years. It has also been documented that the average cost of rolling the land ranged between \$11 and more than \$12 ha^{-1} when an appropriately- and over-sized tractors were employed, respectively (Manitoba Pulse & Soybean Growers Association, 2020).

2.5. Conclusions

Land rolling is a practice that has value in soybean production, as well as in the production of other crops, where stones, corn root-balls and large clods on the soil surface can cause serious equipment damage and delays in field operations. Even on the clay-rich soils of the Red River Valley, most fields have some stones that are large enough to warrant land rolling. The protection gained by this management practice may justify the expense of the land rolling equipment and operation. However, costs associated with the practice of land rolling were not examined in this study as these costs were the focus of a complementary study by another research group. Although land rolling has been shown to increase crop yields in studies in other regions, we were unable to observe any positive effect in our study in the Red River Valley; in fact, we observed a small decrease in yield with land rolling. Results of a statistical power analysis suggested that the number of observations needs to be larger to provide definitive conclusions on the impacts of land rolling on crop production and related economics. Further, rolling after planting led to a change in bulk density and soil drying rate and subsequently the volumetric soil moisture content differed between rolled and non-rolled treatments.

Land rolling smoothes the soil surface and increases wind erosion risk, and this increased vulnerability occurs at or shortly after seeding, after the period of greatest wind erosion risk in the spring when the soil is bare and disturbed. However, this study demonstrated that any increased risk of wind erosion caused by land rolling is unlikely to translate into a measurable increase in soil loss or decrease in crop yield. In general, observed soil loss and sedimentation caused by wind erosion are very small in the Red River Valley and Manitoba. Although the abrasion of crops by wind-transported sediment could have significant agronomic and economic impacts, we did not observe this in our study. Our assessment of off-site sedimentation was observed to be very small, and the costs associated with off-site sedimentation are presumed to be very small as well. It is also worth mentioning that the variation in mass of collected sediment at two heights above the ground was observed, which demonstrates the acceptable efficiency of the wind-transported sediment samplers.

2.6. References

Al-Kaisi, M., Holmes, J., Hanna, M., DeJong-Hughes, J., 2011. Land roller use: challenges and benefits. University of Minnesota Extension. URL http://www.extension.iastate.edu/CropNews/2011/0103alkaisi.html. (accessed 2.17.2021)

Altikat, S., Celik, A., 2011. The effects of tillage and intra-row compaction on seedbed properties and red lentil emergence under dry land conditions. Soil Tillage Res. 114, 1-8. https://doi.org/10.1016/j.still.2011.03.003

Armbrust, D.V., Chepil, W.S., Siddoway, F.H., 1964. Effects of ridges on erosion of soil by wind. Soil Sci. Soc. Am. J. 28, 557-560. https://doi.org/10.2136/sssaj1964.03615995002800040031x

Bai, Z.G., Dent, D.L., Olsson, L., Schaepman, M.E., 2008. Proxy global assessment of land degradation. Soil Use Manag. 24, 223-234. https://doi.org/10.1111/j.1475-2743.2008.00169.x

Barker, D.J., Macadam, J.W., Butler, T.J., Sulc, R.M., 2012. Forage and biomass planting.

Conserv. Outcomes from Pasturel. Hayl. Pract. 41-110.

Barthod, L.R.M., Liu, K., Lobb, D.A., Owens, P.N., Martínez-Carreras, N., Koiter, A.J., Petticrew, E.L., McCullough, G.K., Liu, C., Gaspar, L., 2015. Selecting color-based tracers and classifying sediment sources in the assessment of sediment dynamics using sediment source fingerprinting. J. Environ. Qual. 44, 1605-1616. https://doi.org/10.2134/jeq2015.01.0043

Basaran, M., Erpul, G., Uzun, O., Gabriels, D., 2011. Comparative efficiency testing for a newly designed cyclone type sediment trap for wind erosion measurements. Geomorphology. 130, 343-351. https://doi.org/10.1016/j.geomorph.2011.04.016

Bennell, M.R., Leys, J.F., Cleugh, H.A., 2007. Sandblasting damage of narrow-leaf lupin (Lupinus angustifolius L.): A field wind tunnel simulation. Aust. J. Soil Res. 45, 119-128. https://doi.org/10.1071/SR06066

Bluemle, M.E., 1988. Guide to the geology of Northeastern North Dakota: Cavalier, Grand Forks, Nelson, Pembina, and Walsh Counties, Educational series. North Dakota Geological Survey.

Bohner, H., 2018. What is the best time to roll soybeans?. Ministry of Agriculture, Food and Rural Affairs. Ontario, Canada. URL http://www.omafra.gov.on.ca/english/crops/field/news/croptalk/2018/ct-0318a1.htm (accessed 9.1.2021)

Bossenmaier, E.F., Vogel, C.G., 1974. Wildlife and wildlife habitat in the winnipeg region. Resources Planning, Manitoba Department of Mines, Resources and Environmental Management.

Blake, G.R., Hartge, K.H., 1986. Bulk Density, in: A. Klute (Ed.), Methods of Soil Analysis. John Wiley & Sons, Ltd, pp. 363–375. https://doi.org/https://doi.org/10.2136/sssabookser5.1.2ed.c13

Boudreault, M., Koiter, A.J., Lobab, D.A., Liu, K., Benoy, G., Owens, P.N., Li, S., 2019. Comparison of sampling designs for sediment source fingerprinting in an agricultural watershed in Atlantic Canada. J. Soils Sediments 19, 3302-3318. https://doi.org/10.1007/s11368-019-02306-6

Boyers, N.H., Lenssen, A.W., Moore, K.J., 2020. Post-emergence land rolling influences soybean plant architecture but not yield. Crop. Forage Turfgrass Manag. 6, e20025. https://doi.org/10.1002/cft2.20025

Brown, D.J., Shepherd, K.D., Walsh, M.G., Dewayne Mays, M., Reinsch, T.G., 2006. Global soil characterization with VNIR diffuse reflectance spectroscopy. Geoderma 132, 273-290. https://doi.org/10.1016/j.geoderma.2005.04.025

Bryant, R., Moran, M.S., Thoma, D.P., Holifield Collins, C.D., Skirvin, S., Rahman, M., Slocum, K., Starks, P., Bosch, D., González Dugo, M.P., 2007. Measuring surface roughness height to parameterize radar backscatter models for retrieval of surface soil moisture. IEEE Geosci. Remote Sens. Lett. 4, 137-141. https://doi.org/10.1109/LGRS.2006.887146

Chabot, M., Lindsay, J., Rowlandson, T., Berg, A.A., 2018. Comparing the use of terrestrial LiDAR scanners and pin profilers for deriving agricultural roughness statistics. Can. J. Remote Sens. 44, 153-168. https://doi.org/10.1080/07038992.2018.1461559

Chepil, W.S., 1945. Dynamics of wind erosion: I. Nature of movement of soil by wind. Soil Sci. 60. 305-320.

Chepil, W.S., Milne, R.A., 1941. Wind erosion of soil in relation to roughness of surface. Soil Sci. 52. 417-434.

Cihacek, L.J., Sweeney, M.D., Deibert, E.J., 1993. Characterization of wind erosion sediments in the Red River Valley of North Dakota. J. Environ. Qual. 22, 305-310.

Clay, S.A., DeSutter, T.M., Clay, D.E., 2001. Herbicide concentration and dissipation from surface wind-erodible soil. Weed Sci. 49, 431-436. https://doi.org/10.1614/0043-1745(2001)049[0431:hcadfs]2.0.co;2

Couture, S.J., DiTommaso, A., Asbil, W.L., Watson, A.K., 2004. Influence of seeding depth and seedbed preparation on establishment, growth and yield of fibre flax (Linum usitatissimum L.) in Eastern Canada. J. Agron. Crop Sci. 190, 184-190. https://doi.org/10.1111/j.1439-037X.2004.00091.x

DeJong-Hughes, J., Holen, D., Glogoza P., 2012. Management considerations for rolling soybean in the upper Midwest. University of Minnesota Extension. URL http://pierce.uwex.edu/files/2012/07/Ground-Rolling-in-the-MidWest.pdf. (accessed 1.5.2021)

Dong, Z., Qian, G., 2007. Characterizing the height profile of the flux of wind-eroded sediment. Environ. Geol. 51, 835–845. https://doi.org/10.1007/s00254-006-0363-5

Dong, Z., Sun, H., Zhao, A., 2004. WITSEG sampler: A segmented sand sampler for wind tunnel test. Geomorphology. 59, 119-129. https://doi.org/10.1016/j.geomorph.2003.09.010

Dürr, C., Aubertot, J.N., 2000. Emergence of seedlings of sugar beet (Beta vulgaris L.) as affected by the size, roughness and position of aggregates in the seedbed. Plant Soil. 219, 211-220. https://doi.org/10.1023/a:1004723901989

Endres, G., Henson, B., 2010. Impact of field rolling on soybean performance. North Dakota State University agriculture. URL https://www.ag.ndsu.edu/carringtonrec/documents/agronomyrd/docs2004/04%20Soybean%20Rolling.pdf. (accessed 7.6.2021)

Environment and Climate Change Canada (ECCC)., 2019. 1981-2010 climate normals and averages. Canadian climate normals. URL https://climate.weather.gc.ca/climate_normals/index_e.html. (accessed 3.10.2021)

Faé, G.S., Kemanian, A.R., Roth, G.W., White, C., Watson, J.E., 2020. Soybean yield in relation to environmental and soil properties. Eur. J. Agron. 118, 126070. https://doi.org/10.1016/j.eja.2020.126070

Fryrear, D.W., 1986. A field dust sampler. J. Soil Water Conserv. 41, 117-120.

Fryrear, D.W., 1984. Soil ridges-clods and wind erosion. Trans. ASAE. 27, 445-448. https://doi.org/https://doi.org/10.13031/2013.32808

Gausman, H.W., Gerbermann, A.H., Wiegand, C.L., Leamer, R.W., Rodriguez, R.R., Noriega, J.R., 1975. Reflectance differences between crop residues and bare soils. Soil Sci. Soc. Am. J. 39, 752-755. https://doi.org/https://doi.org/10.2136/sssaj1975.03615995003900040043x

Goossens, D., Offer, Z.Y., 2000. Wind tunnel and field calibration of six aeolian dust samplers. Atmos. Environ. 34, 1043-1057. https://doi.org/10.1016/S1352-2310(99)00376-3

Gray, A.B., Pasternack, G.B., Watson, E.B., 2010. Hydrogen peroxide treatment effects on the particle size distribution of alluvial and marsh sediments. Holocene. 20, 293-301. https://doi.org/10.1177/0959683609350390

Guo, Z., Chang, C., Wang, R., Li, J., 2017. Comparison of different methods to determine wind-erodible fraction of soil with rock fragments under different tillage/management. Soil Tillage Res. 168, 42-49. https://doi.org/10.1016/j.still.2016.12.008

Gürsoy, S., Türk, Z., 2019. Effects of land rolling on soil properties and plant growth in chickpea production. Soil Tillage Res. 195, 104425. https://doi.org/10.1016/j.still.2019.104425

Kuntze, H. Beinhauer, R.T. Tetzlaff, G., 1989. Quantifizierung derBodenerosion durch Wind. Mitt. Dt. Bodenkundl. Ges. 59/II, 1089-1094.

Koiter, A., 2021. Colour analysis scripts. https://doi.org/10.5281/zenodo.5123327

Håkansson, I., Myrbeck, Å., Etana, A., 2002. A review of research on seedbed preparation for small grains in Sweden. Soil Tillage Res. 64, 23-40. https://doi.org/10.1016/S0167-1987(01)00255-0

Halde, C., Hammermeister, A.M., McLean, N.L., Webb, K.T., Martin, R.C., 2011. Soil compaction under varying rest periods and levels of mechanical disturbance in a rotational grazing system. Can. J. Soil Sci. 91, 957-964. https://doi.org/10.4141/CJSS2011-026

Hevia, G.G., Buschiazzo, D.E., Hepper, E.N., Urioste, A.M., Antón, E.L., 2003. Organic matter in size fractions of soils of the semiarid Argentina. Effects of climate, soil texture and management. Geoderma 116, 265-277. https://doi.org/10.1016/S0016-7061(03)00104-6

Hevia, G.G., Mendez, M., Buschiazzo, D.E., 2007. Tillage affects soil aggregation parameters linked with wind erosion. Geoderma. 140, 90-96. https://doi.org/10.1016/j.geoderma.2007.03.001

Hou, T., Filley, T.R., Tong, Y., Abban, B., Singh, S., Papanicolaou, A.T., Wacha, K.M., Wilson, C.G. and Chaubey, I., 2021. Tillage-induced surface soil roughness controls the chemistry and physics of eroded particles at early erosion stage. Soil Tillage Res. 207, 104807. https://doi.org/10.1016/j.still.2020.104807

Huffman, E., Eilers, R.G., Padbury, G., Wall, G., MacDonald, K.B., 2000. Canadian agri-environmental indicators related to land quality: Integrating census and biophysical data to estimate soil cover, wind erosion and soil salinity. Agric. Ecosyst. Environ. 81, 113-123. https://doi.org/10.1016/S0167-8809(00)00185-7

Hugenholtz, C.H., Brown, O.W., Barchyn, T.E., 2013. Estimating aerodynamic roughness (z_0) from terrestrial laser scanning point cloud data over un-vegetated surfaces. Aeolian Res. 10, 161-169. https://doi.org/10.1016/j.aeolia.2013.03.004

Iturri, L.A., Funk, R., Sommer, M., Buschiazzo, D.E., 2021. Elemental composition of wind-blown sediments from contrasting textured soils. Aeolian Res. 48, 100656. https://doi.org/10.1016/j.aeolia.2020.100656

Kheirabadi, H., Mahmoodabadi, M., Jalali, V., Naghavi, H., 2018. Sediment flux, wind erosion and net erosion influenced by soil bed length, wind velocity and aggregate size distribution. Geoderma. 323, 22-30. https://doi.org/10.1016/j.geoderma.2018.02.042

Labiadh, M., Bergametti, G., Kardous, M., Perrier, S., Grand, N., Attoui, B., Sekrafi, S., Marticorena, B., 2013. Soil erosion by wind over tilled surfaces in South Tunisia. Geoderma. 202, 8-17. https://doi.org/10.1016/j.geoderma.2013.03.007

Lal, R., 1997. Soil degradative effects of slope length and tillage methods on alfisols in Western Nigeria. III. Soil physical properties. L. Degrad. Dev. 8, 325–342. https://doi.org/10.1002/(SICI)1099-145X(199712)8:4<325::AID-LDR265>3.0.CO;2-N

Lal, R., 1998. Soil erosion impact on agronomic productivity and environment quality. CRC. Crit. Rev. Plant Sci. 17, 319-464. https://doi.org/10.1080/07352689891304249

Lal, R., 2009. Soil degradation as a reason for inadequate human nutrition. Food Secur. 1, 45-57. https://doi.org/10.1007/s12571-009-0009-z

Larney, F.J., Bullock, M.S., 1994. Influence of soil wetness at time of tillage and tillage implement on soil properties affecting wind erosion. Soil Tillage Res. 29, 83-95. https://doi.org/10.1016/0167-1987(94)90104-X

LaZerte, S.E., Albers, S., Brown, N., 2018. weathercan: Download and format weather data from Environment and Climate Change Canada. J. Open Source Softw., 3(22), 571. https://doi.org/10.21105/joss.00571.

Li, S., Lobb, D.A., Lindstrom, M.J., 2007. Tillage translocation and tillage erosion in cereal-based production in Manitoba, Canada. Soil Tillage Res. 94, 164-182. https://doi.org/10.1016/j.still.2006.07.019

Lobb, D.A., Badreldin, N., Loro, M., Li, S., McConkey, B.G., Soil degradation: The cost to agriculture and the economy. Summit on Canadian Soil Health. Soil Conservation Council of Canada. Guelph, Ontario. August 2017.

Lyles, L., 1988. Basic wind erosion processes. Agric. Ecosyst. Environ. 22, 91-101. https://doi.org/10.1016/0167-8809(88)90010-2

Manitoba Pulse & Soybean Growers Association, 2020. Soybean rolling. URL https://www.manitobapulse.ca/2019/04/should-i-roll-my-soybeans. (accessed 12.23.2021)

McKenna Neuman, C., Maxwell, C., 1999. A wind tunnel study of the resilience of three fungal crusts to particle abrasion during aeolian sediment transport. Catena 38, 151–173. https://doi.org/10.1016/S0341-8162(99)00043

Michels, K., Armbrust, D.V., Allison, B.E., Sivakumar, M.V., 1995. Wind and windblown sand damage to pearl millet. Agron. J. 87, 620-626. https://doi.org/10.2134/agronj1995.00021962008700040003x

Nelson, D.W., Sommers, L.E., 1996. Total carbon, organic carbon, and organic matter, in: Sparks, D.L., Page, A.L., Helmke, P.A., Loeppert, R.H., Soltanpour, P.N., Tabatabai, M.A., Johnston, C.T., Sumner, M.E. (Eds.), Methods of Soil Analysis Part 3. Chemical Methods. Soil Science Society of America Book Series Number 5, pp. 961-1010. Madison, WI.

Nickling, W.G., McKenna Neuman, C., 1997. Wind tunnel evaluation of a wedge-shaped aeolian sediment trap. Geomorphology. 18, 333-345. https://doi.org/10.1016/s0169-555x(96)00040-2

Nield, J.M., Wiggs, G.F.S., 2011. The application of terrestrial laser scanning to aeolian saltation cloud measurement and its response to changing surface moisture. Earth Surf. Process. Landforms. 36, 273-278. https://doi.org/10.1002/esp.2102

Parry, M.L., Carter, T.R., Konijn, N.T., 1988. The effects on potential for wind erosion of soil, in: The Impact of Climatic Variations on Agriculture. Springer Netherlands, 281-292. https://doi.org/10.1007/978-94-009-2943-2_9

Pi, H., Huggins, D.R., Sharratt, B., 2021. Wind erosion of soil influenced by clay amendment in the inland Pacific Northwest, USA. L. Degrad. Dev. 32, 241-255. https://doi.org/10.1002/ldr.3709

R core Team., 2020. R: A language and environment for statistical computing. R foundation for Statistical Computing, Vienna, Austria. https://www.R-project.org/.

Rennie, D.A., 1985. Soil degradation, a western perspective. Can. J. Agric. Econ. 33, 19-29. https://doi.org/10.1111/j.1744-7976.1985.tb03229.x

Riksen, M.J.P.M., De Graaff, J., 2001. On-site and off-site effects of wind erosion on European light soils. L. Degrad. Dev. 12, 1-11. https://doi.org/10.1002/ldr.423

Romaneckas, K., Pilipavičius, V., Šarauskis, E., 2010. Impact of seedbed density on sugar beet (Beta vulgaris L.) seed germination, yield and quality of roots. J. Food, Agric. Environ. 8, 599-601.

Rueber, D., Holmes, J., 2012. Water infiltration following land rolling of soybeans. Iowa State University 2011 Northern Research and Demonstration Farm Progress Report. URL https://lib.dr.iastate.edu/farms_reports/96. (accessed 4.10.2021)

Samson, F., Knopf, F., 1994. Prairie conservation in North America. Bioscience. 44, 418-421. https://doi.org/10.2307/1312365

Shao, Y., 2008. Wind-erosion climatology, in: Physics and Modelling of Wind Erosion. Springer Netherlands, Dordrecht, 13-48. https://doi.org/10.1007/978-1-4020-8895-7_2

Sharratt, B., 2011. Size distribution of windblown sediment emitted from agricultural fields in the columbia plateau. Soil Sci. Soc. Am. J. 75, 1054-1060. https://doi.org/10.2136/sssaj2010.0337

Soy Canada, 2019. Canadian Soybean Industry. URL https://soycanada.ca/statistics/seeded-area-hectares/ (accessed 6.29.2021)

Statistics Canada., 2016. Table 32-10-0153-01. Total area of farms and use of farm land, historical data. URL https://doi.org/10.25318/3210015301-eng. (accessed 6.29.2021)

Statistics Canada., 2020. Table 32-10-0359-01. Estimated areas, yield, production, average farm price and total farm value of principal field crops, in metric and imperial units. URL https://doi.org/10.25318/3210035901-eng. (accessed 6.29.2021)

Stoner, J.D., Lorenz, D.L., Wiche, G.J., Goldstein, R.M., 1993. Red River of the North Basin, Minnesota, North Dakota, and South Dakota. J. Am. Water Resour. Assoc. 29, 575–615. https://doi.org/10.1111/j.1752-1688.1993.tb03229.x

Thangavel, P., Sridevi, G., 2017. Soil security: a key role for sustainable food productivity, in: Dhanarajan, A. (Ed.), Sustainable Agriculture towards Food Security, Springer Singapore, Singapore, pp. 309-325. https://doi.org/10.1007/978-981-10-6647-4_16

Thomsen, L.M., Baartman, J.E.M., Barneveld, R.J., Starkloff, T., Stolte, J., 2015. Soil surface roughness: Comparing old and new measuring methods and application in a soil erosion model. Soil 1, 399-410. https://doi.org/10.5194/soil-1-399-2015

Todhunter, P.E., Cihacek, L.J., 1999. Historical reduction of airborne dust in the Red River Valley of the North. J. Soil Water Conserv. 54, 543–551.

Tong, J., Zhang, Q., Guo, L., Chang, Y., Guo, Y., Zhu, F., Chen, D., Liu, X., 2015. Compaction performance of biomimetic press roller to soil. J. Bionic Eng. 12, 152-159. https://doi.org/10.1016/S1672-6529(14)60109-8

Topp, G.C., Parkin, G.W., Ferré, T.P., 2007. Soil water content, in: Carter, M.R. and Gregorich, E.G. (Eds.), Soil sampling and methods of analysis (2nd ed.), CRC Press. pp. 939-962. https://doi.org/10.1201/9781420005271

Van Pelt, R.S., Zobeck, T.M., Ritchie, J.C., Gill, T.E., 2007. Validating the use of ^{137}Cs measurements to estimate rates of soil redistribution by wind. Catena 70, 455-464. https://doi.org/10.1016/j.catena.2006.11.014

Vermang, J., Norton, L.D., Huang, C., Cornelis, W.M., da Silva, A.M., Gabriels, D., 2015. Characterization of soil surface roughness effects on runoff and soil erosion rates under simulated rainfall. Soil Sci. Soc. Am. J. 79, 903-916. https://doi.org/10.2136/sssaj2014.08.0329

Walther, P.A., 2017. Corn (ZEA MAYS L.) residue management for soybean (GLYCINE MAX L.) production: on-Farm experiment. (Master's dissertation). University of Manitoba, Winnipeg.

Webb, N.P., Strong, C.L., Chappell, A., Marx, S.K., McTainsh, G.H., 2013. Soil organic carbon enrichment of dust emissions: Magnitude, mechanisms and its implications for the carbon cycle. Earth Surf. Process. Landforms. 38, 1662-1671. https://doi.org/10.1002/esp.3404

Wen, J., Yi, Y., Zeng, G., 2016. Effects of modified zeolite on the removal and stabilization of heavy metals in contaminated lake sediment using BCR sequential extraction. J. Environ. Manage. 178, 63-69. https://doi.org/10.1016/j.jenvman.2016.04.046

White, B.R., 1982. Two-phase measurements of saltating turbulent boundary layer flow. Int. J.

Multiph. Flow. 8, 459-473. https://doi.org/10.1016/0301-9322(82)90018-0

Wickham, H., 2016. ggplot2: Elegant Graphics for Data Analysis. Springer-Verlag New York. ISBN 978-3-319-24277-4, https://ggplot2.tidyverse.org.

Wilson, S.J., Cooke, R.U., 1980. Wind erosion, in: Kirkby, M.J., Morgan, R.P.C. (Eds.), Soil Erosion, Wiley, Chichester, 217-251.

Yan, Y., Wang, X., Guo, Z., Chen, J., Xin, X., Xu, D., Yan, R., Chen, B., Xu, L., 2018. Influence of wind erosion on dry aggregate size distribution and nutrients in three steppe soils in northern China. Catena. 170, 159-168. https://doi.org/10.1016/j.catena.2018.06.013

Yates, A.G., Brua, R.B., Corriveau, J., Culp, J.M., Chambers, P.A., 2014. Seasonally driven variation in spatial relationships between agricultural land use and in-stream nutrient concentrations. River Res. Appl. 30, 476-493.

Yates, A.G., Culp, J.M., Chambers, P.A., 2012. Estimating nutrient production from human activities in subcatchments of the Red River, Manitoba. J. Great Lakes Res. 38, 106-114. https://doi.org/10.1016/j.jglr.2011.04.009

Zhang, C.L., Zou, X.Y., Gong, J.R., Liu, L.Y., Liu, Y.Z., 2004. Aerodynamic roughness of cultivated soil and its influences on soil erosion by wind in a wind tunnel. Soil Tillage Res. 75, 53–59. https://doi.org/10.1016/S0167-1987(03)00159-4

Zhao, L., Hou, R., Wu, F., Keesstra, S., 2018. Effect of soil surface roughness on infiltration water, ponding and runoff on tilled soils under rainfall simulation experiments. Soil Tillage Res. 179, 47-53. https://doi.org/10.1016/j.still.2018.01.009

Zobeck, T.M., 1991. Abrasion of crusted soils: Influence of abrader flux and soil properties. Soil Sci. Soc. Am. J. 55, 1091-1097. https://doi.org/10.2136/sssaj1991.03615995005500040033x

Zobeck, T.M., Fryrear, D.W., 1986. Chemical and physical characteristics of windblown sediment

I. Quantities and physical characteristics. Trans. Am. Soc. Agric. Eng. 29, 1032-1036. https://doi.org/10.13031/2013.30265

Zobeck, T.M., Sterk, G., Funk, R., Rajot, J.L., Stout, J.E., Van Pelt, R.S., 2003. Measurement and data analysis methods for field-scale wind erosion studies and model validation. Earth Surf. Process. Landforms 28, 1163-1188. https://doi.org/10.1002/esp.1033

Chapter 3

Agricultural activities lead to sediment infilling of wetlandscapes in the Canadian Prairies: Assessment of soil erosion and sedimentation fluxes

3.1. Abstract

Wetlandscapes are vulnerable to land conversion and sediment infilling from upland agriculture, causing them to act as sinks for sediment deposition and putting at risk their ecosystem services. Wetlandscapes in the Canadian Prairie agroecosystem are particularly susceptible to sediment infilling because of the intensification of human activities and agricultural practices. The rising risk of soil erosion in cultivated landscapes has generated a need to estimate soil redistribution rates and soil loss monitoring tools and techniques. This research examines the effects of agricultural activities on soil loss and sedimentation rates within agricultural landscapes in the Canadian Prairies. Land and atmospheric fluxes of sediment into wetlands are quantified over the past 60 years using catchment-scale tracing (^{137}Cs) and budgeting techniques. Findings indicate that the pattern of ^{137}Cs erosion/deposition varies along catchment toposequences, with erosion near the top of the toposequences (the average annual soil erosion rates were found to be 1.1 kg m^{-2} yr^{-1} for Manitoba and 0.3 kg m^{-2} yr^{-1} for Alberta) and deposition within the wetland ecosystem (total deposition rates were estimated at about -3.6 kg m^{-2} $yr^{-1}$for Manitoba and -0.9 kg m^{-2} yr^{-1} for Alberta). The sediment delivery ratios were approximately 57% and 35% in Manitoba and Alberta, respectively, indicating that a noticeable amount of the mobilized sediment exits the field. These transfers from cultivated fields into wetlands reveal that wetlandscapes in Canadian Prairies are vulnerable to sediment infilling, and soil erosion control practices are needed to achieve sustainable management of agricultural landscapes.

3.2. Introduction

Agricultural landscapes of the Prairie Pothole Region (PPR) of North America cover nearly 777,000 km^2 and contain millions of wetlands embedded within intensively farmed cropland (Doherty et al., 2016). The Canadian portion of the PPR is the nation's largest and most intensive grain crop production area, spanning 312,746 km^2 across three provinces (Manitoba, Saskatchewan and Alberta) and accounting for about 83% of Canada's agricultural land area and about 5% of Canada's total land base (National Wetlands Working Group, 1988; Environment Canada, 1996; Statistics Canada, 2017). Prairie wetlandscapes are amongst the most valuable ecosystems in the world (Creed et al. 2017), providing ecosystem services such as carbon storage, hydrologic regulation, water purification, biodiversity conservation, and recreation and tourism opportunities (Mitsch and Gossilink, 2000; Thorslund et al., 2017; Creed et al., 2022).

Agricultural activities [e.g., land conversion, wetland infilling, surface draining (ditching), subsurface drainage (tiling), channelization and basin consolidation] (Watmough and Schmoll, 2007) within the PPR place these prairie wetlands at risk from soil erosion. As agricultural activities intensify, wetlands are subject to natural and anthropogenic agents acting on the soils over a broad range of spatial and temporal scales (Johnston, 1991; Santhi et al., 2006). Consequently, the intensification of agricultural activities and the associated risk of cycles of land abandonment (e.g., summer fallow) followed by a return to cultivation have accelerated the processes of soil erosion from agricultural landscapes (Redpath, 1993; Dahl and Watmough, 2007; Penfound and Vaz, 2022). Soil erosion is recognized as one of the greatest environmental threats to sustainable management of agricultural landscapes (Montanarella et al., 2016; Thangavel and Sridevi, 2017). Soil erosion and its subsequent sedimentation affects the eroded site, leading to the mass movement of soil and therefore a loss of soil productivity (Schmitter et al., 2010; Lobb, 2011), as well as increased sedimentation (e.g., damage to aquatic reservoirs) (Dercon et al., 2012; Preston et al., 2013).

In the PPR, sediment inputs into wetlands on agricultural landscapes are derived primarily from wind, water, and tillage erosion of upland soil in adjacent areas (Craft and Casey, 2000).

Historically, wind erosion has been considered a severe threat to the sustainability of crop production on the PPR (Rennie, 1985; Lobb et al., 2017). The North American Dust Bowl era of the 1930s is an extreme example of the potential on-farm and off-farm costs of soil erosion by wind. Today, wind erosion continues to be a problem in drought periods throughout the PPR (Wheaton, 1992). Soil loss by wind is most severe on exposed upper slopes of toposequences within landscapes dominated by agriculture. The pattern of wind erosion is driven by the prevailing wind direction including deposition of sediments on the leeward side of nearby vegetation cover, aeolian mixture of snow and soil (snirt), dust abrades and buried plants (Li, 2021). Water erosion is not as noticeable as wind erosion or soil drifting in the PPR (Ripley et al., 1961). However, water runoff contributes largely to the sediment flux into wetlands (Liu et al., 2013). Spring meltwaters represents about 80% of total annual runoff into the wetlands in the Canadian PPR (Bourne et al., 2002; Glozier et al., 2006). Soil transport on cultivated lands not only depends on erosion/deposition by wind and water, but also on agricultural practices, such as the tilling of soils. Tillage erosion is a major form of erosion on agricultural landscapes of the Canadian PPR (Lobb, 2011). In contrast to wind and water erosion, tillage erosion is a nonselective process, and is the net downslope translocation of soils resulting in soil loss over the upper parts of toposequences and deposition over the lower parts of the toposequences, or soil loss from convex toposequence positions and soil accumulation in concave toposequence positions (Li et al., 2008; 2021).

On agricultural landscapes, it is necessary to assess all processes of soil erosion (i.e., wind, water and tillage) to provide a comprehensive estimate of soil erosion, as there are linkages and interactions among these processes. Linkages are the additive effects of different erosion processes, and interactions occur when one erosion process changes the erodibility of the landscape for another process, or when one erosion process works as a delivery mechanism for another erosion process (Li et al., 2007a; Lobb et al., 2003). The catchment sediment budget is introduced as an effective framework for characterizing the sediment mobilization, transport, deposition, and storage within, and sediment output from, a catchment (Slaymaker, 2003; Walling and Collins, 2008; Porto et al., 2016; Goharrokhi et al., 2021). The catchment sediment budget of individual depressional wetlands can be highly variable because of their “closed” material cycle and small catchment size (Hopkinson 1992; Lane and Autrey, 2017). Estimating catchment sediment budgets of depressional wetlands is often challenging (e.g., spatial heterogeneity, limited data availability, complex hydrological processes, and interaction with climate factors). However, tracer-based sediment budget approach can be used to assess soil redistribution rates within, and yields from, the catchment (Wallbrink et al., 2002).

Numerous quantitative and qualitative approaches exist to quantify erosion and sedimentation rates. Recent improvements in remote sensing can contribute to the development of more precise methodologies that can measure soil volumes of sedimentary features by exploiting high-resolution topographic technologies (Cucchiaro et al., 2021). For instance, Airborne Laser Scanning (ALS) and Terrestrial Laser Scanning (TLS) use Light Detection and Ranging (LiDAR) technology to enable a detailed assessment of micro-topography features of soil erosion processes and their spatial patterns. ALS permits airborne mapping of sedimentary features and anthropogenic landforms (e.g., ridges-and-furrows, headlands, and lynchets) across large spatial scales (Chartin et al., 2011; Godone et al., 2018). TLS permits ground-based mapping of detailed land surface features (Hugenholtz et., 2013; Chabot et al., 2018) such as tillage-related landforms (tillage banks/ridges/berms and lynchet) (Li et al., 2009; Turner et al., 2014), gully erosion and alluvial fan deposits (Perroy et al., 2010), and symmetrical ridge associated with prevailing wind direction (Sweeney et al, 2019). Thus, measuring soil surface changes at field scale is another tool to analyze sediment connectivity and can contribute to a better understanding of processes causing soil detachment and transport.

Environmental radionuclides (e.g., ^{137}Cs, $^{210}Pb_{ex}$, ^{7}Be, ^{10}Be) can be used to construct hillslope sediment budgets and quantify sediment delivery ratios over a range of timescales (de Jong et., 1983; Walling and Quine, 1992; Lobb et al., 1995; Matisoff et al., 2002; Pennock, 2003; Li et al., 2008; Tiessen et al., 2009; Jelinski et al., 2019; Owens, 2020). The radioisotope ^{137}Cs has been most used as a sediment tracer (Evrard et al., 2020). ^{137}Cs fallout was produced as a byproduct of the atmospheric testing of thermonuclear-weapons during the period extending from the mid-1950s to early 1960s. ^{137}Cs is almost non-exchangeable, and upon delivery to the land surface is promptly and strongly adsorbed by the surface soil or sediment particles. Its subsequent redistribution over the landscape occurs mainly through physical processes (Walling, 2012). Thus, ^{137}Cs provides a means of measuring multi-decadal rates and distributions of soil erosion within a catchment (Walling and Quine, 1991).

Soil erosion studies have been conducted in the PPR (e.g., de Jong et al., 1983; Li et al., 2007), but there has been limited comprehensive assessment of soil loss and magnitude of the sediment entering wetlands by soil erosion processes (wind, water, and tillage). Here, we quantify soil erosion and fluxes of sediment within the Canadian PPR, which was previously identified as the most soil erosion-prone area in the Northern Great Plains (NGP). Our objectives are to: (1) estimate soil erosion and sedimentation rates using ^{137}Cs; (2) develop integrated budgets of soil loss from agricultural areas and sediment accumulation in wetlands using landscape-scale transect sampling data; and (3) identify and discriminate sedimentary features using LiDAR derived DEM within wetlands.

3.3. Materials and methods

3.3.1. Study area

The Canadian PPR occupies part of three Canadian Provinces (southwestern Manitoba, southern Saskatchewan, southeastern Alberta, and extends westward to central Alberta) (Pennock et al., 2010). The study focused on two sub-watersheds in the Canadian PPR, which contained drained, undrained, and restored depressional wetlands ranging from potholes to large sloughs that formed when subterranean masses of ice melted following the retreat of the Assiniboine and Wisconsin glacial lobes about 20,000-12,000 B.P (at the end of the last ice age).

The Broughton's Creek sub-watershed (26,034 ha) is in the Little Saskatchewan River watershed (49°52'19.87" N, 100° 7'7.20" W), which is a tributary of the Assiniboine River that drains into the Red River and then Lake Winnipeg (Manitoba soil survey report, 2011) (Fig. 3.1). The climate of the study area is semi-arid. The mean annual temperature is 2.2 °C (ranging from -16.6° C in January and 18.5° C in July), and the mean annual precipitation is 474 mm, of which 118 mm (25%) is snow, lasting from November to the following April, based on the 1980-2010 climate normals for Brandon, MB, ID: 5010480 (ECCC, 2022). The topography is hummocky till plain, with a relief of 110 m, ranging from 490 m to 600 m above sea level. The soils are Orthic Black Chernozem overlying moderately to strongly calcareous, loamy morainal till of limestone, granitic, and shale origin (Manitoba soil survey report, 2011). The vegetation of native prairie landscapes is a transitional grassland characterized by oak groves, trembling aspen, intermittent fescue grasslands, and tall mixed shrubs (Watmough and Schmoll, 2007). The land use consists of perennial and annual cropland (73.1%), grassland (10.8%), wetland (9.5%), forest (4.0%), and urban development (2.6%) (Yang et al., 2008).

The Bigstone Creek sub-watershed (725,000 ha) is in the Battle River watershed (52°43'24.71" N, 108°15'19.32" W), which is a tributary of the North Saskatchewan River (Fig. 3.1). The Battle River traverses central Alberta and extends east into Saskatchewan, where it flows into the North Saskatchewan River (NSWA, 2005). The study area lies within a gradient zone between a humid, continental and semiarid climate. The mean annual temperature is 3.0 °C (ranging from -17.2° C in January and 22.9° C in July), and the mean annual precipitation is 438 mm, with a monthly maximum occurring in June or July, based on the 1980-2010 climate normal for Camrose, AB, ID: 3011240 (ECCC, 2022). The undulating topography results in a pock-marked pattern of poorly drained depressions and pothole sloughs, with a relief of 240 m, ranging from 680 and 920 meters above sea level. The soils are deep, well-drained Black Solodized Solonetz developed on a dense yellowish brown to dark grayish brown till, overlying the non-marine sandstone, mudstone, siltstone, and coal strata of the Horse shoe Canyon Formation. The vegetation is in the Dry Mixed Wood and Aspen Parkland natural sub-regions, a transition between boreal and grassland environments. The land use consists of perennial and annual cropland (69%), grassland (19%), wetland (7.4%), forest (3%), and urban development (1.6%) (Alberta soil survey report, 1985; Howitt 1988; NSWA, 2005).

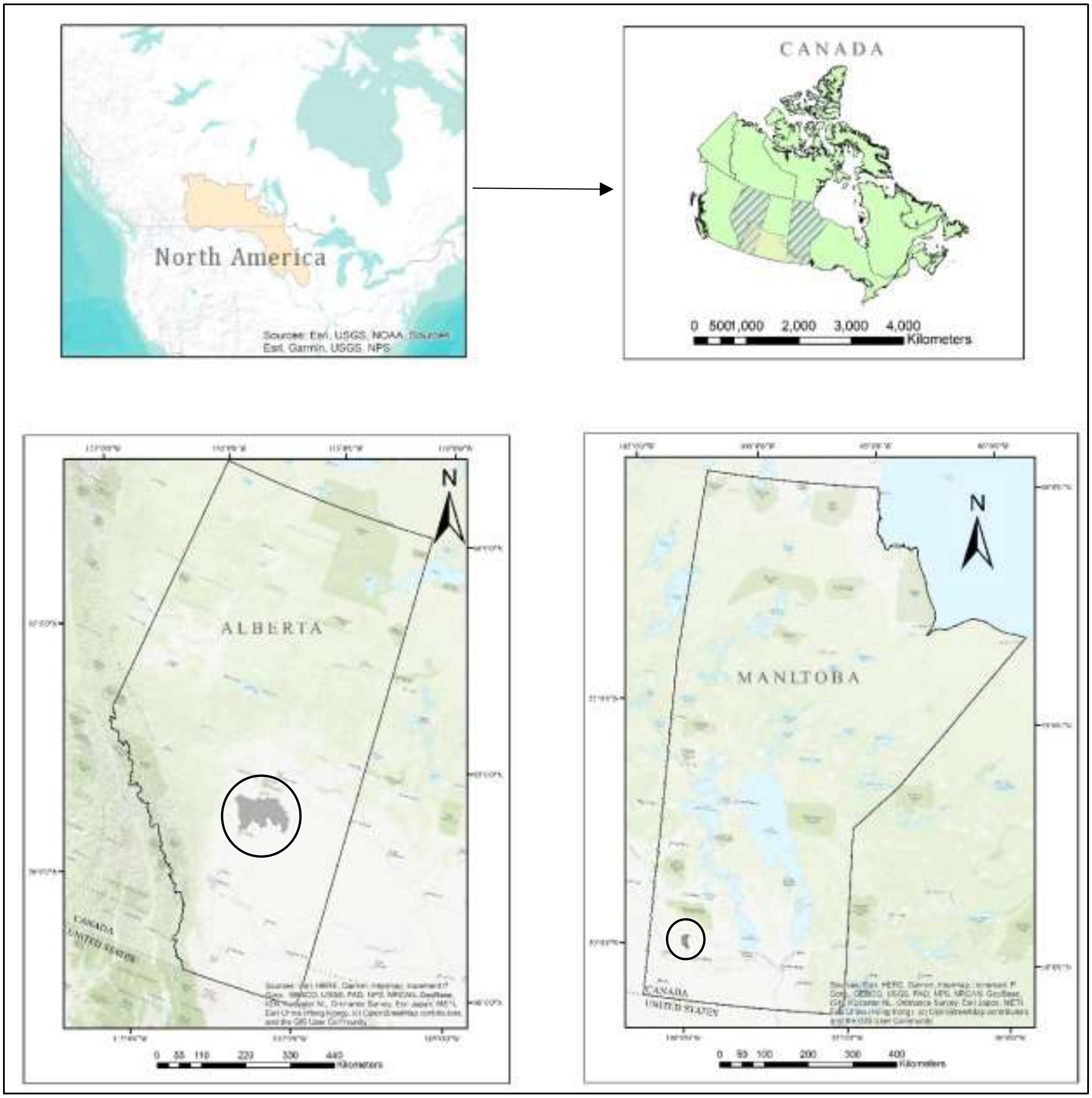

Fig. 3. 1. Geographic location of the studied catchments in Prairie provinces of Manitoba and Alberta, Canada. Light brown area shows the Canadian portion of the Prairie Pothole Region and dark gray areas are Broughton's Creek watershed, Manitoba and Bigstone Creek watershed, Alberta.

3.3.2. Soil sampling

The soil sampling strategy was designed to integrate the spatial variability of soil redistribution processes and the micro-scale spatial variability in ^{137}Cs radionuclides resulting from post-fallout soil redistribution (Walling and Quine, 1993). Wetlands that have never been disturbed by human activity within the sub-watersheds were identified on a series of aerial photographs taken between 1947 and 2018 by Natural Resources Canada (NRCan), and then eight of these wetlands with representative topography were selected for further analysis. The selected wetland catchments were naturally enclosed, which ensured a negligible loss of sediment in runoff from the catchments. The wetlands were embedded within annual croplands (7 wetlands) or a native prairie (1 wetland), of which, four catchments within croplands were in the Broughton's Creek watershed (Manitoba), three catchments within croplands were in the Bigstone Creek watershed (Alberta), and the catchment surrounded by a native prairie landscape was in Manitoba. Three transects were established within each wetland catchment; along each transect, positions were selected based on topographic attributes and dominant vegetation (e.g., upland/cultivated field, riparian and open water/pond center). Riparian, including grass wet meadow and emergent vegetation, is usually a dynamic transitional area between the aquatic system (i.e., open water or pond center) and the surrounding terrestrial system (i.e., upland), with well-defined vegetation covers and soil characteristics.

3.3.2.1. Soil and sediment core collection and processing

Sampling campaigns were carried out in summer 2016 (Alberta) and 2019 (Manitoba). In each wetland catchment, transects were established extending from the uppermost portion of agricultural land to the central area of the wetland, six to nine positions, representing upper slope (or crest and shoulder), middle slope (or backslope), lower slope (or footslope and toeslope) and depression (or wetland/open water) (MacMillan et al., 2000). For each transect within the cultivated portion of wetland catchments, three soil coring locations were chosen to represent three slope positions (upper, middle and lower). Fig. 3.3b is a schematic demonstrating the location of sampling points on different toposequences within wetland catchments. Soil cores were sampled at 10- to 15-cm depth interval, up to a maximum of 10 depth intervals, using a foot-operated stainless steel JMC Backsaver soil sampler (with a 45.7-cm-long, 3.17-cm-diameter slotted sampling tube). The soil cores collected by the Backsaver soil sampler and were sectioned in the field and transferred to the laboratory in coolers and refrigerated at 4° C until further analysis. Soil/sediment cores from riparian areas and the central areas of the wetlands were collected using a stainless steel JMC Backsaver soil sampler and then sectioned into 1-cm, 2-cm, 5-cm, and 10-cm intervals, depending on the locations of sampling. However, where water was present (e.g., in Manitoba), a different soil coring technique was used. At these sites, to sample from the deeper (>1 m) consolidated sediment in riparian area including grass wet meadow and cattail emergent vegetation, a portable and lightweight gas-powered Vibracoring unit (WINK Vibracore Drill Ltd., Vancouver, BC, Canada, at the Department of Geological Sciences, University of Manitoba, Winnipeg, Canada) was used that was equipped with 180-cm long and 7.62-cm diameter aluminum tubes and extracted by a hand-operated winch device. To sample from the central area of the wetland, which was open water, a handheld SDI Vibecore Mini unit (Specialty Devices Inc., Wylie, TX, USA, at the Landscape Dynamics Laboratory, University of Manitoba, Winnipeg, Canada) equipped with 120-cm long and 7.62-cm diameter polycarbonate tubes was used (Fig. 3.2). A hoist, mounted on an inflatable pontoon boat, was used for retrieving the cores from the open water. The retrieved cores were capped, sealed with tape, and labeled for transfer to the laboratory. Cores were allowed to sit for a few hours to make sure any suspended sediment associated with the collection process was allowed to settle. Before being transported to the lab any remaining water above the sediment-water interface was removed by drilling holes in the core tube above the sediment-water interface to reduce the amount of mixing during transportation. The cores were transported vertically (to avoid disturbing of sediment layers) to the laboratory and stored at -20° C. Prior to analysis, the frozen core tubes were split lengthwise with a table saw, then sectioned using a band-saw equipped with a diamond blade. The collected cores from the central area of the wetland were sectioned into 2-cm intervals, and cores from riparian area were sectioned into 1-cm intervals from the surface to a depth of 30-cm, and then at 5-cm intervals to the bottom of the core. In general, fine versus coarse segmentations of cores were chosen to optimize analytical throughput and to provide adequate detail for interpretation of the ^{137}Cs data (e.g., ^{137}Cs peak in sedimentary environment). The average percentage of material loss between slices due to the thickness of the cutting blade (~ 0.7 mm) was estimated at about 3.5% (ranging between 1.9% and 6.3%) in the cores sectioned using this method, which was taken into consideration in calculations.

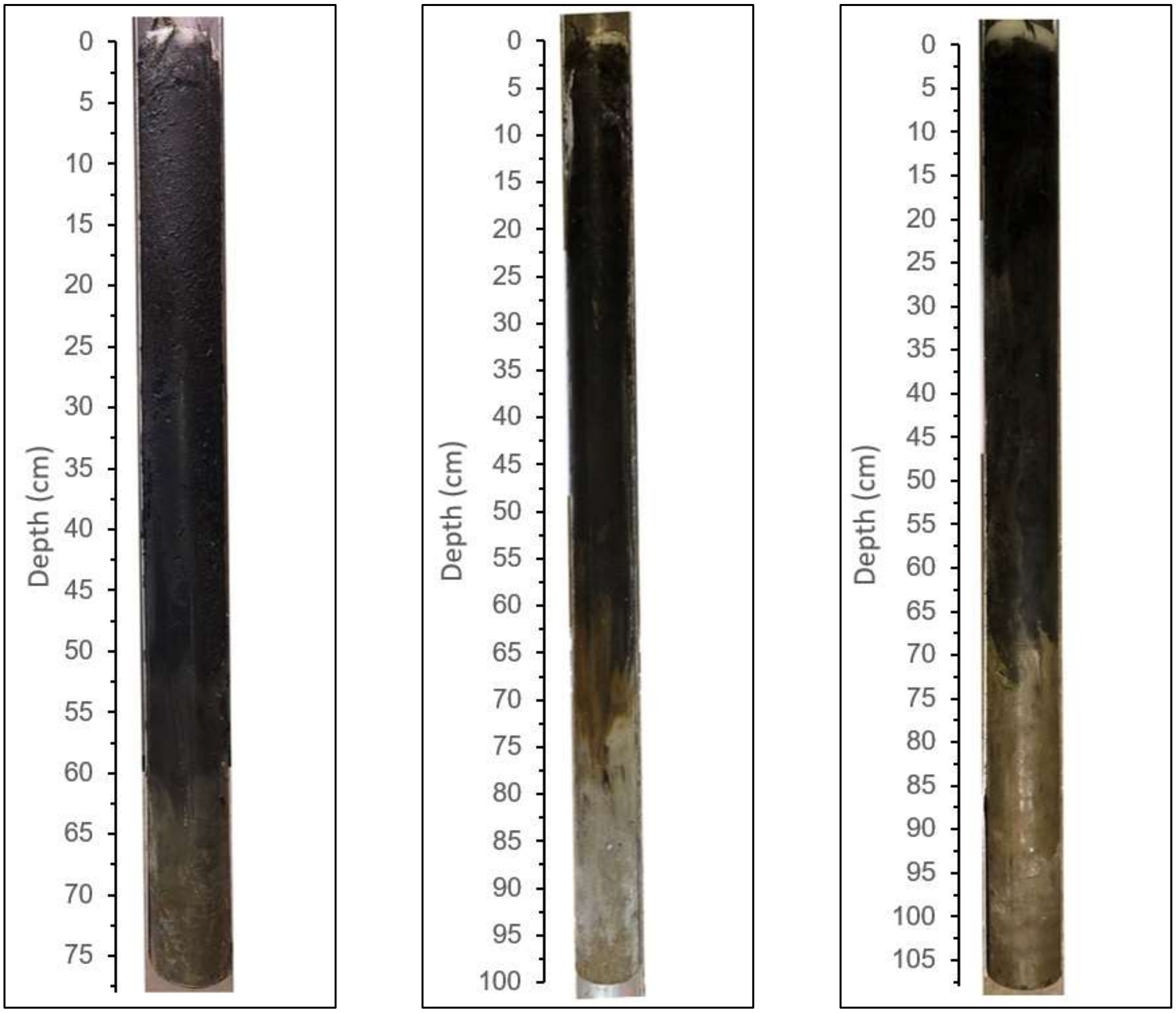

(a) (b) (c)

Fig. 3. 2. Photographs of collected cores in Broughton's Creek watershed, Manitoba, which are retrieved from riparian areas of (a) wetland surrounded by cropland (wetlandA-T1), (b) wetland surrounded by cropland (WetlandJ-T3) and (c) wetland surrounded by native prairie. The cores show the same characteristic pattern with a black organic-rich layer overlaying homogenous parent materials.

3.3.2.2. Measurement of radionuclide activity

After collection and sectioning of the soil/sediment cores, each section was prepared by drying at 70°C for 72 hours and then hand-crushing and sieving through 2-mm mesh to remove stones/large gravel particles and to ensure a constant sample density and geometry (Reddy et al., 2013). Furthermore, the bulk density of each section was determined as the ratio between soil dry weight and the volume corresponding to each section. The bulk density values were adjusted by taking into account the weight of materials larger than 2 mm (i.e., stones and gravels) (Blake and Hartge, 1986). Samples were transferred to plastic containers (i.e., 25-, 60- or 120-mL) based on sample size. ^{137}Cs activity was determined using gamma spectrometry. The gamma assays of the soil and sediment (< 2-mm) were performed in the laboratory by gamma-ray spectrometry using standard and low-background high-purity Germanium gamma detectors including Broad Energy detectors (BE6530) and a high-resolution Small Anode Germanium (SAGe) well detector (GSW275L) (Mirion Technologies, Canberra, Australia Inc., Meriden, CT, USA, at the Landscape Dynamics Laboratory, University of Manitoba, Winnipeg, Canada). The counting time was 12 to 24 h, depending upon the activity of ^{137}Cs in the samples, providing a < 10% detection error (Li et al., 2008). Samples were measured on a single detector to minimize the uncertainties associated with the precision of ^{137}Cs measurement. The spectra were analyzed with Canberra Genie 2000 software. The activity of ^{137}Cs in the samples were derived from the gamma-ray energy lines at 661.6 keV (Lobb et al., 1995). The ^{137}Cs content of the soil samples may be expressed as an activity (Bq kg^{-1}) or on an area basis (Bq m^{-2}) by dividing the total amount of ^{137}Cs in the sample by the internal area of the core sampler. The total inventory of a profile is obtained by the addition of the individual inventories for each depth increment. Calibration for the fallout radionuclides was conducted by the measurement of the mixed radionuclide reference material IAEA-447 (Shakhashiro et al., 2012).

3.3.3. ^{137}Cs reference sites selection

Reference sites are undisturbed sites established prior to 1950 (e.g., cemeteries, schoolyards, airports, parks, lawns, vegetated livestock exclosures) (Owens and Walling, 1996; Li et al., 2011a). In Manitoba, potential reference sites were selected in flat areas (to minimize lateral transport of water/sediments) near the study area (to ensure that both the reference and the wetland catchment had similar initial radioactive fallout). Historic aerial photography from 1947 to the present day, provided by NRCan and Google Earth Pro © images (Google Earth Pro version 7.3), as well as information provided by residents, were used to document the history of changes in the potential reference sites. Three reference sites were then selected, including a schoolyard and two old rural cemeteries next to the studied wetland catchments in Manitoba. At the reference sites, sampling points were more than 5-m away from the nearest tree to avoid the influence of snow and rain shadowing on ^{137}Cs inventories (Owens and Walling, 1996). A total of 27 soil cores (nine per reference site) were sampled up to 60-cm using a 3.17-cm diameter JMC Backsaver soil core sampler. Soil cores were sectioned at 5-cm increments to examine the vertical distribution of ^{137}Cs, an increment that provides sufficient detail to detect soil disturbance within the reference sites (Li et al., 2007b).

In Alberta, ^{137}Cs reference data were derived from a study by Li et al. (2007b), where two undisturbed flat sites were sampled about 60 km from the study area. A total of 24 soil cores (12 per reference site) were sampled at each reference site using up to 100-cm using a Giddings, truck-mounted hydraulic driven probe, with a 6.6-cm-diameter and 100-cm-long soil core sampler. Soil cores were sectioned at 5-cm increments to examine the vertical distribution of ^{137}Cs.

3.3.4. Total sedimentation and soil erosion estimation using ^{137}Cs measurements

Most of the ^{137}Cs fallout across the Prairies occurred during the 1960 to 1965 period, peaking in early 1963 (Kiss et al., 1986). The ^{137}Cs profile of each soil/sediment core was characterized visually to determine key time markers that could be employed to estimate sedimentation rates. Once these time markers were characterized, sedimentation rates were calculated by dividing the associated depth by the number of years between deposition and collection of the soil/sediment core (i.e., years from deposition to cores collection in 2016 for Alberta and 2019 for Manitoba samples) (Lobb et al., 1995; Walling and Quine, 1991). Although information on ^{137}Cs inventories and depth distributions can be used directly to explore qualitative patterns of soil redistribution rates within the landscape, quantitative estimates can provide a basis for establishing the overall sediment budget for the field.

^{137}Cs data were used to explore soil erosion rates, soil redistribution rates and sediment budgets. Point-based ^{137}Cs inventories were converted into point-based total soil erosion rates using the Proportional Model (PM) and Mass Balance Model 2 (MBM2) on disturbed soils, and Profile Distribution Model (PDM) on undisturbed soils (Walling et al., 2002; Li et al., 2010; Walling et al., 2011). To run the PM and MBM2, the "start year of cultivation" was set at 1960. The "mass plough depth" was 235 kg m^{-2} for Manitoba and 190 kg m^{-2} for Alberta, which was determined from the average plough depth (~ 0.2 m) and measured bulk density. Mean bulk density values ranged between 820 and 1380 kg m^{-3} for Manitoba and between 815 to 1075 kg m^{-3} for Alberta throughout the 0.2 m soil profiles. Following the study conducted by Li et al. (2007a) in the PPR, the "relaxation mass depth" (H_{MBM2}), "proportion of annual ^{137}Cs input susceptible to erosion loss" (γ_{MBM2}), and the "particle size correction factor" (P_{MBM2}) were defined as 4.0 kg m^{-2}, 0.75, and 1.0 respectively.

The PM uses a simple linear function to convert the loss (or gain) of ^{137}Cs inventory (relative to measured reference inventory) to a loss (or gain) of soil mass. PM does not simulate ^{137}Cs loss during the ^{137}Cs fallout period and tillage dilution (vertical and lateral) of ^{137}Cs activity due to the incorporation of soil from below the original plough depth. Therefore, PM underestimates the actual magnitude of soil loss in the area of maximum loss. Similarly, the actual deposition rates for the accumulation area can be underestimated since the model does not account for the progressive reduction in the ^{137}Cs activity of the deposited soil as erosion proceeds upslope. The PM also holds approximately closer to the actual budget of ^{137}Cs activity within a landscape, which makes it an appropriate model to simulate soil loss or gain budgeting within a naturally closed system (e.g., wetland catchment). The PM output erosion rates include the effects of all erosion processes.

The MBM2 represents complex processes that account for changes in the ^{137}Cs activity in response to the time-variant ^{137}Cs fallout input and the fate of freshly deposited ^{137}Cs prior to cultivation (e.g., losses/gains due to erosion/deposition, and progressive incorporation of fresh soil from beneath the original plough depth by tillage). Thus, results obtained using the MBM2 are likely to be more realistic for the area of maximum loss within a landscape (e.g., hilltop) in comparison with those of the PM. The MBM2 underestimates sediment deposition in the accumulation area like the PM, as both models were developed/designed mainly for application in eroding areas (Lobb and Kachanoski, 1997; Li et al., 2010; Walling et al., 2011; Zhang et al., 2018).

The PDM is simple and easy to use; however, the "profile shape factor" (h_0PDM) describes the rate of exponential decrease in ^{137}Cs activity with depth for a soil profile from a reference site. h_0PDM was estimated by fitting an exponential decay curve to the relationship between sampling depth in cumulative mass and ^{137}Cs activity (Walling et al., 2011).

The Erosion Calibration Model program developed by Walling et al. (2011), at the University of Exeter, was run to calculate soil loss and deposition rates for each of the downslope transects within wetland catchments. All models have been developed for use with data collected from downslope transects (Walling et al., 2011).

3.3.4.1. Estimation of point-based soil erosion and sedimentation rates

Point-based soil redistribution rates (kg m^{-2} yr^{-1}) were estimated using the MBM2 and based on the degree of reduction in the ^{137}Cs inventory relative to the ^{137}Cs reference inventory derived from local stable sites (off-site ^{137}Cs reference level) in each province. In depositional areas, although results indicated that average ^{137}Cs inventories of collected cores within depositional areas were lower than estimated off-site reference values, most of the cores showed one well-defined ^{137}Cs peak, corresponding to the peak fallout of ^{137}Cs in 1963 from atmospheric nuclear weapons testing. Therefore, sediment deposition rates were reported from the peak of ^{137}Cs activity.

3.3.4.2. Development of soil loss and accumulation budgets

Average soil loss and accumulation budgets were established by carrying out a simple mass balance for the whole wetland catchments in Manitoba and Alberta. The average soil redistribution rate obtained for sampling points on each toposequence position was used to calculate equivalent values of soil loss or deposition (kg yr^{-1}) for the individual position, extending from a particular sampling point to the adjacent sampling point in each direction. Furthermore, the ^{137}Cs inventory values of the sampled points were representative of the entire toposequence position. Previous researchers (Collins et al., 2001; Walling et al., 2003; Estrany et al., 2010; Gaspar et al., 2013) assumed that each transect represents a 1-m wide strip. However, this methodology was modified to adapt it to extrapolate average point values to the area of each toposequence position, which can be calculated using LandMapR™ to take into account the contribution of each toposequence position to soil erosion and achieve accurate sediment export rates from cultivated fields to wetland ecosystems. The PM and catchment-level reference ^{137}Cs values (on-site values) were used for the development of the sediment budgets (Table 3.3). Since the studied wetland catchments are naturally enclosed, it was assumed that negligible ^{137}Cs left the wetland catchments. Therefore, catchment-level reference ^{137}Cs values (on-site values) were calculated by adding up area weighted available ^{137}Cs for each toposequence position within the wetland catchments, and subsequently dividing this sum by the total area of the wetland catchments in each of the two provinces. The resulting areal estimates were summed to provide a sediment budget for the overall catchment, which comprised estimates (~ 60 years) of the total erosion, total deposition, net soil loss and the sediment delivery ratio.

3.3.5. Characterization of landform elements and sedimentary features

High-resolution digital elevation models (1×1 m) (DEMs) were acquired from an airborne Light Detection and Ranging (LIDAR) scanning system. LiDAR point cloud data was acquired for the Broughton's Creek with a vertical accuracy assessed as ±0.15 m at 95% confidence level in flat open terrain (Ducks Unlimited Canada, unpublished data). LiDAR point cloud data for Bigstone Creek were provided by Altalis (Altalis Ltd., Calgary, Alberta, Canada, www.altalis.com). All digital elevation data contain some degree of errors and uncertainties, and the DEM errors could be classified into two distinct groups (e.g., random and systematic errors) (Liu and Jezek, 1999). Systematic errors are usually corrected before release of the DEM (Li et al., 2011b). Random errors are relatively hard to detect and still exist in the DEM. Therefore, data noise suppression can be conducted by smoothing the DEM before using it for landscape classification and hydrological modeling (Li et al., 2011b). DEMs with a cell size of 5 to 10 m are common for characterizing the landform classes and hydrological entities (MacMillan et al., 2003). Therefore, prior to landform characterization, DEMs for both study areas were resampled to a 5-m grid and smoothed using three passes of a mean filter with dimensions of 5 × 5, 5 × 5, and 7 × 7 (MacMillan et al., 2003). After generating the smoothed DEMs, nested hierarchical wetland depressions were identified and their corresponding catchments were delineated using the "Wetland Hydrology Analyst" tool in ArcGIS® 10.6.1, which uses three stand-alone subprograms sequentially (wetland depression tool, wetland catchment tool and flow path tool) (Wu and Lane, 2017).

The smoothed DEM was used for delineation of toposequence positions. Toposequence positions were defined using the LITAP package (V0.6.0; Lazerte and Li, 2021) in R, which is based on the

LandMapR™ software developed by MacMillan et al. (2003). The resulting 15 toposequence classes were grouped into four classes based on typical toposequence positions (upper slope, middle slope, lower slope and depression areas). Fig. 3.3a illustrates the landscape classification map for a quarter section of land in Broughton's Creek Watershed, which includes three studied wetland catchments. The landscape classification maps were produced using Surfer® software (V17; Golden Software, LLC) by over laying on the 5-m DEMs.

LiDAR data were used to identify natural- (wind and water) and human-induced (tillage) depositional features on the agricultural landscapes (Langewitz et al., 2021). The original (unsmoothed) 1-m LiDAR DEMs were used to visually identify depositional patterns around the wetlands (e.g., riparian areas) and to estimate the volume of deposits associated with soil erosion (wind, water and tillage). Depositional patterns were identified through visual assessment of features on the DEMs. The volume of deposits at the boundary of the cultivated field and the riparian area (i.e., wet meadow), which is a transitional zone, were estimated by extracting actual elevation profiles of the depositional features using Surfer® software for multiple transects within wetland catchments. The length, width, depth, and as well as shape of these deposits were characterized on the DEMs and extracted elevation profiles. The mass of deposits was then calculated using the measured bulk density.

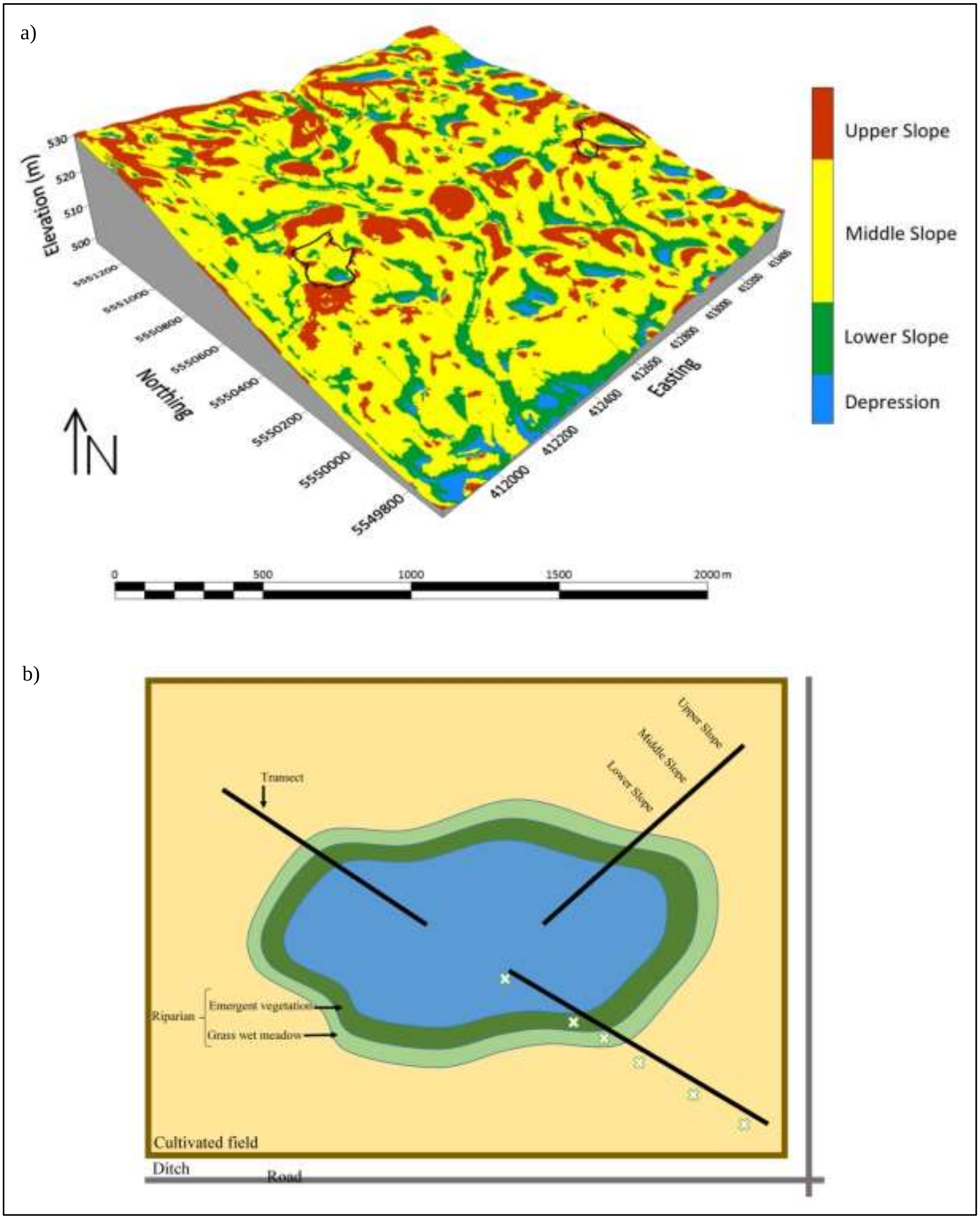

Fig. 3. 3. Three-dimensional (3D) view illustrating the landscape classification in Broughton's Creek Watershed, Manitoba (a) and schematic representation of wetland catchment sampling locations relative to the wetland fringe and boundaries (b). The three studied wetland catchments in a section of land were identified using borderline that was extracted by "Wetland Hydrology Analyst" in ArcGIS®.

3.3.6. Data treatment and statistical analysis

One-way analysis of variance (ANOVA) was performed to investigate the ^{137}Cs inventory variations along different toposequence positions within wetland catchments. Before performing a one-way ANOVA, variables were subjected to the Kolmogorov-Smirnov test for normality and a Levene test for homogeneity of variance. Mean separation between toposequence positions was evaluated using the Tukey-Kramer test with a probability level for significance of 0.1. Analysis of variance was conducted with the Proc Glimmix procedure (V9.4; SAS Institute, Cary, NC) with a lognormal distribution. In addition, descriptive statistics including sample mean, sample standard deviation and coefficient of variation were calculated for each toposequence position within each land use in both provinces. All figures were created using the ggplot2 package (V3.3.3; Wickham, 2016) in R (V4.0.1; R Core team, 2020) and Microsoft Excel 2016.

3.4. Results and discussion

3.4.1. ^{137}Cs reference data

In Manitoba, the depth distribution of ^{137}Cs in two of the three reference sites (the school playground and one of the old rural cemeteries) revealed that soil disturbance had occurred in these two sites since 1954. Therefore, one old rural cemetery was selected as the reference site. The ^{137}Cs areal activity inventory of the reference site had a mean value of 1,430 ±123 Bq m^{-2} decay-corrected to 1 January 2021 with a coefficient of variation of 8.6%. This mean value is close to that estimated by others who reported a value of 1,502 Bq m^{-2} (Li et al., 2008). One of the important indicators of an undisturbed reference site is the expected exponential decrease of ^{137}Cs activity with soil depth (Walling and Quine, 1991; Collins et al., 2001). The ^{137}Cs depth distribution profiles associated with the reference site are depicted in Fig. 3.4 with maximum activities at the surface of the soil. The depth distributions of ^{137}Cs in the reference profiles conform to that expected for a stable undisturbed site, with around 80% of the total inventory occurring in the top 15 cm and a sharp decline in ^{137}Cs activities below this depth.

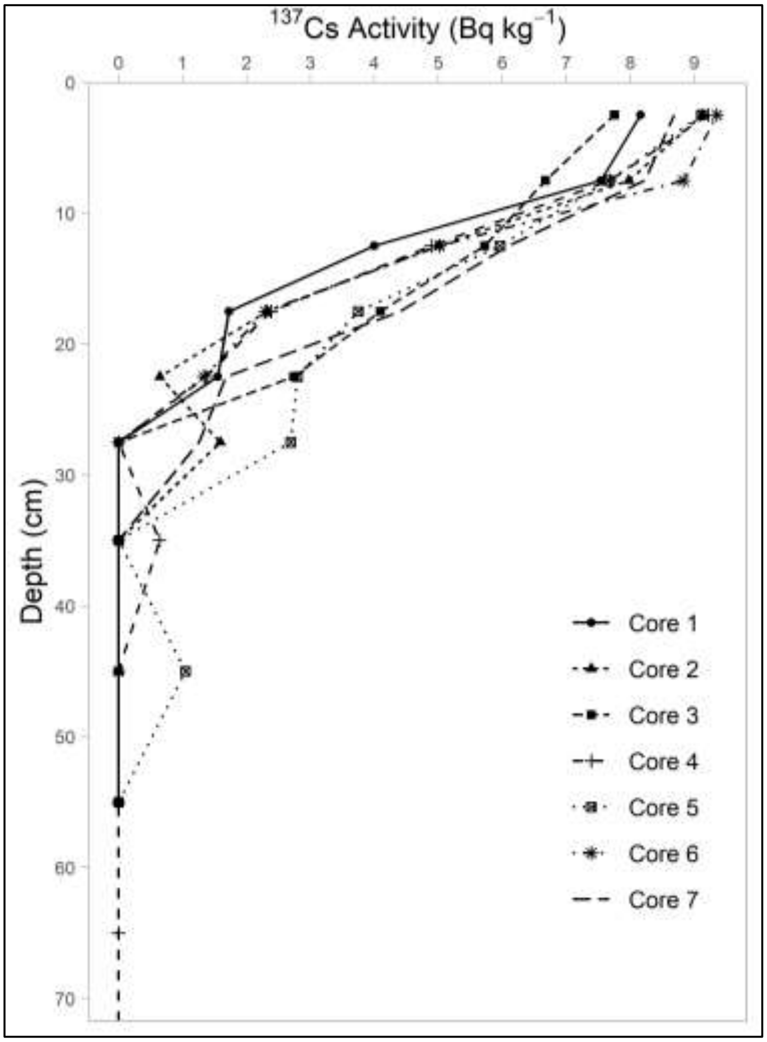

Fig. 3. 4. Depth distribution of ^{137}Cs in soil profiles collected from an old rural cemetery at the Broughton's Creek watershed, Manitoba. Two bulk cores were collected from this reference site, which are not shown in the figure, but were used for estimation of average ^{137}Cs reference inventory.

In Alberta, the ^{137}Cs areal activity inventory of the reference sites (n=24) ranged from 546 to 3,628 Bq m^{-2}, with a mean value of 1,684 ±834 Bq m^{-2} decay-corrected to 1 January 2021, and a coefficient of variation of 49% (Li et al., 2007b). Similar means and coefficients of variation were reported in studies by Basher and Matthews (1993), Owens and Walling (1996), and Baldwin (2015). Baldwin (2015) assessed wind erosion on a low-relief hummocky landscape in southern

Alberta and documented an average ^{137}Cs reference inventory of 914 ±376 Bq m^{-2}, decay-corrected to 1 January 2021, with a coefficient of variation of 41% (n= 19). The regional variability of the measured ^{137}Cs reference inventories between central and southern Alberta can be mainly related to heterogeneity within a reference site (Owens and Walling; 1996) and variability of precipitation in the Canadian Rockies (Haines, 2012). According to Owens and Walling (1996), the ^{137}Cs inventories variability can be attributed to random heterogeneity (i.e., small-scale heterogeneity in topography, soils, and the plants) within reference sites.

3.4.2. ^{137}Cs transect data

Descriptive statistics of ^{137}Cs data collected from the 165 sampling locations along 24 transects within the studied wetland catchments are presented in Table 3.1. In cultivated catchments, the largest variability of ^{137}Cs activities was found at the upper and middle slopes and, in general, the variability decreased to the lower slopes and inner riparian (i.e., emergent vegetation) area. In Manitoba, within cultivated field area about 66% of the ^{137}Cs inventories were significantly smaller than the reference site, indicating soil loss, and 17% were significantly larger, indicating soil deposition. The remaining 17% of the ^{137}Cs inventory values were not significantly different from the reference site, indicating that these sites were essentially stable, experiencing neither loss nor deposition. In Alberta, 78% of the ^{137}Cs inventories were smaller than the reference site, but the differences were not statistically significant. This result could suggest that soil loss and deposition occurred at roughly equivalent rates. The noticeable reduction in the ^{137}Cs inventory, especially in Manitoba, indicated that the majority of the sampling locations have experienced significant soil erosion since 1963, which can cause significant soil redistribution. Lobb (2011) has reported soil erosion as the dominant soil redistribution process within topographically complex landscapes.

Table 3. 1. Descriptive statistics for the ^{137}Cs inventories documented for the sampling points along the transects within wetland catchments with different land uses in Manitoba and Alberta.

Toposequence position	Number of cores	^{137}Cs inventory (Bq m^{-2})			
		Average	Standard Deviation	Coefficient of Variation	Range
Manitoba- Cultivated catchments					
Upper Slope	12	569	461	81	0 - 1610
Middle Slope	12	1055	1269	120	0 - 4826
Lower Slope	12	2493	1902	76	403 - 6919
Outer Riparian	12	2782	1733	62	200 - 6099
Inner Riparian	9	1606	718	45	642 - 2917
Inner Wetland	12	1240	843	68	337 - 2717
Manitoba- Native prairie					
Upper Slope	3	1580	27	2	1557 - 1610
Middle Slope	3	2116	848	40	1284 - 2980
Lower Slope	3	426	229	54	162 - 575
Inner Riparian	3	1011	471	47	637 - 1539
Inner Wetland	3	557	56	10	523 - 622
Alberta- Cultivated catchments					
Upper Slope	9	940	687	73	0 - 2399
Middle Slope	9	1152	475	41	650 - 2011
Lower Slope	9	1896	1073	57	257 - 4056
Outer Riparian	9	1831	1283	70	91 - 3724
Middle Riparian	9	1460	759	52	143 - 2671
Inner Riparian	9	1506	816	54	366 - 2804
Outer Wetland	9	1331	501	38	646 - 2093
Middle Wetland	9	913	508	56	0 - 1634
Inner Wetland	9	1318	603	46	0 - 1954

Toposequence position was a significant factor ($P < 0.1$) in determining the ^{137}Cs inventories within wetland catchments embedded in cultivated fields (Fig. 3.5a). ^{137}Cs inventories of the upper slope position were significantly ($P = 0.022$) smaller than the lower slope position but there was no statistically significant difference between upper and lower slope positions with the middle slope position. The extent of the reduction of ^{137}Cs inventories varied along different transects in the wetland catchments surrounded by cultivated land but followed a similar pattern (Fig. 3.6). This pattern was characterized by a low ^{137}Cs inventory (indicating maximum erosion) near the top of transects with ^{137}Cs inventories increasing downslope. The highest ^{137}Cs inventory values, which exceed the local reference inventory, indicating soil deposition, were found at sampling points near the base of transects. Therefore, due to the combined action of tillage erosion and water erosion, a large amount of soil was deposited at the lower segment of slope (lower slope and/or outer riparian/grass wet meadow). Tillage erosion typically occurs in the upper slope position, and water erosion gradually increases down the slope until it reaches the highest rate in the middle slope or upper lower slope position (Li, 2021; Li et al., 2008; Lobb et al., 1995; Lobb et al., 2007). Despite the lack of statistical significance difference in average ^{137}Cs inventory values between the riparian area (i.e., grass wet meadow and emergent vegetation) and the central area of wetland on theses cultivated catchments, higher ^{137}Cs deposition occurred in the outer riparian (i.e., grass wet meadow) and inner riparian (emergent vegetation) areas, respectively. In addition, this might suggest that more cores may be required for detection of statistical difference within the wetland ecosystems. Furthermore, it is reasonable to argue that the clay particles that made it to the center of the wetland preferentially carry more ^{137}Cs than the larger particles that were deposited at the wetland fringe (He and Walling, 1996). This could be addressed by measuring particle size distributions of those samples.

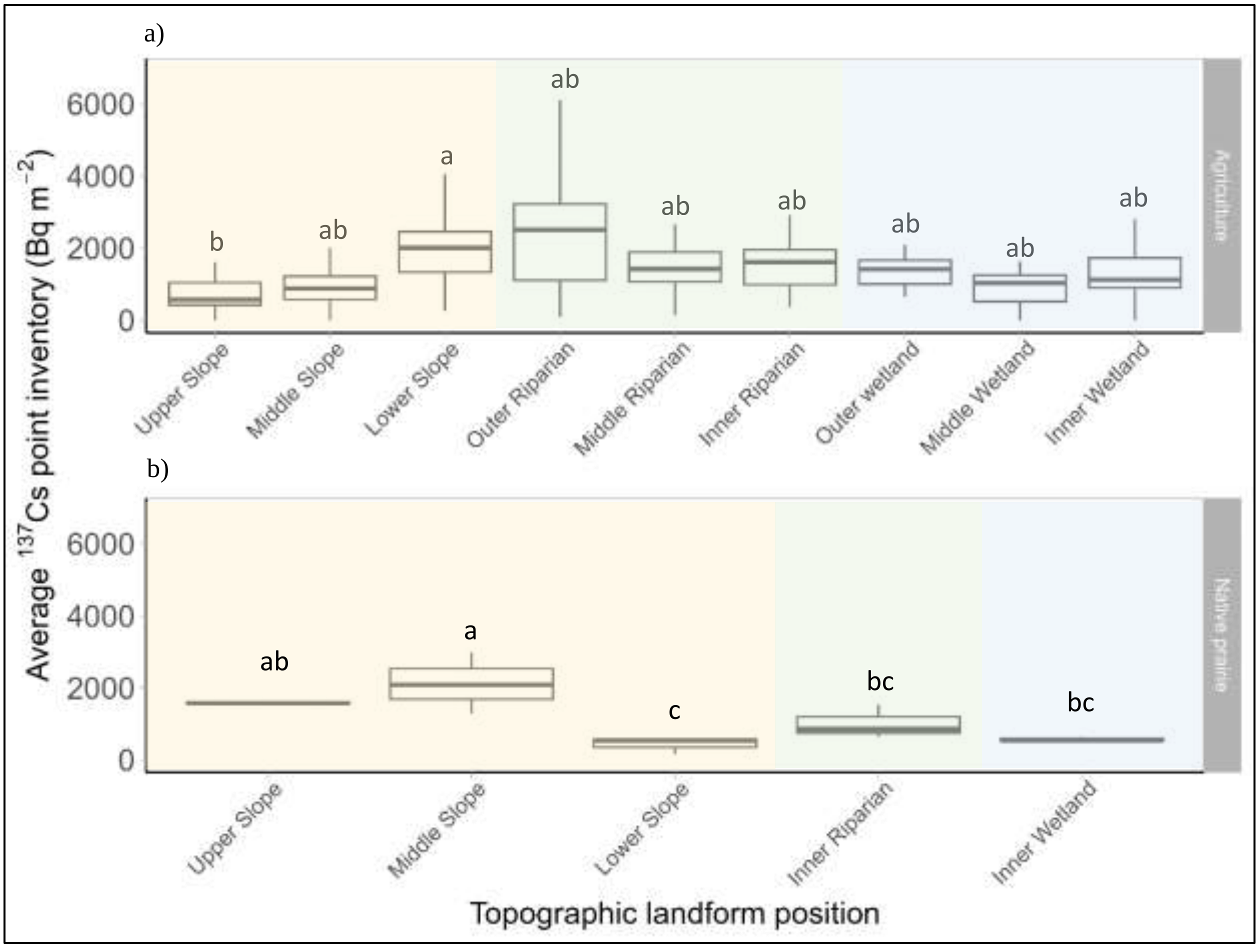

Fig. 3. 5. Difference comparison ($P < 0.1$) of the downslope spatial variations in ^{137}Cs inventories along different toposequence positions in wetland catchments surrounding by (a) cultivated land and (b) native prairie. [Yellow, green and blue colours shown upland, riparian and pond center].

Toposequence position was also a significant factor affecting the ^{137}Cs inventories within wetland catchments embedded in native prairie (Fig. 3.5b). However, the distribution of ^{137}Cs inventory on this undisturbed landscape was distinct from the distribution of ^{137}Cs inventories on cultivated landscapes. In the undisturbed landscape, ^{137}Cs depletion was observed in the lower slope of the wetland catchment, while in the cultivated landscape, ^{137}Cs enrichment was observed in the lower slope. The depositional zone (e.g., lower slope position and riparian area) would be expected to be an area of deposition, thus enriched in ^{137}Cs. However, this was not the case in this study. This could suggest that sediment redistribution within the undisturbed site has been negligible over the past ~ 60 years. Another possible explanation for this discrepancy could be attributed to the location of sampling points and soil surface condition (e.g., micro-relief and vegetation cover). Furthermore, the spatial variability of ^{137}Cs in the native prairie surrounding the wetland has not been documented as rigorously, although it appeared to be significantly lower than the variability at disturbed locations (Table 3.1). This finding supports evidence from previous observations (e.g., Sutherland, 1994; Kaste et al., 2006) that were conducted across the undistributed prairie landscape of the NGP and reported lower ^{137}Cs inventory values on concave landforms. Furthermore, Dalzell et al. (2022) conducted a study in Fillmore County, MN, USA, and reported that agricultural sites exhibited greater variability in total ^{137}Cs inventory compared to grassland sites, which is consistent with the finding of this study.

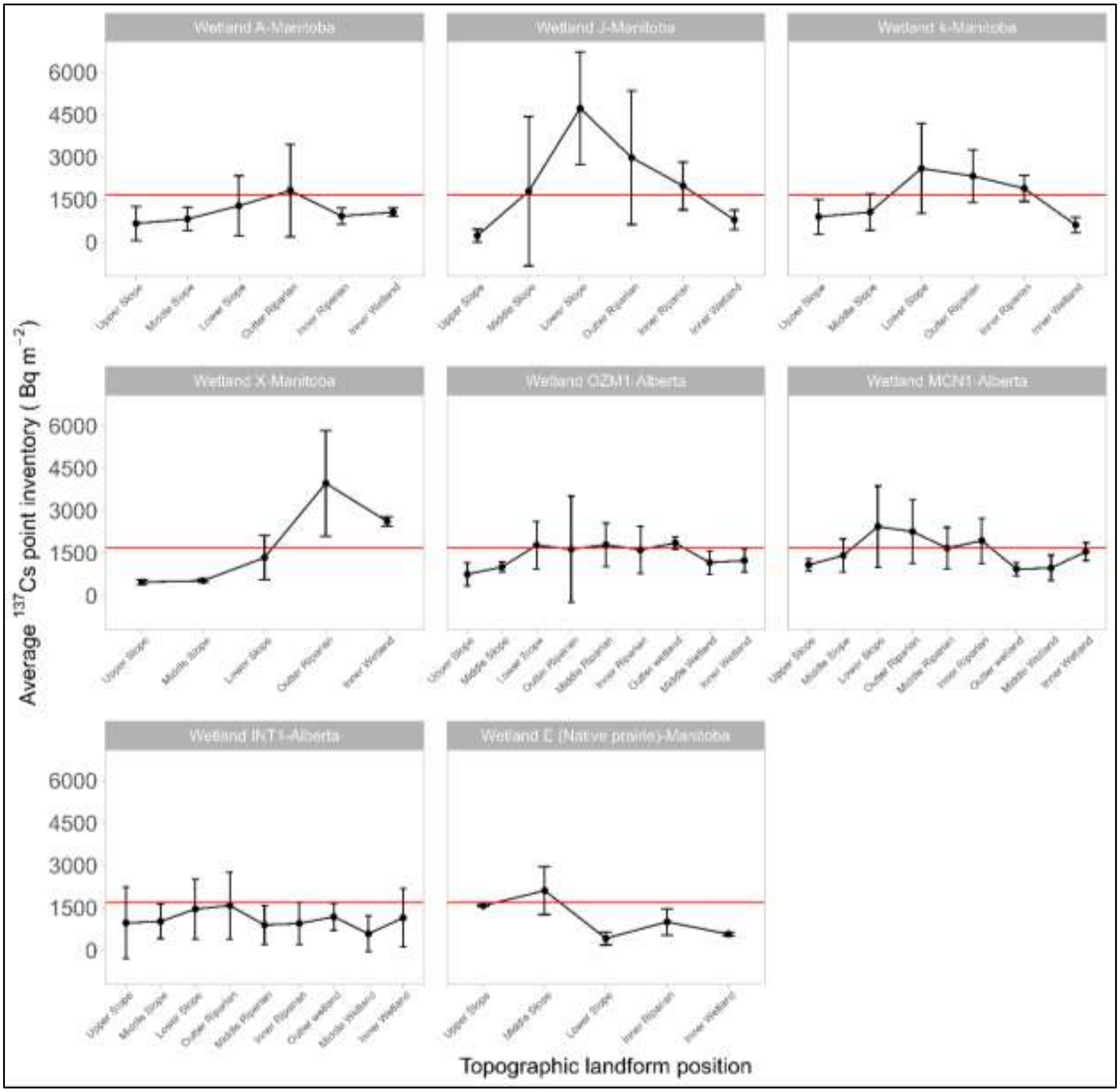

Fig. 3. 6. Spatial variation of ^{137}Cs inventories within wetland catchments in Manitoba and Alberta. The red line shows the reference inventories of the study areas in Manitoba and Alberta.

Fig. 3.7 presents a summary of the observed pattern of the ^{137}Cs inventories on three transects within one wetland catchment located in Broughton's Creek watershed, Manitoba (figures for the other wetland catchments are presented in Appendix A-A1 to -A7. Fig. 3.7 shows that the depth distribution of ^{137}Cs across all soil cores exhibits a decrease in activity, but with different configurations (i.e., the shape of the ^{137}Cs depth profile). The differences in the resulting patterns of ^{137}Cs depth distributions within the wetland may be due to agricultural activities that influence hydrological and biological properties within the soil profile (Paramonova et al., 2017). From upper slope to lower slope positions, the ^{137}Cs depth distributions show a uniform variation in the activity of ^{137}Cs within the plough layer (ranging from 20 to 30 cm) that is characteristic of cultivated land. The ^{137}Cs depth distribution for the depositional areas (i.e., riparian area and pond center) conforms to the normally expected characteristics of a depositional site, in which ^{137}Cs was found at greater depths and greater activities than eroding sites because of soil sedimentation. The collected sediment cores from inner-riparian (i.e., emergent vegetation) and -wetland were characterized by a substantial increased activity of ^{137}Cs down the soil profiles. However, some sampling locations (e.g., Fig 3.7. e), which could be expected to have characteristics of an undisturbed core, are characterized by a near-uniform ^{137}Cs activity down the profile. This can be attributed partially to physical disturbance by animal activities (e.g., ducks and gophers) and intensive agricultural activities over the dry years when water recedes and allows to expand agricultural activities. It is worth mentioning that although the ^{137}Cs depth distributions of soil profiles from different toposequence positions are characterized by different inventory values, they have a similar shape that conforms to that expected for a cultivated landscape and undisturbed land (Meliho et al., 2019). Furthermore, within the wetland catchments, ^{137}Cs was not detected below the ~ 20-cm depth in eroded profiles or the depositional profiles. These results, together with the pronounced accumulation of ^{137}Cs in the top ~ 10 cm of the accumulation areas (i.e., inner-riparian and -wetland), could indicate that very little downward movement of fallout ^{137}Cs has occurred through leaching.

Fig. 3. 7. Depth distribution of ^{137}Cs and their variation according to toposequence positions on three transects within one wetland catchment (Wetland K) embedded in cultivated land in Manitoba. The points are showing analyzed depth of each core. ^{137}Cs activity was measured down to 80-cm depth in some cores, but are not shown in the figure. The dashed line shows the approximate depth of tillage that is the zone of frequent mixing in the cultivated land.

Wetland catchments displayed oscillating behaviour of the ^{137}Cs inventories (Fig. 3.6), suggesting a variation of soil erosion and deposition along transects. Since, accordingly to historic aerial photographs, the central area of the studied wetlands has not experienced disturbance by anthropogenic activities, it was anticipated that ^{137}Cs inventories associated with open water would be at least close to non-eroded off-site reference ^{137}Cs values (i.e., local stable sites). However, the sediment cores from the pond center of wetland catchments showed lower ^{137}Cs inventories than reference sites. There are a few possible reasons to explain this inconsistency. ^{137}Cs dynamics between sediment and the overlying water column within the pond center could have contributed to this pattern. Remobilization of ^{137}Cs can be caused by physical disturbances, chemical (e.g., ion exchange) and biological processes (e.g., foliar uptake). The physical disturbances can be caused by bioturbation of sediments (e.g., salamanders, snakes, turtles, and aquatic insects) that result in resuspension of low-density sediment and organic matter, and by wind, both of which lead to lower ^{137}Cs inventories within the pond center. Remobilization may also occur due to the ion-exchange replacement of Cs^+ from sediment by cesium competing cations (e.g., K^+ and NH_4^+), which can be released in anoxic settings, associated with the wetland ecosystems (Ries et al., 2019; Funaki et al., 2022). For example, NH_4^+ that is formed by the decomposition of organic matter under anaerobic environments (e.g., wetlands) could be a more important competing ion to Cs^+ than K^+ because NH_4^+ is nearly five times more selectively bound to clay particles compared to K^+ (Wauters et al., 1996); NH_4^+ is therefore more likely to displace Cs^+ from binding sites. Remobilization of ^{137}Cs can also occur by foliar absorption of Cs^+ by aquatic macrophytes (e.g., vascular plants, mosses, and algal bloom) (Sarosik et al., 1980; Pinder et al., 2006). Moreover, the feeding habits of ducks on algal blooms can create a dynamic connection among different wetland areas, resulting in the movement of nutrients (e.g., carbon, nitrogen, and phosphorus) as well as ^{137}Cs out of the system, although it is likely a small portion of the "missing" ^{137}Cs inventory.

3.4.3. Soil erosion and sedimentation rates

Table 3.2 presents the mean ^{137}Cs loss/gain and point-based soil erosion and deposition rates using the MBM2 and non-eroded off-site reference ^{137}Cs values along the transects within the wetland catchments. The soil erosion rates are presented as positive values, while the deposition rates as negative values. The mean soil erosion rate within the boundary of the cultivated field was 1.7 kg m^{-2} yr^{-1} in Manitoba and 1.2 kg m^{-2} yr^{-1} in Alberta. If each transect represents a 1-m wide strip, the total soil loss from the eroding area of the cultivated field was estimated at 18 kg yr^{-1} in Manitoba and 22 kg yr^{-1} in Alberta. The eroding zone covered around 73% of the upland field area in both provinces, mostly located in the upper and middle slope positions. The mean soil erosion rates in the cultivated field decreased downslope (see Table 3.2), providing evidence of the downslope movement of the eroded soil and deposited in the lowest part of the slope (lower slope and outer riparian/wet meadow areas) at rates of -1.7 kg m^{-2} yr^{-1} in Manitoba and -1.5 kg m^{-2} yr^{-1} in Alberta. The depositing zone covered the remaining 27% of the upland field area. The nature of the presented results in this section will be discussed in the next section (3.4.) to further characterize soil redistribution within wetland catchments. Appendix A-A8 displays detailed results for individual wetland catchments in Manitoba and Alberta.

Table 3. 2. Point soil loss and deposition rates within the wetland catchments using ^{137}Cs reference value estimated from individual local stable sites.

Province	Toposequence Position	Number of cores	^{137}Cs inventory (Bq m^{-2})	^{137}Cs loss or gain (% of reference ^{137}Cs)	Soil loss (+) or deposition (-) (kg m^{-2} yr^{-1})			Sedimentation rate (kg m^{-2} yr^{-1})[4]
					Power model[1]	Power model[2]	Linear model[3]	
Individual reference site								
Manitoba	Flat landscape	9	1430	-	-	-	-	-
Alberta	Flat landscape	24	1684	-	-	-	-	-
Cultivated catchments								
Manitoba	Upper Slope	12	569	39.8	2.6	-	2.4	-
Manitoba	Middle Slope	12	1055	73.8	0.8	-	1.0	-
Manitoba	Lower Slope	12	2493	174.3	-2.9	-	-2.9	2.0
Manitoba	Outer Riparian	12	2782	194.5	-3.7	-	-3.7	2.3
Manitoba	Inner Riparian	9	1606	112.3	-0.5	-	-0.5	1.4
Manitoba	Inner Wetland	12	1240	86.7	0.3	-	0.4	1.0
Native prairie								
Manitoba	Upper Slope	3	1580	110.5	-	n.d.	n.d.	1.1
Manitoba	Middle Slope	3	2116	148.0	-	n.d.	n.d.	0.8
Manitoba	Lower Slope	3	426	29.8	-	7.4	2.8	0.0
Manitoba	Inner Riparian	3	1011	70.7	-	2.1	1.2	0.3
Manitoba	Inner Wetland	3	557	39.0	-	5.6	2.4	1.0
Cultivated catchments								
Alberta	Upper Slope	9	940	55.9	1.5	-	1.5	-
Alberta	Middle Slope	9	1152	68.6	0.9	-	1.1	-
Alberta	Lower Slope	9	1896	112.9	-0.4	-	-0.4	1.4
Alberta	Outer Riparian	9	1831	109.0	-0.3	-	-0.3	2.1
Alberta	Middle Riparian	9	1460	86.9	0.4	-	0.5	2.8
Alberta	Inner Riparian	9	1506	89.6	0.3	-	0.4	1.3
Alberta	Outer Wetland	9	1331	79.2	0.6	-	0.7	1.3
Alberta	Middle Wetland	9	913	54.4	1.5	-	1.6	1.3
Alberta	Inner Wetland	9	1318	78.5	0.6	-	0.7	1.8

[1]Power model: Mass Balance Model (MBM2) was used for wetland embedded within agricultural landscape.
[2]Power model: Profile Distribution Model was used for wetlands embedded in native prairie.
[3]Linear model: Proportional Model was used for wetlands embedded in agricultural and native prairie landscapes.
[4]Sedimentation rate was calculated using the peak of ^{137}Cs activity.
n.d.: not determined by developed excel add-in software.

3.4.4. Soil loss and accumulation budgets

Table 3.3 displays the mean ^{137}Cs loss/gain and point-based soil erosion and deposition rates using the PM and catchment-level (on-site) reference ^{137}Cs values along the transects within each wetland catchment (see Appendix A-A9 for individual wetland catchments' results in Manitoba and Alberta). Most of the exported sediment beyond the cultivated field was deposited in the riparian areas and a small amount of sediment moved to the open water or pond center.

Table 3. 3. Point soil loss and deposition rates within the wetland catchments using catchment-level ^{137}Cs reference value.

Province	Toposequence Position	Number of cores	^{137}Cs inventory (Bq m^{-2})	^{137}Cs loss or gain (% of reference ^{137}Cs)	Soil loss (+) or deposition (-) (kg m^{-2} yr^{-1})			Sedimentation rate (kg m^{-2} yr^{-1})[4]
					Power model[1]	Power model[2]	Linear model[3]	
Cultivated catchments								
Catchment-level ref. ^{137}Cs			**1310**					
Manitoba	Upper Slope	12	569	50.7	2.3	-	2.2	-
Manitoba	Middle Slope	12	1055	80.2	0.6	-	0.8	-
Manitoba	Lower Slope	12	2493	182.5	-3.4	-	-3.6	2.0
Manitoba	Outer Riparian	12	2782	239.2	-4.3	-	-4.4	2.3
Manitoba	Inner Riparian	9	1606	116.2	-0.7	-	-0.9	1.4
Manitoba	Inner Wetland	12	1240	117.7	0.1	-	0.1	1.0
Native prairie								
Catchment-level ref. ^{137}Cs			**1460**					
Manitoba	Upper Slope	3	1580	109.0	-	n.d	n.d	1.1
Manitoba	Middle Slope	3	2116	145.9	-	n.d	n.d	0.8
Manitoba	Lower Slope	3	426	29.4	-	7.5	2.8	0.0
Manitoba	Inner Riparian	3	1011	69.7	-	2.2	1.2	0.3
Manitoba	Inner Wetland	3	557	38.4	-	5.7	2.4	1.0
Cultivated catchments								
Catchment-level ref. ^{137}Cs			**1221**					
Alberta	Upper Slope	9	940	77.4	0.6	-	0.8	-
Alberta	Middle Slope	9	1152	94.2	0.1	-	0.2	-
Alberta	Lower Slope	9	1896	154.1	-1.5	-	-1.9	1.4
Alberta	Outer Riparian	9	1831	149.6	-1.4	-	-1.7	2.1
Alberta	Middle Riparian	9	1460	120.1	-0.5	-	-0.7	2.8
Alberta	Inner Riparian	9	1506	122.2	-0.6	-	-0.8	1.3
Alberta	Outer Wetland	9	1331	114.2	-0.2	-	-0.3	1.3
Alberta	Middle Wetland	9	913	75.7	0.7	-	0.9	1.3
Alberta	Inner Wetland	9	1318	108.3	-0.2	-	-0.3	1.8

[1]Power model: Mass Balance Model (MBM2) was used for wetland embedded within agricultural landscape.
[2]Power model: Profile Distribution Model was used for wetlands embedded in native prairie.
[3]Linear model: Proportional Model was used for wetlands embedded in agricultural and native prairie landscapes.
[4]Sedimentation rate was calculated using the peak of ^{137}Cs activity.
n.d.: not determined by developed excel add-in software.

Furthermore, Fig. 3.8a and b clearly show that there is evidence of both soil loss and deposition within the wetland catchments. The mean soil erosion rate in the cultivated fields was 1.2 kg m^{-2} yr^{-1} (gross erosion rate of 1.1 kg m^{-2} yr^{-1}) for Manitoba and 0.3 kg m^{-2} yr^{-1} (gross erosion rate of

0.3 kg m^{-2} yr^{-1}) for Alberta. The mean soil deposition rates within the boundary of cultivated fields were -3.6 kg m^{-2} yr^{-1} (gross deposition rate of -0.4 kg m^{-2} yr^{-1}) for Manitoba, whereas those for Alberta were around -1.9 and -0.2 kg m^{-2} yr^{-1}, respectively. The overall net soil loss rates associated with the cultivated field was about 0.6 (equivalent to 12,287 kg yr^{-1}) and 0.1 (equivalent to 3,530 kg yr^{-1}) kg m^{-2} yr^{-1} in Manitoba and Alberta, respectively (see Appendix for detailed results on sediment budgets for individual wetland catchments in Manitoba (Appendix A-A10) and Alberta (Appendix A-A11)). The resulting sediment delivery ratio, which corresponds to the ratio of the net sediment output to the gross erosion, was around 57% and 35% in Manitoba and Alberta, respectively. This indicates that a relatively high amount of the mobilized sediment was exported beyond the cultivated fields towards the wetland ecosystems, mostly deposited in riparian areas. Furthermore, the disparity between soil erosion rates in Manitoba and Alberta could be attributed to regional farming practices (e.g., tillage equipment) in different provinces, and differences in sediment deposition caused by changing land use. In addition, considering the variable climate and the alternating drawdown and emergent phases of PPR wetlands, constant sedimentation rates seem unlikely (Freeland, 1999). Previous studies in Canada (e.g., Kachanoski et al., 1992; Lobb et al., 1995; Lobb and Kachanoski, 1999; Li et al., 2007a; Tiessen et al., 2009) have found that soil erosion rates from cultivated fields ranged from 2.5 to 15 kg m^{-2} yr^{-1} exceeding the soil loss tolerance limit of 0.6 kg m^{-2} yr^{-1} (~ 6 t ha^{-1}) that is typically considered sustainable for most soils in Canada (van Vliet et al., 2005), and that the soil deposition rates in cultivated fields ranged from -2.7 to -15.4 kg m^{-2} yr^{-1}. Additionally, in accordance with the present results, a study by Freeland et al. (1999) in Stutsman County, North Dakota, USA reported that the mean soil erosion and deposition rates ranged from 3.5 to -1.6 kg m^{-2} yr^{-1} within cultivated fields surrounding the northern prairie wetlands.

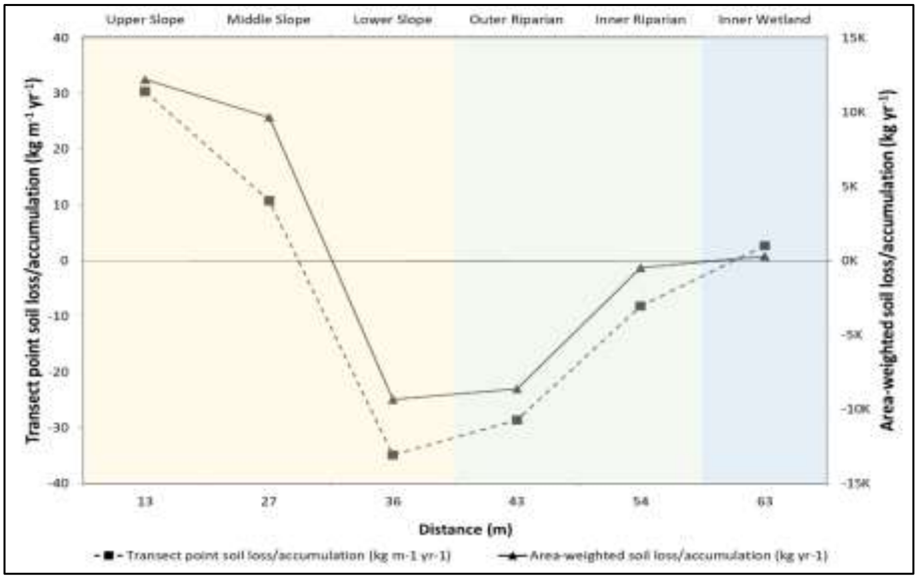

(a)

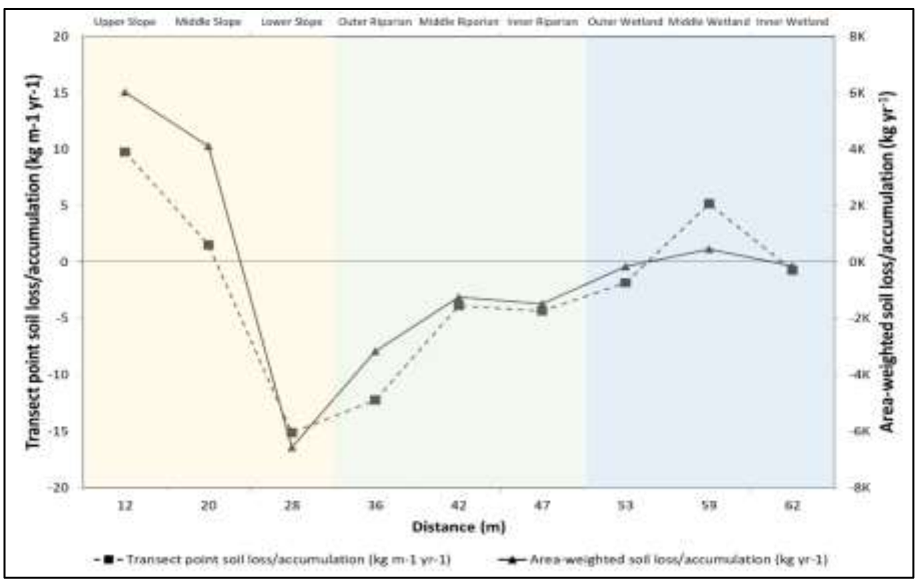

(b)

Fig. 3. 8. Soil redistribution assessment estimated from ^{137}Cs measurement along transects using catchment-level reference value and PM in Manitoba (a) and Alberta (b).

Within the wetland ecosystems (riparian area and water body), total soil deposition rates were -3.6 kg m^{-2} yr^{-1} in Manitoba and -0.9 kg m^{-2} yr^{-1} in Alberta, respectively. Overall, the results confirm that the upper and middle slope positions are indeed net sediment exporting units, and that the lower slope position and riparian area experienced deposition. These findings indicate that almost all the exported sediment beyond the cultivated field deposited in riparian area with only a small amount of sediment moving to the central open water area of the wetlands. Research conducted by VandenBygaart et al. (2012) within depositional areas in different agroecosystems across Canada including Alberta, Saskatchewan, Manitoba, Ontario, New Brunswick, and Prince Edward Island, reported that soil deposition rates ranging between -4.0 and -15.2 kg m^{-2} yr^{-1}, with the greatest rates occurring in New Brunswick and Saskatchewan. The findings of this study compare favourably with those of Craft and Casey (2000), who studied deposition rates in depressional wetlands in Baker County, Georgia, USA and reported average soil deposition rates of -0.12 kg m^{-2} yr^{-1} and -0.95 kg m^{-2} yr^{-1} using ^{137}Cs (~ 30 years) and $^{210}Pb_{ex}$ (~ 100 years). However, the findings of this study do not compare favourably with those of Buris and Skagen (2013) and Skagen et al. (2016), who concluded that a large percentage of wetlands (e.g., depressional and playas) would be filled by > 50% with sediment within the next 100 years.

The estimates of soil erosion and deposition rates were sensitive to the conversion model. The results acquired by the PM in this study could be seen as being more realistic, in spite of the fact that the PM is the simplest model and requires little input data, avoiding large errors introduced in soil erosion estimations. The model's simplicity could be important, especially if the model is to be used to establish sediment budgets for catchments. Although the MBM2 requires the most comprehensive set of input data that can lead to the introduction of errors, the model normally provides the most realistic results for the area of maximum loss within the catchment.

There are uncertainties associated with the ^{137}Cs-estimated erosion rates derived from the reference ^{137}Cs levels. The conversion models were highly sensitive to the input values of the reference ^{137}Cs and tillage depth. Two reference ^{137}Cs values (off-site and on-site reference ^{137}Cs levels) were used to estimate point-based soil erosion rates and sediment budgets. The on-site and off-site reference

^{137}Cs levels were close, especially in Manitoba (See tables 3.2 and 3.3 for ^{137}Cs reference values), which confirms the almost "closed" material cycles of the catchments. Off-site reference ^{137}Cs levels may be biased, due to local and regional variability of ^{137}Cs fallout, which can be reduced by taking multiple samples within a site (Li et al., 2011a). Therefore, in a closed system (e.g., depressional wetlands), on-site reference ^{137}Cs can lead to more accurate erosion rate estimates, in spite of random errors associated with this method. However, the random errors can be reduced by increasing the number of cores per site and using the spatially averaged erosion rates for data interpretation.

3.4.5. Sedimentary features

Linear sedimentary features, also known as lynchets, were observed within the studied wetland catchments surrounded by cultivated fields in the unsmoothed 1-m DEMs. There was a break-in the slope that was 2- to 8-m wide and reached about 0.15- to 0.3-m height, creating a discontinuity in the landscape. The sedimentary features were oriented perpendicularly to the steepest slope and were predominantly shaped by the progressive accumulation of soil materials at the bottom of the slope by tillage, water, and wind erosion (see Fig. 3.9). The mean mass of soil materials stored in the sedimentary features was estimated at ~ -131,000 kg for Manitoba and -114,000 kg for Alberta, representing < 1% by mass of the total soil material present in the studied catchments in both provinces. The results showed that the DEM-estimated soil accumulation was not consistent with the ^{137}Cs-estimated net soil loss associated with the cultivated field. However, given the amount of soil stored at the bottom of the slope and mainly profile of the depositional feature, it can be attributed to tillage erosion process. In addition, it has been documented that with each tillage pass, the tillage ridge/berm height increases while the berm's top width decreases (Fig. 3.9c) (Vieira and Dabney, 2011). Furthermore, the evaluation of DEMs revealed that one wetland catchment in

Alberta (Wetland INT1) had no detectable tillage-induced berms or lynchet, which could have resulted in the deposition of sediment further down-gradient. However, spatial variation of ^{137}Cs inventory values along transects (Fig. 3.6) indicated that most of the mobilized sediment was deposited in the outer riparian or wet meadow area within this wetland catchment. Several reasons might have contributed to the formation and continued reinforcement of tillage berms in one field and not in the other such as farming practices.

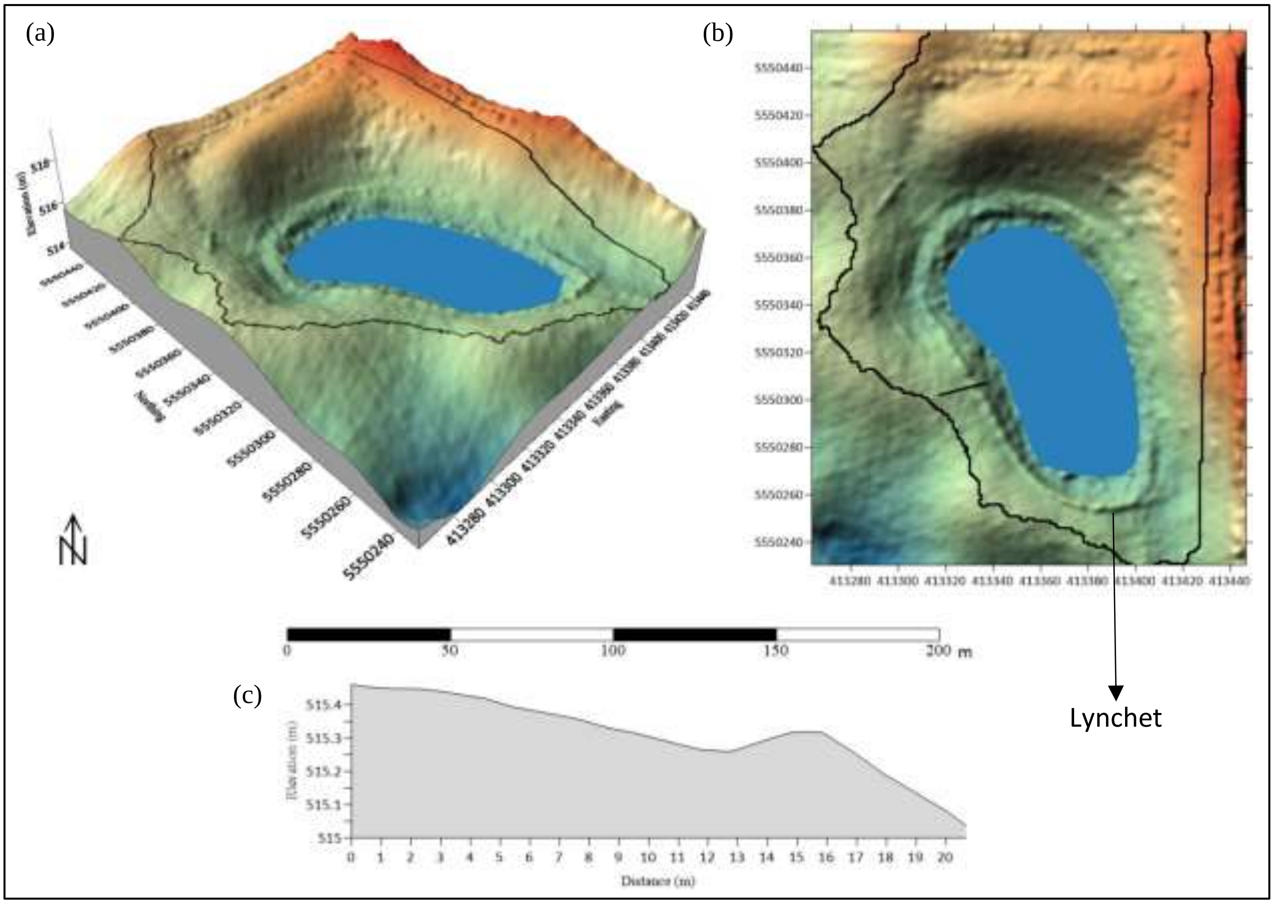

Fig. 3. 9. Original unsmoothed 1-m DEM of one wetland catchment: (a) three-dimensional (3D) view of the catchment, (b) colour relief view of the catchment and (c) geometrical characteristics of the sedimentary features for the shown transect in the colour relief view.

Lynchets are common in the depressional wetlands of the Canadian Prairies. Interaction between erosion and deposition processes at the interface between the cultivated field and the riparian area can lead to the development of sedimentary features of several meters in width (e.g., tillage ridges/berms and steps, headlands, and lynchets). In other studies, lynchets had a mean thickness of ~1.08 m and contained ~15% of the total soil material in the studied field (Chartin et al. 2011). These lynchets acted as barriers to water and sediment fluxes, and sites of large carbon sequestration within cultivated hillslopes (Chartin et al., 2013; Zádorová et al., 2018).

3.4.6. Potential error sources in discrimination of sedimentary features using LiDAR DEM

Identifying and understanding the limitations of the LiDAR-based estimation of soil accumulation in the lynchet areas at the lower part of hillslopes is necessary for improving estimation accuracy and establishing standard estimation designs and procedures. The advantages that LiDAR technology provides for the identification of sedimentary features include: accurate and high-resolution DEM data, a relatively cost- and time-effective method of data collection, the capability of penetrating vegetation; and an adequate representation of human-induced and topographic features. However, there are several factors that can contribute to uncertainties associated with this method. The accuracy of DEMs can be impacted by the interpolation methods and the filtering algorithm to categorize LiDAR points as ground or non-ground (Simpson et al., 2017). In addition, transformation of raw LiDAR points into elevation surfaces requires interpolation from points onto a grid cell, which can present a level of uncertainty into DEMs, although LiDAR points are collected at very short separation distances (Sailer et al., 2013). The uncertainty associated with grid size variations for resampling can also impact a DEM's accuracy. The accuracy of DEMs can also be affected by the shape of the interpolator than the actual terrain (e.g., interpolation artifacts will become significant) (Albani et al., 2004). Most accurate DEMs can be generated from grids, which have an identical spacing to the original points. The vertical accuracy of DEMs can also be affected by the field conditions including vegetation cover and morphological properties (e.g., slope gradient and surface roughness). Dense canopy vegetation can lead to large vertical errors in

LiDAR derived DEMs due to the reduced ground point density (Sailer et al., 2013; Salekin et al., 2018). Furthermore, horizontal-scanning LiDAR can do well to go through dense canopy (e.g., forests), but vertical or airborne LiDAR can be affected by vegetation density. Recently, advances in new technologies, such as ground-based LiDAR and backpack LiDAR will hopefully improve the accuracy of ground surveys.

3.5. Conclusions

Identifying areas according to the level of soil erosion risk is imperative in agriculture-intensive regions such as the Canadian PPR. This study attempted a comprehensive overview of soil erosion in wetlandscapes using a ^{137}Cs tracer to provide important insights into the rates and processes of erosion acting on the hummocky landscapes. The results showed that ^{137}Cs inventories at all the sampling points on the upper and middle slope positions were reduced relative to the reference inventories in both provinces, indicating that erosion had occurred. In addition, the inventory of ^{137}Cs decreased with depth and its penetration increased along the slope and became higher in the depositional areas. These results clearly show increased soil loss in the upland catchments (upper and middle slope positions) of wetlands surrounded by cropland, with deposition occurring on the lower slope position and riparian areas. Additionally, with increased soil redistribution within cropland catchments, there might be considerable potential for soil carbon movement along toposequence positions towards the wetland ecosystem resulting in carbon sequestration in the riparian area surrounding the wetland. The large quantities of soil redistributed in these landscapes indicate that a large part of eroded soil remains within the field and/or field-riparian borders, which is attributed to tillage erosion. Furthermore, little sediment is delivered to the central open water of wetlands, which suggests that the accumulation of carbon at the center of the wetland basin is more likely autochthonous in nature and generated by the accumulation of plant and algal litter.

As the average annual soil erosion rates for the studied catchments were found to be higher than the tolerable value of soil loss, well-planned watershed management activities are vital to restoring degraded areas and combating soil erosion from the watershed. Improvement of erosion control measures, which are feasible and can be easily implemented by the agricultural producers (e.g., counter tillage, topsoil replacement, buffer strips and riparian corridors), can assist to counteract the downward soil redistribution and maintain the field erosion rate within the tolerance limit. Further modelling studies are necessary for better understanding of soil redistribution and erosion processes within cultivated Prairie landscapes.

3.6. References

Albani, M., Klinkenberg, B., Andison, D.W., Kimmins, J.P., 2004. The choice of window size in approximating topographic surfaces from Digital Elevation Models. Int. J. Geogr. Inf. Sci. 18, 577-593. https://doi.org/10.1080/13658810410001701987

Alberta soil survey report, 1985. Soil Survey of the County of Two Hills No. 21, Alberta. Terrain Sciences Department, Natural Resources Division, Alberta Research Council, Edmonton, Alberta, Canada. URL https://sis.agr.gc.ca/cansis/publications/surveys/ab/ab35/index.html (accessed 11.01.2022)

Baldwin, C.D.G., 2015. An assessment of wind erosion on highly sensitive soil landscapes in the Canadian prairies. (Master's dissertation). University of Manitoba, Winnipeg.

Basher, L.R., Matthews, K.M., 1993. Relationship between ^{137}Cs in some undisturbed new zealand soils and rainfall. Aust. J. Soil Res. 31, 655-663. https://doi.org/10.1071/SR9930655

Blake, G.R., Hartge, K.H., 1986. Bulk Density. In: Klute, A. (Ed.), Methods of Soil Analysis. John Wiley & Sons, Ltd, pp. 363–375. https://doi.org/10.2136/ sssabookser5.1.2ed.c13.

Bourne, A., Armstrong, N., Jones, G.. 2002. A preliminary estimate of total nitrogen and total phosphorus loading to streams in Manitoba, Canada. Rep. 2002-2004. Water Qual. Manage. Sect., Manitoba Conservation, Winnipeg, Manitoba, Canada.

Burris, L., Skagen, S.K., 2013. Modeling sediment accumulation in North American playa wetlands in response to climate change, 1940-2100. Clim. Change 117, 69-83. https://doi.org/10.1007/s10584-012-0557-7

Chabot, M., Lindsay, J., Rowlandson, T., Berg, A.A., 2018. Comparing the use of terrestrial LiDAR scanners and pin profilers for deriving agricultural roughness statistics. Can. J. Remote Sens. 44, 153-168. https://doi.org/10.1080/07038992.2018.1461559

Chartin, C., Bourennane, H., Salvador-Blanes, S., Hinschberger, F., Macaire, J.J., 2011. Classification and mapping of anthropogenic landforms on cultivated hillslopes using DEMs and soil thickness data - Example from the SW Parisian Basin, France. Geomorphology 135, 8-20. https://doi.org/10.1016/j.geomorph.2011.07.020

Chartin, C., Evrard, O., Salvador-Blanes, S., Hinschberger, F., Van Oost, K., Lefèvre, I., Daroussin, J., Macaire, J.J., 2013. Quantifying and modelling the impact of land consolidation and field borders on soil redistribution in agricultural landscapes (1954-2009). Catena 110, 184-195. https://doi.org/10.1016/j.catena.2013.06.006

Collins, A.L., Walling, D.E., Sichingabula, H.M., Leeks, G.J.L., 2001. Using ^{137}Cs measurements to quantify soil erosion and redistribution rates for areas under different land use in the Upper Kaleya River basin, southern Zambia. Geoderma 104, 299-323. https://doi.org/10.1016/S0016-7061(01)00087-8

Craft, C.B., Casey, W.P., 2000. SedimCraft, C. B., Casey, W. P., 2000. Sediment and nutrient accumulation in floodplain and depressional freshwater wetlands of Georgia, USA. Wetlands, 20(2), 323-332. https://doi.org/10.1672/0277-5212(2000)020[0323:SANAIF]2.0.CO;2ent and nutrient accu. Wetlands 20, 323-332.

Creed, I.F., Badiou, P., Enanga, E., Lobb, D.A., Pattison-Williams, J.K., Lloyd-Smith, P., Gloutney, M., 2022. Can restoration of freshwater mineral soil wetlands deliver naturebased climate solutions to agricultural landscapes? Front. Ecol. Evol. 10, 1–12. https://doi.org/10.3389/fevo.2022.932415

Creed, I.F., Lane, C.R., Serran, J.N., Alexander, L.C., Basu, N.B., Calhoun, A.J.K., Christensen, J.R., Cohen, M.J., Craft, C., D'Amico, E., De Keyser, E., Fowler, L., Golden, H.E., Jawitz, J.W., Kalla, P., Katherine Kirkman, L., Lang, M., Leibowitz, S.G., Lewis, D.B., Marton, J., McLaughlin, D.L., Raanan-Kiperwas, H., Rains, M.C., Rains, K.C., Smith, L., 2017. Enhancing protection for vulnerable waters. Nat. Geosci. 10, 809–815. https://doi.org/10.1038/NGEO3041

Cucchiaro, S., Paliaga, G., Fallu, D.J., Pears, B.R., Walsh, K., Zhao, P., Van Oost, K., Snape, L., Lang, A., Brown, A.G., Tarolli, P., 2021. Volume estimation of soil stored in agricultural terrace systems: A geomorphometric approach. Catena 207, 105687. https://doi.org/10.1016/j.catena.2021.105687

Dahl, T.E., Watmough, M.D., 2007. Current approaches to wetland status and trends monitoring in prairie Canada and the continental United States of America. Can. J. Remote Sens. 33, S17-S27. https://doi.org/10.5589/m07-050

Dalzell, B.J., Fissore, C., Nater, E.A., 2022. Topography and land use impact erosion and soil organic carbon burial over decadal timescales. Catena 218, 106578. https://doi.org/10.1016/j.catena.2022.106578

de Jong, E., Begg, C.B.M., Kachanoski, R.G., 1983. Estimates of soil erosion and deposition for some Saskatchewan soils. Can. J. of Soil Sci. 63, 607-617. https://doi.org/10.4141/cjss83-061

Dercon, G., Mabit, L., Hancock, G., Nguyen, M.L., Dornhofer, P., Bacchi, O.O.S., Benmansour, M., Bernard, C., Froehlich, W., Golosov, V.N., Haciyakupoglu, S., Hai, P.S., Klik, A., Li, Y., Lobb, D.A., Onda, Y., Popa, N., Rafiq, M., Ritchie, J.C., Schuller, P., Shakhashiro, A., Wallbrink, P., Walling, D.E., Zapata, F., Zhang, X., 2012. Fallout radionuclide-based techniques for assessing the impact of soil conservation measures on erosion control and soil quality: An overview of the main lessons learnt under an FAO/IAEA Coordinated Research Project. J. Environ. Radioact. 107, 78-85. https://doi.org/10.1016/j.jenvrad.2012.01.008

Doherty, K.E., Howerter, D.W., Devries, J.H., 2016. The Wetland Book. Wetl. B. 1-10. https://doi.org/10.1007/978-94-007-6173-5

Environment Canada, 1996. The state of Canada's environment. URL https://publications.gc.ca/site/eng/9.881686/publication.html (accessed 5.12.2022)

Environment and Climate Change Canada (ECCC)., 2022. 1981-2010 climate normals and averages. Canadian climate normals. URL https://climate.weather.gc.ca/climate_normals/index_e.html. (accessed 5.12.2022)

Estrany, J., Garcia, C., Walling, D.E., 2010. An investigation of soil erosion and redistribution in a Mediterranean lowland agricultural catchment using caesium-137. Int. J. Sediment Res. 25, 1-16. https://doi.org/10.1016/S1001-6279(10)60023-6

Evrard, O., Chaboche, P.A., Ramon, R., Foucher, A., Laceby, J.P., 2020. A global review of sediment source fingerprinting research incorporating fallout radiocesium (^{137}Cs). Geomorphology 362, 107103. https://doi.org/10.1016/j.geomorph.2020.107103

Freeland, J.A., Richardson, J.L., Foss, L.A. 1999. Soil indicators of agricultural impacts on northern prairie wetlands: Cottonwood lake research area, north Dakota, USA. Wetlands 19, 56-64. https://doi-org.uml.idm.oclc.org/10.1007/BF03161733

Funaki, H., Tsuji, H., Nakanishi, T., Yoshimura, K., Sakuma, K., Hayashi, S., 2022. Remobilisation of radiocaesium from bottom sediments to water column in reservoirs in Fukushima, Japan. Sci. Total Environ. 812, 152534. https://doi.org/10.1016/j.scitotenv.2021.152534

Gaspar, L., Navas, A., Walling, D.E., Machín, J., Gómez Arozamena, J., 2013. Using ^{137}Cs and 210Pbex to assess soil redistribution on slopes at different temporal scales. Catena 102, 46-54. https://doi.org/10.1016/j.catena.2011.01.004

Glozier, N.E., Elliott, J.A., Holliday, B., Yarotski, J., Harker, B.. 2006. Water quality characteristics and trends in a small agricultural watershed: South Tobacco Creek, Manitoba, 1992-2001. Environment Canada. Ottawa, Ontario, Canada.

Godone, D., Giordan, D., Baldo, M., 2018. Rapid mapping application of vegetated terraces based on high resolution airborne lidar. Geomatics, Nat. Hazards Risk 9, 970-985. https://doi.org/10.1080/19475705.2018.1478893

Goharrokhi, M., McCullough, G.K., Owens, P.N., Lobb, D.A., 2021. Sedimentation dynamics within a large shallow lake and its role in sediment transport in a continental-scale watershed. J. Great Lakes Res. 47, 725-740. https://doi.org/10.1016/j.jglr.2021.03.022

Haines, H.A., 2012. Changes in the hydrological regime in the Upper Bow and Upper Athabasca Watersheds during the 20th century. (Master's dissertation). University of Western Ontario, London.

He, Q., Walling, D.E., 1996. Interpreting particle size effects in the adsorption of ^{137}Cs and unsupported ^{210}Pb by mineral soils and sediments. J. Environ. Radioact. 30, 117–137. https://doi.org/https://doi.org/10.1016/0265-931X(96)89275-7

Hopkinson, C.S., 1992. A comparison of ecosystem dynamics in freshwater wetlands. Estuaries

15, 549-562. https://doi.org/10.2307/1352397

Howitt RW., 1988. Soil survey of the County of Beaver (Vol. 47): Alberta soil survey report. URL https://open.alberta.ca/publications/ss-47 (accessed 5.12.2022)

Hugenholtz, C.H., Brown, O.W., Barchyn, T.E., 2013. Estimating aerodynamic roughness (z_0) from terrestrial laser scanning point cloud data over un-vegetated surfaces. Aeolian Res. 10, 161-169. https://doi.org/10.1016/j.aeolia.2013.03.004

Jelinski, N.A., Campforts, B., Willenbring, J.K., Schumacher, T.E., Li, S., Lobb, D.A., Papiernik, S.K., Yoo, K., 2019. Meteoric Beryllium-10 as a tracer of erosion due to postsettlement land use in west-central Minnesota, USA. J. Geophys. Res. Earth Surf. 124, 874-901. https://doi.org/10.1029/2018JF004720

Johnston, C.A., 1991. Critical Reviews in Environmental control sediment and nutrient retention by freshwater wetlands : Effects on surface water quality sediment and nutrient retention by freshwater wetlands : Effects on surface water quality. Crit. Rev. Environ. Control 37-41.

Kachanoski, R.G., Protz, R.D., Gregorich, E.G., 1992. Management of farm field variability. I. Quantification of soil loss in complex topography, in: Kachanoski, R.G., Miller, M.H., Lobb, D.A., Protz, R.D., Gregorich, E.G. (Eds.), Management of Farm Field Variability, SWEEP/TED report No. 38. Centre for Soil and Water Conservation, University of Guelph, Guelph, p. 156.

Kaste, J.M., Heimsath, A.M., Hohmann, M., 2006. Quantifying sediment transport across an undisturbed prairie landscape using cesium-137 and high resolution topography. Geomorphology 76, 430-440. https://doi.org/10.1016/j.geomorph.2005.12.007

Lane, C.R., Autrey, B.C., 2017. Sediment accretion and accumulation of P, N and organic C in depressional wetlands of three ecoregions of the United States. Mar. Freshw. Res. 68, 2253-

2265. https://doi.org/10.1071/MF16372

Langewitz, T., Wiedner, K., Polifka, S., Eckmeier, E., 2021. Pedological properties related to formation and functions of ancient ridge and furrow cultivation in Central and Northern Germany. Catena 198, 105049. https://doi.org/10.1016/j.catena.2020.105049

LaZerte, S., Li, S., 2021. LITAP: Landscape Integrated Terrain Analysis Package. R package version 0.6.0, https://github.com/FRDC-SHL/LITAP.

Li, S., 2021. Landscape Integrated Soil and Water Conservation (LISWC) system for sloping landscapes in Atlantic Canada. Agric. 11. https://doi.org/10.3390/agriculture11050427

Li, S., Lobb, D.A., Lindstrom, M.J., Farenhorst, A., 2008. Patterns of water and tillage erosion on topographically complex landscapes in the North American Great Plains. J. Soil Water Conserv. 63, 37-46. https://doi.org/10.2489/63.1.37

Li, S., Lobb, D.A., Lindstrom, M.J., Farenhorst, A., 2007a. Tillage and water erosion on different landscapes in the northern North American Great Plains evaluated using ^{137}Cs technique and soil erosion models. Catena 70, 493-505. https://doi.org/10.1016/j.catena.2006.12.003

Li, S., Lobb, D.A., McConkey, B.G., Walker, B., Goddard, T., 2007b. Tillage and water erosion under different tillage systems in Alberta, Canada. In ASA-CSSA-SSSA International Annual Meetings (November 4-8, 2007). ASA-CSSA-SSSA

Li, S., Lobb, D.A., Tiessen, K.H.D., 2009. Modeling tillage-induced morphological features in cultivated landscapes. Soil Tillage Res. 103, 33-45. https://doi.org/10.1016/j.still.2008.09.005

Li, S., Lobb, D.A., Tiessen, K.H.D., McConkey, B.G., 2010. Selecting and applying Cesium-137 conversion models to estimate soil erosion rates in cultivated fields. J. Environ. Qual. 39, 204-219. https://doi.org/10.2134/jeq2009.0144

Li, S., Lobb, D.A., Kachanoski, R.G., McConkey, B.G., 2011a. Comparing the use of the traditional and repeated-sampling-approach of the ^{137}Cs technique in soil erosion estimation. Geoderma 160, 324–335. https://doi.org/10.1016/j.geoderma.2010.09.029

Li, S., MacMillan, R.A., Lobb, D.A., McConkey, B.G., Moulin, A., Fraser, W.R., 2011b. Lidar DEM error analyses and topographic depression identification in a hummocky landscape in the prairie region of Canada. Geomorphology 129, 263-275. https://doi.org/10.1016/j.geomorph.2011.02.020

Liu, H., Jezek, K.C., 1999. Investigating DEM error patterns. Geogr. Anal. 31, 249-266.

Liu, K., Elliott, J.A., Lobb, D.A., Flaten, D.N., Yarotski, J., 2013. Critical factors affecting field-scale losses of nitrogen and phosphorus in spring snowmelt runoff in the Canadian Prairies. J. Environ. Qual. 42, 484-496. https://doi.org/10.2134/jeq2012.0385

Lobb, D.A., 2011. Understanding and managing the causes of soil variability. J. Soil Water Conserv. 66, 175-179. https://doi.org/10.2489/jswc.66.6.175A

Lobb, D.A., Kachanoski, R.G., 1997. The impact of tillage translocation and tillage erosion on the estimation of soil loss using ^{137}Cs. Poster presentation at Soil and Water Conservation Society, Annual Conference, 1st International Symposium on Tillage Translocation and Tillage Erosion. Toronto, Ontario, Canada. July 1997.

Lobb, D.A., Badreldin, N., Loro, M., Li, S., McConkey, B.G., 2017.Soil degradation: The cost to agriculture and the economy. Summit on Canadian Soil Health. Soil Conservation Council of Canada. Guelph, Ontario, Canada. August 2017.

Lobb, D.A., Huffman, E., Reicosky, D.C., 2007. Importance of information on tillage practices in the modelling of environmental processes and in the use of environmental indicators. J. Environ. Manage. 82, 377-387. https://doi.org/10.1016/j.jenvman.2006.04.019

Lobb, D.A., Kachanoski, R.G., 1999. Modelling tillage erosion in the topographically complex landscapes of southwestern Ontario, Canada. Soil Tillage Res. 51, 261–277. https://doi.org/10.1016/S0167-1987(99)00042-2

Lobb, D.A., Kachanoski, R.G., Miller, M.H., 1995. Tillage translocation and tillage erosion on shoulder slope landscape positions measured using ^{137}Cs as a tracer. Can. J. Soil Sci. 75, 211-218. https://doi.org/10.4141/cjss95-029

Lobb, D.A., Lindstrom, M.J., Schumacher, T.E., 2003. Soil erosion processes and their interactions: implications for environmental indicators, in: Agricultural Impacts on Soil Erosion and Soil Biodiversity: Developing Indicators for Policy Analysis. Proceedings from an OECD Expert Meeting-Rome, Italy, March. 325-336.

MacMillan, R.A., Martin, T.C., Earle, T.J., Mc Nabb, D.H., 2003. Automated analysis and classification of landforms using high-resolution digital elevation data: Applications and issues. Can. J. Remote Sens. 29, 592-606. https://doi.org/10.5589/m03-031

MacMillan, R.A., Pettapiece, W.W., Nolan, S.C., Goddard, T.W., 2000. A generic procedure for automatically segmenting landforms into landform elements using DEMs, heuristic rules and fuzzy logic. Fuzzy Sets Syst. 113, 81-109. https://doi.org/10.1016/S0165-0114(99)00014-7

Manitoba soil survey report, 2011. Soils of the Rural Municipality of Blanshard No. 91, Manitoba. Soil and Landscape Management Section, Agri-Environment knowledge Center, Manitoba Agriculture, Food and Rural Initiatives, Winnipeg, Manitoba, Canada. URL https://sis.agr.gc.ca/cansis/publications/surveys/mb/mbd91/index.html (accessed 11.01.2022)

Matisoff, G., Bonniwell, E.C., Whiting, P.J., 2002. Soil erosion and sediment sources in an ohio watershed using Beryllium-7, Cesium-137, and Lead-210. J. Environ. Qual. 31, 54-61.

https://doi.org/10.2134/jeq2002.5400

Meliho, M., Nouira, A., Benmansour, M., Boulmane, M., Khattabi, A., Mhammdi, N., Benkdad, A., 2019. Assessment of soil erosion rates in a Mediterranean cultivated and uncultivated soils using fallout ^{137}Cs. J. Environ. Radioact. 208-209, 106021. https://doi.org/10.1016/j.jenvrad.2019.106021

Mitsch, W.J., Gossilink, J.G., 2000. The value of wetlands: Importance of scale and landscape setting. Ecol. Econ. 35, 25-33. https://doi.org/10.1016/S0921-8009(00)00165-8

Montanarella, L., Pennock, D.J., McKenzie, N., Badraoui, M., Chude, V., Baptista, I., Mamo, T., Yemefack, M., Aulakh, M.S., Yagi, K., Hong, S.Y., Vijarnsorn, P., Zhang, G.L., Arrouays, D., Black, H., Krasilnikov, P., Sobocká, J., Alegre, J., Henriquez, C.R., Mendonça-Santos, M. de L., Taboada, M., Espinosa-Victoria, D., AlShankiti, A., AlaviPanah, S.K., Mustafa Elsheikh, E.A. El, Hempel, J., Arbestain, M.C., Nachtergaele, F., Vargas, R., 2016. World's soils are under threat. Soil. 2, 79-82. https://doi.org/10.5194/soil-2-79-2016

National Wetlands Working Group., 1988. Wetlands of Canada. Sustainable Development Branch, Environment Canada, and Polysciences Publications Inc. Ottawa, Ontario. Ecological Land Classification Series No. 24. URL https://publications.gc.ca/site/eng/9.867553/publication.html (accessed 5.12.2022)

North Saskatchewan Watershed Alliance (NSWA), 2005. State of the North Saskatchewan watershed report 2005 - A foundation for collaborative watershed management. North Saskatchewan Watershed Alliance, Edmonton, Alberta.

Owens, P.N., 2020. Soil erosion and sediment dynamics in the Anthropocene: A review of human impacts during a period of rapid global environmental change. J. Soils Sediments 20, 4115-4143. https://doi.org/10.1007/s11368-020-02815-9

Owens, P.N., Walling, D.E., 1996. Spatial variability of caesium-137 inventories at reference sites: An example from two contrasting sites in England and Zimbabwe. Appl. Radiat. Isot. 47, 699-707. https://doi.org/10.1016/0969-8043(96)00015-2

Paramonova, T., Belyaev, V., Komissarova, O., Ivanov, M., 2017. Homo/Heterogeneity of Cs-137 Vertical Distribution Within Plough Horizons of Cultivated Chernozems - 30 Years After Chernobyl Accident. RAD Assoc. J. 2. https://doi.org/10.21175/radj.2017.03.039

Penfound, E., Vaz, E., 2022. Analysis of 200 years of change in ontario wetland systems. Appl. Geogr. 138, 102625. https://doi.org/10.1016/j.apgeog.2021.102625

Pennock, D.J., 2003. Terrain attributes, landform segmentation, and soil redistribution. Soil Tillage Res. 69, 15-26. https://doi.org/10.1016/S0167-1987(02)00125-3

Pennock, D., Yates, T., Bedard-Haughn, A., Phipps, K., Farrell, R., McDougal, R., 2010. Landscape controls on N_2O and CH_4 emissions from freshwater mineral soil wetlands of the Canadian Prairie Pothole region. Geoderma 155, 308–319. https://doi.org/10.1016/j.geoderma.2009.12.015

Perroy, R.L., Bookhagen, B., Asner, G.P., Chadwick, O.A., 2010. Comparison of gully erosion estimates using airborne and ground-based LiDAR on Santa Cruz Island, California. Geomorphology 118, 288-300. https://doi.org/10.1016/j.geomorph.2010.01.009

Pinder, J.E., Hinton, T.G., Whicker, F.W., 2006. Foliar uptake of cesium from the water column by aquatic macrophytes. J. Environ. Radioact. 85, 23-47. https://doi.org/10.1016/j.jenvrad.2005.05.005

Porto, P., Walling, D.E., Cogliandro, V., Callegari, G., 2016. Exploring the potential for using $^{210}Pb_{ex}$ measurements within a re-sampling approach to document recent changes in soil redistribution rates within a small catchment in southern Italy. J. Environ. Radioact. 164, 158-

168. https://doi.org/10.1016/j.jenvrad.2016.06.026

Preston, T.M., Sojda, R.S., Gleason, R.A., 2013. Sediment accretion rates and sediment composition in Prairie Pothole wetlands under varying land use practices, Montana, United States. J. Soil Water Conserv. 68, 199 LP – 211. https://doi.org/10.2489/jswc.68.3.199

R core Team., 2020. R: A language and environment for statistical computing. R foundation for Statistical Computing, Vienna, Austria. https://www.R-project.org/.

Reddy, K.R., Clark, M.W., DeLaune, R.D., Kongchum, M., 2013. Physicochemical Characterization of Wetland Soils, in: DeLaune, R.D., Reddy, K.R., Richardson, C.J., Megonigal, J.P. (Eds), Methods in Biogeochemistry of Wetlands. John Wiley & Sons, Ltd, pp. 41-54. https://doi.org/https://doi.org/10.2136/sssabookser10.c3

Redpath, K., 1993. Reporting on the state of Canada's environment. Soc. Indic. Res. 30, 39-47. https://doi.org/10.1007/BF01080331

Rennie, D.A., 1985. Soil degradation, a western perspective. Can. J. Agric. Econ. 33, 19-29. https://doi.org/10.1111/j.1744-7976.1985.tb03229.x.

Ries, T., Putyrskaya, V., Klemt, E., 2019. Long-term distribution and migration of ^{137}Cs in a small lake ecosystem with organic-rich catchment: A case study of Lake Vorsee (Southern Germany). J. Environ. Radioact. 198, 89-103. https://doi.org/10.1016/j.jenvrad.2018.12.017

Ripley, P.O., Kalbfleisch, W., Bourget , S.J., Cooper, D.J., 1961. Soil erosion by water. Minister of Supply and Services Canada Publication 1083. URL https://atrium.lib.uoguelph.ca/xmlui/handle/10214/15182 (accessed 11.7.2022)

Sailer, R., Rutzinger, M., Rieg, L., Wichmann, V., 2013. Digital elevation models derived from airborne laser scanning point clouds: Appropriate spatial resolutions for multi-temporal characterization and quantification of geomorphological processes. Earth Surf. Process.

Landforms 39, 272-284. https://doi.org/10.1002/esp.3490

Salekin, S., Burgess, J.H., Morgenroth, J., Mason, E.G., Meason, D.F., 2018. A comparative study of three non-geostatistical methods for optimising digital elevation model interpolation. ISPRS Int. J. Geo-Information 7, 1-15. https://doi.org/10.3390/ijgi7080300

Santhi, C., Srinivasan, R., Arnold, J.G., Williams, J.R., 2006. A modeling approach to evaluate the impacts of water quality management plans implemented in a watershed in Texas. Environ. Model. Softw. 21, 1141-1157. https://doi.org/10.1016/j.envsoft.2005.05.013

Sarosik, J., Kamiński, R., Szczerbiński, K., 1980. Radiosensitivity of the moss Drepanocladus aduncus (Hedw.) Mnkm. Acta Soc. Bot. Pol. 49, 511–525.

Schmitter, P., Dercon, G., Hilger, T., Thi Le Ha, T., Huu Thanh, N., Lam, N., Duc Vien, T., Cadisch, G., 2010. Sediment induced soil spatial variation in paddy fields of Northwest Vietnam. Geoderma 155, 298-307. https://doi.org/10.1016/j.geoderma.2009.12.014

Shakhashiro, A., Tarjan, S., Ceccatelli, A., Kis-Benedek, G., Betti, M., 2012. IAEA-447: A new certified reference material for environmental radioactivity measurements. Appl. Radiat. Isot. 70, 1632-1643. https://doi.org/10.1016/j.apradiso.2012.03.024

Simpson, J.E., Smith, T.E.L., Wooster, M.J., 2017. Assessment of errors caused by forest vegetation structure in airborne LiDAR-derived DTMs. Remote Sens. 9. https://doi.org/10.3390/rs9111101

Skagen, S.K., Burris, L.E., Granfors, D.A., 2016. Sediment accumulation in prairie wetlands under a changing climate: the relative roles of landscape and precipitation. Wetlands. 36, 383-395. https://doi.org/10.1007/s13157-016-0748-5

Slaymaker, O., 2003. The sediment budget as conceptual framework and management tool. Hydrobiologia 494, 71-82. https://doi.org/10.1023/A:1025437509525

Statistics Canada, 2017. Seeding decisions harvest opportunities for Canadian farmers. URL https://www150.statcan.gc.ca/n1/pub/95-640-x/2016001/article/14813-eng.htm (accessed 11.07.2022).

Sutherland, R.A., 1994. Spatial variability of ^{137}Cs and the influence of sampling on estimates of sediment redistribution. Catena 21, 57–71. https://doi.org/https://doi.org/10.1016/0341-8162(94)90031-0

Sweeney, M.R., Fischer, B., Wermers, K., Cowman, T., 2019. Eolian and fluvial modification of Missouri River sandbars deposited by the 2011 flood, USA. Geomorphology 327, 111-125. https://doi.org/10.1016/j.geomorph.2018.10.018

Thangavel, P., Sridevi, G., 2017. Soil Security: A key role for sustainable food productivity, in: Dhanarajan, A. (Ed.), sustainable agriculture towards food security. Springer Singapore, Singapore, pp. 309-325. https://doi.org/10.1007/978-981-10-6647-4_16

Thorslund, J., Jarsjo, J., Jaramillo, F., Jawitz, J.W., Manzoni, S., Basu, N.B., Chalov, S.R., Cohen, M.J., Creed, I.F., Goldenberg, R., Hylin, A., Kalantari, Z., Koussis, A.D., Lyon, S.W., Mazi, K., Mard, J., Persson, K., Pietro, J., Prieto, C., Quin, A., Van Meter, K., Destouni, G., 2017. Wetlands as large-scale nature-based solutions: Status and challenges for research, engineering and management. Ecol. Eng. 108, 489–497. https://doi.org/10.1016/j.ecoleng.2017.07.012

Tiessen, K.H.D., Li, S., Lobb, D.A., Mehuys, G.R., Rees, H.W., Chow, T.L., 2009. Using repeated measurements of ^{137}Cs and modelling to identify spatial patterns of tillage and water erosion within potato production in Atlantic Canada. Geoderma 153, 104-118. https://doi.org/10.1016/j.geoderma.2009.07.013

Turner, R., Panciera, R., Tanase, M.A., Lowell, K., Hacker, J.M., Walker, J.P., 2014. Estimation of soil surface roughness of agricultural soils using airborne LiDAR. Remote Sens. Environ. 140, 107-117. https://doi.org/10.1016/j.rse.2013.08.030

VandenBygaart, A.J., Kroetsch, D., Gregorich, E.G., Lobb, D., 2012. Soil C erosion and burial in cropland. Glob. Chang. Biol. 18, 1441-1452. https://doi.org/10.1111/j.1365-2486.2011.02604.x

van Vliet, L.J.P., Padbury, G.A., Rees, H.W., Matin, M.A., 2005. Water erosion, in: Lefebvre, A., Eilers, W.D., Chunn, B. (Eds.), Environmental Sustainability of Canadian Agriculture: Agri-Environmental Indicator Report Series- Report No. 2. Agriculture and Agri-Food Canada, Ottawa, ON., pp. 90-96.

Vieira, D.A.N., Dabney, S.M., 2011. Modeling edge effects of tillage erosion. Soil Tillage Res. 111, 197–207. https://doi.org/10.1016/j.still.2010.10.007

Wallbrink, P.J., Roddy, B.P., Olley, J.M., 2002. A tracer budget quantifying soil redistribution on hillslopes after forest harvesting. Catena 47, 179-201. https://doi.org/10.1016/S0341-8162(01)00185-0

Walling, D.E., Collins, A.L., 2008. The catchment sediment budget as a management tool. Environ. Sci. Policy 11, 136-143. https://doi.org/10.1016/j.envsci.2007.10.004

Walling, D.E., Collins, A.L., Sichingabula, H.M., 2003. Using unsupported lead-210 measurements to investigate soil erosion and sediment delivery in a small Zambian catchment. Geomorphology 52, 193-213. https://doi.org/10.1016/S0169-555X(02)00244-1

Walling, D.E., He, Q., Appleby, P.G., 2002. Conversion Models for Use in Soil-Erosion, Soil-Redistribution and Sedimentation Investigations, in: Zapata, F. (Ed.), Handbook for the Assessment of Soil Erosion and Sedimentation Using Environmental Radionuclides. Springer Netherlands, Dordrecht, pp. 111-164. https://doi.org/10.1007/0-306-48054-9_7

Walling, D.E., Quine, T.A., 1993. Use of caesium-137 as a tracer of erosion and sedimentation: Handbook for the application of the caesium-137 technique. UK Overseas Dev. Adm. Res. Scheme R 4579.

Walling, D.E., Quine, T.A., 1992. The use of caesium-137 measurements in soil erosion surveys. Eros. sediment Monit. Program. river basins. Proc. Int. Symp. Oslo, 1992 143-152.

Walling, D.E., Quine, T.A., 1991. Use of ^{137}Cs measurements to investigate soil erosion on arable fields in the UK: potential applications and limitations. J. Soil Sci. 42, 147-165. https://doi.org/10.1111/j.1365-2389.1991.tb00099.x

Walling, D.E., Zhang, Y., He, Q., 2011. Models for deriving estimates of erosion and deposition rates from fallout radionuclide (Caesium-137, Excess Lead-210, and Beryllium-7) measurements and the development of user-friendly software for model implementation, in: Impact of soil conservation measures on erosion control and soil quality, EA-TECDOC-1665, IAEA Publication, Vienna, Austria, pp. 11-33.

Watmough, M.D., Schmoll, M.J., 2007. Environment Canada's Prairie & Northern Region Habitat Monitoring Program Phase II: Recent habitat trends in the Prairie Habitat Joint Venture. 135.

Wauters, J., Madruga, M.J., Vidal, M., Cremers, A., 1996. Solid phase speciation of radiocaesium in bottom sediments. Stud. Environ. Sci. 68, 165. https://doi.org/10.1016/S0166-1116(09)70092-5

Wheaton, E.E., 1992. Prairie dust storms - A neglected hazard. Nat. Hazards 5, 53-63. https://doi.org/10.1007/BF00127139

Wickham, H., 2016. ggplot2: Elegant Graphics for Data Analysis. Springer-Verlag New York. ISBN 978-3-319-24277-4, https://ggplot2.tidyverse.org.

Wu, Q., Lane, C.R., 2017. Delineating wetland catchments and modeling hydrologic connectivity using lidar data and aerial imagery. Hydrol. earth Syst. Sci. 21, 3579-3595.

Yang, W., Wang, X., Gabor, S., Boychuk, L., Badiou, P., 2008, Water quantity and quality benefits from wetland conservation and restoration in the Broughton's Creek watershed, Ducks Unlimited Canada publication, 48.

Zádorová, T., Penížek, V., Žížala, D., Matějovský, J., Vaněk, A., 2018. Influence of former lynchets on soil cover structure and soil organic carbon storage in agricultural land, Central Czechia. Soil Use Manag. 34, 60-71. https://doi.org/10.1111/sum.12406

Zhang, X.C., Liu, B.Y., Wei, X., Garbrecht, J.D., 2018. Evaluating sediment deposition prediction by three ^{137}Cs erosion conversion models . Soil Sci. Soc. Am. J. 82, 931-938. https://doi.org/10.2136/sssaj2018.02.0080

Chapter 4

Agricultural activities lead to sediment infilling of wetlandscapes in the Canadian Prairies: Assessment of contributions by tillage, water and wind erosion

4.1. Abstract

Soil erosion and sediment delivery models have been increasingly employed in studies of catchment sediment dynamics in current years. These models are also used to represent the spatial interaction of soil erosion and sediment transport processes, thereby providing spatially-distributed predictions of soil redistribution rates for agricultural landscapes. It has been widely recognized that individual soil erosion processes and their interactions contribute towards total soil erosion; however, quantifying the rates and patterns of soil erosion processes and their interactions within topographically complex landscapes is challenging. Therefore, the objective of this research was to estimate and model the relative contributions of tillage, water and wind erosion towards total soil erosion in the Canadian Prairie provinces of Manitoba and Alberta using ^{137}Cs, a fallout radionuclide tracer, and three well-established models: (i) Tillage Erosion Model (TillEM); (ii) Revised Universal Soil Loss Equation, version 2 (RUSLE2); and (iii) Single-event Wind Erosion Evaluation Program (SWEEP). The findings indicate that the patterns of ^{137}Cs-estimated soil erosion closely matched with the erosion pattern predicted by TillEM and suggests that tillage erosion dominates the pattern of total soil erosion on the knolls of hummocky landscapes. Additionally, soil particle size variation within the wetland catchments reflected the modeled patterns of water and tillage erosion. Furthermore, our findings confirmed that colour coefficients are useful in identifying spatial heterogeneity of soil within wetland catchments and reflect the patterns of soil loss and gains. These results indicate that water and tillage erosion, and also their interactions, are main erosion processes in the Canadian Prairie Pothole Region (PPR), but that soil movement by tillage practices has been the predominant redistribution process.

4.2. Introduction

Soil loss by erosion processes has been recognized as major threats affecting soil health, agricultural productivity, and ecosystem services, and this concern still persists across diverse agro-ecosystems (Panagos et al., 2020). Soil erosion refers to process of detachment, transport, and deposition of soil and associated particles by erosive forces, while soil loss defines as the quantity of soil materials removed in a specified time period across an area of land (Nearing et al., 1994). Soil erosion is a natural process that contributes to soil formation and landscape evolution. However, anthropogenic activities have dramatically accelerated soil erosion rates mostly due to increased removal of vegetation cover and expansion of farming on marginal lands, resulting in widespread soil degradation throughout the world's agricultural regions (Borrelli et al., 2017).

Total soil erosion rates and patterns across the landscape is the result of combined impacts of distinct processes: water erosion, wind erosion, tillage erosion and/or erosion due to crop harvesting (Kuhwald et al., 2022). Historically, soil erosion due to wind and water were assumed to be the main forms of soil erosion. However, during the past decades tillage erosion has been identified as another major form of soil erosion within sloping cultivated fields in many different agro-environments (e.g., Lobb et al., 1995; Li et al., 2007b; Tiessen et al., 2009). Harvest erosion usually occurs in potato and sugar beet production, where soil is in direct contact with the harvested product (Ruysschaert et al., 2004). Overall, each soil erosion process has its characteristic pattern across the landscape and each will contribute partially to the total soil erosion within agricultural landscapes (Papiernik et al., 2005; Li et al., 2007b).

Water erosion occurs when a landscape experiences erosive rainfall events and snowmelt runoff (Ghadiri, 2004). Particles detached by raindrops are entrained and transported downhill by overland flow (e.g., sheet and interrill erosion), which form small and ephemeral concentrated flow paths (rill or ephemeral gully erosion). Water erosion increases down the slope and reaches the highest rate in the middle slope and/or upper-lower slope segment, and then it gradually decreases towards depressional areas (Blanco-Canqui and Lal, 2008). In cold-climate areas, such as the Canadian portion of PPR of the Northern Great Plains, snowmelt runoff often exceeds rainfall runoff on an annual basis. As a result, snowmelt erosion can contribute considerably to annual soil losses. Freezing and thawing of soil are the main mechanisms detaching soil particles. Further, snowmelt usually occurs over frozen soil with little infiltration, in a short period of time, resulting in high runoff volumes (Tiessen et al., 2010). Plot-scale soil erosion research was conducted by Knisel (1980) in Morris, Minnesota, USA, and documented that only about seven percent of the annual erosion at that location was associated with erosion by snowmelt during the spring thaw.

Wind erosion is most common in arid and semiarid regions, occurring when soil is dry and wind velocity is higher than the threshold wind speed (Lal, 1998). Soil loss in landscapes dominated by wind erosion is most severe on exposed upper slope segments and the pattern of loss is driven by the prevailing wind direction. Generally, the pattern of wind erosion is normally asymmetric with maximum soil loss on the windward upper slope areas. Therefore, wind erosion pattern can be distinguished from that of tillage erosion; where, directionality is evident, but does not match the prevailing wind direction (Lobb, 2011). Furthermore, the pattern of wind erosion is evident within prairie wetland landscapes can be observed as deposition of sediment in nearby vegetation on leeward side of fields (e.g., treed wind breaks, grassed/treed riparian areas), aeolian mixture of snow and soil (snirt), infilling of roadside ditches, and dust abraded and buried plants.

Tillage erosion is defined as redistribution of soil within a landscape by tillage operations (Lobb and Kachanoski, 1999; Govers et al., 1999). The magnitude and severity of tillage erosion rates are dependent on the erosivity of the tillage system and the erodibility of the landscape (Lobb and Kachanoski, 1999). Tillage induced soil loss occurs on the upper-convex portion of slope, whereas tillage-induced soil accumulation occurs on lower concave portions of the slope. The middle linear portion of slope serves as a transition zone where translocation occurs, with no net gain or loss of soil (Li, 2021). Tillage erosion also leads to undercutting of field boundaries (fences, hedges, diversion terraces and grass strips) on the downslope side and burial on the upslope side (Li, 2009). The pattern of soil erosion exhibits complexity due to the interactions and linkages between the erosion processes. Linkages refer to simple additive effects between different forms of erosion, which may reinforce each other on the upper slope positions (i.e., wind erosion and tillage erosion reinforce each other); whereas, erosion processes may cancel each other on the middle and lower slope position (i.e., tillage erosion and water erosion can cancel each other). Interactions between distinct erosion processes occur when one erosion process changes the erodibility of the landscape for another process and/or when one erosion process works as a delivery mechanism for another process. For example, soil accumulated on lower slope position may be poorly structured and therefore more susceptible to water induced soil loss and/or tillage operation may deposit sediments into ephemeral gullies that can subsequently be moved by water erosion (Lobb et al., 2003; Li et al., 2013). Therefore, the observed soil redistribution pattern in agricultural land is an integrated result of all forms of soil erosion.

In general, modelling is intended to quantitatively characterize the complex earth-surface processes (e.g., soil erosion and flooding) (Croke and Nethery, 2006). Soil erosion can be quantified through modeling or field measurements (Heuvelink et al., 2006). Modelling soil erosion is the process of mathematically illustrating soil materials detachment, entrainment, transport, and deposition across landscape (Nearing et al., 2017). Soil erosion models are aimed at constructing watershed- and field-scale sediment budgets, improving our understanding of soil erosion processes, and enable us to test different scenarios (e.g., identify dominant driving forces of change for specific periods, under various conditions). Erosion is a complex process as it is, influenced by interactions between various factors (e.g., soil properties, landscape, management practices, and climate) and their spatial and temporal variability. Due to this complexity, models were developed to assess water, wind, and tillage erosion processes individually (Li et al., 2007b). However, the accuracy of model-predicted total soil erosion, including all forms of erosion, has been limited due to high uncertainty associated with erosion models and overlooked linkages and/or interactions between different erosion processes (Van Oost et al., 2000; Heuvelink et al., 2006).

Although field measurements provide another approach to quantify soil erosion, there are limitations associated with these field-based methods due to various variables, including temporal and spatial variability, resolution of the collected data, operational constraints, cost and reliability of results (Mabit et al, 2014). The use of environmental fallout radionuclides (e.g., ^{137}Cs, $^{210}Pb_{ex}$ and ^{7}Be) as tracers has proven to be an excellent approach in soil erosion studies and possesses many advantages compared to other methods (e.g., experimental plots and air photo interpretation) (Millard et al., 2009). The use of ^{137}Cs as a tracer has been, and continues to be, widely adopted and successfully applied in soil erosion studies because of its properties and behaviour in the environment (e.g., de Jong et al., 1983, Quine et al., 1997, Lobb et al., 1999, Pennock, 2003; Li et al., 2007b; Tiessen et al., 2009; Cabrera et al., 2023). Based on the fact that ^{137}Cs-estimated erosion includes all three soil erosion processes and their interactions, it is possible to assess the relative contributions of various erosion processes towards the total soil erosion by comparing model estimates to the ^{137}Cs-estimates.

The preferential adsorption of ^{137}Cs by the fine-grained and organic-rich fraction of soil and sediment coupled with the preferential mobilization, transport, and deposition of particles based on size and organic matter content results in unique patterns that reflect the erosional history of the landscape (Koiter et al., 2013; Zarrinabadi et al., 2023). It has been documented that the degree of selectivity is a function of environmental factors including physico-chemical properties of the soil, surface characteristics and more importantly the nature of the eroding process (e.g., tillage, water and wind) (Asadi et al., 2011). Typically, the greater the energy of the erosive process, the lesser the particle selectivity. Agricultural activities and erosional processes redistribute the soil down through the soil profile (i.e., vertical redistribution) and across the landscape (i.e., horizontal redistribution). Therefore, natural soil/sediment properties (e.g., ^{137}Cs activity, particle size distribution, organic matter content and spectral reflectance) can facilitate the discrimination between riparian and cultivated areas and eroded and depositional zones as well as aiding in the identification of the dominant erosional process (Koiter et al., 2013).

Quantitative assessment of soil erosion using ^{137}Cs technique in the Canadian Prairies started in the early 1980s. Despite qualitative evidence of significant wind and water erosion, limited studies were conducted prior to the 1980s to assess erosion in the Canadian Prairies, with reported soil losses ranging from 0.2 to 8.7 kg m^{-2} yr^{-1}, mostly associated with water erosion (Toogood, 1963; Nicholaichuk and Read, 1978; Shaw, 1980). Subsequent investigations by other researchers (e.g., de Jong et al., 1983; Jenkins et al., 1984; Southerland and de Jong, 1990) using the ^{137}Cs technique revealed soil loss on upper slope positions and soil accumulation on lower slope and depressional positions, with soil erosion rates ranging between 3.0 and -4.6 kg m^{-2} yr^{-1} over a 20-year period. In a recent study by Li et al. (2007b) in Manitoba, average soil erosion rate was reported at about 1.2 kg m^{-2} yr^{-1} (ranging between 4.2 and -2.7 kg m^{-2} yr^{-1}).

Since agricultural landscapes in the PPR are continuously recognized as soil erosion-prone region, it highlights the ongoing challenges associated with soil erosion in this region. Therefore, concerns over accelerated soil loss due to farming activities and climate change have emphasized the need for improved characterization and understanding of the patterns, and relative contribution of the three soil erosion processes within these landscapes. As the typical spatial patterns of soil loss by tillage, water, and wind erosion are not fundamentally similar, it is possible to predict their relative contributions towards total soil erosion in a wetland landscape using erosion models. To date, there has been little comprehensive study on the application of erosion models to these environments for characterizing soil erosion processes, especially wind erosion models. The general aim of this study was to characterize the impacts of agricultural activities on soil redistribution processes using soil erosion models and field measurements of soil loss within the Canadian Prairie provinces of Manitoba and Alberta. The specific objectives of this study were to: (1) predict tillage, water, and wind erosion rates and patterns within agricultural wetland landscape using currently accepted models; (2) compare the relative contributions of predicted tillage, water and wind erosion to total soil erosion estimated by ^{137}Cs within wetland landscapes; (3) validate estimated soil erosion using mass budget models of predicted wind, water and tillage erosion; (4) identify the relative contributions of tillage, water and wind erosion using ^{137}Cs activity, particle size distribution, and colour in soil/sediment.

4.3. Materials and methods

4.3.1. Description of the study area

The study area includes two sub-watersheds in the PPR, within the Canadian portion of the Northern Great Plains. The two sub-watersheds are Broughton’s Creek and Bigstone Creek watersheds, which are located in Manitoba and Alberta, respectively (Fig. 4.1). The PPR of Canada spans southeastern Alberta, southern Saskatchewan, and southwestern Manitoba. It was formed between 20,000 and 12,000 years ago when glaciers retreated (Wisconsin and Assiniboine glacial lobes) and left behind numerous small potholes (wetlands) and fertile soil parent materials. Geomorphologically, surficial properties of the study area are broadly characterized by irregular undulating to hummocky terrain, composed of chaotically arranged knolls and depressions (Pennock et al., 1987).

The climate of the PPR is characterized as semi-arid to sub-humid with the total annual precipitation increasing from 250 mm to 550 mm along a west to east gradient. Long, cold winters, short growing seasons, and dry wind further characterize the region (Coupland, 1973). The watersheds are located within the Canadian Aspen Forests and Parklands ecoregion, which extends in a broad arc from southwestern Manitoba, northwestward through Saskatchewan to its northern limit in central Alberta. The parkland is a transitional region between the boreal forest to the north and the grasslands to the south (Millet et al., 2009).

The Broughton's Creek watershed is a sub-watershed of the Little Saskatchewan River watershed located in southwestern Manitoba. Based on the climate normal (1981-2010; Brandon, Manitoba, ID: 5010480), the average annual precipitation is 474 mm, with monthly maximum average rainfalls of 80 and 73 mm occurring in June and July, respectively, and maximum average snowfalls of 25 and 23 mm in December and January, respectively. Overall, around 118 mm (~25%) of the average annual precipitation manifests occurs in the form of snow, lasting from November to the following April. The annual temperature average is 2.2° C with the mean monthly temperature reaching a high of 18.5° C in July, and dropping to a low of -16.6° C in January (ECCC, 2022). The soils throughout the study area are characterized as Orthic Black Chernozem soils (Newdale Soil Association) with solum depth ranging from 25- to 98-cm (Manitoba soil survey report, 2011).

The Bigstone Creek watershed is the western-most sub-watershed of the Battle River watershed located in east-central Alberta. According to the 1981-2010 climate normal data (Camrose, Alberta, ID: 3011240), average annual precipitation is 438 mm, with monthly peak precipitation of 74 and 85 mm in June and July, respectively. Snowfall represented ~25% (113 mm) of the annual precipitation, extending from October to April. The mean monthly maximum and minimum temperature are 22.9° C (July) and -17.2° C (January), respectively, with annual mean of 3.0° C (ECCC, 2022). Soils in this area of Alberta are dominated by well-drained Black Solodized Solonetz soils, which have loam texture (Alberta soil survey report, 1985; Howitt 1988).

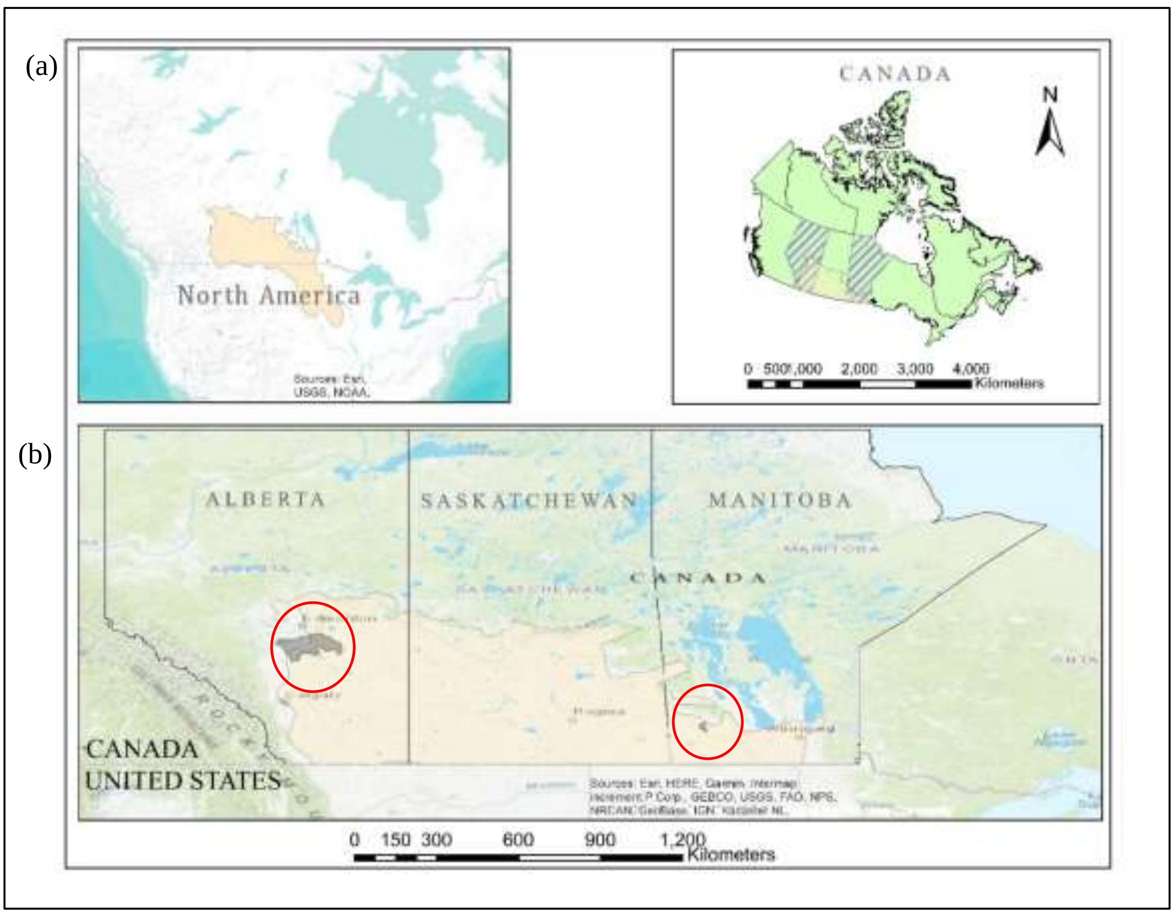

Fig. 4. 1. Geographic location of (a) the Prairie Pothole Region (PPR) in North America and (b) the studied wetland catchments in Prairie provinces of Manitoba and Alberta, Canada.

The hourly historical wind velocity and direction data were obtained from the weather stations in Manitoba (Brandon, Manitoba; ID: 5010480) and Alberta (Camrose, Alberta, ID: 3011240). Fig. 4.2a and b show the historical wind direction and speed of the selected stations in Manitoba and Alberta over all seasons (winter, spring, summer and fall) and the months of April, May and June. The main wind directions for all winds over the entire year are northwest and west in both watersheds, whilst the most frequent direction of erosive winds during the months of April, May and June are the Northwest and Southeast in Alberta, and Northwest, Northeast and East in Manitoba. The erosive winds from the South and Southwest directions are less erosive. It has been reported that a wind speed of 6.2 m s-1 is required to entrain and displace fine-textured soils (Chepil, 1945).

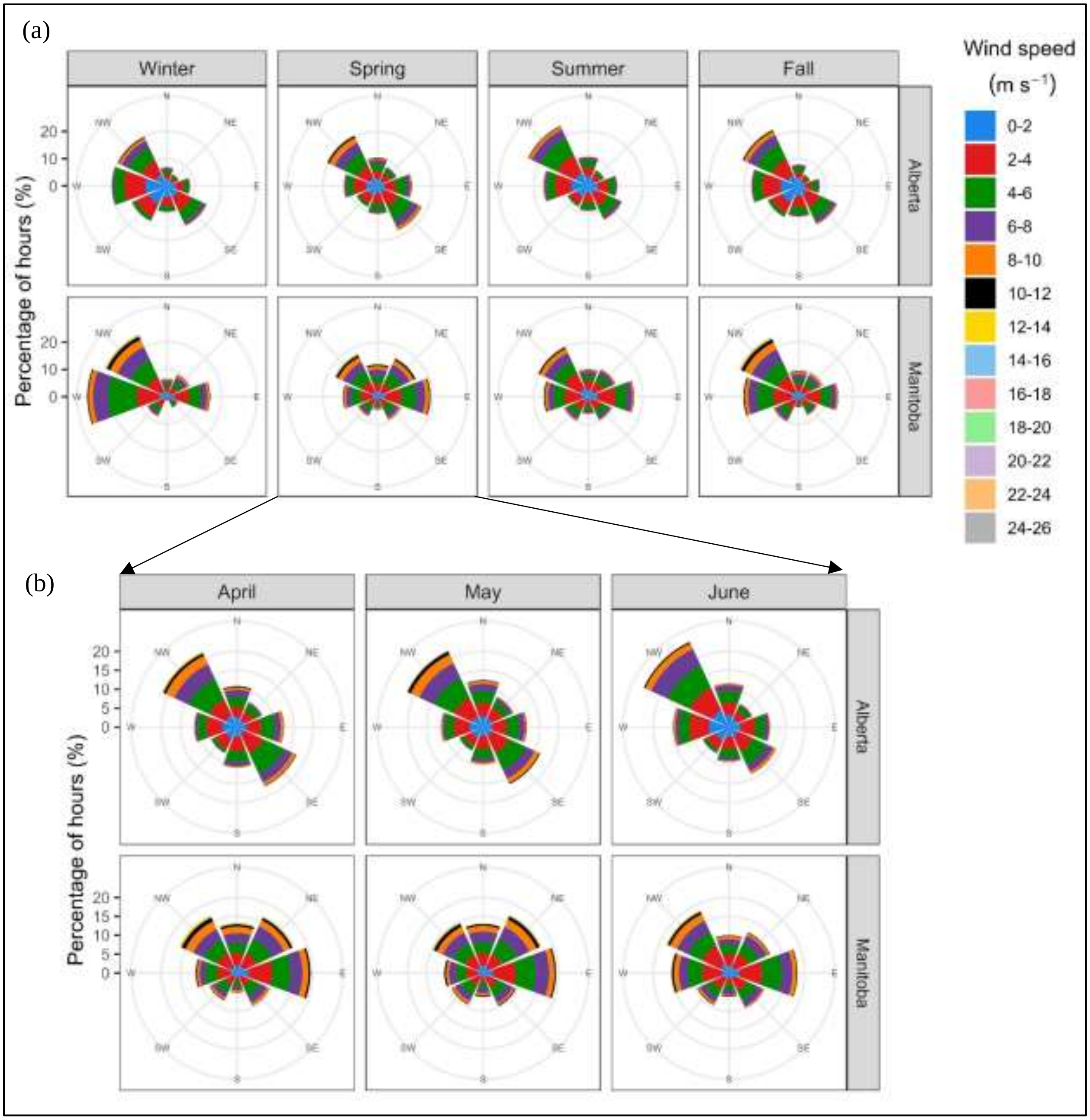

Fig. 4. 2. Historical distribution of wind speeds and directions for each season in the Broughton's Creek (Manitoba) and Bigstone Creek (Alberta) watersheds, measured at ECCC stations (ID: 5010480, Brandon, Manitoba and ID: 3011240, Camrose, Alberta). Historical wind data for the months that soil surface is not fully protected are presented as well.

4.3.2. Soil sampling and laboratory analysis

A total of eight wetland catchments were selected for this study. Five wetland catchments were located in the Broughton's Creek watershed (Manitoba) and three wetland catchments were located in the Bigstone Creek watershed (Alberta). The wetland ecosystems were individual depressions (i.e., closed basins) with topography typical of the cultivated land in the two prairie watersheds. Seven of the selected wetlands were embedded within agricultural landscapes and one was embedded within a native prairie landscape. The catchment within the native prairie landscape is located in the Broughton's Creek watershed and has not been cultivated since at least the 1950s. Furthermore, the aerial photographs showed that the selected agricultural landscapes were under cultivation since 1947. Depending on the water balance, these wetlands vary from being shallow and seasonal to relatively permanent.

To evaluate the spatial variability of soil redistribution processes using ^{137}Cs, a multiple independent transect approach, extending from different directions, was adopted as the sampling strategy. Three transects were established within each wetland catchment to capture the variability resulting from the topographic complexity of these landscapes. In each wetland catchment, 15 to 27 cores were collected along the three transects from six to nine toposequence positions extending from the uppermost portion of the catchment to the central area of the wetland. Toposequence positions were selected based on the topographic attributes and dominant vegetation (e.g., upland, riparian and open water) as shown in Fig. 4.3b.

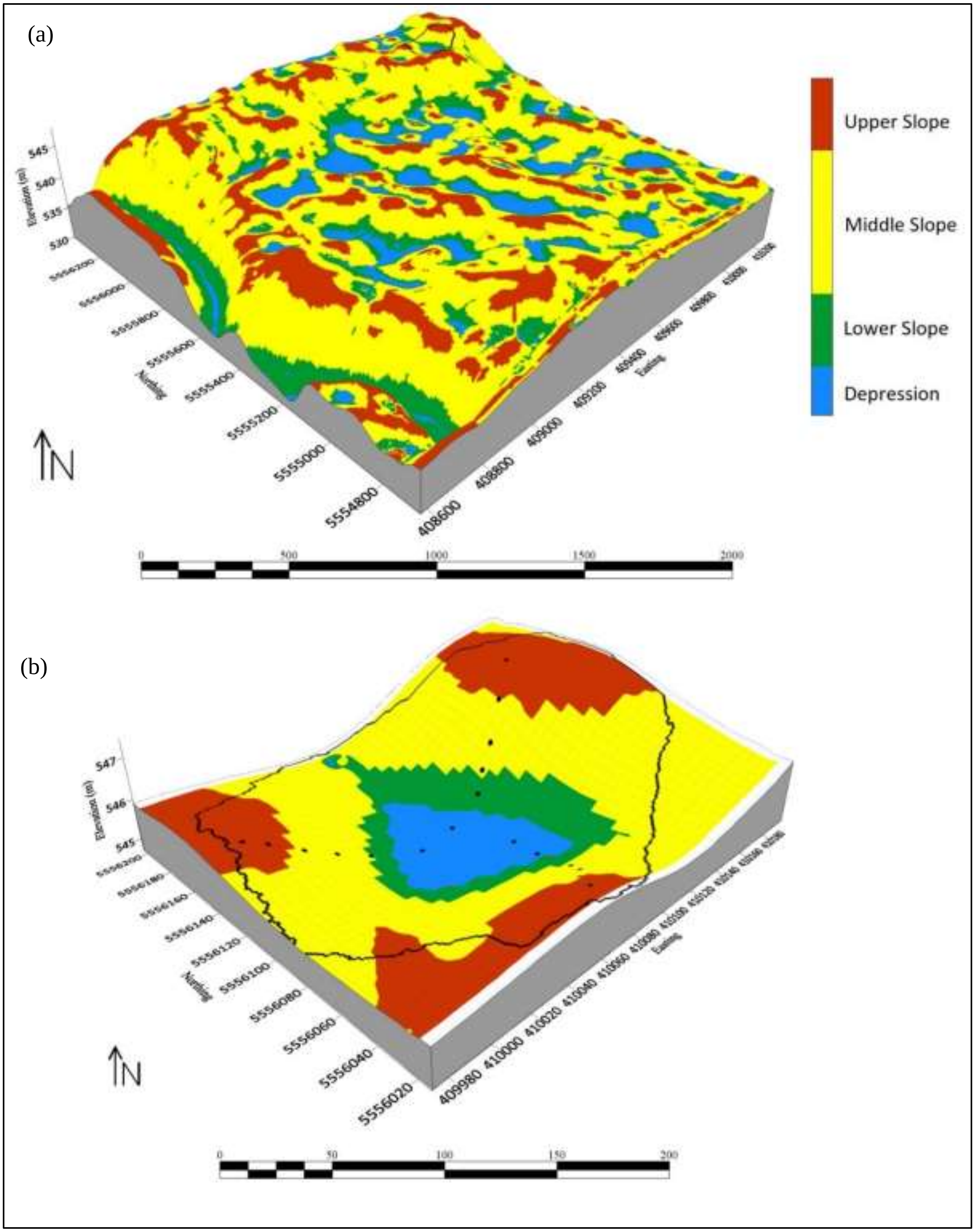

Fig. 4. 3. Three-dimensional (3D) view illustrating the landscape classification of (a) one section of land and (b) one individual wetland landscape (WetlandA) located within the section of land in Broughton's Creek Watershed, Manitoba. Sampling points on three individual transects extending from upper slope position to the central area of wetland are shown.

Soil/sediment cores from upland field (upper, middle, and lower), riparian area and the central area of the wetland were collected using a foot-operated stainless steel JMC Backsaver soil sampler (with a 45.7-cm-long, 3.17-cm-diameter slotted sampling tube). However, where water was present (e.g., in Manitoba), a different soil coring technique was used. At these sites, a portable and lightweight gas-powered Vibracoring unit (WINK Vibracore Drill Ltd., Vancouver, BC, Canada, at the Department of Geological Sciences, University of Manitoba, Winnipeg, Canada) equipped with 180-cm long and 7.62-cm diameter aluminum tubes was used to collect deeper (>1 m) consolidated samples in the wetland riparian area (i.e., riparian grass and cattail). A handheld SDI Vibecore Mini unit (Specialty Devices Inc., Wylie, TX, USA, at the Landscape Dynamics Laboratory, University of Manitoba, Winnipeg, Canada) equipped with 120-cm long and 7.62-cm diameter polycarbonate tubes was used to sample from the central area of the wetland, which was open water. In order to retrieve the cores, a hoist mounted on an inflatable pontoon boat and a winch device were used in the central area of the wetland and the riparian area, respectively. The cores collected using the Backsaver sampler were sectioned into 1-cm, 2-cm, 5-cm, 10-cm and 15-cm intervals in the field, and samples were transferred to laboratory in coolers and refrigerated at 4° C until further analysis. The remainder of the collected cores were kept and transported vertically (to avoid disturbing sediment layers) to the laboratory and stored at -20° C. The frozen cores from the central area of the wetland were sectioned into 2-cm intervals, and cores from riparian area were sectioned into 1-cm intervals from the surface to a depth of 30-cm, and then at 5-cm intervals to the bottom of the core. These frozen cores were sectioned using a band-saw equipped with a fine grit-size diamond blade. The mass that was ground away between slices by the diamond blade cut (~ 0.7 mm) was ranged between 1.9% and 6.3% (averaged 3.5%), which was taken into consideration in calculations.

Following sectioning, each increment was dried at 70°C for 72 hours and sieved through 2-mm mesh (in order to remove stones/large gravel particles and to ensure a constant sample density and geometry) (Reddy et al., 2013). In order to quantify soil erosion rate, discriminate type of erosional processes, and characterize the properties of soil/sediment samples, ^{137}Cs activity, ultimate particle size distribution, and spectral reflectance were measured in the laboratory. The radioactivity of ^{137}Cs in soil and sediment samples was measured by gamma-ray spectrometry, determined using 661.6 keV gamma emissions on standard and low-background high-purity Germanium gamma detectors (including Broad Energy detectors and a high-resolution coaxial HPGe well detector) (Mirion Technologies (Canberra) Inc., Meriden, CT, USA, at the Landscape Dynamics Laboratory, University of Manitoba, Winnipeg, Canada). The samples were counted on the detectors for approximately 12-24 hours, depending upon the radioactivity of the samples, providing a detection error < 10% (Li et al., 2007b; 2008).

The reference site used for determining the ^{137}Cs baseline value (non-eroded off-site value) was selected in an unused portion of an old rural cemetery in Manitoba, which was not disturbed since the 1950s and located within a distance range of 1 to 5 km of the studied wetland catchments. At the reference site, nine soil cores were taken in 5-cm depth increments to 60-cm. The average inventory of 1430 ±123 Bq m^{-2} decay-corrected to 1 January 2021 was estimated as the reference ^{137}Cs level (non-eroded off-site value) for the studied catchments in Manitoba. In Alberta, Li et al. (2007c) reported the ^{137}Cs reference inventories of 1684 ±834 Bq m^{-2} decay-corrected to 1 January 2021, which was used as the reference ^{137}Cs level (non-eroded off-site value) in this study and located around 60 km northeast of the study area. Additionally, it was assumed that ^{137}Cs loss out of the wetland catchment was negligible because of the enclosed topography. Thereby, catchment-level reference ^{137}Cs values (on-site values) were calculated to develop field-based mass budgets and further comparison with mass budget models of wind, water, and tillage erosion. The on-site values of ^{137}Cs varied from 931 to 1450 Bq m^{-2} in Manitoba, and from 1086 to 1488 Bq m^{-2} in Alberta.

Reflectance spectrometry readings were collected and colour coefficients (i.e., Commission Internationale de l'éclairage (CIE) colour space models) were calculated following the procedures described by Barthod et al. (2015), using a spectroradiometer (ASD FieldSpec Pro, Analytical Spectral Device Inc., Boulder, CO, USA, at the Landscape Dynamics Laboratory, University of Manitoba, Winnipeg, Canada). The ultimate particle size distribution of samples was obtained after oxidizing organic material with hydrogen peroxide (H_2O_2, 30%), and using hexametaphosphate as a dispersant (Gray et al., 2010; Zarrinabadi et al., 2022) by laser diffraction in water using a Mastersizer 3000 (Malvern Instruments, Malvern, England, at the Landscape Dynamics Laboratory, University of Manitoba, Winnipeg, Canada).

4.3.3. Total soil erosion estimated from ^{137}Cs Measurements

The Mass Balance Model2 (MBM2) and Proportional Model (PM) were used to convert point ^{137}Cs inventories into point total soil erosion rates. The MBM2 represents complex processes that accounts for changes in the ^{137}Cs concentration in response to the time-variant ^{137}Cs fallout input and the fate of freshly deposited ^{137}Cs prior to cultivation (e.g., losses/gains due to erosion/deposition, and progressive incorporation of fresh soil from beneath the original plough depth by tillage) (Walling et al., 2011). Results obtained using this model are likely to be more realistic for the area of maximum loss within a landscape (e.g., hilltop) in comparison with those of the PM (Lobb and Kachanoski, 1997). Furthermore, the MBM2 underestimates sediment deposition in the accumulation area, as this model was developed/designed mainly for application in eroding areas. The PM was used to develop soil loss and accumulation budgets, since it assumes that all the ^{137}Cs deposited in the year 1963, when the majority of the fallout was accumulated on the surface, and the ^{137}Cs concentration at the soil surface available for erosion remains relatively constant through time. Furthermore, the loss or gain of ^{137}Cs in the profile is linearly and directly proportional to the loss of soil in the profile (Li et al., 2010; Walling et al., 2011).

To run the PM and MBM2, the “start year of cultivation” was set at 1963. The “mass plough depth” was determined from the average plough depth (~ 0.2 m) and bulk density of the collected soil/sediment cores (235 kg m^{-2} and 190 kg m^{-2} for Manitoba and Alberta, respectively). Mean bulk density values ranged between 820 and 1380 kg m^{-3} for Manitoba and between 815 to 1075 kg m^{-3} for Alberta throughout the 0.2 m soil profiles. Following the study conducted by Li et al. (2007a) in the PPR, the “relaxation mass depth” (H_{MBM2}), “proportion of annual ^{137}Cs input susceptible to erosion loss” (γ_{MBM2}) and the “particle size correction factor” (P_{MBM2}) were assumed to be 4.0 kg m^{-2}, 0.75 and 1.0, respectively. These two models were implemented within the Erosion Calibration Model program developed in Visual Basic by Walling et al. (2011). The program was run to calculate soil loss and deposition rates for each of the transects within wetland catchments.

Although average ^{137}Cs inventories in some of collected cores within depositional areas were lower than estimated off-site reference values, the cores showed one well-defined ^{137}Cs peak, corresponding to the peak fallout of ^{137}Cs in 1963. In such cases, sediment deposition rates were calculated by dividing the associated depth with the peak of ^{137}Cs concentration by the number of years between deposition and collection of the core (that is, years from deposition to sample collection in 2016 and 2019 for Alberta and Manitoba samples, respectively) (Lobb et al., 1995; Walling and Quine, 1991). The calculated sediment deposition rates were converted to sediment masses using representative values of sediment bulk density and area of the topographic position.

4.3.4. Modelling tillage, water, and wind erosion

Three established models were employed to predict tillage, water, and wind erosion in this study. These models include (i) the Tillage Erosion Model (TillEM) developed by Li et al. (2007a); (ii) the Revised Universal Soil Loss Equation, version 2 (RUSLE2), developed cooperatively by the United States Department of Agriculture (USDA)-Agricultural Research Service (ARS), the USDA-Natural Resources Conservation Service (NRCS), and the University of Tennessee (USDA-ARS, 2008); and (iii) the Single-event Wind Erosion Evaluation Program (SWEEP) developed by USDA-ARS (USDA-ARS, 2020).

4.3.4.1 Tillage erosion- TillEM

TillEM is based on the tillage translocation model, which was developed and introduced by Lobb and Kachanoski, (1999) to predict tillage erosion in topographically complex landscapes. Li et al. (2007a) expanded on the work of Lobb and Kachanoski (1999) and further developed the TillEM, which uses a multiple linear function of slope gradient and slope curvature to simulate tillage erosion in the direction of tillage following the equation:

$$T_M = \alpha + \beta\theta + \gamma\varphi \qquad (1)$$

where: T_M is the translocation in mass per unit width of tillage (kg m^{-1} pass^{-1}); The coefficient α is the intercept of the linear regression equation, representing translocation unaffected by slope gradient and/or slope curvature or the tillage translocation that occurs on level ground (kg m^{-1} pass^{-1}); β is the erosivity coefficient, describing additional translocation resulting from slope gradient (kg m^{-1} %$^{-1}$ pass^{-1}); θ is slope gradient, negative when upslope and positive when downslope (%); γ is the erosivity coefficient for slope curvature, describing the additional tillage translocation due to slope curvature (kg m^{-1} (%$^{-1}$ m) pass^{-1}); and φ is slope curvature, negative for concave and positive for convex (% m^{-1}).

TillEM runs on lines both parallel and perpendicular to the direction of tillage, representing forward and lateral tillage translocation, respectively. TillEM simulates point-tillage erosion rates for each grid point/cell across the landscape using a diffusion/dispersion equation similar to that used by Govers et al. (1994). Tillage erosion is calculated as:

$$E_{Ti} = -\frac{\partial T_M}{\partial s} = -\left(\beta\frac{\partial\theta}{\partial s} + \gamma\frac{\partial\varphi}{\partial s}\right) \qquad (2)$$

Where: E_{Ti} is the predicted tillage erosion rate, negative for soil accumulation and positive for soil loss (kg m^{-2} yr^{-1}); M is the mass of soil per unit area (kg m^{-2}); t is time (year); s is the distance in any specified horizontal direction (m).

TillEM assumes that tillage operations (over time) are conducted equally in opposing directions. Therefore, tillage erosion is predicted at each point across a landscape based on the changes in slope gradient and slope curvature between adjacent points and one-half of their separation distance (Lobb and Kachanoski, 1999). The values of α, β and γ coefficients for a full sequence of tillage operations (one pass of deep-tiller, one pass of light-cultivator followed by air-seeder and two passes of spring-tooth-harrow) were adopted from a field study conducted by Li et al. (2007a) in the PPR. Furthermore, it was assumed that extra pass of farming operations had been conducted in the lower slope and outer riparian positions during dry years when water had receded (see Appendix B-B1).

4.3.4.2 Water erosion- RUSLE2

RUSLE2 was developed and enhanced after its predecessors, Universal Soil Loss Equation (USLE) (Wischmeier and Smith, 1965, 1978) and Revised Universal Soil Loss Equation, version 1 (RUSLE1), in 2001 (Renard et al., 2010). RUSLE2 is a process-based daily time-step and land use independent model that simulates the effects of agricultural cropping practices and rotations on field-scale soil erosion and sediment delivery by rainfall and overland flow path (USDA-ARS, 2008).

RUSLE2 can simulate erosion over irregular and complex topography landscape (e.g., rolling, undulating and hummocky) with spatially variable overland flow (converging and diverging flows). Hillslope profile is conceived as being composed of three layers of variable (topography, soil, and management) and each of these layers can be segmented independently to compute both temporal and spatially variable effect on soil movement (USDA-ARS, 2008; Dabney et al., 2010). Thereby, RUSLE2 can represent any complex hillslopes as a series of segments comprising each unique combination of the variables (Dabney et al., 2010). The effects of spatial variation of soil erodibility, slope steepness and curvature, and soil cover management along a hillslope profile on detachment, transport, and deposition can be predicted in this model (Dabney et al., 2011). This model predicts the sediment yield resulting from rill and inter-rill erosion at the base of the drainage area by considering variations in transport capacity across segmented hillslope. Furthermore, contributions from multiple events are used to determine overall cumulative sediment yield over time (USDA-ARS, 2008; Dabney et al., 2013).

RUSLE2 is supported by extensive databases that include information describing the climate (e.g., precipitation, temperature, erosivity density (the EI_{30} per unit quantity of rain)), soils (e.g., texture, organic matter, soil erodibility, soil hydrologic class), vegetation (e.g., growth over time), residue (decomposition and biomass/cover relationships), cropping systems (e.g., rotations), and field management scenarios. Each scenario was developed by combining field operation descriptions that take place on specified dates (e.g., tillage, planting, applying synthetized fertilizers, harvesting, burning, frost, ripping, grading, and grazing events) and impact hydrologically important properties (e.g., soil surface roughness and residue cover) (USDA-ARS, 2008; Dabney et al., 2012).

Databases of five counties (i.e., Towner, Renville, and Bottineau in North Dakota, and Toole and Glacier in Montana) in the PPR of Northern United States (e.g., climate data, soil database, location database, and management operations) were imported for use with RUSLE2 program. The counties were selected based on geographic characteristics to represent a range of topographic, climatic, and agricultural land conditions nearly identical to the Canadian PPR. The climate data for the selected counties were imported from the climate database provided on the NRCS website. In addition, the soil type for the studied wetland catchments was identified from the Soil Survey database for each county. Based on Manitoba Agricultural Services Corporation (MASC) data spanning 2000-2021, the most widely practiced crop rotations in Manitoba was spring wheat and canola (MASC, 2021). Therefore, the input variable of a multi-year phase rotation (spring wheat and canola) was selected for the cultivated segments of the wetland catchments as an agricultural management practice. As for field management operations, two regional scenarios along with associated dates for each operation were developed using the extensive agricultural practices and crop rotations database in RUSLE2. The tillage direction has been selected as one way to right or down in the management databases. The proposed agricultural practices' scenarios were designed to simulate regional development of tillage practices over two different periods of time for the past 60 years (see Appendix B-B2): (i) 1960 to 1990 (conventional tillage practices), and (ii) 1990 to 2020 (conservation tillage practices).

4.3.4.3 Wind erosion- SWEEP

The Single-event Wind Erosion Evaluation Program (SWEEP), a stand-alone version of the Wind Erosion Prediction System (WEPS) Erosion submodel released in 2007 (Feng and Sharratt, 2009), was used to simulate topsoil loss and dust emission by wind. The SWEEP estimates potential soil loss for user defined surface conditions and management practices (e.g., wind barriers) for a single wind-storm event on hourly and sub-hourly basis (e.g., ≤ 24 hour). In addition to simulating total soil loss, the model subdivides total soil loss into three transport components that include creep/saltation, suspension, and PM_{10} (Particulate Matter ≤ 10 µm) emission (Tatarko et al., 2016). The SWEEP model has been tested and validated for total soil loss and soil discharge from agricultural and non-agricultural lands (e.g., dam and mine tailings) around the world (e.g., Feng and Sharratt, 2009; Jia et al., 2014; Liu et al., 2014; Pi et al., 2016; Zhang et al., 2017; Nerger et al., 2017).

SWEEP initiates the simulation of site-specific soil movement (loss/deposition) for a single erosion event only when friction velocity exceeds the static threshold friction velocity for soil particles entrainment. The calculation of both the friction velocity and the static threshold friction velocity by SWEEP is based on soil physical and surface characteristics (e.g., flat and standing biomass, clods, crust, coarse fragments (>2 mm in diameter), soil aggregate characteristics, and surface water content) in a rectangular region. The model determines the probability of an erosion event and wind parameters by direction and month for defined surface conditions and selected weather stations (Tatarko et al., 2016).

SWEEP simulates the components of wind erosion in response to input parameters required by SWEEP for a single erosion event including site geometry (e.g., fetch length, width, orientation, and wind barriers, if present), soil properties (e.g., particle and aggregate size distribution, volume of rocks, and aggregate density, and stability), soil surface conditions (e.g., crust and loose material cover, crust stability, ridge and random roughness, and surface soil wetness), standing biomass characteristics, residue cover, and wind characteristics (e.g., wind direction and wind speed) with average intervals ranging from 5 to 60 minutes (Feng and Sharratt, 2009). All input parameters for soil properties were obtained from the NRCS SSURGO soil database, which can be downloaded in the SWEEP software. The locations in the northern United States were selected based on geographic location, in the PPR of the United States, to represent a range of agricultural land conditions nearly identical to the PPR of Canada.

Land management practices, soil erodibility and wind erosivity are main factors in wind erosion assessment. In order to simulate the impacts of alternate land management practices and conditions on wind erosion and dust emission in the Canadian PPR, three different scenarios including conservation tillage, conventional tillage, and summer-fallow were developed to simulate the potential of soil loss by creep, saltation, and suspension using the SWEEP model. The proposed management scenarios were designed to simulate regional land management practices over the 60 years, beginning in 1960s.

Scenario 1, conservation tillage, was developed to simulate the effect of crop residues on wind erosion. Conservation tillage is an effective approach to soil surface management with minimum or no-tillage (Unger and McCalla, 1980). Conservation tillage has been well accepted as an efficient method to minimize wind-induced erosion since it retains a significant amount of standing and flat crop residues on the surface of soil (Buschiazzo and Zobeck, 2008). This scenario was formulated by maintaining the surface residues from harvest (late September) to the next planting season (late April).

Scenario 2, conventional tillage and conventional field management, was formulated to simulate lower crop residues on the soil surface. The subsequent surface protection loss due to the removal of surface residues and low productivity of the dryland agricultural crops greatly increases the susceptibility of soil to wind erosion. On conventionally managed fields, tillage ridges are the most effective soil roughness element that contributes to reducing wind erosion in early spring, before the plant canopy develops and protects the soil surface.

Scenario 3, summer fallow, produced a worst-case situation and was designated as a reference for alternative management practices. Producers on the semi-arid PPR have historically selected crop rotations that include fallow every second or third year (Campbell et al., 1990), which intensifies the wind erosion problem by burying crop residues, drying the soil surface and destroying soil aggregates as result of raindrop impacts. However, it is worth noting that the practice of fallowing has been mostly discontinued in the study areas now. Furthermore, as fallow is often used as a strategy for managing excess moisture in the soil, producers in Manitoba practice fallow when the soil is too wet for planting.

4.3.5. Landscape segmentation

The classification of landscapes into toposequence positions was conducted using smoothed DEM of the studied catchments and the LITAP package, Version 0.6.0, in R (Lazerte and Li, 2021), which is based on the LandMapR™ software developed by MacMillan et al. (2003). Detailed descriptions about the algorithms and methodology used in the LandMapR™ programs can be found in the original publication (MacMillan et al., 2000) and previous studies (MacMillan, 2003; Li et al., 2011b). The landscape was then classified into four classes based on typical landscape positions (upper slope, middle slope, lower slope, and depression areas) to calculate the area of each toposequence position so as to develop soil loss and accumulation budgets within wetland catchments. Fig. 4.3 illustrates the landscape classification map for one section of land and one wetland catchment (WetlandA) in Broughton's Creek Watershed, which shows sampling points on three independent transects within the wetland catchment as well.

4.3.6. Statistical analysis

The predicted tillage, water and wind erosion data, soil ultimate particle size distribution, and the ^{137}Cs estimated total soil erosion of the sampling points were statistically analyzed with SAS, Version 9.4 (SAS Institute, Cary, NC, USA). In addition, three-dimension Principal Component Analysis (PCA) was performed using Origin(Pro), Version 2022b (OriginLab Corporation, Northampton, MA, USA). PCA was conducted on standardized variables to eliminate the effect of different measurement units on the determination of factor loading. PCA shows how the data clusters based on similarity across more than two variables. In contrast, correlation analysis compares a pair of variables. Correlation analysis is more likely to be affected by the errors associated with individual variables, especially when the correlations are not strong (Li et al., 2007b).

The data from the top 20-cm depth of collected soil and sediment cores were subjected to statistical analyses since this is the layer mainly influenced by soil erosion processes, particularly tillage erosion. The spectral reflectance data and six colour space models were employed to determine 15 colour coefficients (parameters) of collected soil and sediment samples using R, Version 4.0.1, (R core Team, 2020) following the approach presented by Boudreault et al. (2019) and colour analysis R scripts (Koiter, 2021). Additionally, to aid with visualization the hue, saturation, and value (HVS colour model) and hexadecimal color values were calculated. The non-parametric Kruskal-Wallis test was then applied to identify which of the colour coefficients were significantly different ($P < 0.1$) between at least two landscape classes within studied catchments, eroded (upper, middle and lower slope positions) and accumulation (riparian areas and the central area of wetlands); thereby, allowing discrimination between these areas. Furthermore, Linear Canonical Discriminant Analysis (LCDA) was used for source aggregation (Liu et al., 2017) using Origin(Pro), Version

2022b. The canonical coefficients indicate the relative importance of each variable in discriminating between the pre-defined groups or classes. The variables with larger absolute canonical coefficients are considered more important in discriminating between the groups. Weather data for the weather stations were downloaded from Environment and Climate Change Canada's website using the Weathercan R package, Version 0.6.2 (LaZerte et al., 2018). Figures were created using the ggplot2 package, Version 3.3.3 (Wickham, 2016), Origin(Pro), Version 2022b, and Microsoft Excel 2016.

4.4. Results and discussion

4.4.1. Patterns and magnitudes of predicted tillage, water, and wind erosion

4.4.1.1. TillEM

Tillage erosion rates predicted by TillEM at the cultivated transect points varied from 3.0 (soil loss) to -6.1 (soil accumulation) kg m^{-2} yr^{-1}, and 6.3 to -5.9 kg m^{-2} yr^{-1} in Manitoba and Alberta, respectively. The most severe soil losses due to tillage were found on upper slope positions, while TillEM predicted soil accumulation in concave landscape positions with maximum accumulation rates predicted at the bottom of the field (outer segment riparian area) with little change occurring on positions with uniform or linear slopes (Table 4.1). Generally, soil redistribution pattern predicted by TillEM varied mainly with local topography and was consistent with the findings of previous studies conducted in Canada (e.g., Lobb and Kachanoski, 1999; Li et al., 2007b; Tiessen et al., 2009). As tillage erosion results in soil redistribution within cultivated fields rather than exporting soil from the cultivated fields, losses should equal gains. However, as water recedes in wetlands during drought years, terrestrial portions and riparian zones of prairie wetlands are often tilled to increase the crop production area. The periodic tillage of these areas can result in extra passes of tillage operations and soil movement out of permanently cultivated fields. The TillEM results also indicated that the 60-year annual average soil flux by tillage erosion, from cultivated fields to riparian areas, was approximately 25,000 kg yr^{-1} in Manitoba and 48,000 kg yr^{-1} in Alberta.

Table 4. 1. Average point soil loss and deposition rates within the individual wetland catchments using ^{137}Cs and soil erosion models.

Province	Toposequence position	Average ^{137}Cs inventory (Bq m^{-2})	Toposequence Area (m^2)	Average soil loss (+) or deposition (-) (kg m^{-2} yr^{-1})				
				Power model[1]	Linear model[2]	Tillage erosion model[3]	Water erosion model[4]	Wind erosion model[5]
Wetland A (Cultivated catchment)								
Catchment-level ref. ^{137}Cs		**944**						
MB	Upper Slope		6675	2.2	1.2	1.82	0.05	
MB	Middle Slope	819	15975	1.5	0.5	0.50	0.10	
MB	Lower Slope	1289	2425	0.3	-1.4	-0.16	0.05	0.06
MB	Outer Riparian	1826	-	-1.0	-3.7	-2.16	-	-
MB	Inner Riparian	926	-	1.2	0.1	-	-	-
MB	Inner Wetland	1060	-	0.8	-0.5	-	-	-
Wetland J (Cultivated catchment)								
Catchment-level ref. ^{137}Cs		**1898**						
MB	Upper Slope	233	5025	5.4	3.5	2.24	0.07	
MB	Middle Slope	1802	15950	-1.7	0.2	0.53	0.14	
MB	Lower Slope	4732	3450	-14.8	-5.9	-0.48	0.19	0.06
MB	Outer Riparian	2990	-	-7.0	-2.3	-2.28	-	-
MB	Inner Riparian	1992	-	-2.5	0.2	-	-	-
MB	Inner Wetland	794	-	1.6	2.3	-	-	-
Wetland K (Cultivated catchment)								
Catchment-level ref. ^{137}Cs		**1314**						
MB	Upper Slope	901	7950	1.3	1.2	2.86	0.03	
MB	Middle Slope	1067	13425	0.8	0.7	1.42	0.13	
MB	Lower Slope	2605	3475	-2.7	-3.9	-0.76	0.23	0.05
MB	Outer Riparian	2338	-	-2.1	-3.1	-3.51	-	-
MB	Inner Riparian	1901	-	-1.1	-1.8	-	-	-
MB	Inner Wetland	609	-	2.4	2.1	-	-	-
Wetland X (Cultivated catchment)								
Catchment-level ref. ^{137}Cs		**936**						
MB	Upper Slope	478	1600	1.9	1.9	2.45	0.07	
MB	Middle Slope	532	4025	1.6	1.7	1.96	0.13	
MB	Lower Slope	1345	5225	-1.6	-1.7	-0.37	0.09	0.02
MB	Outer Riparian	3971	-	-11.9	-12.8	-4.05	-	-
MB	Inner Wetland	2626	-	-6.7	-7.1	-	-	-
Wetland E (Native prairie)								
Catchment-level ref. ^{137}Cs		**1460**						
MB	Upper Slope	1580	-	-	n.d	-	-	-
MB	Middle Slope	2116	-	-	n.d	-	-	-

Province	Toposequence position	Average ^{137}Cs inventory (Bq m^{-2})	Toposequence Area (m^{2})	Average soil loss (+) or deposition (-) (kg m^{-2} yr^{-1})				
				Power model[1]	Linear model[2]	Tillage erosion model[3]	Water erosion model[4]	Wind erosion model[5]
MB	Lower Slope	426	-	-	2.8	-	-	-
MB	Inner Riparian	1011	-	-	1.2	-	-	-
MB	Inner Wetland	575	-	-	2.4	-	-	-
		Wetland OZM1 (Cultivated catchment)						
Catchment-level ref. ^{137}Cs		**1100**						
AB	Upper Slope	757	6800	2.0	1.1	2.77	0.14	
AB	Middle Slope	1013	23350	1.3	0.3	1.08	0.13	
AB	Lower Slope	1782	3325	-0.2	-2.1	-1.04	0.18	0.02
AB	Outer Riparian	1641	-	0.1	-1.7	-2.81	-	-
AB	Middle Riparian	1798	-	-0.2	-2.2	-	-	-
AB	Inner Riparian	1621	-	0.1	-1.6	-	-	-
AB	Outer Wetland	1864	-	-0.4	-2.4	-	-	-
AB	Middle Wetland	1170	-	0.9	-0.2	-	-	-
AB	Inner Wetland	1247	-	0.7	-0.5	-	-	-
		Wetland MCN1 (Cultivated catchment)						
Catchment-level ref. ^{137}Cs		**1477**						
AB	Upper Slope	1090	11325	1.1	0.9	2.86	0.12	
AB	Middle Slope	1420	28875	0.4	0.1	0.82	0.13	
AB	Lower Slope	2441	3325	-1.3	-2.2	-0.71	0.12	0.02
AB	Outer Riparian	2265	-	-1.0	-1.8	-2.98	-	-
AB	Middle Riparian	1683	-	0.0	-0.5	-	-	-
AB	Inner Riparian	1942	-	-0.4	-1.1	-	-	-
AB	Outer Wetland	942	-	1.4	1.2	-	-	-
AB	Middle Wetland	979	-	1.3	1.1	-	-	-
AB	Inner Wetland	1554	-	0.2	-0.2	-	-	-
		Wetland INT1 (Cultivated catchment)						
Catchment-level ref. ^{137}Cs		**1086**						
AB	Upper Slope	972	4975	1.5	0.4	4.58	0.07	
AB	Middle Slope	1023	12175	1.4	0.2	1.71	0.08	
AB	Lower Slope	1464	1970	0.4	-1.2	-1.78	0.09	0.01
AB	Outer Riparian	1588	-	0.2	-1.6	-4.51	-	-
AB	Middle Riparian	899	-	1.7	0.6	-	-	-
AB	Inner Riparian	954	-	1.6	0.4	-	-	-
AB	Outer Wetland	1188	-	1.0	-0.3	-	-	-
AB	Middle Wetland	590	-	2.9	1.6	-	-	-
AB	Inner Wetland	1154	-	1.0	-0.2	-	-	-

[1]Power model: Mass Balance Model (MBM2) and off-site reference ^{137}Cs values were used for wetland embedded within agricultural landscape.

[2]Linear model: Proportional Model and catchment-level (on-site) reference ^{137}Cs values were used for wetlands embedded in agricultural and native prairie landscapes.

[3]Tillage erosion model: TillEM was used to predict tillage erosion within the cultivated portion of wetland catchments.

[4]Water erosion model: RUSLE2 was used to predict water erosion within the cultivated portion of wetland catchments.

[5]Wind erosion model: SWEEP was used to predict wind erosion within the cultivated portion of wetland catchments.

n.d.: not determined by developed excel add-in software.

4.4.1.2. RUSLE2

RUSLE2 predicted water erosion rates for cultivated field within wetland landscapes varied from 0.3 to -0.14 kg m^{-2} yr^{-1}, and 0.21 and 0.04 kg m^{-2} yr^{-1} in Manitoba and Alberta, respectively. The predicted average water erosion rate for upper, middle and lower slope positions were estimated to be 0.05, 0.13 and 0.14 kg m^{-2} y^{-1} for Manitoba, and 0.11, 0.11 and 0.13 kg m^{-2} yr^{-1} for Alberta (Table 4.1). The spatial pattern of water erosion, predicted by RUSLE2, shows lower soil losses due to water erosion at the upper slope position of the field, while maximum soil loss rates occurred in the positions with the steepest slope gradients (middle slope and lower slope positions). The results of this study are consistent with previous studies (e.g., Schumacher et al., 2005; Li et al., 2007b; Tiessen et al., 2009) that predicted soil loss by water using different water erosion models (e.g., Water and Tillage Erosion Model (WaTEM) and Water Erosion Prediction Project (WEPP). It is also worth mentioning that the water erosion rates from the cultivated field are below the guideline tolerable soil loss limit of 0.6 kg m^{-2} yr^{-1} in Canada (van Vliet et al., 2005). The primary reason for lower water erosion rates can be attributed to the shorter slope length around the wetland environments, at the studied catchments (Demissie et al., 2022). Additionally, model-predicted average sediment delivery by water erosion from cultivated field to riparian area was estimated at about 2,500 kg yr^{-1} for Manitoba and 3,600 kg yr^{-1} for Alberta. The different findings observed in Manitoba and Alberta could be explained by the variations in their respective regional climate and soil characteristics.

4.4.1.3. SWEEP

According to the SWEEP simulation, the minimum threshold wind velocity ranged from 12.0 m s^{-1} (summer fallow with ridge parallel to wind direction) to 18 m s^{-1} (conservation tillage with ridge perpendicular to wind direction). Wind data analysis for Manitoba (1958 to 2021) and Alberta

(1994 to 2021) showed that 330 and 91 erosive days occurred during April, May and June in the Manitoba and Alberta, respectively (Appendix B-B3 and -B4). The total wind erosion rates predicted by SWEEP averaged 0.05 kg m^{-2} y^{-1} for Manitoba and 0.02 kg m^{-2} yr^{-1} for Alberta (Table 4.1). The lower wind erosion rates can be attributed to a smaller effective field length and/or more wind barriers (e.g., riparian areas) within wetland catchments. Additionally, predicted sediment output by wind from cultivated field was predicted to be approximately 1,026 kg yr^{-1} for Manitoba and 617 kg yr^{-1} for Alberta. The results also indicated that wind-eroded sediment traveling in suspension was the main component of soil loss, accounting approximately 47% (summer fallow) to 83% (conservation tillage) of the eroded soil, and this portion for sediment moving by creep/saltation varied approximately between 17% (conservation tillage) and 52% (summer fallow). The proportion of PM10 particles remained very low and stable (at about 2% of the total), regardless of the ridge orientation and height, and amounted to approximately ≤0.001 kg m^{-2} yr^{-1}. These results demonstrated that saltation and suspension processes are the dominant mode in summer fallow practice. The findings of this research are in agreement with recent studies (e.g., Zhang et al., 2017; Nerger et al., 2017), that reported that the majority of wind-blown sediments are transported by suspension in SWEEP simulation. The results also revealed that soil erosion by wind decreased with increasing percentage of residue cover and ridge height. Although the findings of this study are not consistent to previous studies (e.g., Chepil, 1945; Lyles, 1988) that have suggested that between 50% and 80% of total transport is by creep/saltation depending on soil texture, our objectives were to assess soil management scenarios affecting transitory properties (e.g., soil surface roughness) on wind erosion risk rather than stable properties (e.g., texture and organic matter content).

4.4.2. Discrimination of sources of soil erosion

4.4.2.1. Soil redistribution and spatial patterns of ^{137}Cs

Summary of the ^{137}Cs data collected, and ^{137}Cs and model estimated erosion rates of wetland landscapes are presented in Table 4.1. The estimates of soil redistribution reflect the effects of all erosion processes and represent mean annual values since the early 1960s. The estimated point-based soil redistribution rates with the wetland catchments, using a power model (MBM2) and off-site ^{137}Cs reference values, for the 84 and 81 individual sampling points ranged from a maximum soil loss rate of 28.6 to a maximum deposition rate of -32.4 kg m^{-2} yr^{-1}, and from a maximum soil loss rate of 25.0 to a maximum deposition rate of -7.7 kg m^{-2} yr^{-1} in Manitoba and Alberta, respectively. This indicated that both loss and deposition rates varied greatly with the toposequence position. The pattern of soil redistribution indicates that highest soil loss rates are generally found on the upper slope position, while the areas characterized by deposition are largely located in the lower slope positions and particularly the outer riparian area that receive sediment delivered from the eroded areas. Overall, it can be seen from the data in Table 4.1 that the area subject to soil loss greatly exceeds the area where deposition is found, and the field portion of wetland catchments are characterized by average erosion rate between 5.4 and -14.8 kg m^{-2} yr^{-1} for Manitoba, and between 2.0 and -1.3 kg m^{-2} yr^{-1} for Alberta.

Fig. 4.4a and b indicate the pattern of average ^{137}Cs estimated soil erosion, model-predicted tillage erosion and model-predicted total soil erosion (tillage + water + wind). Using linear model (PM) and on-site ^{137}Cs reference values, the sediment delivery ratios for cultivated fields range from 1% to 87% (averaged 57%) for Manitoba, and from 12% to 51% (averaged 34%) for Alberta. The sediment delivery ratios suggest that a reasonable proportion of the sediment mobilized by erosion processes is exported beyond the field boundary with the majority of sediment being deposited in the outer riparian areas, which receive extra pass of field operations during dry years. This in turn can emphasize tillage erosion as a main driver of soil redistribution within the cultivated portion of wetland landscapes (Li et al., 2007b).

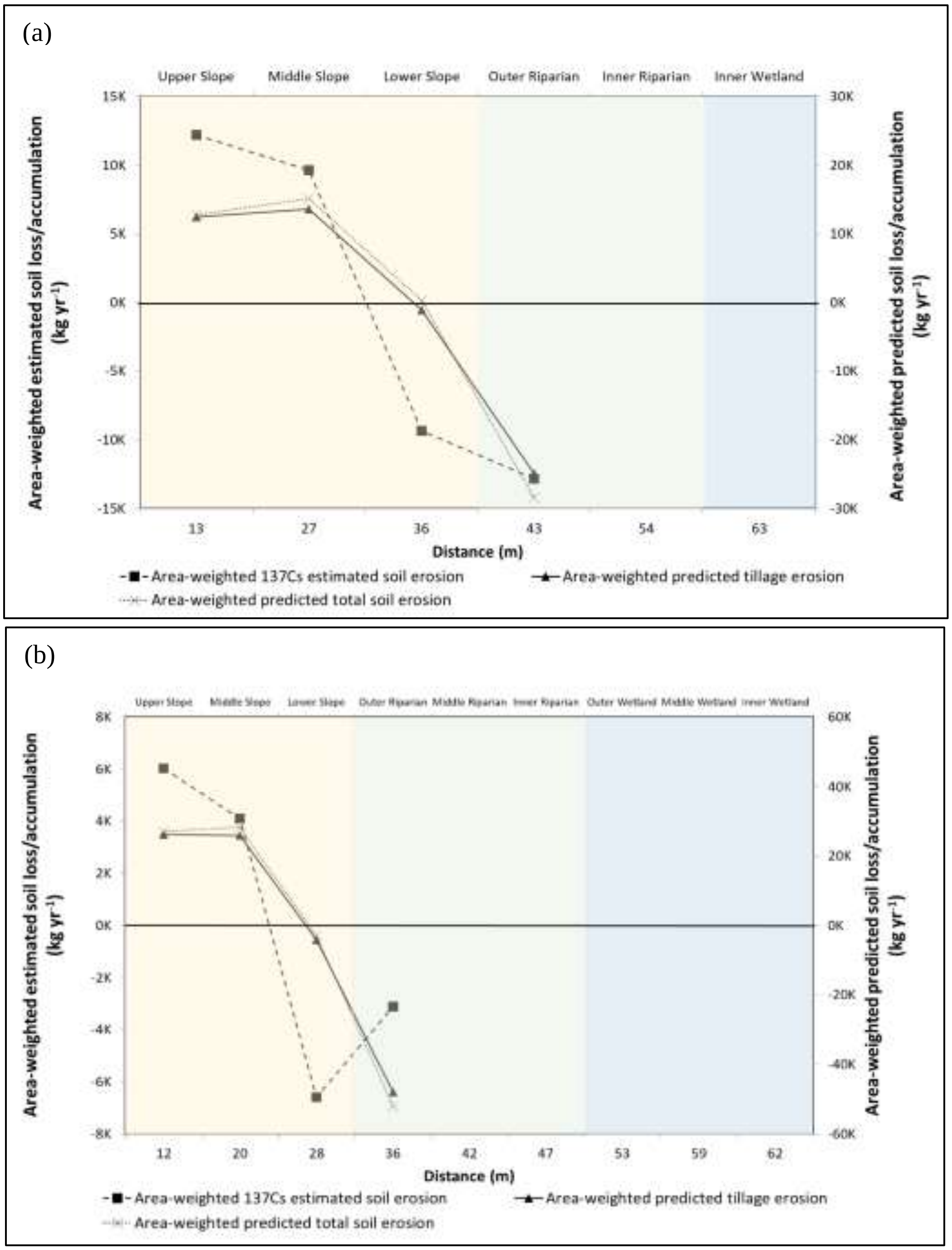

Fig. 4. 4. Average soil redistribution estimated by ^{137}Cs and soil erosion models along transect using a linear model and catchment-level reference value (on-site values) in Manitoba (a) and Alberta (b). Soil erosion models only applied to the field portion of wetland landscapes.

Additionally, as can be seen from the Fig 4.4a and b, the pattern of ^{137}Cs-estimated total erosion showed better agreement with that of the TillEM prediction compared to other erosion processes, while model-predicted soil redistribution rates failed to exhibit any relation with ^{137}Cs-estimated rates. This suggests that tillage erosion is likely the key erosional process for both watersheds. The large discrepancy between the models (i.e., TillEM, RUSLE2 and SWEEP) and ^{137}Cs estimates suggests that there might be systematic errors in these models. These errors were likely caused by the absence of data relating to the current and historically used tillage implements and possible discrepancies of the weather data due to the distance between the weather stations and field sites (Li et al., 2007b). These results are consistent with previous studies (Lobb and Kachanoski, 1999; Li et al., 2007b), who documented that tillage erosion was primarily responsible for the soil redistribution patterns observed in their research, which dominates the eroding portion of landscapes (e.g., hilltops and knolls). Additionally, comparison of the findings with those of other studies (e.g., He and Walling, 2003; Warren et al., 2005) confirms that other soil erosion models (e.g., ANSWERS, AGNPS, WEPP and USLE) yielded quite different predictions compared to tracer-estimated erosion and deposition (e.g., ^{137}Cs and ^{210}Pb$_{ex}$). In addition, although a greater number of cores is required to characterize the spatial pattern of soil redistribution within wetland catchments, the data presented in this study are still able to provide a meaningful representation of erosional land depositional patterns.

4.4.2.2. Principal Component Analysis (PCA)

The average mean values of 10 variables for the sampling points including the ^{137}Cs estimated total soil erosion, model-predicted soil erosion (water, wind, and tillage), soil properties measurements within the tillage depth (~20 cm) such as HSV colour attributes (hue, saturation, and value), and percentage of clay, sand and silt fractions were used for PCA analysis. According to the results of three-dimension PCA, the first principal component (PC1) accounted for 30.2% of the total variance within the data, while the second (PC2) and third (PC3) components explained 27.5% and 15.8% of the total variance, respectively (Fig. 4.5). The first axis (PC1) represented hue, saturation, value and the proportions of clay and silt suggesting that soil colour was strongly affected by these particles. For the second axis (PC2), high contribution values (coefficients), positive or negative, were attributed to tillage erosion (E_{Till}), water erosion (E_{Wat}), model predicted total soil erosion (E_{all}), ^{137}Cs estimated soil erosion (E_{137Cs}), and the proportion of sand. The second axis differentiated the effects of water and tillage erosion given that E_{Till} scored positively, but E_{Wat} scored negatively. E_{Till} and E_{all} were strongly and closely correlated with E_{137Cs}, suggesting that tillage erosion model was the dominant erosional process within the landscape. With respect to the impacts of tillage erosion, E_{Till} was closely correlated with sand content suggesting that the variation of sand across the landscape were influenced by the pattern of tillage erosion. Additionally, water erosion is demonstrating some particle size selectivity (see Appendix B-B5). Including the third component (PC3) into PCA analysis was able to assist with showing the effect of tillage erosion on variations of soil colour attributes (i.e., hue, saturation, and value) within cultivated portion of the wetland catchment. This in turn can confirm that the spatial variability of these variables across the wetland landscapes could be attributed to soil erosion by tillage as well. Furthermore, it showed that the variation of ^{137}Cs within the landscape was closely related to that of clay. This supports the hypothesis that the clay fraction of soil has a high affinity for sorption of ^{137}Cs.

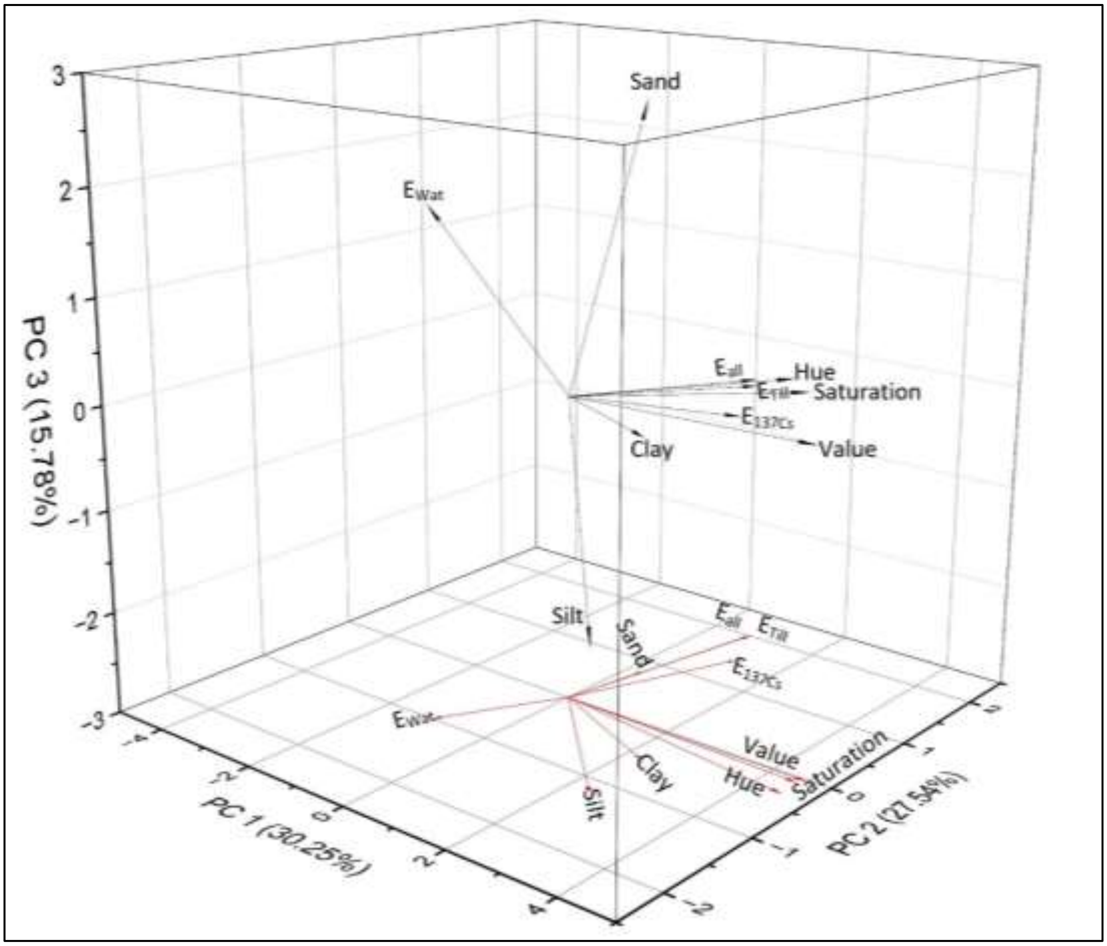

Fig. 4. 5. Three-dimension Principal Components Analysis biplot of the measured and modelled data. Field-measured variables (~20-cm depth) including ^{137}Cs estimated soil erosion (E_{Cs}), hue, saturation, value, sand, silt and clay, and model-estimated variables including tillage erosion (E_{Till}), water erosion (Ewat) and total erosion (E_{all}, tillage- + water- + wind-erosion). Eigenvalues for the first, second and third axis are 3.0, 2.7 and 1.5, respectively, which are standardized to 1.000 and the cumulative percentage variance of each axis is shown in the following bracket. Two-dimension Principal Components Analysis projection using PC1 and PC2 was shown in red and each vector was labelled.

4.4.2.3. Spatial pattern of soil and sediment properties

The spatial distribution pattern of soil primary particles for sampling points along toposequene positions within one wetland catchment (Wetland A) located in Broughton’s Creek watershed, Manitoba is presented in Fig. 4.6 (figures associated with the other wetland catchments in Manitoba and Alberta are presented in the Appendix B-B6 to –B11. The spatial variation of soil particle size within the cultivated portion across the landscape exhibits almost identical distributions on upper, middle, and lower slope positions. It seems reasonable that this pattern may be due to soil redistribution by erosion processes, especially tillage, since tillage erosion is known as a non-selective erosion process. It involves the movement of soil particles across the field, where both finer and coarser particles are transported in a relatively uniform manner. Studies conducted in Canada (Lobb et al., 1995, 1999; Li et al., 2007a, 2007b, 2008; Tiessen et al., 2009) and elsewhere in the world (Lindstrom et al., 1992; Govers et al., 1999; Tiessen et al., 2010) have documented that tillage moves a tremendous amount of soil within cultivated landscapes and is unlikely to have a high degree of particle size selectivity. However, the result of PCA analysis showed that tillage and water erosion contributed to the variation of sand and clay across the landscape, respectively. Furthermore, from Fig. 4.6, it can be seen that smaller particles, mainly clays and silts, are transported further relative to larger, heavier particles, like sand into the central area of wetland catchments that are selectively eroded during surface runoff and erosive wind events. This mainly reflects that finer particles are less prone to deposition in the riparian area and may remain suspended in runoff and pass straight through riparian zones with little retention (Owens et al., 2007).

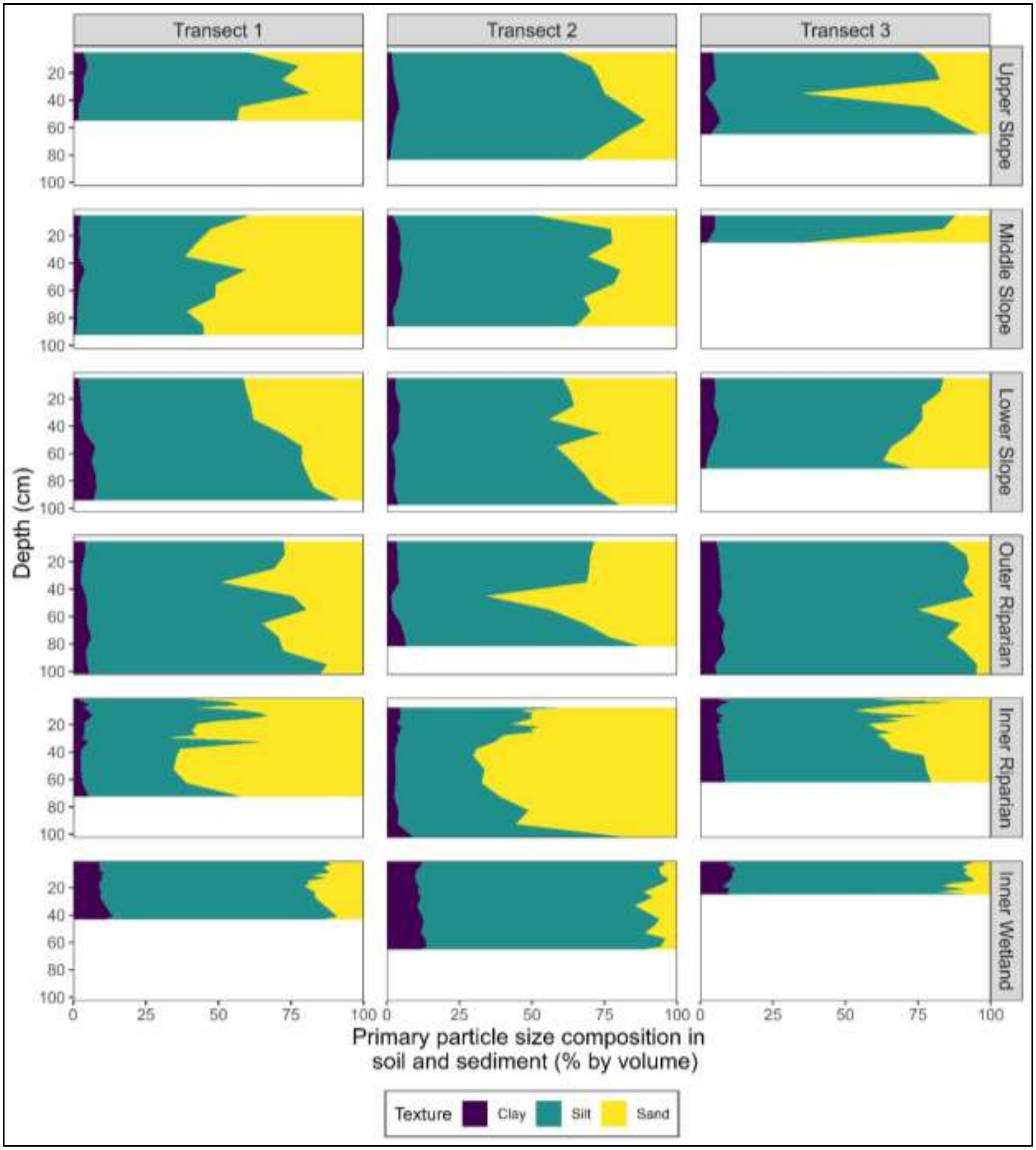

Fig. 4. 6. Average particle size composition of collected soil and sediment samples from different toposequence positions on three transects within one wetland catchment (WetlandA) in Broughton's Creek watershed, Manitoba. Particle size composition is represented by the clay (≤0.002 mm), silt (0.002–0.063 mm) and sand (0.063–2 mm) content of collected samples.

The Kruskal-Wallis test revealed that all colour coefficients were significantly different between the two areas (eroded and accumulation), except for CIE xyZ colour space value *x* and the CIE

L*a*b* colour space value *a**. Furthermore, the LCDA results demonstrate that samples collected in the upland area of wetland catchments at three various toposequence positions (e.g., upper, middle and lower slope positions) were similar, as shown by the close grouping in Fig. 4.7, but were separated from sediments collected at the riparian areas and the central area of wetlands. This significant difference between cultivated upland and wetland environment could be attributed to the upland's soil organic matter depletion and enrichment of soil organic matter in the accumulation zone, which is likely a result of soil and associated constituents (e.g., nutrients) flux via dominant soil erosion process, tillage and water erosion, and production of biomass within wetland environments. Additionally, tillage practices create a more oxidative environment, which accelerates decomposition of crop residue and soil organic matter (Doran, 1980). In general, as organic matter content increases, soil reflectance decreases throughout the entire visible, near-infrared and shortwave-infrared range (VNIR-SWIR) (Baumgardner et al., 1985).

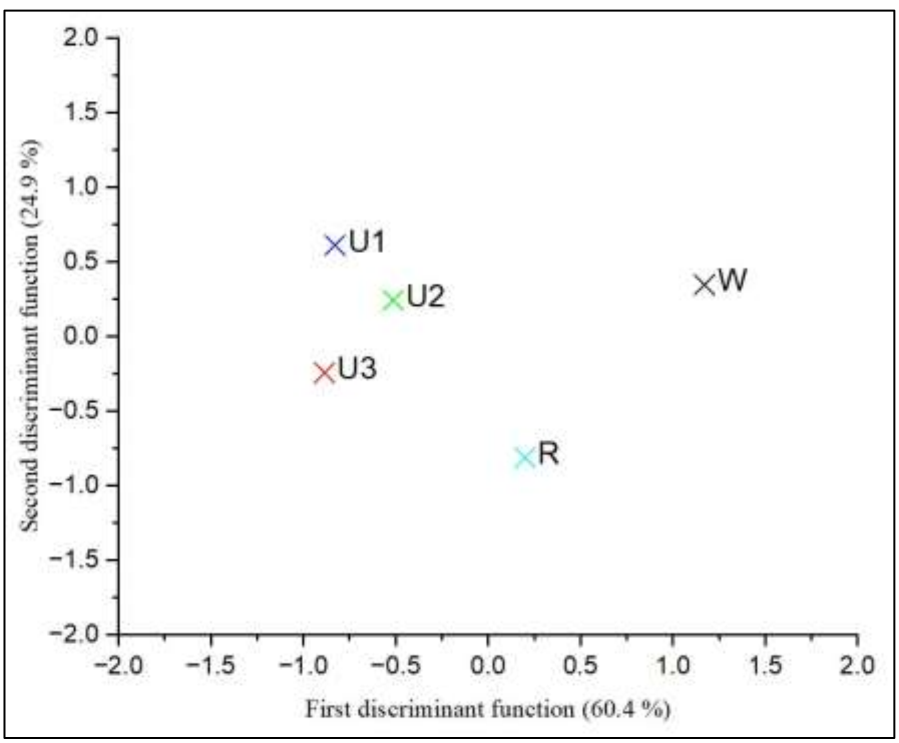

Fig. 4. 7. Colour coefficients properties of soil and sediment collected (~20-cm depth) at different toposequence positions (U1; upper slope position, U2; middle slope position, U3; lower slope position, R; riparian areas, W; water body (central area)) in the studied agricultural catchments. Points are the average across studied wetland catchments.

As can be seen from Fig. 4.8, samples collected from different toposequence positions of one wetland catchment in Manitoba (WetlandA) were characterized by colour attributes of hue, saturation and value, which was used to aid in distinguishing between the eroded and accumulated zones. Therefore, according to the depth distribution of HSV colour attributes, it seems reasonable that organic matter contents of collected cores decreased with depth. Overall, it could be argued that soil/sediment colour can be, at least in part, determined by soil organic matter and primary soil particles (i.e., clay and silt). It is worth mentioning that soil colour might not be a good indicator of stability of soil structure. These findings are consistent with that of Fu et al. (2020), who documented that the darker color of soil was highly correlated to the amount of organic matter, which consequently exhibited lower reflectance. Depth characterization of HSV colour attributes associated with the other wetland catchments are presented in the Appendix B-B12 to -B18. Hexadecimal colour codes were used to visualize the colour composition of each layer of soil and sediment cores within wetland catchments (Appendix B-B19 to -B26).

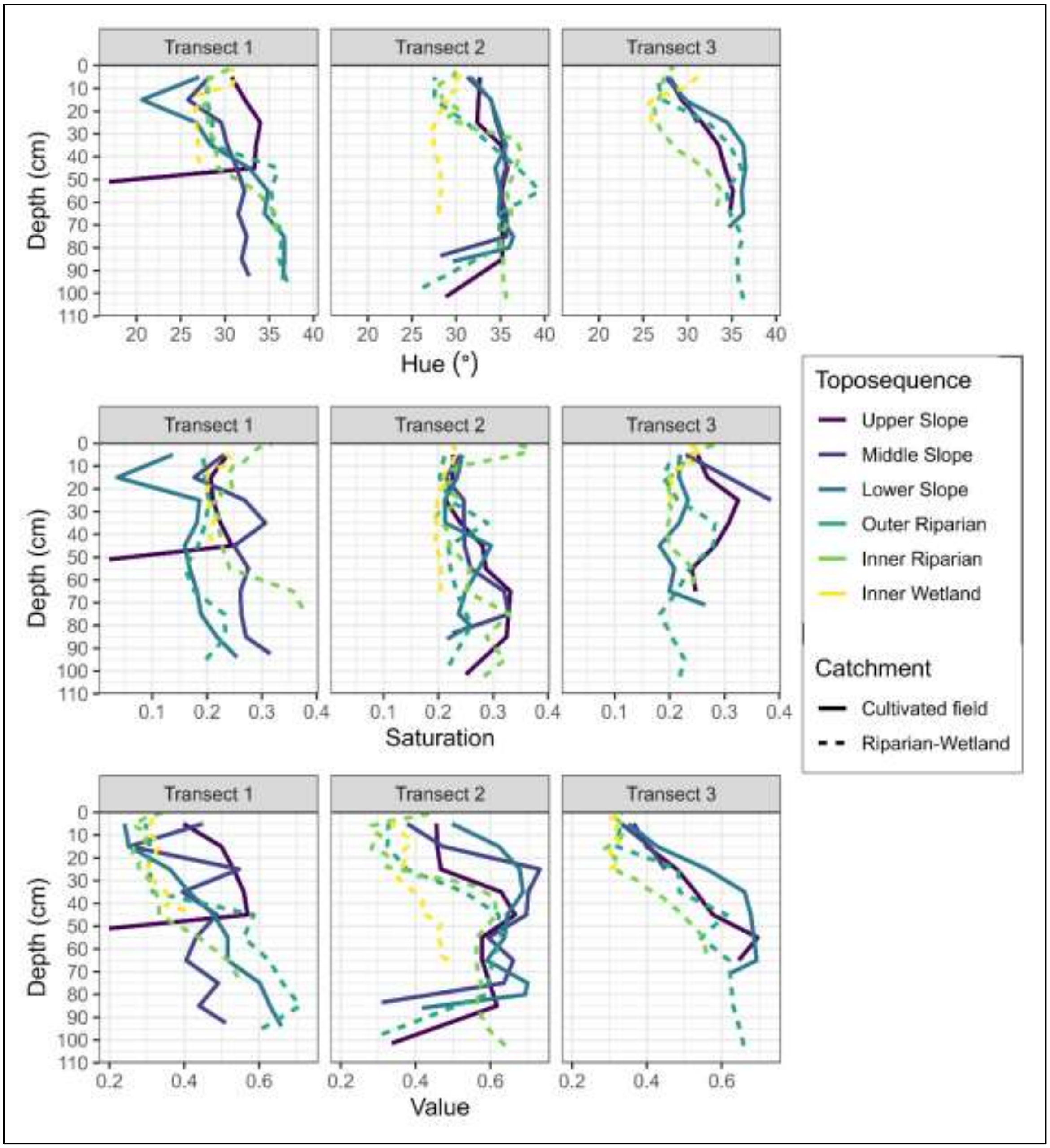

Fig. 4. 8. Depth characterization of HSV colour attributes of hue (e.g., colour itself), saturation (e.g., colour brilliance) and value (e.g., lightness/darkness) for different toposequence position within one wetland catchment (WetlandA) in Broughton's Creek, Manitoba. HSV colour attributes have been used for quantitative descriptions of soil colour.

4.4.3. Uncertainties associated with the soil erosion models

Every erosion model has limitations, which can cause a level of uncertainty in the accuracy of the predicted results. Uncertainty and variability associated with RUSLE2 and SWEEP are a product of error propagated through the model from input data, in the form of real parameters, boundary conditions and effective parameters, but also from model structural errors (Kinnel, 2017). The most important of those are the uncertainties caused by inaccuracy of input data including the weather data, soil, management (e.g., tillage practices, surface conditions, crop rotation), and topographic data, which can contribute errors to the models' predictions (Li et al., 2007b). Increasing model's complexity can also lead to increased model uncertainty due to not examined equations, interactions among variables, numerous input parameters, and non-availability of accurate datasets (Brazier et al., 2000; Nearing and Hairsine, 2010). The errors deriving from more input parameters in the models often outweigh the potential improvement in prediction. Additionally, in contrast to RUSLE2, the current version of SWEEP could not account for the effects of topography (Zhang et al., 2017), which can contribute high uncertainties in predicted wind erosion rates in topographically complex landscapes of PPR. Despite high degrees of uncertainty and variability, water erosion models are deemed as being useful for identifying water erosion patterns in North American PPR (Li et al., 2007b; Kinnel, 2017).

Compared to water erosion and wind erosion models, the tillage erosion model is a relatively simple model (Li et al., 2007b). The estimated tillage erosion rates by TillEM are mainly affected by the values of slope curvature (φ) and slope gradient (θ), since these parameters vary across the landscapes, which impacts the magnitude of the estimated tillage erosion rates. Lobb et al. (1999) reported that predicted tillage erosion rate is likely to be more sensitive to slope gradient. Furthermore, research performed by Li et al. (2007b) reported low uncertainties associated with TillEM estimated tillage erosion rates and indicated that pattern of estimated tillage erosion was not sensitive to slope curvature and gradient.

4.4.5. Discrepancies between the model-predicted and ^{137}Cs-estimated soil erosion

One of the main reasons for high modelling uncertainty is that soil erosion measurements contain a considerable amount of uncertainty (e.g., each measurement technique constrained by either spatial scale, accuracy, or repeatability of measurements) (Alewell et al., 2019). Therefore, this uncertainty can lead to unavoidable discrepancies between soil loss rates derived from ^{137}Cs inventories and those from soil erosion models (e.g., TillEM, RUSLE2 and SWEEP). The large discrepancy between the models (i.e., TillEM, RUSLE2 and SWEEP) and ^{137}Cs estimates can be attributed to differences in spatial and temporal resolution of methods and possible influence of individual extreme events on results yielded by the ^{137}Cs method as well as systematic errors in the models (Belyaev et al., 2009). For example, the ^{137}Cs technique estimated a greater soil accumulation at the lower slope position in comparison to the predictions by soil erosion models. There are a number of possible reasons to explain these discrepancies. The first is that the tillage erosion could be underestimated using the parameters obtained from Li et al. (2007a) because more intensive tillage operations might have been used at the studied wetland catchments. For instance, speed of tillage, greater depth, larger equipment, and more tillage passes were often used before the 1990s, which could have increased tillage erosion and the soil movement, compared to that predicted by the models (Tiessen et al., 2009). Second, the discrepancies for RUSLE2-based predictions arise from the temporal and spatial resolutions of the rainfall data, differences in hydrologic processes and simplifications in vegetation and soil erodibility. An instance of this is the utilization of climate and soil databases from different counties in this study, which aimed to resemble the topographic, climatic, and agricultural land conditions of the studied catchments within the Canadian PPR. Furthermore, RUSLE2 does not estimate erosion by snowmelt in late winter and early spring, which could be the most important water erosion event in areas where snow covers the soil for most of the winter months (USDA-ARS, 2008). Third, previous studies (e.g., Feng and Sharratt 2009; Zhang et al., 2017) reported that SWEEP tended to underestimate the observed wind erosion rates, due to: (i) an overestimation of the threshold friction velocity, and (ii) the needed model inputs were not measured, so average parameter values for the specific soils were substituted for these inputs. Another possible reason for differences is that discrepancies often exist between the erosion rates estimated using the different conversion models for a given set of ^{137}Cs data (Porto et al., 2003; Li et al., 2010). In this study, the linear model (i.e., PM) was used to convert the ^{137}Cs inventory values into soil loss and accumulation rates. It has been documented that discrepancy due to different conversion models is larger in the situations of higher ^{137}Cs losses (Li, 2021).

4.5. Conclusions

Information concerning agricultural catchment soil and sediment dynamics is important for understanding the mobilization and transfer of soil and soil-associated constituents. Therefore, to strengthen field-based erosion assessments, the spatial patterns of soil erosion predicted by three erosion models (TillEM, RUSLE2 and SWEEP) were complemented with the pattern of erosion estimated using ^{137}Cs, which allowed a spatial interpretation of the soil redistribution in the wetland catchments. Overall, the spatial patterns of tillage- and water-induced erosion are fundamentally different across hummocky landscapes. On the knoll of these landscapes, tillage-induced erosion dominates the pattern of total soil erosion, and the impacts of wind- and water-induced erosion are minor. Although close agreement between model-predicted and ^{137}Cs-estimated spatial patterns of soil erosion will afford some degree of validation, it will not provide conclusive confirmation of the validity of the magnitude of soil redistribution within the catchment predicted by the models. The results also showed greater uncertainties with water erosion

(RUSLE2) and wind erosion (SWEEP) models than Tillage erosion (TillEM) model. Despite the complexity of the studied catchments, the results indicated that tillage- and water-induced soil erosion were considered to be a major factor for the spatial variation of soil properties within the landscapes. Besides, soil and sediment colour measurements, and close correlation between HSV colour attributes and primary soil particles (i.e., clay and silt) confirmed soil organic matter enrichment in the accumulation areas of the wetland catchments. Furthermore, the complexity of soil redistribution pattern is greatly affected by tillage, which consequently can influence soil organic matter dynamics in the topographically complex landscape. Therefore, implementing effective soil conservation measures should be considered to minimize the effects of tillage erosion in this region.

4.6. References

Alberta soil survey report, 1985. Soil Survey of the County of Two Hills No. 21, Alberta. Terrain Sciences Department, Natural Resources Division, Alberta Research Council, Edmonton, Alberta, Canada. URL https://sis.agr.gc.ca/cansis/publications/surveys/ab/ab35/index.html (accessed 11.01.2022)

Alewell, C., Borrelli, P., Meusburger, K., Panagos, P., 2019. Using the USLE: Chances, challenges and limitations of soil erosion modelling. Int. Soil Water Conserv. Res. 7, 203–225. https://doi.org/10.1016/j.iswcr.2019.05.004

Asadi, H., Moussavi, A., Ghadiri, H., Rose, C.W., 2011. Flow-driven soil erosion processes and the size selectivity of sediment. J. Hydrol. 406, 73–81. https://doi.org/10.1016/j.jhydrol.2011.06.010

Barthod, L.R.M., Liu, K., Lobb, D.A., Owens, P.N., Martínez-Carreras, N., Koiter, A.J., Petticrew, E.L., McCullough, G.K., Liu, C., Gaspar, L., 2015. Selecting color-based tracers and classifying sediment sources in the assessment of sediment dynamics using sediment source fingerprinting. J. Environ. Qual. 44, 1605-1616. https://doi.org/10.2134/jeq2015.01.0043

Baumgardner, M.F., Silva, L.F., Biehl, L.L., Stonery, E.R., 1985. Reflectance properties of soils. Adv. Agron. 38, 1-44. https://doi.org/10.1016/S0065-2113(08)60672-0

Belyaev, V.R., Golosov, V.N., Kuznetsova, J.S., Markelov, M.V., 2009. Quantitative assessment of effectiveness of soil conservation measures using a combination of ^{137}Cs radioactive tracer and conventional techniques. Catena 79, 214–227. https://doi.org/10.1016/j.catena.2009.05.006

Blanco-Canqui, H., Lal, R., 2008a. Soil and Water Conservation, in: Blanco-Canqui, H., Lal, R. (Eds.), Principles of Soil Conservation and Management. Springer Netherlands, Dordrecht, pp. 1–19. https://doi.org/10.1007/978-1-4020-8709-7_1

Blanco-Canqui, H., Lal, R., 2008b. Water Erosion, in: Blanco-Canqui, H., Lal, R. (Eds.), Principles of Soil Conservation and Management, Springer Netherlands, Dordrecht, pp. 21–53. https://doi.org/10.1007/978-1-4020-8709-7_2

Borrelli, P., Robinson, D.A., Fleischer, L.R., Lugato, E., Ballabio, C., Alewell, C., Meusburger, K., Modugno, S., Schütt, B., Ferro, V., Bagarello, V., Oost, K. Van, Montanarella, L., Panagos, P., 2017. An assessment of the global impact of 21st century land use change on soil erosion. Nat. Commun. 8. https://doi.org/10.1038/s41467-017-02142-7

Boudreault, M., Koiter, A.J., Lobb, D.A., Liu, K., Benoy, G., Owens, P.N., Li, S., 2019. Comparison of sampling designs for sediment source fingerprinting in an agricultural watershed in Atlantic Canada. J. Soils Sediments 19, 3302–3318. https://doi.org/10.1007/s11368-019-02306-6

Brazier, R.E., Beven, K.J., Freer, J., Rowan, J.S., 2000. Equifinality and uncertainty in physically based soil erosion models: Application of the glue methodology to WEPP- the water erosion prediction project- for sites in the UK and USA. Earth Surf. Process. Landforms 25, 825–845. https://doi.org/10.1002/1096-9837(200008)25:8<825::AID-ESP101>3.0.CO;2-3

Buschiazzo, D.E., Zobeck, T.M., 2008. Validation of WEQ, RWEQ and WEPS wind erosion for different arable land management systems in the Argentinean Pampas. Earth Surf. Process. Landforms 33, 1839–1850. https://doi.org/https://doi.org/10.1002/esp.1738

Cabral, P., Tejeda, S., Cabrera, M., Sanabria, R., Gonz, J., Zarazua, G., Melgar-paniagua, E., Tassano, M., 2023. Using ^{137}Cs and ^{210}Pb$_{ex}$ to assess soil redistribution at different temporal scales along with lithogenic radionuclides to evaluate contrasted watersheds in the Uruguayan Pampa grassland. Geoderma. 435, 116502. https://doi.org/10.1016/j.geoderma.2023.116502

Campbell, C.A., R.P Zentner, H.H. Janzen, and K.E. Bowren., 1990. Crop Rotation Studies on the Canadian Prairies. Publ. 1841/E, Research Branch, Agriculture Canada, Ottawa, Ontario 133 pp.

Chepil, W.S., 1945. Dynamics of wind erosion: I. Nature of movement of soil by wind. Soil Sci. 60. 305-320.

Coupland, R.T., 1973. Theme study of natural grassland in western Canada. Unpublished report. National and Historic Parks Branch, Canada Department of Indian Affairs and Northern Development. Ottawa, ON.

Croke, J., Nethery, M., 2006. Modelling runoff and soil erosion in logged forests: Scope and application of some existing models. Catena 67, 35–49. https://doi.org/10.1016/j.catena.2006.01.006

Dabney, S.M., 2010. Modeling runoff and erosion from construction sites in 2-D with RUSLE2. 19th World Congr. Soil Sci. Soil Solut. a Chang. World 14–17.

Dabney, S.M., Vieira, D.A.N., Yoder, D.C., 2013. Effects of topographic feedback on erosion and deposition prediction 56, 727–736.

Dabney, S.M., Yoder, D.C., Vieira, D.A.N., 2012. The application of the Revised Universal Soil Loss Equation, Version 2, to evaluate the impacts of alternative climate change scenarios on runoff and sediment yield. J. Soil Water Conserv. 67, 343–353. https://doi.org/10.2489/jswc.67.5.343

Dabney, S.M., Yoder, D.C., Vieira, D.A.N., Bingner, R.L., 2011. Enhancing RUSLE to include runoff-driven phenomena. Hydrol. Process. 25, 1373–1390. https://doi.org/10.1002/hyp.7897

de Jong, E., Begg, C.B.M., Kachanoski, R.G., 1983. Estimates of soil erosion and deposition for some Saskatchewan soils. Can. J. Soil Sci. 63, 607–617. https://doi.org/10.4141/cjss83-061

Demissie, S., Meshesha, D.T., Adgo, E., Haregeweyn, N., Tsunekawa, A., Ayana, M., Mulualem, T., Wubet, A., 2022. Effects of soil bund spacing on runoff, soil loss, and soil water content in the Lake Tana Basin of Ethiopia. Agric. Water Manag. 274, 107926. https://doi.org/10.1016/j.agwat.2022.107926

Doran, J.W., 1980. Soil Microbial and Biochemical Changes Associated with Reduced Tillage. Soil Sci. Soc. Am. J. 44, 765–771. https://doi.org/https://doi.org/10.2136/sssaj1980.03615995004400040022x

Environment and Climate Change Canada (ECCC), 2022. 1981-2010 climate normals and averages. Canadian climate normals. URL https://climate.weather.gc.ca/climate_normals/index_e.html. (accessed 5.12.2022)

Feng, G., Sharratt, B., 2009. Evaluation of the SWEEP model during high winds on the Columbia Plateau. Earth Surf. Process. Landforms 34, 1461–1468. https://doi.org/https://doi.org/10.1002/esp.1818

Fu, Y., Taneja, P., Lin, S., Ji, W., Adamchuk, V., Daggupati, P., Biswas, A., 2020. Predicting soil organic matter from cellular phone images under varying soil moisture. Geoderma. 361, 114020. https://doi.org/10.1016/j.geoderma.2019.114020

Ghadiri, H., 2004. Crater formation in soils by raindrop impact. Earth Surf. Process. Landforms 29, 77–89. https://doi.org/10.1002/esp.1014

Govers, G., Lobb, D.A., Quine, T.A., 1999. Tillage erosion and translocation: emergence of a new paradigm in soil erosion research. Soil Tillage Res. 51, 167-174.

Govers, G., Vandaele, K., Desmet, P., Poesen, J., Bunte, K., 1994. The role of tillage in soil redistribution on hillslopes. Eur. J. Soil Sci. 45, 469–478. https://doi.org/10.1111/j.1365-2389.1994.tb00532.x

Gray, A.B., Pasternack, G.B., Watson, E.B., 2010. Hydrogen peroxide treatment effects on the particle size distribution of alluvial and marsh sediments. Holocene 20, 293–301. https://doi.org/10.1177/0959683609350390

He, Q., Walling, D.E., 2003. Testing distributed soil erosion and sediment delivery models using ^{137}Cs measurements. Hydrol. Process. 17, 901–916. https://doi.org/10.1002/hyp.1169

Heuvelink, G.B.M., Schoorl, J.M., Veldkamp, A., Pennock, D.J., 2006. Space-time Kalman filtering of soil redistribution. Geoderma. 133, 124–137. https://doi.org/10.1016/j.geoderma.2006.03.041

Howitt R.W., 1988. Soil survey of the County of Beaver (Vol. 47): Alberta soil survey report. URL https://open.alberta.ca/publications/ss-47 (accessed 5.12.2022)

Jenkins, C. Shaykewich, C.F. and de Jong, E., 1984. Potential for the use of Cesium-137 as a tracer for soil erosion in Manitoba. 27th Manitoba Soil Science Society Meeting, Winnipeg, Manitoba, 181-187.

Jia, Q., Al-Ansari, N., Knutsson, S., 2014. Modeling of wind erosion of the Aitik tailings dam using SWEEP model. Engineering 06, 355–364. https://doi.org/10.4236/eng.2014.67038

Kinnell, P.I.A., 2017. A comparison of the abilities of the USLE-M, RUSLE2 and WEPP to model event erosion from bare fallow areas. Sci. Total Environ. 596–597, 32–42. https://doi.org/10.1016/j.scitotenv.2017.04.046

Knisel, W. G. (editor). 1980. CREAMS : a field scale model for Chemicals, Runoff, and Erosion from Agricultural Management Systems. Conservation Research Report No. 26. U.S. Department of Agriculture, Science and Education Administration, Washington, DC.

Koiter, A., 2021. Colour analysis scripts. https://doi.org/10.5281/zenodo.5123327

Koiter, A.J., Owens, P.N., Petticrew, E.L., Lobb, D.A., 2013. The behavioural characteristics of sediment properties and their implications for sediment fingerprinting as an approach for identifying sediment sources in river basins. Earth-Science Rev. 125, 24–42. https://doi.org/10.1016/j.earscirev.2013.05.009

Kuhwald, M., Busche, F., Saggau, P., Duttmann, R., 2022. Is soil loss due to crop harvesting the most disregarded soil erosion process? A review of harvest erosion. Soil Tillage Res. 215, 105213. https://doi.org/10.1016/j.still.2021.105213

Lal, R., 1998. Soil Erosion Impact on Agronomic Productivity and Environment Quality. CRC. Crit. Rev. Plant Sci. 17, 319–464. https://doi.org/10.1080/07352689891304249

LaZerte, S.E., Albers, S., Brown, N., 2018. weathercan: Download and format weather data from Environment and Climate Change Canada. J. Open Source Softw. 3(22), 571. https://doi.org/10.21105/joss.00571

LaZerte, S., Li, S., 2021., LITAP: Landscape Integrated Terrain Analysis Package. R package version 0.6.0, https://github.com/FRDC-SHL/LITAP

Li, S., 2021. Landscape Integrated Soil and Water Conservation (LISWC) system for sloping landscapes in Atlantic Canada. Agric. 11, 427. https://doi.org/10.3390/agriculture11050427

Li, S., Lobb, D.A., Lindstrom, M.J., 2007a. Tillage translocation and tillage erosion in cereal-based production in Manitoba, Canada. Soil Tillage Res. 94, 164–182. https://doi.org/10.1016/j.still.2006.07.019

Li, S., Lobb, D.A., Lindstrom, M.J., Farenhorst, A., 2008. Patterns of water and tillage erosion on topographically complex landscapes in the North American Great Plains. J. Soil Water Conserv. 63, 37–46. https://doi.org/10.2489/63.1.37

Li, S., Lobb, D.A., Lindstrom, M.J., Farenhorst, A., 2007b. Tillage and water erosion on different landscapes in the northern North American Great Plains evaluated using ^{137}Cs technique and soil erosion models. Catena 70, 493–505. https://doi.org/10.1016/j.catena.2006.12.003

Li, S., Lobb, D.A., McConkey, B.G., Walker, B., Goddard, T., 2007c. Tillage and water erosion under different tillage systems in Alberta, Canada. In ASA-CSSA-SSSA International Annual Meetings (November 4-8, 2007).

Li, S., Lobb, D.A., Tiessen, K.H.D., 2009. Modeling tillage-induced morphological features in cultivated landscapes. Soil Tillage Res. 103, 33–45. https://doi.org/10.1016/j.still.2008.09.005

Li, S., Lobb, D.A., Tiessen, K.H.D., 2013. Soil Erosion and Conservation, In: El-Shaarawi, A.H., Piegorsch, W.W., (Eds.), Encyclopedia of Environmetrics. John Wiley & Sons, Ltd. https://doi.org/https://doi.org/10.1002/9780470057339.vas031.pub2

Li, S., Lobb, D.A., Tiessen, K.H.D., McConkey, B.G., 2010. Selecting and applying Cesium-137 conversion models to estimate soil erosion rates in cultivated fields. J. Environ. Qual. 39, 204–219. https://doi.org/10.2134/jeq2009.0144

Li, S., MacMillan, R.A., Lobb, D.A., McConkey, B.G., Moulin, A., Fraser, W.R., 2011. Lidar DEM error analyses and topographic depression identification in a hummocky landscape in the prairie region of Canada. Geomorphology 129, 263–275. https://doi.org/10.1016/j.geomorph.2011.02.020

Lindstrom, M.J., Nelson, W.W., Schumacher, T.E., 1992. Quantifying tillage erosion rates due to moldboard plowing. Soil Tillage Res. 24, 243–255. https://doi.org/10.1016/0167-1987(92)90090-X

Liu, B., Qu, J., Niu, Q., Han, Q., 2014. Comparison of measured wind tunnel and SWEEP simulated soil losses. Geomorphology 207, 23–29. https://doi.org/10.1016/j.geomorph.2013.10.024

Liu, K., Lobb, D.A., Miller, J.J., Owens, P.N., Caron, M.E.G., 2017. Determining sources of fine-grained sediment for a reach of the lower little bow river, Alberta, using a colour-based sediment fingerprinting approach. Can. J. Soil Sci. 98, 55–69. https://doi.org/10.1139/cjss-2016-0131

Lobb, D.A., 2011. Understanding and managing the causes of soil variability. J. Soil Water Conserv. 66, 175–179. https://doi.org/10.2489/jswc.66.6.175A

Lobb, D.A., Kachanoski, R.G., (1997, July). The impact of tillage translocation and tillage erosion on the estimation of soil loss using ^{137}Cs. Poster presentation at Soil and Water Conservation Society, Annual Conference, 1st International Symposium on Tillage Translocation and Tillage Erosion. Toronto, Ontario, Canada.

Lobb, D.A., Kachanoski, R.G., 1999. Modelling tillage erosion in the topographically complex landscapes of southwestern Ontario, Canada. Soil Tillage Res. 51, 261–277. https://doi.org/10.1016/S0167-1987(99)00042-2

Lobb, D.A., Kachanoski, R.G., Miller, M.H., 1995. Tillage translocation and tillage erosion on shoulder slope landscape positions measured using ^{137}Cs as a tracer. Can. J. Soil Sci. 75, 211–218. https://doi.org/10.4141/cjss95-029

Lobb, D.A., Lindstrom, M.J., Schumacher, T.E., 2003. Soil erosion processes and their interactions: implications for environmental indicators, in: Agricultural Impacts on Soil Erosion and Soil Biodiversity: Developing Indicators for Policy Analysis. Proceedings from an OECD Expert Meeting—Rome, Italy, March. 325–336.

Lyles, L., 1988. Basic wind erosion processes. Agric. Ecosyst. Environ. 22, 91-101. https://doi.org/10.1016/0167-8809(88)90010-2

Mabit, L., Zapata, F., Benmansour, M., Bernard, C., Dercon, G., Walling, D.E., 2014. Assessment of soil erosion and sedimentation: the role of fallout radionuclides: The Role of Fallout Radionuclides, IAEA-TECDOC-1741, IAEA Publication, Vienna, Austria, 3, 3-26.

MacMillan, R.A., Martin, T.C., Earle, T.J., Mc Nabb, D.H., 2003. Automated analysis and classification of landforms using high-resolution digital elevation data: Applications and issues. Can. J. Remote Sens. 29, 592–606. https://doi.org/10.5589/m03-031

MacMillan, R.A., Pettapiece, W.W., Nolan, S.C., Goddard, T.W., 2000. A generic procedure for automatically segmenting landforms into landform elements using DEMs, heuristic rules and fuzzy logic. Fuzzy Sets Syst. 113, 81–109. https://doi.org/10.1016/S0165-0114(99)00014-7

Manitoba Agricultural Services Corporation (MASC), 2021. Yield Manitoba. https://www.masc.mb.ca/masc.nsf/ym_2021_full_issue.pdf (accessed 10.12.2022)

Millard, K., Burke, C., Stiff, D., Redden, A., 2009. Detection of a low-relief 18th-century British siege trench using LiDAR vegetation penetration capabilities at Fort Beauséjour-Fort Cumberland National Historic Site, Canada. Geoarchaeology 24, 576–588. https://doi.org/10.1002/gea.20281

Manitoba soil survey report, 2011. Soils of the Rural Municipality of Blanshard No. 91, Manitoba. Soil and Landscape Management Section, Agri-Environment knowledge Center, Manitoba Agriculture, Food and Rural Initiatives, Winnipeg, Manitoba, Canada. URL https://sis.agr.gc.ca/cansis/publications/surveys/mb/mbd91/index.html (accessed 11.01.2022)

Millett, B., Johnson, W.C., Guntenspergen, G., 2009. Climate trends of the North American prairie pothole region 1906-2000. Clim. Change 93, 243–267. https://doi.org/10.1007/s10584-008-9543-5

Nearing, M.A., Hairsine, P.B., 2010. The Future of Soil Erosion Modelling, in: Morgan, R. P. C., Nearing M. A., (Eds.), Handbook of Erosion Modelling. pp. 387–397. https://doi.org/https://doi.org/10.1002/9781444328455.ch20

Nearing, M.A., Lane, L.J., Lopes, V.L., 1994. Modeling soil erosion. In: Lal, R. (Ed.), Soil Erosion: Research Methods, Soil and Water Conservation Society and St. Lucie Press, Ankeny, Iowa, pp. 127–156.

Nearing, M.A., Lane, L.J., Lopes, V.L., 2017. Modeling Soil Erosion, in: Lal, R. (Ed.), Soil Erosion Research Methods. Routledge, pp. 127–158.

Nerger, R., Funk, R., Cordsen, E., Fohrer, N., 2017. Application of a modeling approach to designate soil and soil organic carbon loss to wind erosion on long-term monitoring sites (BDF) in Northern Germany. Aeolian Res. 25, 135–147. https://doi.org/10.1016/j.aeolia.2017.03.006

Nicholaichuk, W., Read, D.W.L., 1978. Nutrient runoff from fertilized and unfertilized fields in western Canada. J. Environ. Qual. 7, 542–544. https://doi.org/https://doi.org/10.2134/jeq1978.00472425000700040015x

Owens, P.N., Duzant, J.H., Deeks, L.K., Wood, G.A., Morgan, R.P.C., Collins, A.J., 2007. Evaluation of contrasting buffer features within an agricultural landscape for reducing sediment and sediment-associated phosphorus delivery to surface waters. Soil Use Manag. 23, 165–175. https://doi.org/10.1111/j.1475-2743.2007.00121.x

Panagos, P., Borrelli, P., Robinson, D., 2020. FAO calls for actions to reduce global soil erosion. Mitig. Adapt. Strateg. Glob. Chang. 25, 789–790. https://doi.org/10.1007/s11027-019-09892-3

Papiernik, S.K., Lindstrom, M.J., Schumacher, J.A., Farenhorst, A., Stephens, K.D., Schumacher, T.E., Lobb, D.A., 2005. Variation in soil properties and crop yield across an eroded prairie landscape. J. Soil Water Conserv. 60, 388–395.

Pennock, D.J., 2003. Terrain attributes, landform segmentation, and soil redistribution. Soil Tillage Res. 69, 15–26. https://doi.org/10.1016/S0167-1987(02)00125-3

Pennock, D.J., Zebarth, B.J., de Jong, E., 1987. Landform classification and soil distribution in hummocky terrain, Saskatchewan, Canada. Geoderma. 40, 297–315. https://doi.org/10.1016/0016-7061(87)90040-1

Pi, H., Sharratt, B., Feng, G., Lei, J., Li, X., Zheng, Z., 2016. Validation of SWEEP for creep, saltation, and suspension in a desert-oasis ecotone. Aeolian Res. 20, 157–168. https://doi.org/10.1016/j.aeolia.2016.01.006

Porto, P., Walling, D.E., Ferro, V., Di Stefano, C., 2003. Validating erosion rate estimates provided by Caesium-137 measurements for two small forested catchments in Calabria, Southern Italy. L. Degrad. Dev. 14, 389–408. https://doi.org/10.1002/ldr.561

Quine, T.A., Govers, G., Walling, D.E., Zhang, X., Desmet, P.J.J., Zhang, Y., Vandaele, K., 1997. Erosion processes and landform evolution on agricultural land - New perspectives from Caesium-137 measurements and topographic-based erosion modelling. Earth Surf. Process. Landforms 22, 799–816. https://doi.org/10.1002/(sici)1096-9837(199709)22:9<799::aid-esp765>3.0.co;2-r

R core Team., 2020. R: A language and environment for statistical computing. R foundation for Statistical Computing, Vienna, Austria. https://www.R-project.org/

Reddy, K.R., Clark, M.W., DeLaune, R.D., Kongchum, M., 2013. Physicochemical Characterization of Wetland Soils, in: DeLaune, R.D., Reddy, K.R., Richardson, C.J., Megonigal, J.P., (Eds.), Methods in Biogeochemistry of Wetlands. John Wiley & Sons, Ltd, pp. 41–54. https://doi.org/https://doi.org/10.2136/sssabookser10.c3

Renard, K.G., Yoder, D.C., Lightle, D.T., Dabney, S.M., 2010. Universal Soil Loss Equation and Revised Universal Soil Loss Equation, in: Morgan, R. P. C., Nearing M. A., (Eds.), Handbook of Erosion Modelling. pp. 135–167. https://doi.org/https://doi.org/10.1002/9781444328455.ch8

Ruysschaert, G., Poesen, J., Verstraeten, G., Govers, G., 2004. Soil loss due to crop harvesting: Signficance and determining factors. Prog. Phys. Geogr. 28, 467–4501. https://doi.org/10.1191/0309133304pp421oa

Schumacher, J.A., Kaspar, T.C., Ritchie, J.C., Schumacher, T.E., Karlen, D.L., Venteris, E.R., McCarty, G.W., Colvin, T.S., Jaynes, D.B., Lindstrom, M.J., Fenton, T.E., 2005. Identifying spatial patterns of erosion for use in precision conservation. J. Soil Water Conserv. 60, 355-362.

Shaw, G.A. 1980. Predicted soil erosion by water for various soil types in Manitoba. 24th Manitoba Soil Science Society Meeting, Winnipeg, Manitoba. pp. 63-70

Sutherland, R.A., de Jong, E., 1990. Estimation of sediment redistribution within agricultural fields using caesium-137, Crystal Springs, Saskatchewan, Canada. Appl. Geogr. 10, 205–221. https://doi.org/https://doi.org/10.1016/0143-6228(90)90022-H

Tatarko, J., van Donk, S.J., Ascough, J.C., Walker, D.G., 2016. Application of the WEPS and SWEEP models to non-agricultural disturbed lands. Heliyon 2, e00215. https://doi.org/10.1016/j.heliyon.2016.e00215

Tiessen, K.H.D., Elliott, J.A., Yarotski, J., Lobb, D.A., Flaten, D.N., Glozier, N.E., 2010. Conventional and conservation tillage: Influence on seasonal runoff, sediment, and nutrient losses in the Canadian Prairies. J. Environ. Qual. 39, 964–980. https://doi.org/10.2134/jeq2009.0219

Tiessen, K.H.D., Li, S., Lobb, D.A., Mehuys, G.R., Rees, H.W., Chow, T.L., 2009. Using repeated measurements of ^{137}Cs and modelling to identify spatial patterns of tillage and water erosion within potato production in Atlantic Canada. Geoderma 153, 104–118. https://doi.org/10.1016/j.geoderma.2009.07.013

Toogood, J.A. 1963. Water erosion in Alberta. J. Soil Water Conserv. 6: 238-240.

Unger, P.W., Mccalla, T.M., 1980. Conservation tillage systems. Adv. Agron. 33, 2–58.

United States Department of Agriculture-Agricultural Research Service (USDA-ARS), 2008. User's reference guide: Revised universal soil loss equation. Version 2. https://www.ars.usda.gov/ARSUserFiles/60600505/RUSLE/RUSLE2_Science_Doc.pdf (accessed 10.12.2022)

United States Department of Agriculture-Agricultural Research Service (USDA-ARS), 2020. The Wind Erosion Prediction System (WEPS): Technical Documentation, ed. J. Tatarko, 533. USDA Agriculture Handbook 727. Beltsville, MD: USDA ARS. https://naldc.nal.usda.gov/catalog/7105679 (accessed 10.12.2022)

Van Oost, K., Govers, G., Desmet, P., 2000. Evaluating the effects of changes in landscape structure on soil erosion by water and tillage. Landsc. Ecol. 15, 577–589. https://doi.org/10.1023/A:1008198215674

van Vliet, L.J.P., Padbury, G.A., Rees, H.W., Matin, M.A., 2005. Water Erosion, in: Lefebvre, A., Eilers, W.D., Chunn, B. (Eds.), Environmental Sustainability of Canadian Agriculture: Agri-Environmental Indicator Report Series- Report No. 2. Agriculture and Agri-Food Canada, Ottawa, ON., pp. 90-96.

Walling, D.E., Quine, T.A., 1991. Use of ^{137}Cs measurements to investigate soil erosion on arable fields in the UK: potential applications and limitations. J. Soil Sci. 42, 147–165.

https://doi.org/10.1111/j.1365-2389.1991.tb00099.x

Walling, D.E., Zhang, Y., He, Q., 2011. Models for deriving estimates of erosion and deposition rates from fallout radionuclide (Caesium-137, Excess Lead-210, and Beryllium-7) measurements and the development of user-friendly software for model implementation, in: Impact of soil conservation measures on erosion control and soil quality, EA-TECDOC-1665, IAEA Publication, Vienna, Austria, pp. 11-33.

Warren, S.D., Mitasova, H., Hohmann, M.G., Landsberger, S., Iskander, F.Y., Ruzycki, T.S., Senseman, G.M., 2005. Validation of a 3-D enhancement of the Universal Soil Loss Equation for prediction of soil erosion and sediment deposition. Catena 64, 281–296. https://doi.org/10.1016/j.catena.2005.08.010

Wickham, H., 2016. ggplot2: Elegant Graphics for Data Analysis. Springer-Verlag New York. ISBN 978-3-319-24277-4, https://ggplot2.tidyverse.org.

Wischmeier, W.H., Smith, D.D., 1965. Predicting rainfall-erosion losses from cropland east of the Rocky Mountains. Guide for selection of practices for soil and water conservation. Agric. Handbook, 282. US Gov. Print. Office, Washington, DC.

Wischmeier, W.H., Smith, D.D., 1978. Predicting rainfall erosion losses- a guide to conservation planning. Agriculture Handbook No. 537. US Department of Agriculture Science and Education Administration, Washington, DC, USA, pp 163.

Zarrinabadi, E., Lobb, D.A., Enanga, E., Badiou, P., Creed, I.F., 2023. Agricultural activities lead to sediment infilling of wetlandscapes in the Canadian Prairies : Assessment of soil erosion and sedimentation fluxes. Geoderma. 436, 116525. https://doi.org/10.1016/j.geoderma.2023.116525

Zarrinabadi, E., Lobb, D.A., Koiter, A.J., Goharrokhi, M., 2022. Assessment of the effects of land rolling on wind erosion and crop growth in soybean production in the Red River Valley, Canada. Soil Tillage Res. 222, 105439. https://doi.org/10.1016/j.still.2022.105439

Zhang, J.Q., Zhang, C.L., Chang, C.P., Wang, R. De, Liu, G., 2017. Comparison of wind erosion based on measurements and SWEEP simulation: A case study in Kangbao County, Hebei Province, China. Soil Tillage Res. 165, 169–180. https://doi.org/10.1016/j.still.2016.08.006

Chapter 5

Summary and Conclusions

5.1. Context of thesis research

In the Canadian Prairie provinces, there have been concerns among agronomists and producers that soil erosion, specifically wind erosion is a serious form of soil degradation and consequently a threat to the sustainability of agriculture across these provinces. The Red River Valley and Prairie Pothole regions of Canada are an ideal study area for assessing soil erosion potential due to their historical susceptibility to wind, water, and tillage erosion. This Ph.D. study was undertaken in the framework of the research project "**Soil erosion and fluxes of sediment within landscapes of the Canadian Prairies**". The project was set up to understand the link between farming activities and soil erosion rates and patterns within the Canadian Prairie Pothole Region during the last several decades using a joint field- and model- based soil erosion assessment, providing a basis for policymakers to apply suitable measures to combat land degradation in these areas. The field measurement of total past soil erosion since the early 1960s was conducted using the ^{137}Cs technique, while tillage, water and wind erosion predictions were performed to discriminate the contributions on wind, water and tillage erosion processes using accepted soil erosion models (i.e., TillEM, RUSLE2 and SWEEP) that were validated by comparison to the total soil erosion estimates. In addition, soil/sediment properties were analyzed to discriminate the contributions of individual erosion processes. This research demonstrated the importance of using an integrated budget of soil erosion using landscape-scale transect sampling data. This study also allowed us to demonstrate that erosion models capture the relative spatial variability of soil loss and accumulation for topographically complex landscape.

5.2. Major Findings

5.2.1. Assessment of the impacts of farming practices on wind erosion

This work focused on assessing the potential impacts of land rolling on plant growth, soil/sediment properties, and the risk of wind erosion during soybean production in the Red River Valley. This study is the first one to examine the impact of the practice of land rolling on wind erosion risk for the agricultural region of Red River Valley. Additionally, soil surface roughness changes affected by land rolling were measured using a terrestrial laser scanner. Passive uni-directional wind erosion sediment samplers were developed and fabricated in this study to assess the movement of wind-transported sediment in rolled and non-rolled fields.

One of the most surprising aspects of this study was that although land rolling smoothed the soil surface roughness, the increased risk of wind erosion was unlikely to translate into a measurable increase in soil loss or to decrease in crop yield. Our results also demonstrated that field surveys following soybean harvest and land rolling, after wind events revealed very little evidence of sediment blowing off the fields. Another important finding of this study was the difference in sediment properties (^{137}Cs, organic matter, particle size distribution, and colour) collected by wind-transported sediment samplers at two heights (5 cm and 20 cm) above the ground, which confirmed the acceptable efficiency of the wind-transported sediment samplers. This study has provided a proof of concept for the design and use of the passive wind erosion samplers.

5.2.2. Assessment of total soil loss and accumulation rates using ^{137}Cs

This was the first comprehensive study to measure total soil erosion rates using ^{137}Cs within wetland catchments located in the Canadian Prairie Pothole Region. Mass balance budgets of soil loss and accumulation were constructed using landscape-scale transect sampling data.

Throughout each transect from uphill to downhill, four landform positions, including upper slope, middle slope, lower slope and foot slope (i.e., riparian area and water body) were investigated.

One of the important contributions of this study was the establishment of an ideal reference site for estimating ^{137}Cs reference level in Manitoba. The use of ^{137}Cs along with the characterization of terrain attributes allowed us to identify erosional patterns for each study sites. The results of this study demonstrated that a consistent pattern in ^{137}Cs profile from the upslope positions in most of fields were characterized by ^{137}Cs inventories lower than profiles located in the mid and downslope positions of the fields. This pattern provides strong evidence of soil redistribution within field. This pattern of inventories is also reflected in differences in the activity-depth distributions with lower maximum depth of elevated ^{137}Cs activity in the eroding zones and elevated ^{137}Cs activity at greater depths in the downslope cores.

The results of ^{137}Cs analysis confirmed a high rate of soil loss in the upper slope and middle slope positions, and a high rate of deposition in lower slope and foot slope positions of wetland landscapes. The budgets obtained allowed for the first quantitative estimation of the potential flux of sediments to the wetland ecosystem (i.e., riparian area and water body). The areal average of transect data provided a sediment delivery ratio estimates of 57% for Manitoba and 35% for Alberta. Therefore, a bit more than 40% and 65% of mobilized sediment and associated constituents (e.g., carbon) by erosion processes was deposited along the slopes before reaching the wetland ecosystems in Manitoba and Alberta, respectively.

A significant proportion of sediment along the slopes was trapped along the hillslopes (i.e., riparian area) and not all the soil and associated constituents transported reached directly to the central area of the wetland. The riparian area acts as a transitional zone between cultivated land

and the central area of the wetland created hydrological disconnection reducing runoff and sediment supply into wetland ecosystems. The ^{137}Cs tracer results also provide strong support for the suitability of this approach for tracing and studying soil redistribution in this environment. The integrated approach employed provides a useful basis for estimating and improving our understanding of mobilization, transport, and storage of soil and sediment in the landscape. This study provided valuable insight on erosion severity for the management of natural and Prairie agricultural environments.

5.2.3. Improved understanding of soil erosion processes

This study focused on estimating and modelling the relative contributions of tillage, water and wind erosion in the Canadian Prairie province of Manitoba and Alberta using the ^{137}Cs technique and three established models: (i) the Tillage Erosion Model (TillEM); (ii) the Revised Universal Soil Loss Equation, version 2 (RUSLE2); and (iii) the Single-event Wind Erosion Evaluation Program (SWEEP).

This study characterized spatial patterns of soil erosion severity at a local scale for a given landscape elements. In topographically complex landscapes, the pattern of ^{137}Cs variation within cultivated fields is consistent with the influence of both tillage and water erosion within the wetland catchments. The results demonstrated that tillage erosion dominated the pattern of total soil erosion on the upper slope position of hummocky landscapes. We believe that a reduction in both tillage- and water-induced erosion is necessary to slow and eventually reverse soil degradation of tilled hillslopes in the Canadian Prairie Pothole Region. Furthermore, soil/sediment properties (e.g., colour and particle size distribution) analyses provided useful results for discriminating sources of soil erosion by tillage, water and wind. Particle size analysis confirmed that tillage erosion is a dominant soil redistribution process in cultivated landscapes. Furthermore, soil/sediment colour properties were useful in discriminating between source (i.e., cultivated field) and sink (i.e., wetland environment) within wetland catchments.

While the use of ^{137}Cs for soil erosion estimations is a valuable tool, it mainly depends on accurate and comprehensive historical data on land use, cropping patterns, and tillage practices. The limitations in available data and the potential variability in these practices over time can introduce uncertainties into the estimated rates. Integrating ^{137}Cs and ^{210}Pb data can help mitigate these limitations and provide a more accurate understanding of soil loss and sedimentation dynamics within wetland catchments.

5.3. Implications

The broader goal that this study sought to address was the understanding of soil physical degradation processes (i.e., soil erosion) to ensure sustainable land use and environmental preservation. Soil erosion, the process of soil redistribution by various erosive agents (e.g., wind, water, and tillage), poses significant challenges to agricultural productivity, water quality, ecosystem and human health, overall land sustainability, and economic stability. Our study in the Canadian PPR worked toward this goal by quantifying soil loss and sedimentation rates, identifying patterns of soil erosion, and assessing potential impacts on land productivity.

This study aimed to quantify the rates of soil loss and sedimentation within the PPR of Canada due to the unique characteristics of this ecosystem. This study can assist researchers and land managers to understand the extent of the problem of soil erosion and its potential impacts on the landscape. Additionally, identifying the patterns of soil erosion across wetland landscapes is crucial information for targeted mitigation strategies. Furthermore, the outcome of this thesis can inform the development of effective soil conservation and erosion control strategies. These strategies could involve altering land management practices, implementing erosion-resistant farming techniques (e.g., equipment selection, and reduced tillage speed and depth), and establishing required buffer zones. Moreover, this research has the potential to enhance stakeholders' education by raising awareness among farmers, landowners, policymakers, and the general public, about the importance of preventing soil erosion and adopting sustainable land management practices. Therefore, through evidence-based recommendations, this study can encourage the adoption of sustainable land management practices that minimize erosion within the study area, while supporting agricultural productivity and ecological balance. The implications of this study extend beyond scientific research, influencing conservation efforts, land management practices, and policy decisions to ensure the long-term health of soil as an important natural resource in this ecologically significant region.

5.4. Suggested field- and laboratory- based method improvements

From the experience gained while evaluating soil erosion within Prairie Pothole region, several areas for potential improvement were noted.

1. Development and fabrication of passive uni-directional wind erosion samplers for quantifying wind-eroded sediment transport in soybean production is the unique novelty of this study, which was designed to improve sediment collection efficiency. These wind-blown sediment samplers are affordable and can be easily fabricated on site to quantify wind-eroded sediment transport mass during erosive wind events over growing season. Samplers can be operated and maintained by farmers, agronomists, or community volunteers.
2. Consolidated sample collection from the aquatic portion of wetland ecosystem was a challenge in this study. Therefore, a portable and lightweight gas-powered Vibracoring unit

(WINK Vibracore Drill Ltd., Vancouver, BC, Canada, at the Department of Geological Sciences, University of Manitoba, Winnipeg, Canada) and a handheld SDI Vibecore Mini unit (Specialty Devices Inc., Wylie, TX, USA, at the Landscape Dynamics Laboratory, University of Manitoba, Winnipeg, Canada) were used for sampling from this environment. An inflatable pontoon boat was used for sampling from the central area of wetland ecosystem (i.e., water body).

3. Undisturbed sample extrusion was another issue raised during sample collection, which was addressed by developing a new method for core extrusion. The collected cores were transported vertically (to avoid disturbing of sediment layers) to the laboratory and stored in a walk-in freezer at -20° C. The frozen cores' tubes were split lengthwise with a table saw; then, the cores were sectioned, while still frozen using a band-saw equipped with a diamond blade. Due to presence of stones in core material, regular blades did not work properly; therefore, a diamond blade was used that cut easily through different materials (e.g., stones) without causing disturbance to the cores.

5.5. Recommendation and further research direction

Although this thesis has provided appreciable observations and results, there are a number of key areas that were identified as being in need of further research.

1. While the new wind-eroded sediment collector that was developed for quantification of sediment transport by wind (at the Landscape Dynamics Laboratory, University of Manitoba, Winnipeg, Canada) has proved to be feasible in sediment collection in soybean production, further investigation is needed to examine this collector under different cropping systems and treatments. The collection efficiency of samplers should also be investigated under controlled condition (i.e., wind tunnel experiments), and compared with

commonly used wind-blown sediment collectors (e.g., BSNE and MWAC). It is worth mentioning that the developed wind-eroded sediment collector has since been used by researchers at the Agriculture and Agri-Food Canada's wind erosion study site (e.g., Carbery, Manitoba) and by potato producers as well.

2. According to the results of this study, there is good evidence for the applicability of using the ^{137}Cs technique for assessing soil loss and accumulation in the study region. Therefore, the accuracy of the estimation of soil erosion rates can be improved by additional studies in order to obtain reliable local values of ^{137}Cs reference inventories in different parts of the Canadian Prairie Pothole Region.

3. The amount of particulate and dissolved forms of carbon, nitrogen and phosphorus within wetlands and their surrounding riparian areas are the products of atmospheric deposition (i.e., wind erosion) and terrestrial transport (i.e., tillage and water erosion) from surrounding upland areas. Therefore, there is a clear need to study landscape-scale nutrients fluxes within wetland catchments to gain insights into the relationship among soil erosion processes, soil nutrients dynamics and soil quality, and to explore the relative importance of erosion processes on fluxes of soil and associated constituents. Such work could incorporate the transect data obtained in this study. Furthermore, estimating carbon sequestration potential within the central area of wetlands (i.e., water body) is dealt with in another complementary study; however, the carbon sequestration assessment should be expanded to riparian areas, which was presented as a hotspot for sediment accumulation containing two sources of carbon (i.e., input from cultivate field and biomass production in the riparian area). Thereby, the relative contribution of the two sources to this carbon sink can be explored in wetlands.

4. With the remarkable increase in potato production area during the past decade over the Prairie provinces and the greater risk of tillage erosion during the production of potatoes compared to the other major cropping systems, it seems reasonable to expand soil erosion assessments using ^{137}Cs to potato production in this region. Therefore, additional studies are required to investigate how soil redistribution by erosion processes impact soil properties and crop yield in potato production in complex hilly landscapes of the Prairie Pothole Region.
5. The combined effect of tillage, water and wind erosion substantially contribute to total erosion rates in most agricultural landscapes of the Prairie provinces. However, the impact of these three processes is generally assess separately. Therefore, further research should also be performed to develop integrated tillage-water-wind erosion modelling approach for agricultural landscapes of the Canadian Prairie Pothole Region in order to estimate total soil erosion and assess the overall effects of soil erosion processes on soil properties and crop productivity in topographically complex landscapes. The integrated soil erosion modelling approach to estimate the impacts of tillage, water and wind erosion in agricultural landscapes can provide critical information for land managers and policy-makers since wind and water erosion is more likely to increase in the face of climate change. However, tillage erosion models are more universal because the erosive agent is not related to climate in comparison to wind and water erosion models. Therefore, fully integrated corrective measures are required for soil conservation.
6. Model-predicted soil loss and sedimentation magnitudes highly depend on how the erosion controlling factors and boundary conditions is defined in the models; therefore, spatial validation of modelled outputs still require further assessment. For example, remote

sensing technologies (i.e., satellite sensors, Airborne Laser Scanning (ALS) and Terrestrial Laser Scanning (TLS)) are developing rapidly, and so are their spatial and temporal resolutions. These high-resolution cameras can produce very high-resolution ($\leq$ 1cm) Digital Surface Models (DSMs). These very high-resolution DSM could also be employed to estimate changes in surface conditions following agricultural practices (e.g., land rolling). These estimates could also be correlated to predictions and contribute to the validation of erosion patterns at local and regional scales.

7. The impact of sediment accumulation on wetland functions, particularly within sediment-rich riparian areas, in agriculturally-dominated ecosystem has been inadequately studied. This research gap is notable, given the substantial accumulation of sediment due to the combined actions tillage and water erosion. The cumulative effects of these processes make it necessary to investigate the complex interactions between sediment deposition and the functions of these ecosystems including disrupting ecosystem resilience and balance (e.g., reduced biodiversity, species extinctions, and economic and social impacts).

Appendices

Appendix A

Supplementary materials for Chapter 3

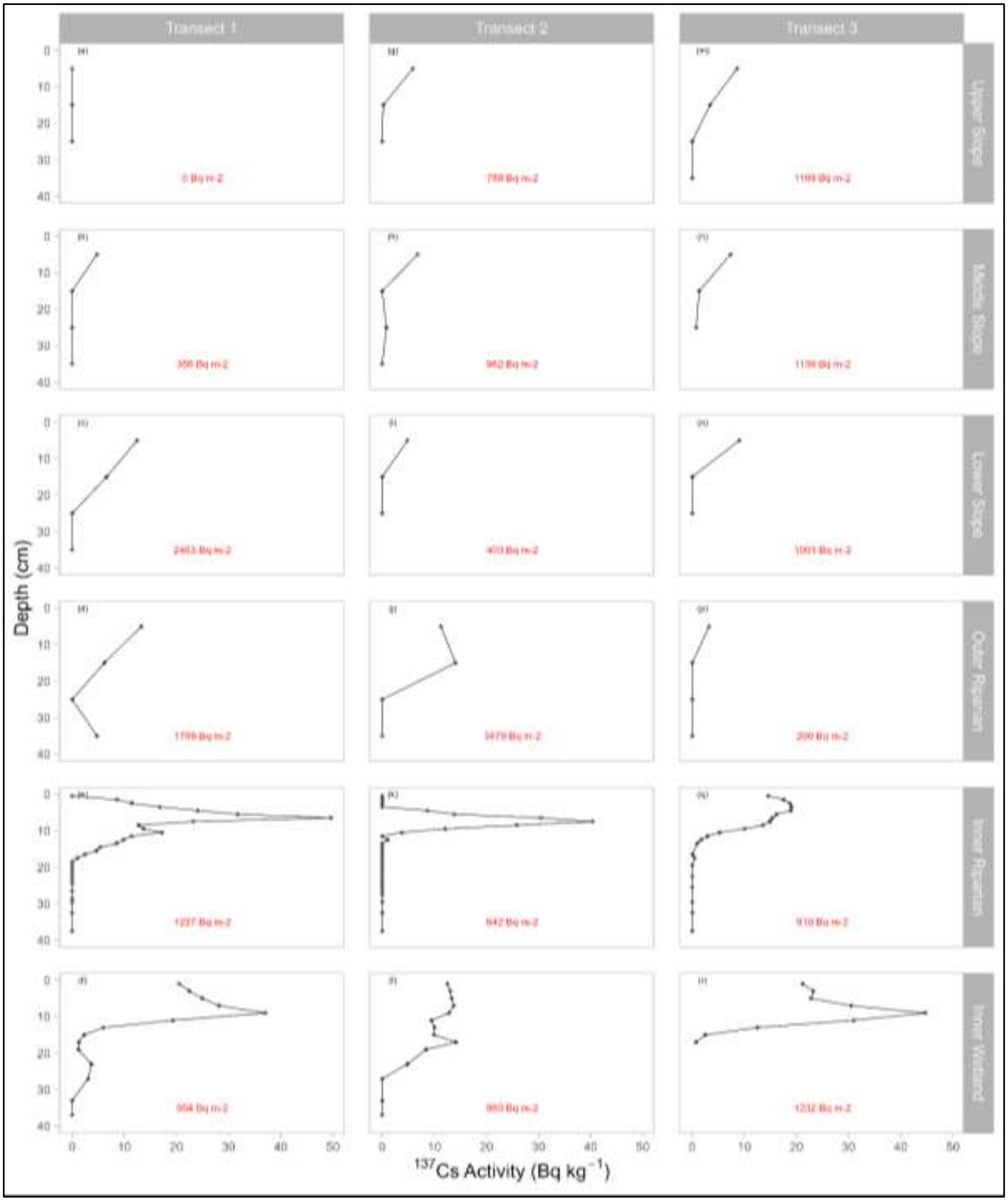

A1. Depth distribution of ^{137}Cs and their variation according to toposequence positions on three transects within one wetland catchment (Wetland A) embedded in cultivated land in Manitoba. The points are showing analyzed depth of each core.

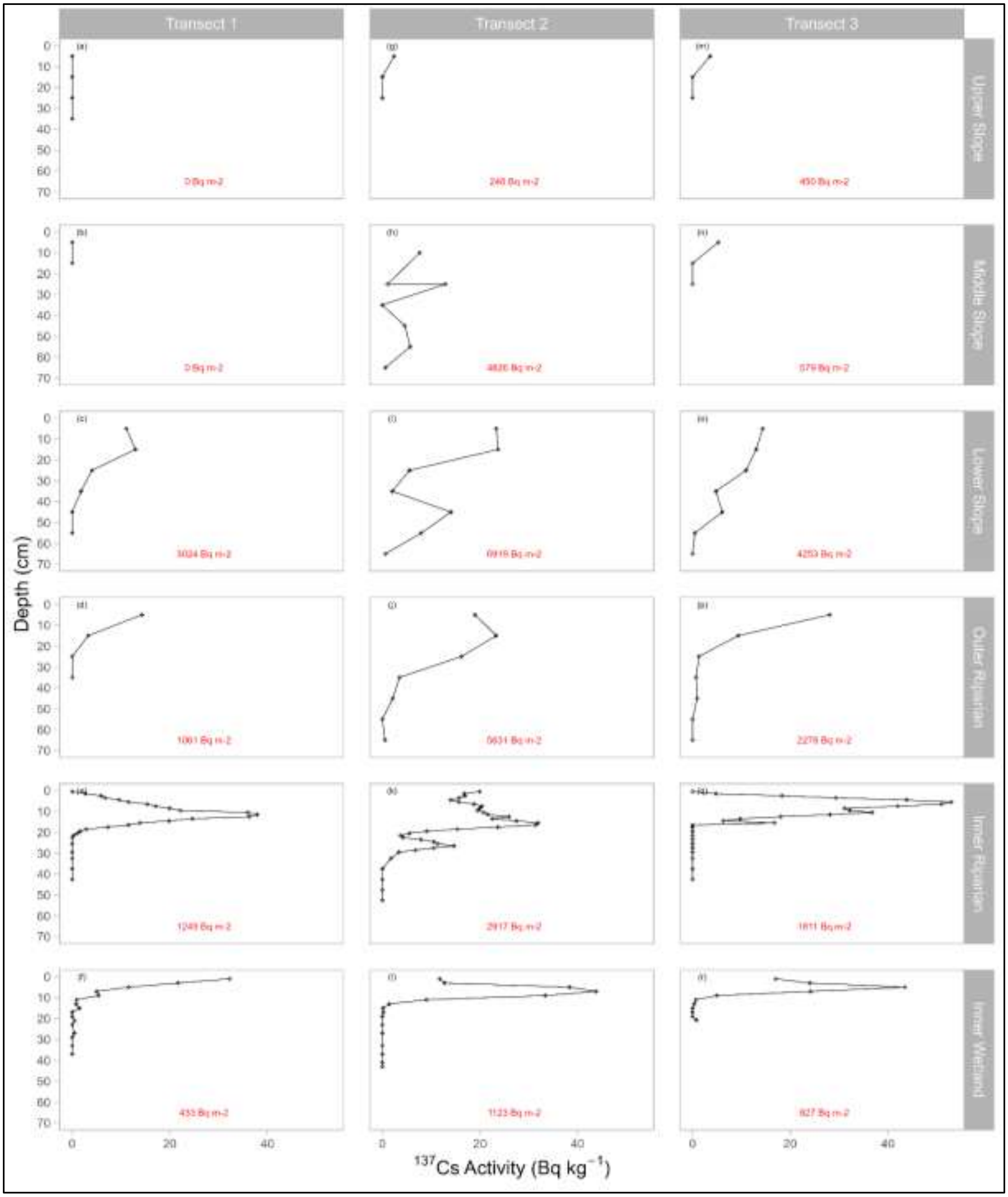

A2. Depth distribution of ^{137}Cs and their variation according to toposequence positions on three transects within one wetland catchment (Wetland J) embedded in cultivated land in Manitoba. The points are showing analyzed depth of each core.

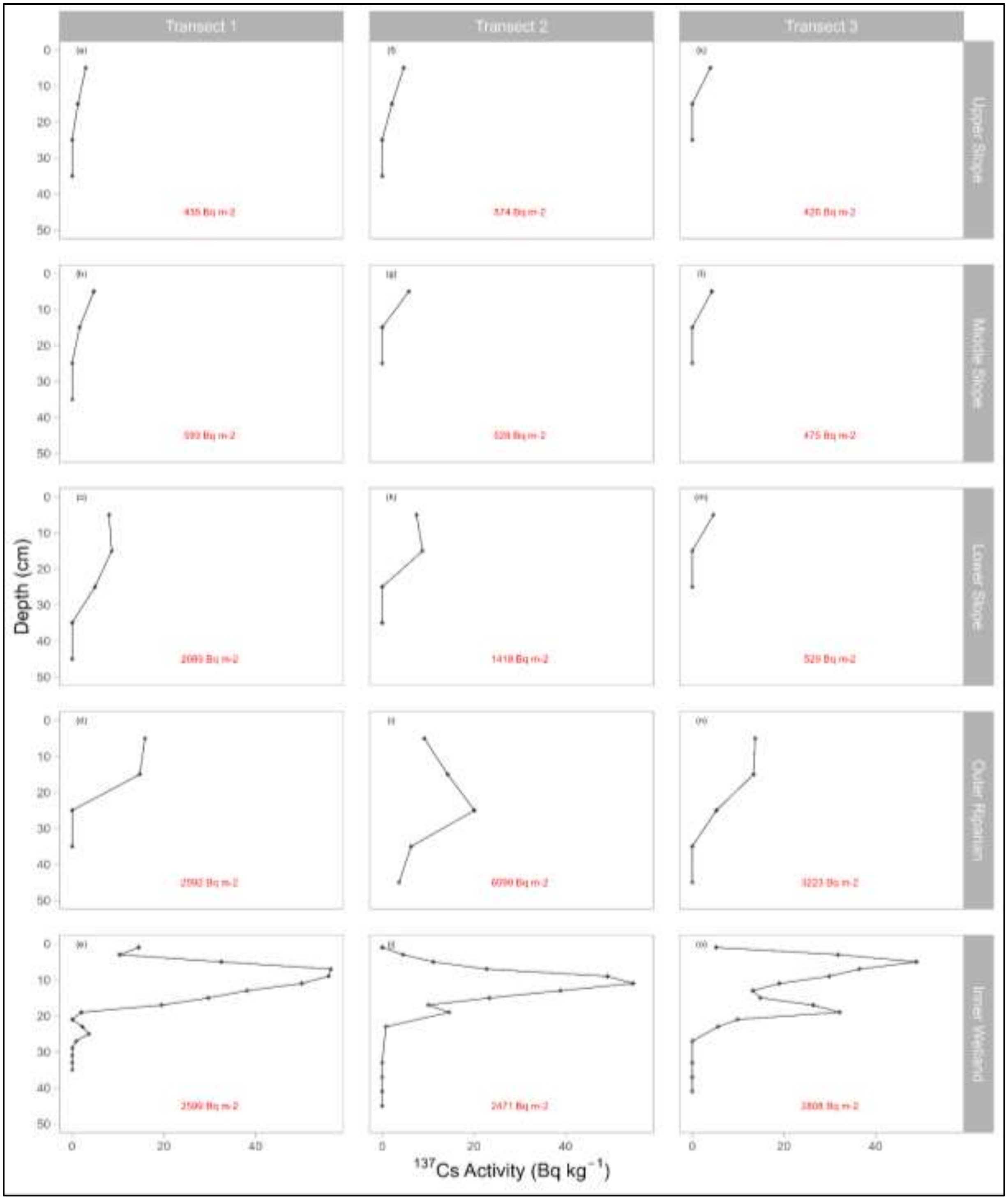

A3. Depth distribution of ^{137}Cs and their variation according to toposequence positions on three transects within one wetland catchment (Wetland X) embedded in cultivated land in Manitoba. The points are showing analyzed depth of each core.

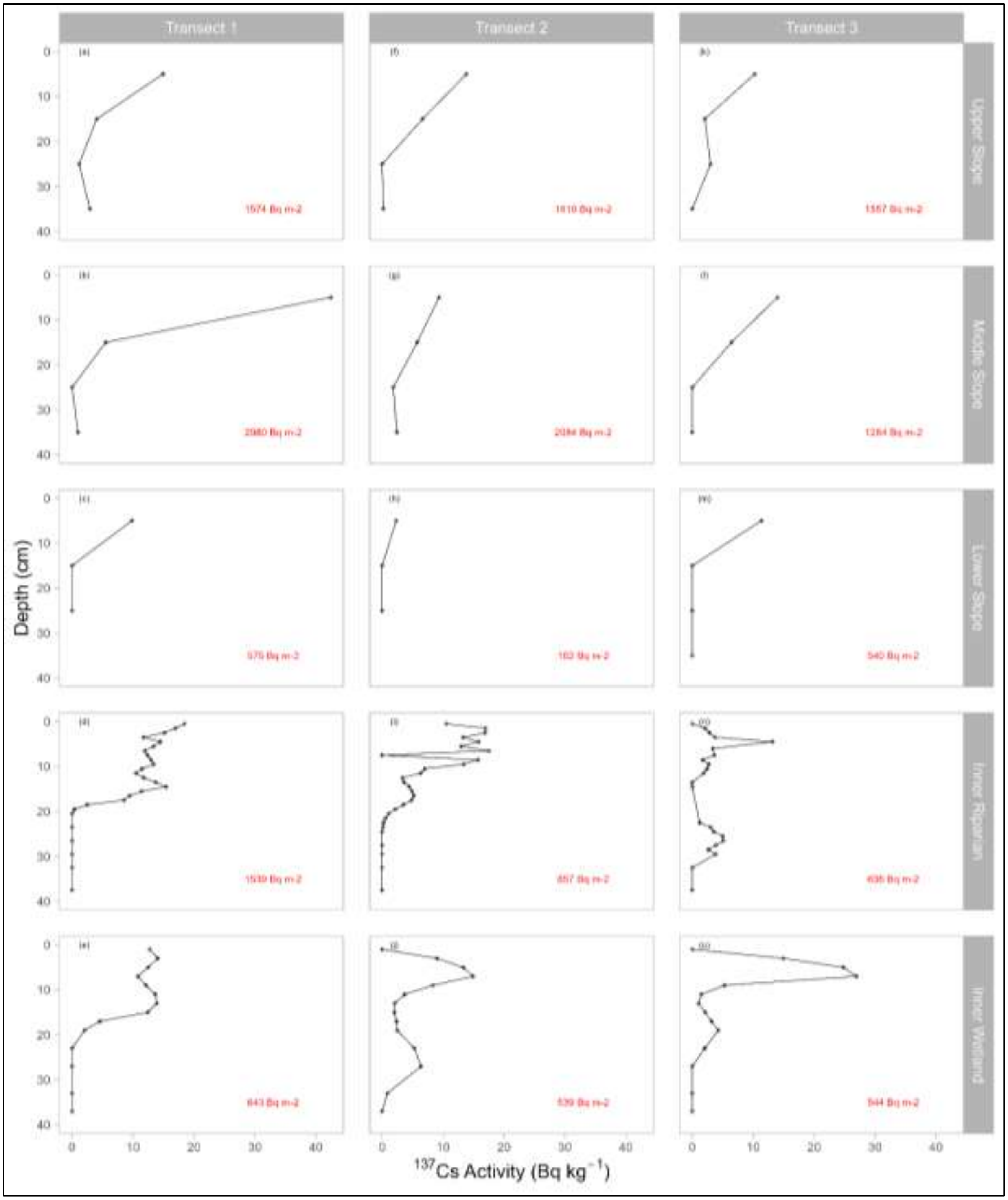

A4. Depth distribution of ^{137}Cs and their variation according to toposequence positions on three transects within one wetland catchment (Wetland E) embedded in native prairie in Manitoba. The points are showing analyzed depth of each core.

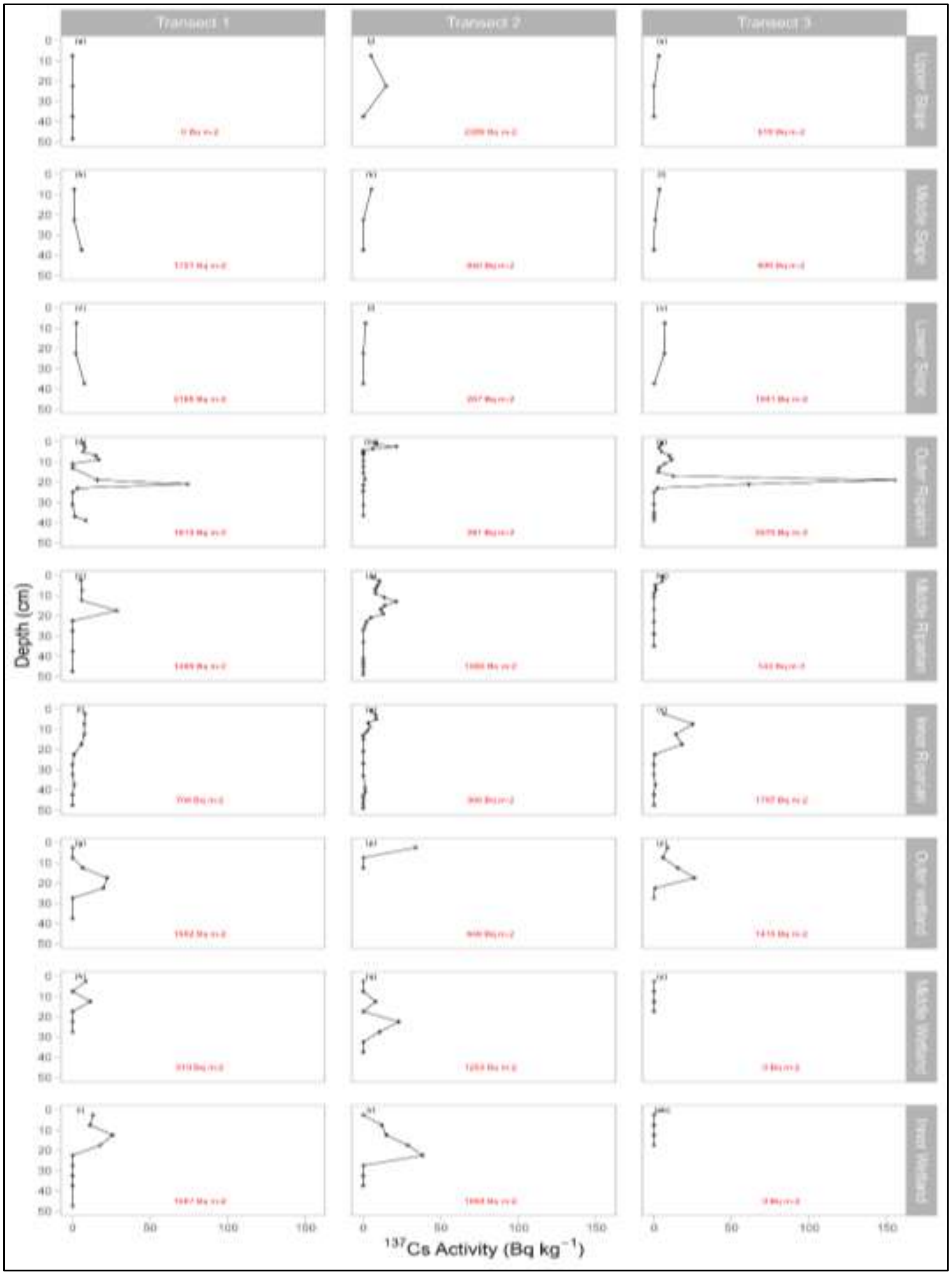

A5. Depth distribution of ^{137}Cs and their variation according to toposequence positions on three transects within one wetland catchment (Wetland INT1) embedded in cultivated land in Alberta. The points are showing analyzed depth of each core.

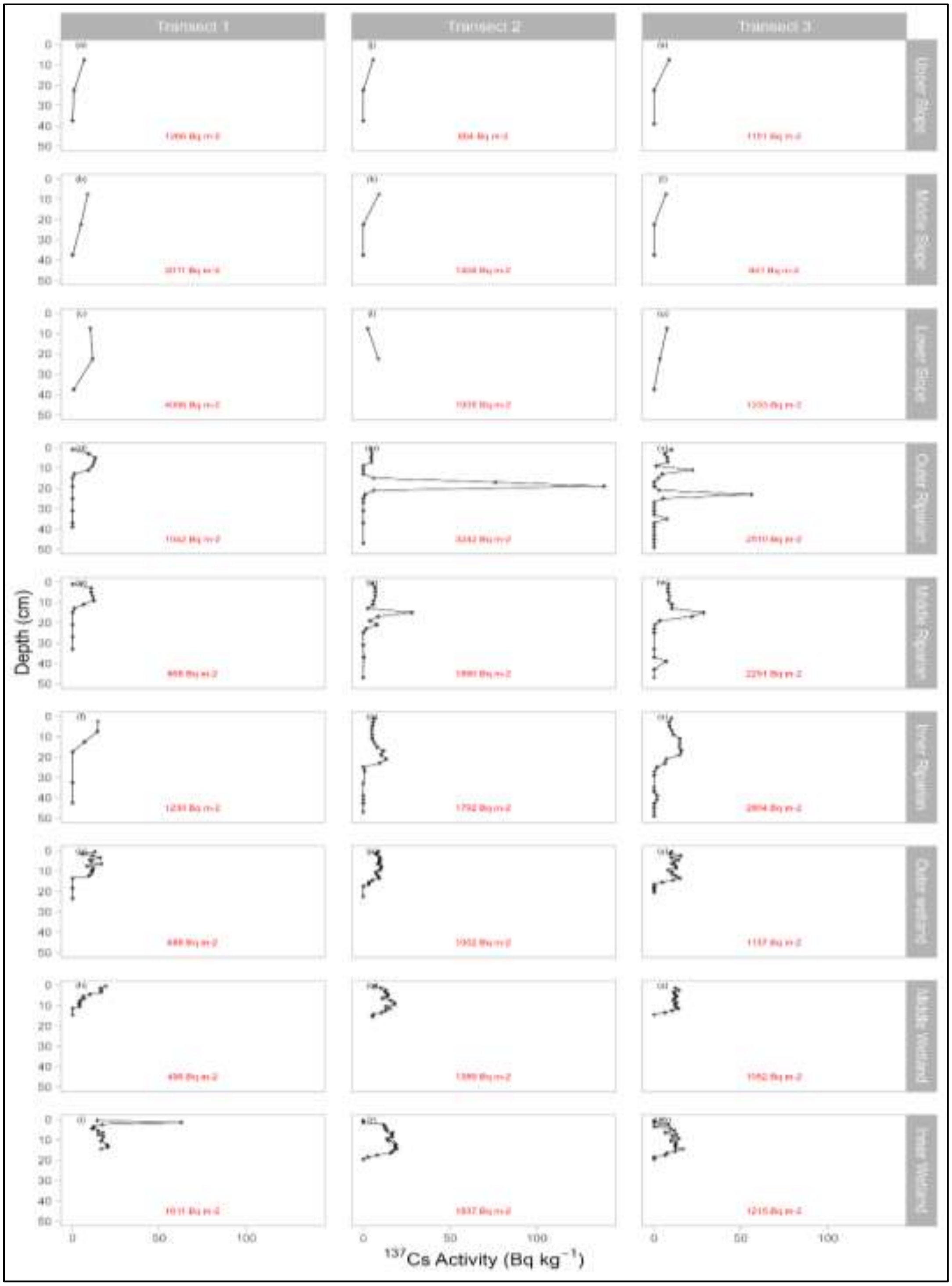

A6. Depth distribution of ^{137}Cs and their variation according to toposequence positions on three transects within one wetland catchment (Wetland MCN1) embedded in cultivated land in Alberta. The points are showing analyzed depth of each core.

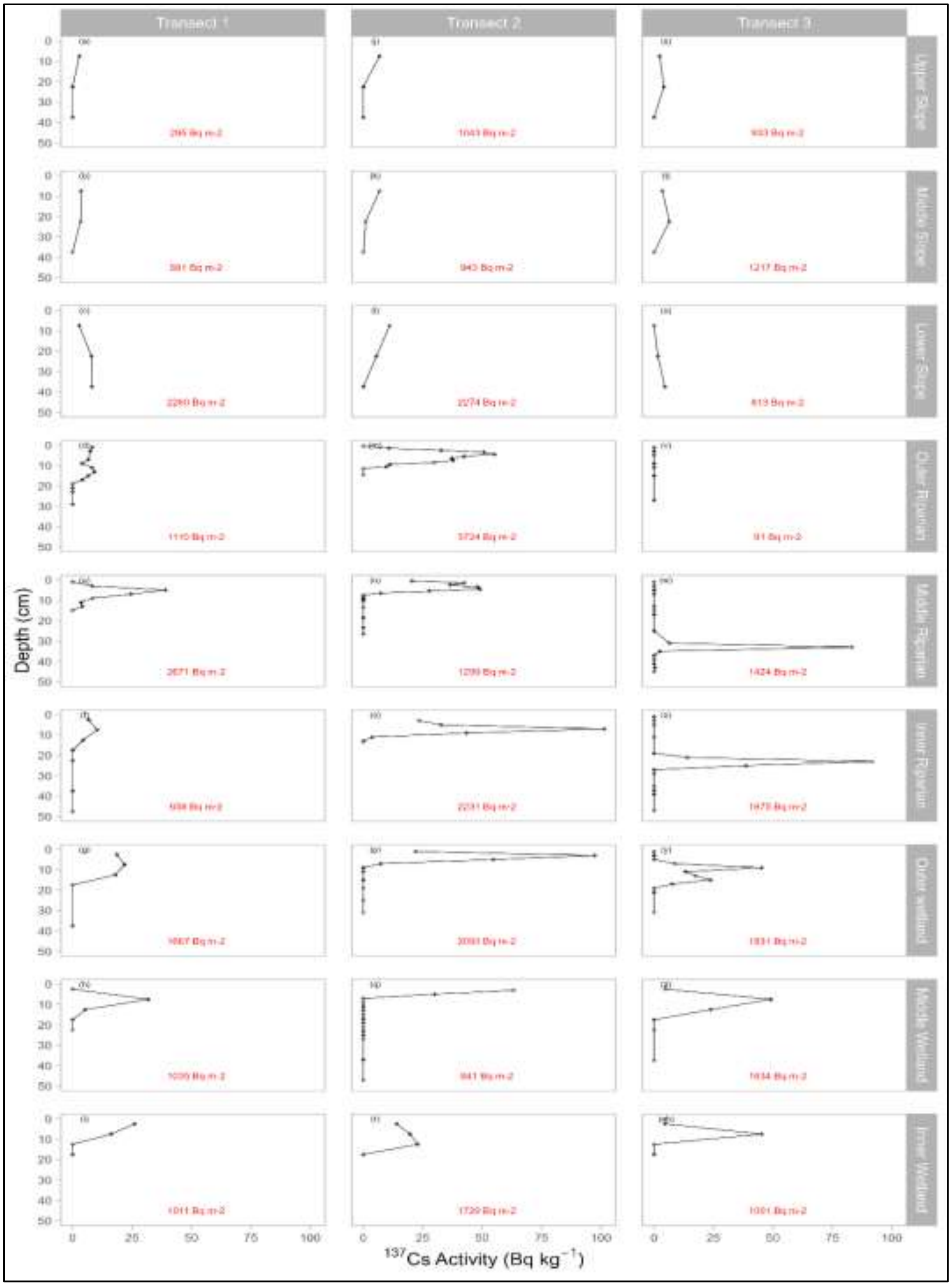

A7. Depth distribution of ^{137}Cs and their variation according to toposequence positions on three transects within one wetland catchment (Wetland OZM1) embedded in cultivated land in Alberta. The points are showing analyzed depth of each core.

A8. Point soil loss and deposition rates within the individual wetland catchments using ^{137}Cs reference value estimated from individual local stable sites.

Province	Toposequence position	^{137}Cs inventory ($Bq\ m^{-2}$)	^{137}Cs loss or gain (% of reference ^{137}Cs)	Soil loss (+) or deposition (-) ($kg\ m^{-2}\ yr^{-1}$)			Sedimentation rate ($kg\ m^{-2}\ yr^{-1}$)
				Power model[1]	Power model[2]	Linear model	
Individual reference sites							
MB	Flat landscape	1430	-	-	-	-	-
AB	Flat landscape	1684	-	-	-	-	-
Wetland A (Cultivated catchment)							
MB	Upper Slope	663	46.3	2.2	-	2.1	-
MB	Middle Slope	819	57.3	1.5	-	1.7	-
MB	Lower Slope	1289	90.1	0.3	-	0.4	0.4
MB	Outer Riparian	1826	127.7	-1.0	-	-1.1	1.9
MB	Inner Riparian	926	64.8	1.2	-	1.4	1.3
MB	Inner Wetland	1060	74.1	0.8	-	1.0	1.7
Wetland J (Cultivated catchment)							
MB	Upper Slope	233	16.3	5.4	-	3.3	-
MB	Middle Slope	1802	126.0	-1.7	-	-1.0	-
MB	Lower Slope	4732	330.9	-14.8	-	-9.1	5.6
MB	Outer Riparian	2990	209.1	-7.0	-	-4.3	2.4
MB	Inner Riparian	1992	139.3	-2.5	-	-1.5	1.6
MB	Inner Wetland	794	55.6	1.6	-	1.7	0.5
Wetland K (Cultivated catchment)							
MB	Upper Slope	901	63.0	1.3	-	1.5	-
MB	Middle Slope	1067	74.6	0.8	-	1.0	-
MB	Lower Slope	2605	182.2	-2.7	-	-3.2	1.6
MB	Outer Riparian	2338	163.5	-2.1	-	-2.5	1.5
MB	Inner Riparian	1901	132.9	-1.1	-	-1.3	1.3
MB	Inner Wetland	609	42.6	2.4	-	2.3	0.5
Wetland X (Cultivated catchment)							
MB	Upper Slope	478	33.4	3.1	-	2.6	-
MB	Middle Slope	532	37.2	2.8	-	2.5	-
MB	Lower Slope	1345	94.1	0.2	-	0.2	1.1
MB	Outer Riparian	3971	277.7	-7.9	-	-7.0	3.4
MB	Inner Wetland	2626	183.6	-3.7	-	-3.3	1.2
Wetland E (Native prairie)							
MB	Upper Slope	1580	110.5	-	n.d	n.d	1.1
MB	Middle Slope	2116	148.0	-	n.d	n.d	0.8
MB	Lower Slope	426	29.8	-	7.4	2.8	-
MB	Inner Riparian	1011	70.7	-	2.1	1.2	0.3
MB	Inner Wetland	575	40.2	-	5.6	2.4	1.0
Wetland OZM1 (Cultivated catchment)							
AB	Upper Slope	757	45.1	2.0	-	1.9	-
AB	Middle Slope	1013	60.3	1.3	-	1.4	-
AB	Lower Slope	1782	106.1	-0.2	-	-0.2	1.2
AB	Outer Riparian	1641	97.7	0.1	-	0.1	0.3
AB	Middle Riparian	1798	107.0	-0.2	-	-0.2	3.6
AB	Inner Riparian	1621	96.5	0.1	-	0.1	2.5
AB	Outer Wetland	1864	110.9	-0.4	-	-0.4	1.1
AB	Middle Wetland	1170	69.6	0.9	-	1.0	1.2

Province	Toposequence position	^{137}Cs inventory ($Bq\ m^{-2}$)	^{137}Cs loss or gain (% of reference ^{137}Cs)	Soil loss (+) or deposition (-) ($kg\ m^{-2}\ yr^{-1}$)			Sedimentation rate ($kg\ m^{-2}\ yr^{-1}$)
				Power model[1]	Power model[2]	Linear model	
AB	Inner Wetland	1247	74.2	0.7	-	0.9	1.6
Wetland MCN1 (Cultivated catchment)							
AB	Upper Slope	1090	64.9	1.1	-	1.2	-
AB	Middle Slope	1420	84.5	0.4	-	0.5	-
AB	Lower Slope	2441	145.3	-1.3	-	-1.5	1.3
AB	Outer Riparian	2265	134.8	-1.0	-	-1.2	3.2
AB	Middle Riparian	1683	100.2	0.0	-	0.0	2.7
AB	Inner Riparian	1942	115.6	-0.4	-	-0.5	1.1
AB	Outer Wetland	942	56.1	1.4	-	1.5	0.7
AB	Middle Wetland	979	58.3	1.3	-	1.4	1.2
AB	Inner Wetland	1554	92.5	0.2	-	0.3	1.5
Wetland INT1 (Cultivated catchment)							
AB	Upper Slope	972	57.9	1.4	-	1.6	-
AB	Middle Slope	1023	60.9	1.2	-	1.5	-
AB	Lower Slope	1464	87.2	0.3	-	0.5	1.7
AB	Outer Riparian	1588	94.5	0.2	-	0.2	2.8
AB	Middle Riparian	899	53.5	1.6	-	1.8	2.2
AB	Inner Riparian	954	56.8	1.4	-	1.6	0.2
AB	Outer Wetland	1188	70.7	0.9	-	1.1	2.0
AB	Middle Wetland	590	35.1	2.7	-	2.4	1.5
AB	Inner Wetland	1154	68.7	0.9	-	1.2	2.3

[1]Power model: Mass Balance Model (MBM2) was used for wetland embedded within agricultural landscape.
[2]Power model: Profile Distribution Model was used for one wetland embedded in native prairie landscape.
Linear model: Proportional Model was used for wetlands embedded in agricultural and native prairie landscapes.
n.d.: not determined by developed excel add-in software.

A9. Point soil loss and deposition rates within the individual wetland catchments using catchment-level ^{137}Cs reference value.

Province	Toposequence position	^{137}Cs inventory (Bq m^{-2})	^{137}Cs loss or gain (% of reference ^{137}Cs)	Soil loss (+) or deposition (-) (kg m^{-2} yr^{-1})			Sedimentation rate (kg m^{-2} yr^{-1})
				Power model[1]	Power model[2]	Linear model	
Wetland A (Cultivated catchment)							
Catchment-level ref. ^{137}Cs		**944**					
MB	Upper Slope	663	70.6	1.0	-	1.2	-
MB	Middle Slope	819	87.2	0.4	-	0.5	-
MB	Lower Slope	1289	137.3	-1.1	-	-1.4	0.4
MB	Outer Riparian	1826	194.5	-2.9	-	-3.7	1.9
MB	Inner Riparian	926	92.4	0.1	-	0.1	1.3
MB	Inner Wetland	1060	109.4	-0.4	-	-0.5	1.7
Wetland J (Cultivated catchment)							
Catchment-level ref. ^{137}Cs		**1898**					
MB	Upper Slope	233	12.3	6.3	-	3.5	-
MB	Middle Slope	1802	95.1	0.1	-	0.2	-
MB	Lower Slope	4732	249.7	-10.4	-	-5.9	5.6
MB	Outer Riparian	2990	157.8	-4.0	-	-2.3	2.4
MB	Inner Riparian	1992	98.4	-0. 3	-	0.2	1.6
MB	Inner Wetland	794	40.7	2.4	-	2.3	0.5
Wetland K (Cultivated catchment)							
Catchment-level ref. ^{137}Cs		**1314**					
MB	Upper Slope	901	68.6	1.0	-	1.2	-
MB	Middle Slope	1067	81.3	0.6	-	0.7	-
MB	Lower Slope	2605	198.4	-3.1	-	-3.9	1.6
MB	Outer Riparian	2338	178.1	-2.5	-	-3.1	1.5
MB	Inner Riparian	1901	135.5	-1.4	-	-1.8	1.3
MB	Inner Wetland	609	45.1	2.2	-	2.1	0.5
Wetland X (Cultivated catchment)							
Catchment-level ref. ^{137}Cs		**936**					
MB	Upper Slope	478	51.3	1.9	-	1.9	-
MB	Middle Slope	532	57.2	1.6	-	1.7	-
MB	Lower Slope	1345	144.5	-1.6	-	-1.7	1.1
MB	Outer Riparian	3971	426.6	-11.9	-	-12.8	3.4
MB	Inner Wetland	2626	275.8	-6.7	-	-7.1	1.2
Wetland E (Native prairie)							
Catchment-level ref. ^{137}Cs		**1460**					
MB	Upper Slope	1580	109.0	-	n.d	n.d	1.1
MB	Middle Slope	2116	145.9	-	n.d	n.d	0.8
MB	Lower Slope	426	29.4	-	7.5	2.8	-
MB	Inner Riparian	1011	65.2	-	2.2	1.2	0.3
MB	Inner Wetland	575	38.4	-	5.7	2.4	1.0
Wetland OZM1 (Cultivated catchment)							
Catchment-level ref. ^{137}Cs		**1100**					
AB	Upper Slope	757	68.8	0.9	-	1.1	-
AB	Middle Slope	1013	92.1	0.2	-	0.3	-
AB	Lower Slope	1782	162.0	-1.8	-	-2.1	1.2
AB	Outer Riparian	1641	149.2	-1.4	-	-1.7	0.3
AB	Middle Riparian	1798	163.4	-1.8	-	-2.2	3.6
AB	Inner Riparian	1621	147.4	-1.3	-	-1.6	2.5

Province	Toposequence position	^{137}Cs inventory (Bq m^{-2})	^{137}Cs loss or gain (% of reference ^{137}Cs)	Soil loss (+) or deposition (-) (kg m^{-2} yr^{-1})			Sedimentation rate (kg m^{-2} yr^{-1})
				Power model[1]	Power model[2]	Linear model	
AB	Outer Wetland	1864	169.4	-2.0	-	-2.4	1.1
AB	Middle Wetland	1170	106.4	-0.2	-	-0.2	1.2
AB	Inner Wetland	1247	113.4	-0.4	-	-0.5	1.6
Wetland MCN1 (Cultivated catchment)							
Catchment-level ref. ^{137}Cs		**1477**					
AB	Upper Slope	1090	73.8	0.8	-	0.9	-
AB	Middle Slope	1420	96.2	0.1	-	0.1	-
AB	Lower Slope	2441	165.3	-1.8	-	-2.2	1.3
AB	Outer Riparian	2265	153.4	-1.5	-	-1.8	3.2
AB	Middle Riparian	1683	113.9	-0.4	-	-0.5	2.7
AB	Inner Riparian	1942	131.5	-0.9	-	-1.1	1.1
AB	Outer Wetland	942	63.8	1.1	-	1.2	0.7
AB	Middle Wetland	979	66.3	1.0	-	1.2	1.2
AB	Inner Wetland	1554	105.2	-0.2	-	-0.2	1.5
Wetland INT1 (Cultivated catchment)							
Catchment-level ref. ^{137}Cs		**1086**					
AB	Upper Slope	972	89.5	0.3	-	0.4	-
AB	Middle Slope	1023	94.2	0.2	-	0.2	-
AB	Lower Slope	1464	134.8	-0.9	-	-1.2	1.7
AB	Outer Riparian	1588	146.2	-1.2	-	-1.6	2.8
AB	Middle Riparian	899	82.8	0.5	-	0.6	2.2
AB	Inner Riparian	954	87.8	0.3	-	0.4	0.2
AB	Outer Wetland	1188	109.4	-0.2	-	-0.3	2.0
AB	Middle Wetland	590	54.4	1.5	-	1.6	1.5
AB	Inner Wetland	1154	106.2	-0.2	-	-0.2	2.3

[1]Power model: Mass Balance Model (MBM2) was used for wetland embedded within agricultural landscape.
[2]Power model: Profile Distribution Model was used for wetlands embedded in native prairie.
[3]Linear model: Proportional Model was used for wetlands embedded in agricultural and native prairie landscapes.
[4]Sedimentation rate was calculated using the peak of ^{137}Cs activity.
n.d.: not determined by developed excel add-in software.

A10. Sediment budget based on ^{137}Cs transect data set at studied individual wetland catchments in Manitoba

Sediment budget	Studied Catchments in Manitoba			
	Wetland A	Wetland J	Wetland K	Wetland X
Total area of cultivated field (m^2)	25075	24425	24850	6375
Eroded area within cultivated field (m^2)	22650	20975	21375	5625
Deposition area within cultivated field (m^2)	2425	3450	3475	750
Mean erosion[1] (kg m^{-2} yr^{-1})	0.71	0.98	0.92	1.76
Mean deposition[1] (kg m^{-2} yr^{-1})	-1.44	-5.88	-3.87	-1.72
Gross erosion[2] (kg m^{-2} yr^{-1})	0.64	0.84	0.80	1.56
Gross deposition[2] (kg m^{-2} yr^{-1})	-0.14	-0.83	-0.54	-0.20
Net erosion[3] (kg m^{-2} yr^{-1})	0.50	0.01	0.25	1.35
Sediment delivery ratio[4] (%)	78.0	1.0	32.0	87.0
Total soil exported from cultivated (kg yr^{-1})	12,656	269	6,322	8,625

[1]Mean erosion/deposition rate is equal to the total erosion/deposition divided by the eroded/deposition area of the cultivated field.
[2]The gross erosion/deposition rate is equal to the total erosion divided by the total area of cultivated field.
[3]The net erosion rate is the rate of soil export from the sampled area, and is equal to the gross erosion rate minus the gross deposition rate within cultivated field (gross erosion - gross sedimentation).
[4]The sediment delivery ratio is equal to the net erosion rate divided by gross erosion rate.

Table A11. Sediment budget based on ^{137}Cs transect data set at studied individual wetland catchments in Alberta

Sediment budget	Studied Catchments in Alberta		
	Wetland OZM1	Wetland MCN1	Wetland INT1
Total area of cultivated field (m^2)	19120	43525	35375
Eroded area within cultivated field (m^2)	17150	40200	30150
Deposition area within cultivated field (m^2)	1970	3325	5225
Mean erosion[1] ($kg\ m^{-2}\ yr^{-1}$)	0.50	0.34	0.23
Mean deposition[1] ($kg\ m^{-2}\ yr^{-1}$)	-2.11	-2.22	-1.18
Gross erosion[2] ($kg\ m^{-2}\ yr^{-1}$)	0.45	0.32	0.20
Gross deposition[2] ($kg\ m^{-2}\ yr^{-1}$)	-0.22	-0.17	-0.17
Net erosion[3] ($kg\ m^{-2}\ yr^{-1}$)	0.23	0.15	0.02
Sediment delivery ratio[4] (%)	51.0	47.0	12.0
Total soil exported from cultivated ($kg\ yr^{-1}$)	4,373	6,447	816

[1]Mean erosion/deposition rate is equal to the total erosion/deposition divided by the eroded/deposition area of the cultivated field.
[2]The gross erosion/deposition rate is equal to the total erosion divided by the total area of cultivated field.
[3]The net erosion rate is the rate of soil export from the sampled area, and is equal to the gross erosion rate minus the gross deposition rate within cultivated field (gross erosion - gross sedimentation).
[4]The sediment delivery ratio is equal to the net erosion rate divided by gross erosion rate.

Appendix B

Supplementary materials for Chapter 4

B1. The values of α, β and γ coefficients that were adopted from Li et al. (2007a) to model the magnitude of tillage erosion in the study area.

Translocation	Coefficients		
	α kg m^{-1} pass^{-1}	β kg m^{-1} %$^{-1}$ pass^{-1}	γ kg m^{-1} (%$^{-1}$ m) pass^{-1}
Forward translocation	50.73	1.7	6.4
Lateral translocation	0	0.85	3.2
Lateral translocation (riparian zone)	25.365	0	0

B2. Management input data representing typical farming practices of the study area (Manitoba and Alberta).

Date (m/d/y)	Farming operations	
	Moderate tillage practices	Intensive tillage practices
9/4/2000	Chisel, sweep shovel	Moldboard plow
4/26/2001	Fertilizer application- Surface broadcast	Fertilizer application- Deep placement heavy shank
4/26/2001	Cultivator, field 6-12 in sweeps	Cultivar, row
4/27/2001	Sprayer, pre-emergence	Sprayer, pre-emergence
4/27/2001	Harrow, coiled tine	Disk, tandem secondary operation
5/15/2001	Drill or airseeder, double disk opener, with fertilizer openers	Drill, deep furrow
6/25/2001	Sprayer. Post emergence	Sprayer. Post emergence
9/10/2001	Harvest, killing crop (50% standing stubble)	Harvest, killing crop (10% standing stubble)
9/20/2001	Chisel, sweep shovel	Moldboard plow
4/24/2002	Fertilizer application. Surface broadcast	Fertilizer application. Deep placement heavy shank
4/25/2002	Cultivator, field 6-12 in sweeps	Cultivar, row
4/25/2002	Harrow, coiled tine	Disk, tandem secondary operation
4/27/2002	Drill or airseeder, double disk opener, with fertilizer openers	Drill, deep furrow, 7 to 10 in spacing
5/8/2002	Sprayer, post emergence	Sprayer. Post emergence
6/25/2002	Sprayer, fungicide	Sprayer, fungicide
8/27/2002	Harvest, killing crop (60% standing stubble)	Harvest, killing crop (10% standing stubble)

B3. The cumulative days of hourly average wind speed from 1958 to 2021 over the months of April, May and June for Manitoba.

Year	Cumulative days of erosive events for various wind speed (m s^{-1})														Total
	13-14	14-15	15-16	16-17	17-18	18-19	19-20	20-21	21-22	22-23	23-24	24-25	25-26	26-27	
1958	0	0	0	0	0	0	0	0	0	0	0	0	0	0	0
1959	5	1	4	0	0	0	1	1	0	0	0	0	0	0	12
1960	7	1	3	0	2	0	0	1	0	0	0	0	0	0	14
1961	4	1	0	1	1	0	0	0	0	0	0	0	0	0	7
1962	7	0	2	0	1	0	0	0	0	0	0	0	0	0	10
1963	7	0	4	1	0	0	0	0	0	1	0	0	0	0	13
1964	5	3	2	5	0	0	0	0	0	0	0	0	0	0	15
1965	3	2	0	1	0	0	0	0	0	0	0	0	0	0	6
1966	1	2	2	0	0	0	0	1	0	0	0	0	0	0	6
1967	6	2	4	1	2	0	0	0	0	0	0	0	0	0	15
1968	3	1	0	0	1	0	0	0	0	0	0	0	0	0	5
1969	1	2	2	0	0	0	0	0	0	0	0	0	0	0	5
1970	5	1	2	0	0	1	0	0	0	1	0	0	0	0	10
1971	4	0	0	1	1	0	0	0	0	0	0	0	0	0	6
1972	2	1	1	0	0	0	0	0	0	0	0	0	0	0	4
1973	6	1	4	1	0	0	0	0	0	0	0	0	0	0	12
1974	2	2	0	0	0	0	0	0	0	0	0	0	0	0	4
1975	3	1	1	0	0	0	0	0	0	0	0	0	0	0	5
1976	4	0	0	0	2	0	0	0	0	0	0	0	0	0	6
1977	1	1	2	0	0	0	0	0	0	0	0	0	0	0	4
1978	3	2	0	0	0	0	0	0	0	0	0	0	0	0	5
1979	1	1	1	0	0	0	0	0	0	0	0	0	0	0	3
1980	1	0	0	0	0	0	0	0	0	0	0	0	0	0	1
1981	3	1	0	0	0	0	0	0	0	0	0	0	0	0	4
1982	1	2	1	0	0	0	0	0	0	0	0	0	0	0	4
1983	0	0	0	0	0	0	0	0	0	0	0	0	0	0	0
1984	0	1	3	1	0	1	0	0	0	1	0	0	0	0	7
1985	6	0	2	0	0	0	0	0	0	0	1	0	0	0	9

Year	Cumulative days of erosive events for various wind speed (m s^{-1})														Total
	13-14	14-15	15-16	16-17	17-18	18-19	19-20	20-21	21-22	22-23	23-24	24-25	25-26	26-27	
1986	3	0	1	0	0	1	0	0	0	0	0	0	0	0	5
1987	2	1	0	0	0	0	0	0	0	0	0	0	0	0	3
1988	2	1	2	0	1	0	0	0	0	0	0	0	0	0	6
1989	2	2	0	0	0	0	1	0	0	0	0	0	0	0	5
1990	0	0	0	0	0	0	0	0	0	0	0	0	0	0	0
1991	0	1	0	0	0	0	0	1	0	0	0	0	0	0	2
1992	4	1	0	0	0	0	0	0	0	0	0	0	0	0	5
1993	0	0	0	0	0	0	0	0	0	0	0	0	0	0	0
1994	2	1	3	0	0	0	0	0	0	0	0	0	0	0	6
1995	0	0	2	0	0	0	0	0	0	0	0	0	0	0	2
1996	0	0	0	0	0	0	0	0	0	0	0	0	0	0	0
1997	1	1	0	0	0	0	0	0	0	0	0	0	0	0	2
1998	1	0	0	0	0	0	0	0	0	0	0	0	0	0	1
1999	1	0	0	0	0	0	0	0	0	0	0	0	0	0	1
2000	0	1	0	0	0	0	0	0	0	0	0	0	0	0	1
2001	0	0	0	0	0	0	0	0	0	0	0	0	0	0	0
2002	1	0	2	0	1	0	0	0	0	0	0	0	0	1	5
2003	0	0	0	0	0	0	0	0	0	0	0	0	0	0	0
2004	1	0	0	0	0	0	0	0	0	0	0	0	0	0	1
2005	0	1	3	0	0	0	0	0	0	0	0	0	0	0	4
2006	0	0	0	0	0	0	0	0	0	0	0	0	0	0	0
2007	0	2	1	0	0	0	0	0	0	0	0	0	0	0	3
2008	2	1	1	0	0	0	0	0	0	0	0	0	0	0	4
2009	0	1	0	0	0	0	0	0	0	0	0	0	0	0	1
2010	1	0	5	1	0	0	0	0	0	0	0	0	0	0	7
2011	2	3	0	1	0	0	0	0	0	0	0	0	0	0	6
2012	1	0	3	0	0	0	0	0	0	0	0	0	0	0	4
2013	4	3	2	0	0	0	1	0	0	0	0	0	0	0	10
2014	2	0	0	0	0	0	0	1	0	0	0	0	0	0	3
2015	5	1	2	0	1	0	0	0	0	0	0	0	0	0	9

Year	Cumulative days of erosive events for various wind speed ($m\ s^{-1}$)														Total
	13-14	14-15	15-16	16-17	17-18	18-19	19-20	20-21	21-22	22-23	23-24	24-25	25-26	26-27	
2016	2	7	0	1	0	0	0	0	1	0	0	0	0	0	11
2017	4	2	1	0	0	0	0	0	0	0	0	0	0	0	7
2018	2	1	1	1	0	0	0	0	0	0	0	0	0	0	5
2019	6	3	1	0	0	0	0	0	0	0	0	0	0	0	10
2020	4	2	2	0	0	0	0	0	0	0	0	0	0	0	8
2021	1	1	0	0	0	0	0	0	0	0	0	0	0	0	2
Total	147	66	72	16	13	3	3	5	1	3	1	0	0	1	331

B4. The cumulative days of hourly average wind speed from 1994 to 2021 over the months of April, May and June for Alberta.

Year	Cumulative days of erosive events for various wind speed (m s-1)							Total
	12-13	13-14	14-15	15-16	16-17	17-18	18-19	
1994	2	2	0	0	0	0	0	4
1995	2	0	0	0	0	0	0	2
1996	0	1	0	0	1	0	0	2
1997	3	1	0	0	0	0	0	4
1998	1	1	0	0	1	0	0	3
1999	3	3	1	1	0	0	0	8
2000	2	1	2	1	0	0	0	6
2001	3	2	2	1	0	0	0	8
2002	4	0	0	0	0	0	0	4
2003	0	1	1	0	1	0	0	3
2004	4	2	0	0	1	0	0	7
2005	1	0	0	0	0	0	0	1
2006	4	0	0	0	0	0	0	4
2007	1	0	0	0	0	0	0	1
2008	1	1	0	0	0	0	0	2
2009	1	2	0	0	0	0	0	3
2010	3	0	0	1	0	1	0	5
2011	1	1	0	1	0	0	0	3
2012	0	1	0	0	0	0	0	1
2013	3	1	1	0	0	0	0	5
2014	1	1	0	0	0	0	0	2
2015	3	1	0	1	0	0	0	5
2016	2	2	1	0	1	0	0	6
2017	0	0	0	0	1	0	0	1
2018	0	0	0	0	0	0	0	0
2019	0	0	0	0	0	0	0	0
2020	0	0	0	0	0	0	0	0
2021	1	0	0	0	0	0	0	1

Year	Cumulative days of erosive events for various wind speed (m s-1)							Total
	12-13	13-14	14-15	15-16	16-17	17-18	18-19	
Total	46	24	8	6	6	1	0	91

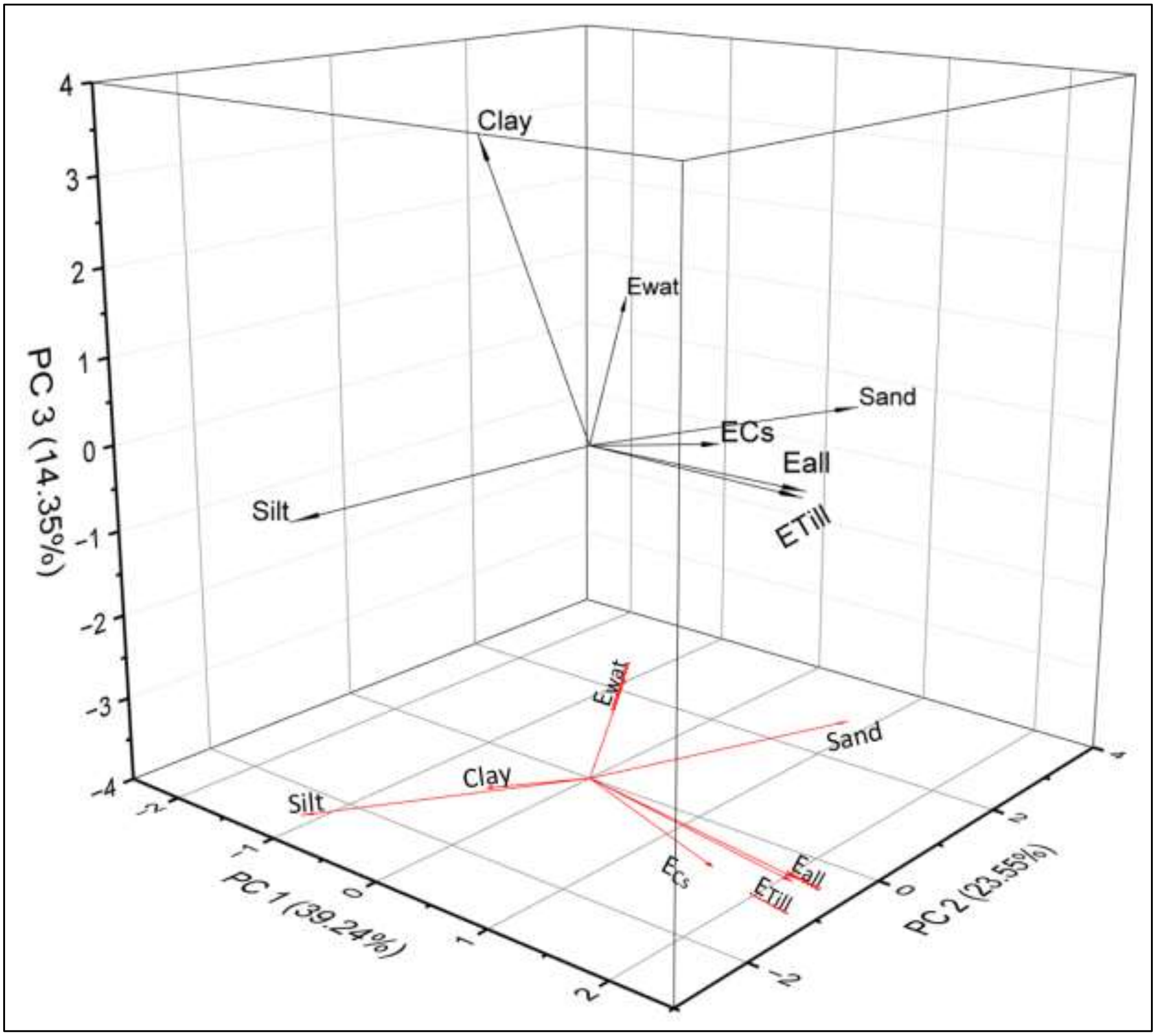

B5. Three-dimension Principal Components Analysis biplot of the measured and modelled data. Field-measured variables (~20-cm depth) including ^{137}Cs estimated soil erosion (E_{Cs}), sand, silt and clay, and model-estimated variables including tillage erosion (E_{Till}), water erosion (E_{wat}) and total erosion (E_{all}, tillage- + water- + wind-erosion). Eigenvalues for the first, second and third axis are 2.7, 1.6 and 1.0, respectively, which are standardized to 1.0 and the cumulative percentage variance of each axis is shown in the following bracket. Two-dimension Principal Components Analysis projection using PC1 and PC2 was shown in red and each vector was labelled.

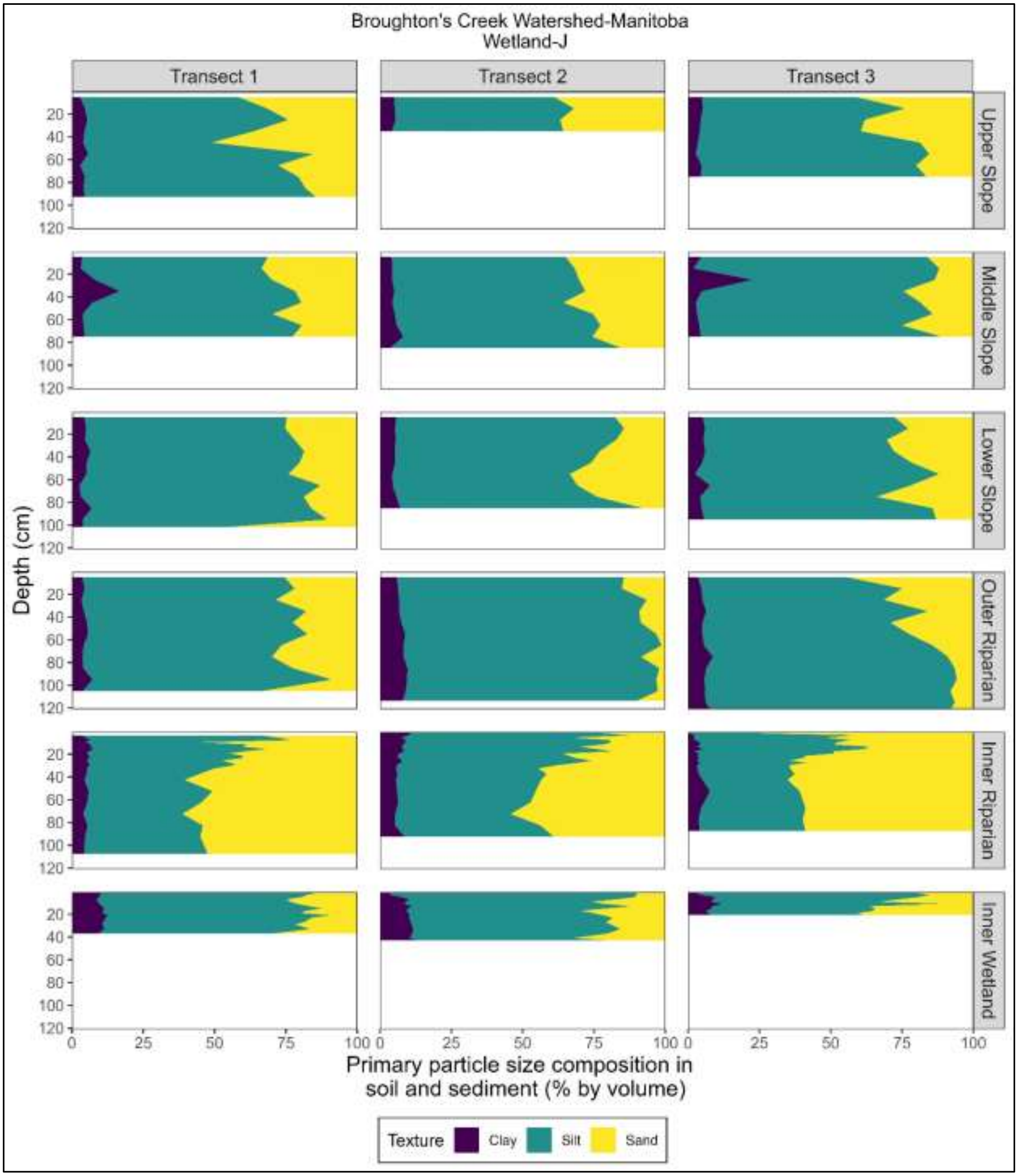

B6. Average particle size composition of collected soil and sediment samples from different toposequence positions on three transects within one wetland catchment (WetlandJ) in Broughton's Creek watershed, Manitoba. Particle size composition is represented by the clay (≤0.002 mm), silt (0.002–0.063 mm) and sand (0.063–2 mm) content of collected samples.

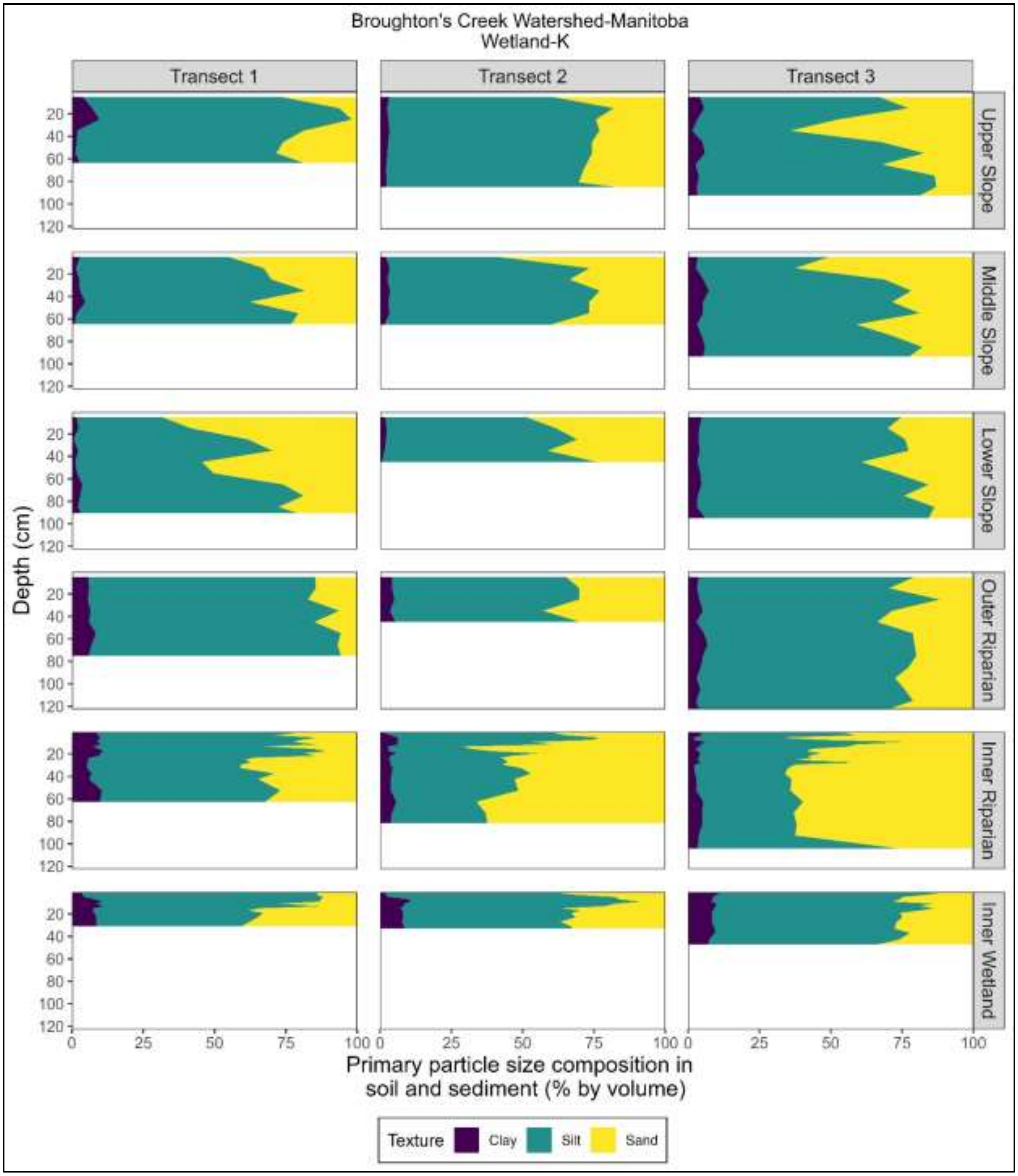

B7. Average particle size composition of collected soil and sediment samples from different toposequence positions on three transects within one wetland catchment (WetlandK) in Broughton's Creek watershed, Manitoba. Particle size composition is represented by the clay (≤0.002 mm), silt (0.002–0.063 mm) and sand (0.063–2 mm) content of collected samples.

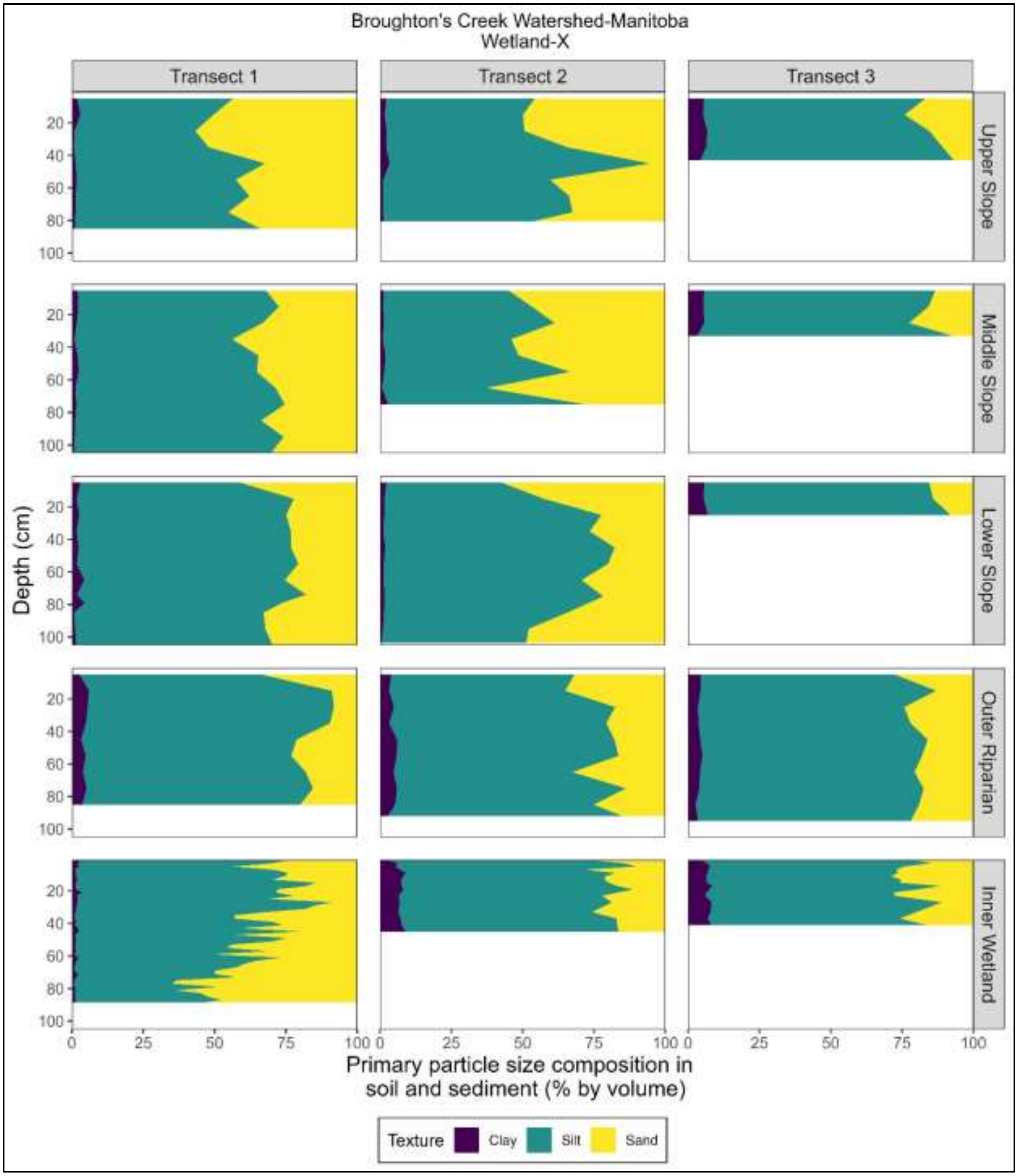

B8. Average particle size composition of collected soil and sediment samples from different toposequence positions on three transects within one wetland catchment (WetlandX) in Broughton's Creek watershed, Manitoba. Particle size composition is represented by the clay (≤0.002 mm), silt (0.002–0.063 mm) and sand (0.063–2 mm) content of collected samples.

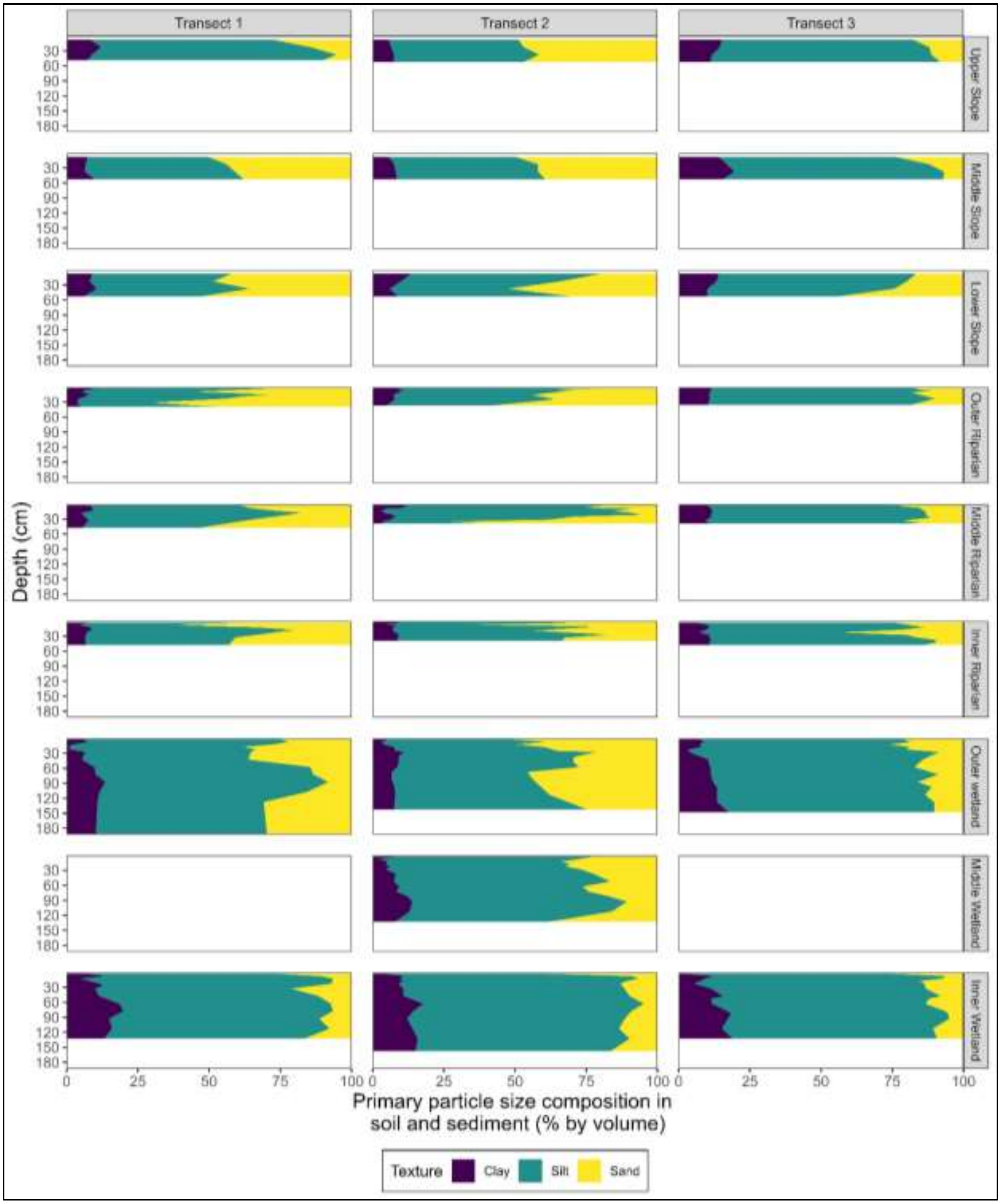

B9. Average particle size composition of collected soil and sediment samples from different toposequence positions on three transects within one wetland catchment (WetlandINT1) in Bigstone Creek watershed, Manitoba. Particle size composition is represented by the clay (≤0.002 mm), silt (0.002–0.063 mm) and sand (0.063–2 mm) content of collected samples.

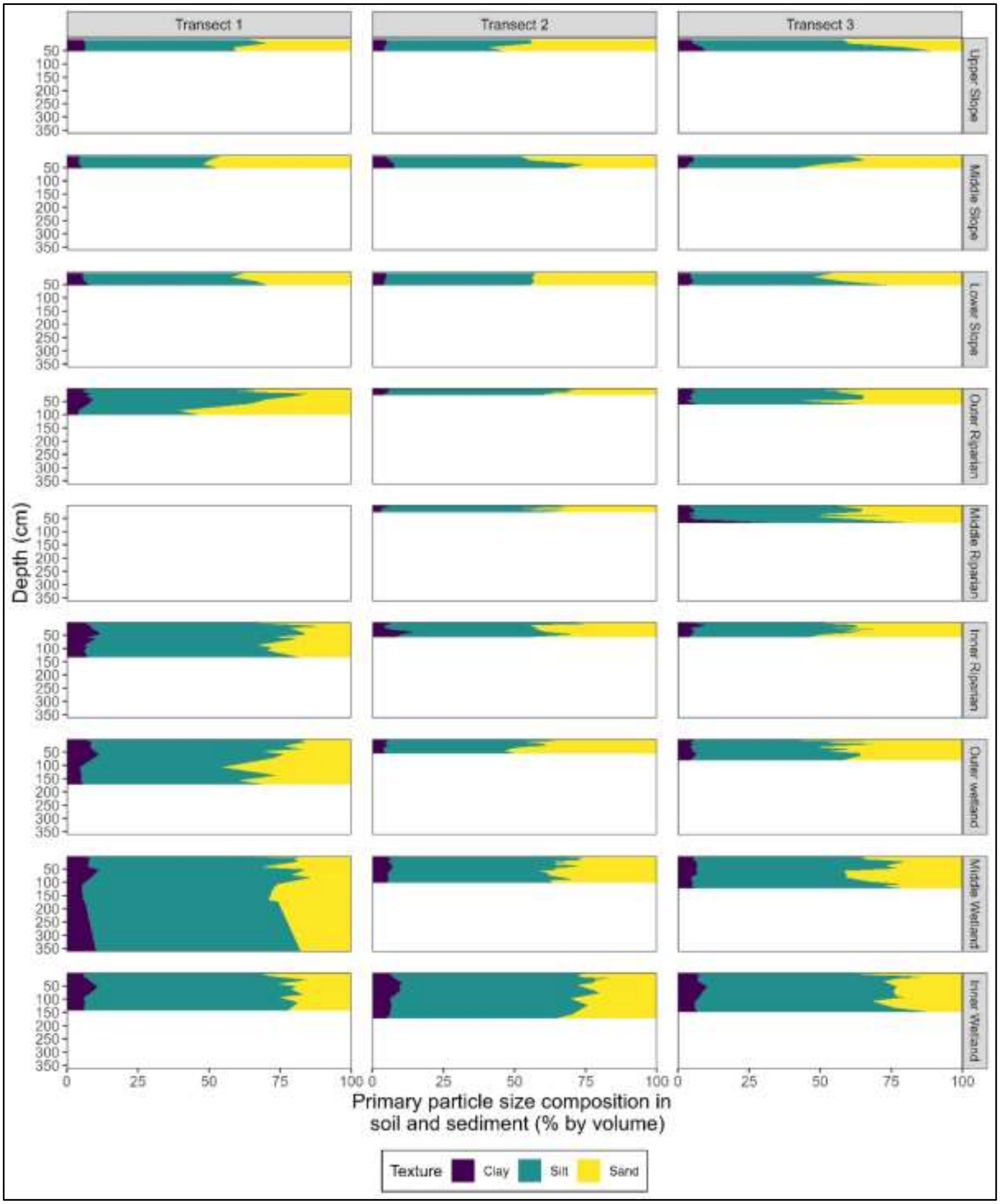

B10. Average particle size composition of collected soil and sediment samples from different toposequence positions on three transects within one wetland catchment (WetlandOZM1) in Bigstone Creek watershed, Manitoba. Particle size composition is represented by the clay (≤0.002 mm), silt (0.002–0.063 mm) and sand (0.063–2 mm) content of collected samples.

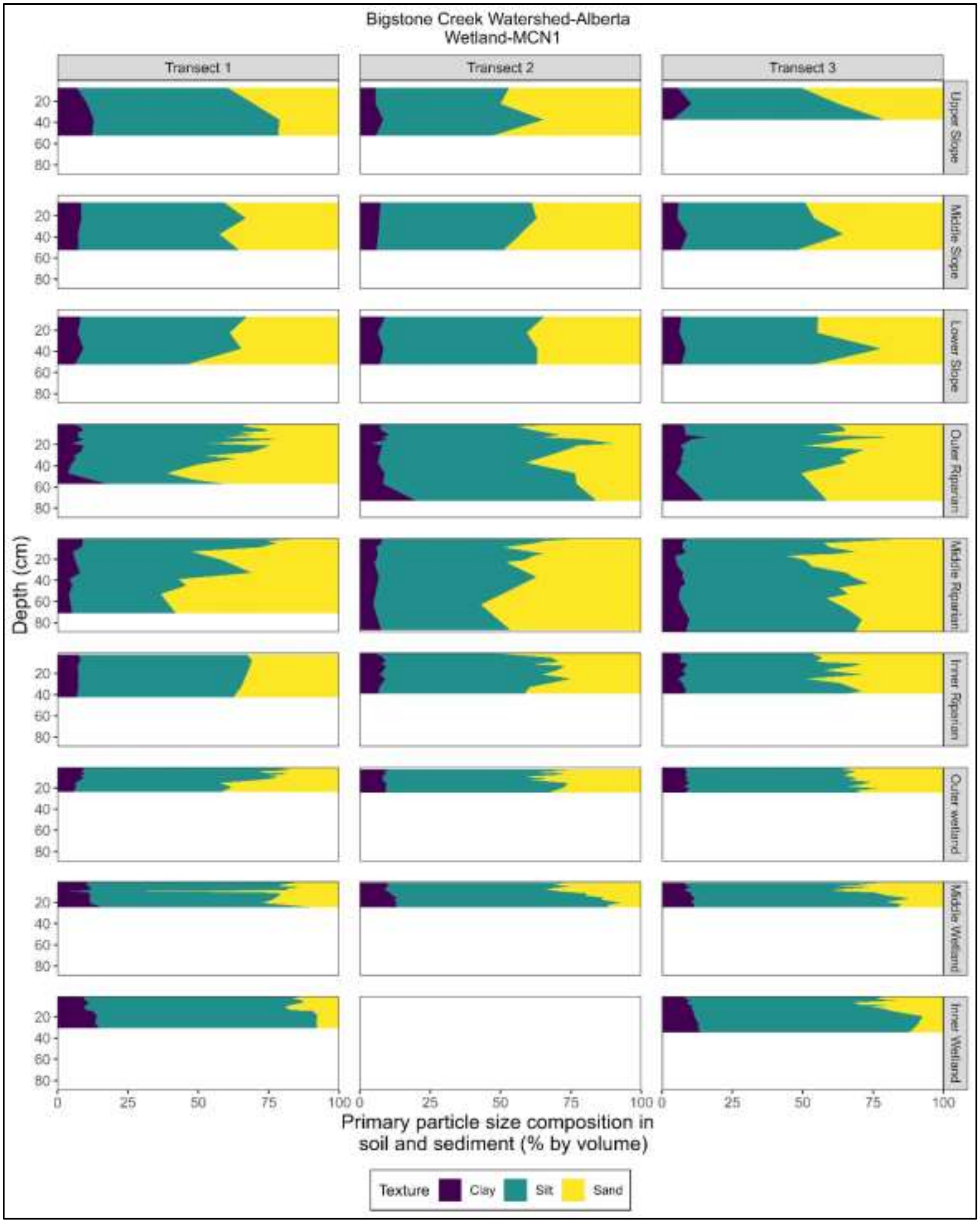

B11. Average particle size composition of collected soil and sediment samples from different toposequence positions on three transects within one wetland catchment (WetlandMCN1) in Bigstone Creek watershed, Manitoba. Particle size composition is represented by the clay (≤0.002 mm), silt (0.002–0.063 mm) and sand (0.063–2 mm) content of collected samples.

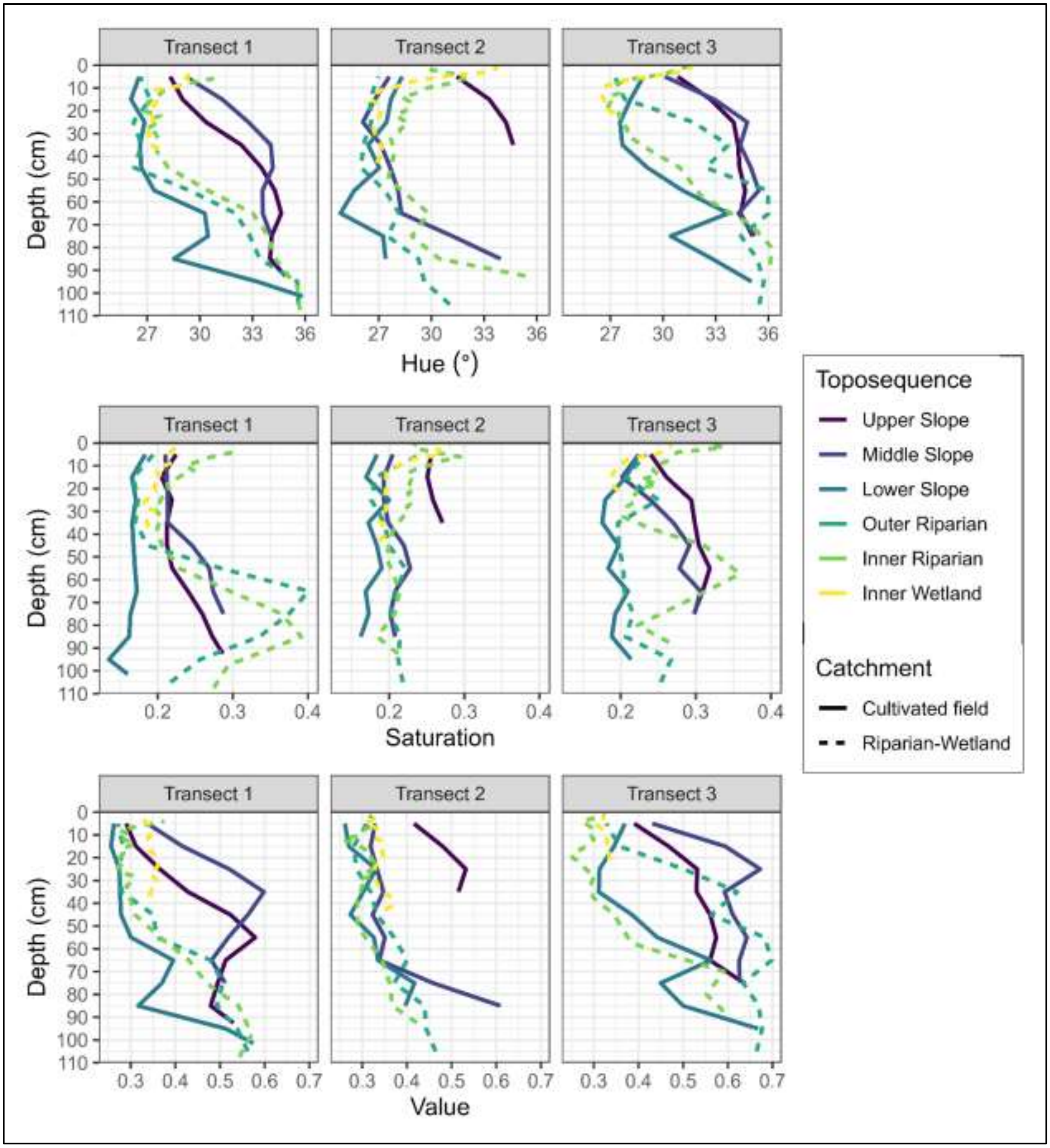

B12. Depth characterization of Munsell colour attributes of hue (e.g., colour itself), saturation (e.g., colour brilliance) and value (e.g., lightness/darkness) for different toposequence position within one wetland catchment (WetlandJ) in Broughton's Creek, Manitoba. Munsell colour attributes have been used for quantitative descriptions of soil colour.

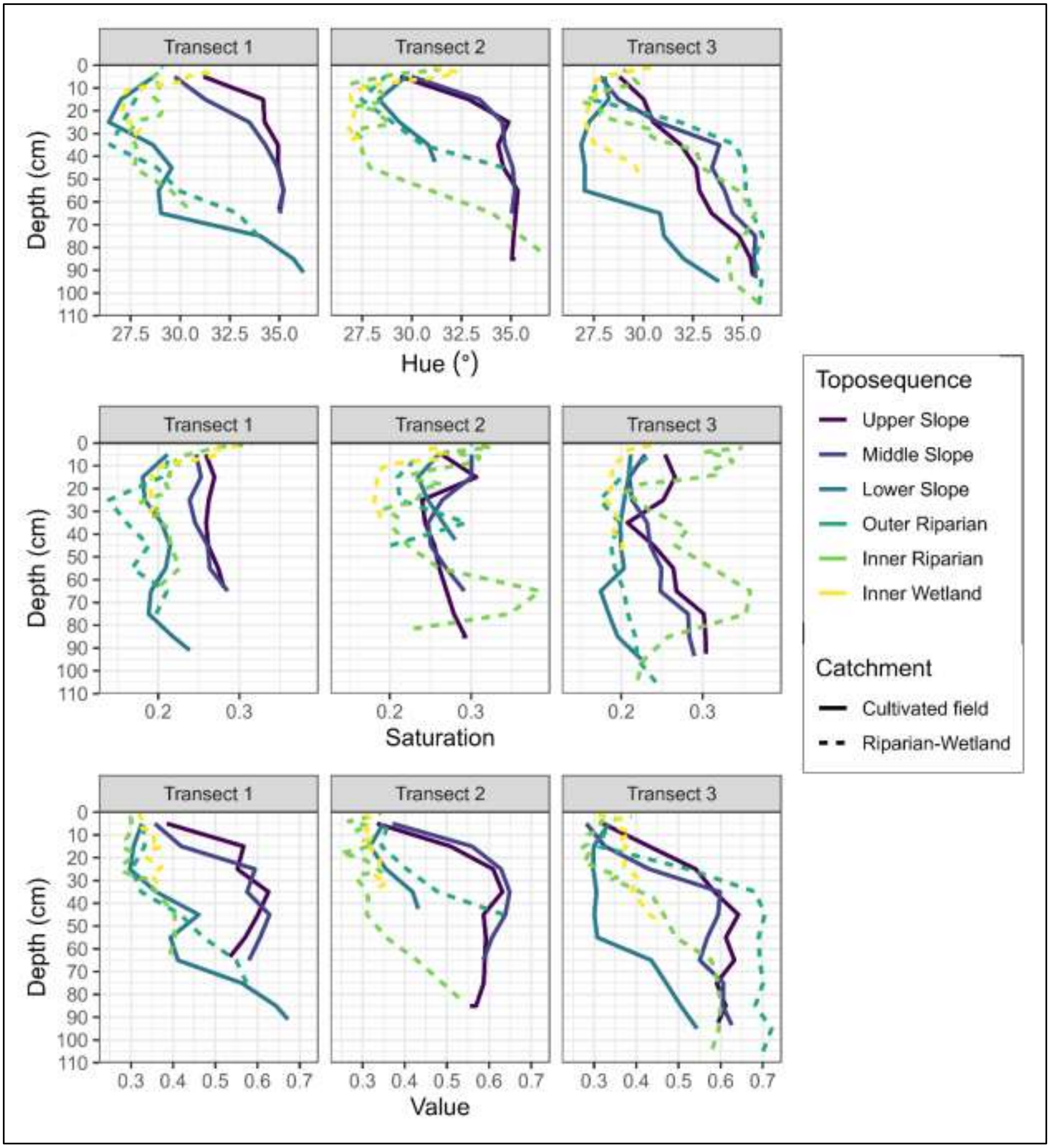

B13. Depth characterization of Munsell colour attributes of hue (e.g., colour itself), saturation (e.g., colour brilliance) and value (e.g., lightness/darkness) for different toposequence position within one wetland catchment (WetlandK) in Broughton's Creek, Manitoba. Munsell colour attributes have been used for quantitative descriptions of soil colour.

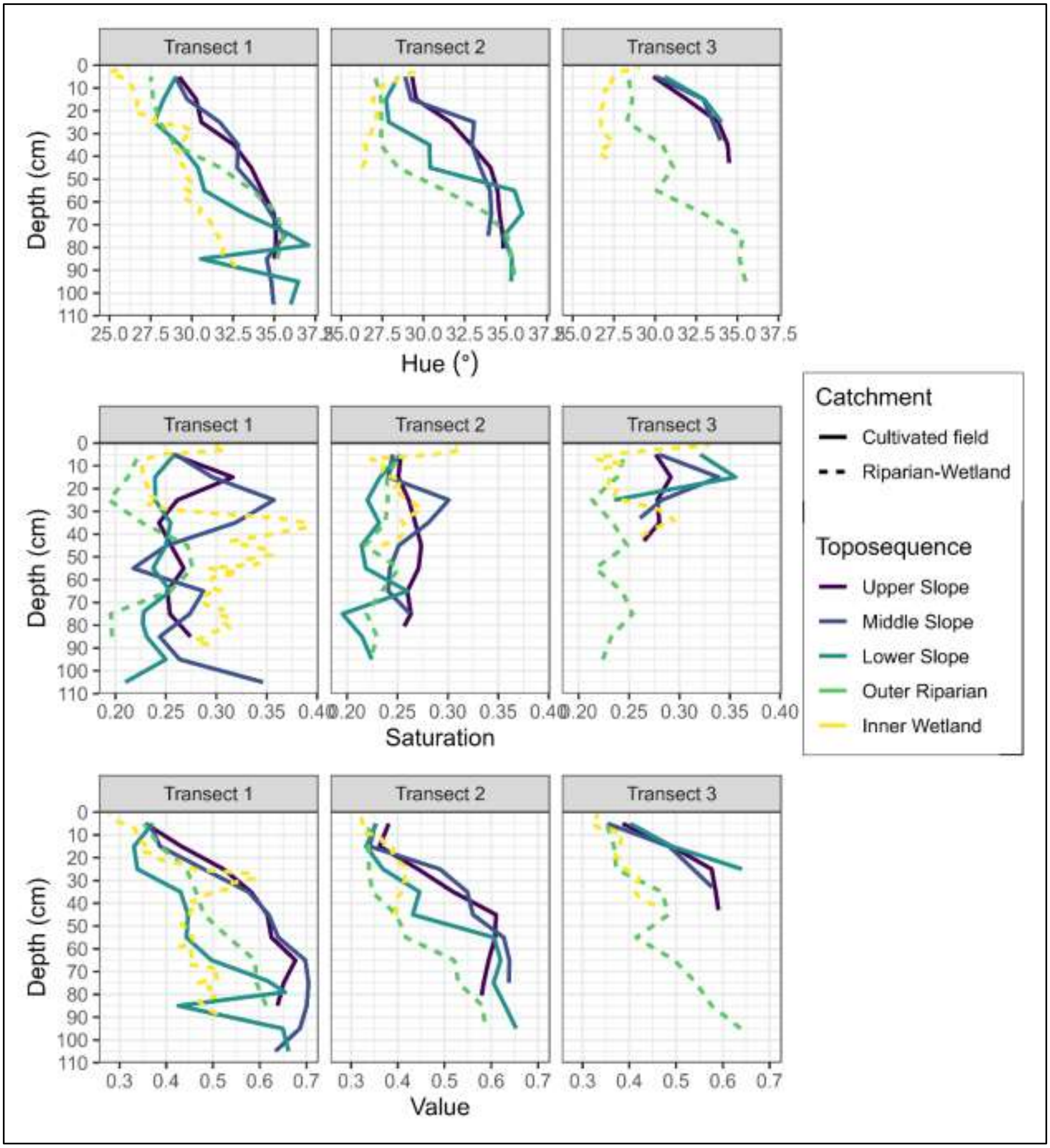

B14. Depth characterization of Munsell colour attributes of hue (e.g., colour itself), saturation (e.g., colour brilliance) and value (e.g., lightness/darkness) for different toposequence position within one wetland catchment (WetlandX) in Broughton’s Creek, Manitoba. Munsell colour attributes have been used for quantitative descriptions of soil colour.

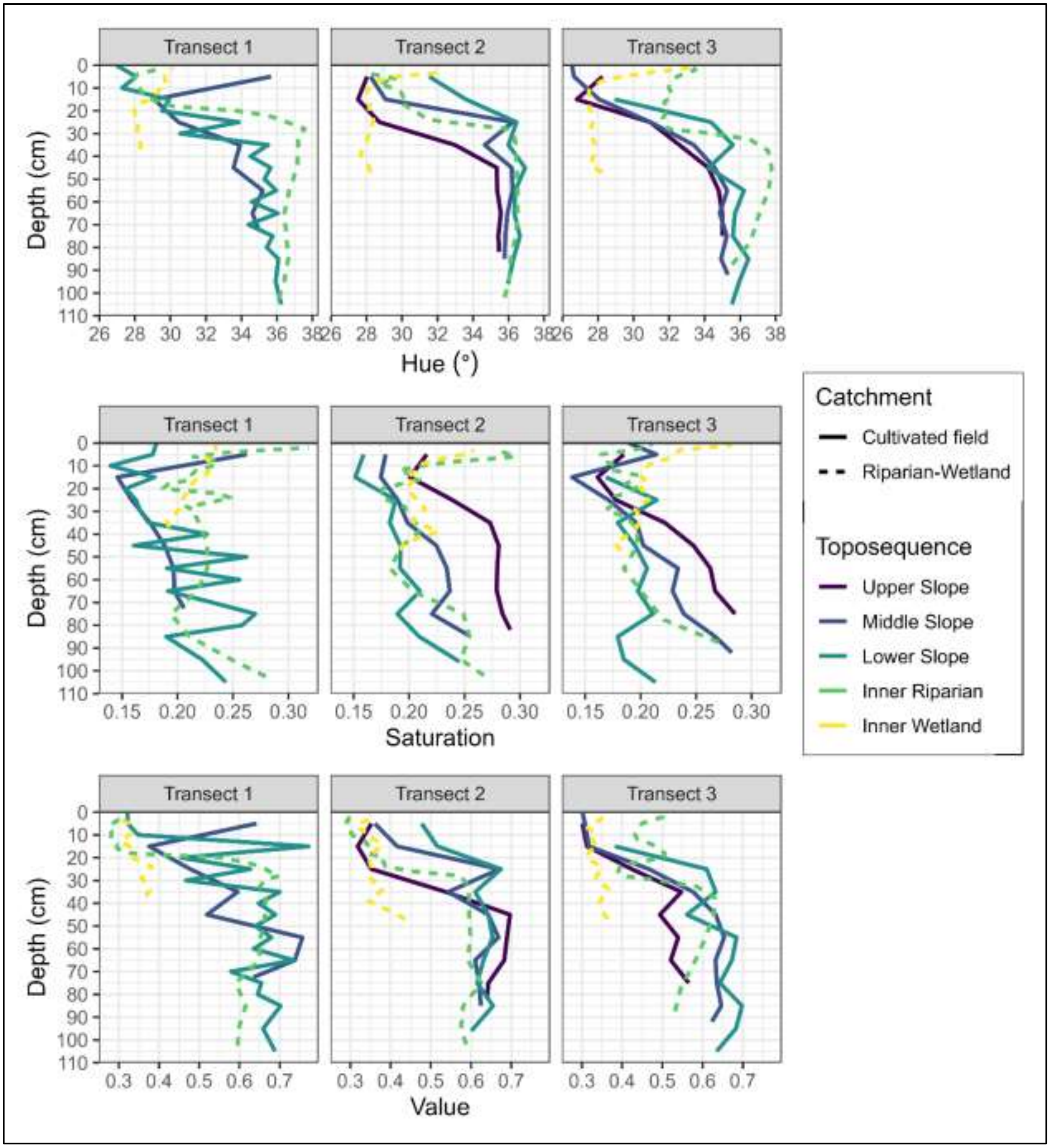

B15. Depth characterization of Munsell colour attributes of hue (e.g., colour itself), saturation (e.g., colour brilliance) and value (e.g., lightness/darkness) for different toposequence position within one wetland catchment (WetlandE- Native Prairie) in Broughton's Creek, Manitoba. Munsell colour attributes have been used for quantitative descriptions of soil colour.

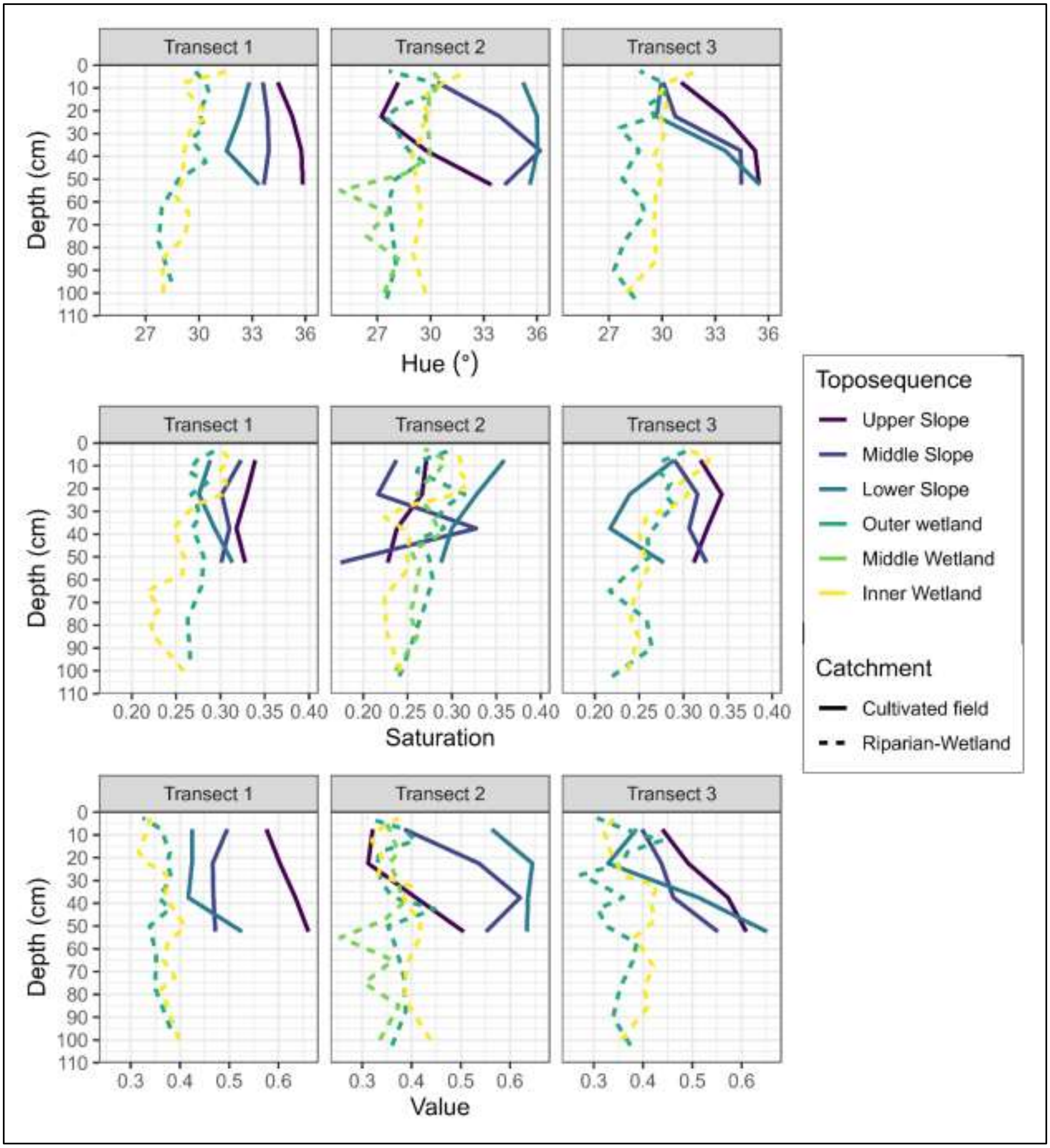

B16. Depth characterization of Munsell colour attributes of hue (e.g., colour itself), saturation (e.g., colour brilliance) and value (e.g., lightness/darkness) for different toposequence position within one wetland catchment (WetlandINT1) in Bigstone's Creek, Alberta. Munsell colour attributes have been used for quantitative descriptions of soil colour.

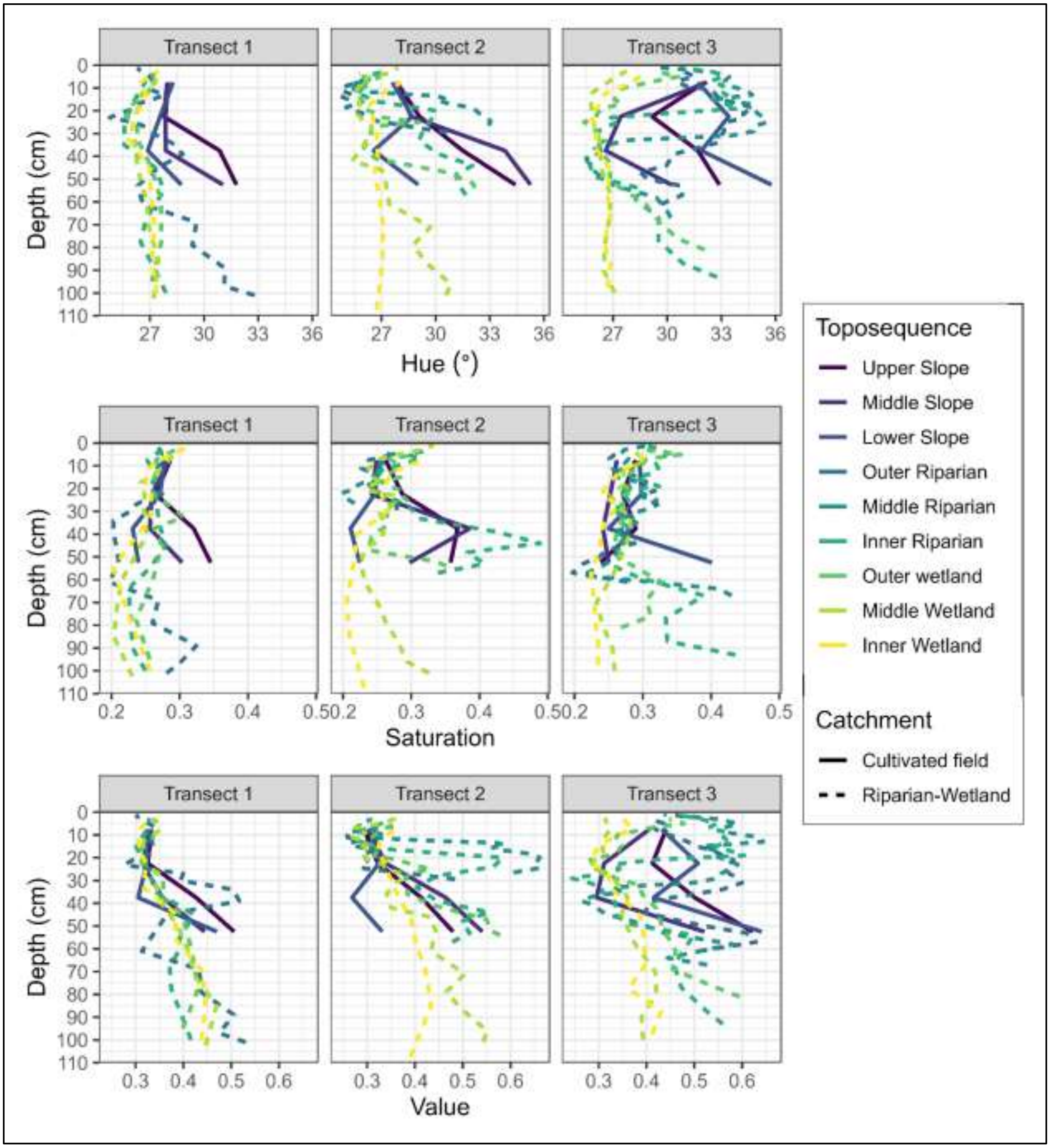

B17. Depth characterization of Munsell colour attributes of hue (e.g., colour itself), saturation (e.g., colour brilliance) and value (e.g., lightness/darkness) for different toposequence position within one wetland catchment (WetlandOZM1) in Bigstone's Creek, Alberta. Munsell colour attributes have been used for quantitative descriptions of soil colour.

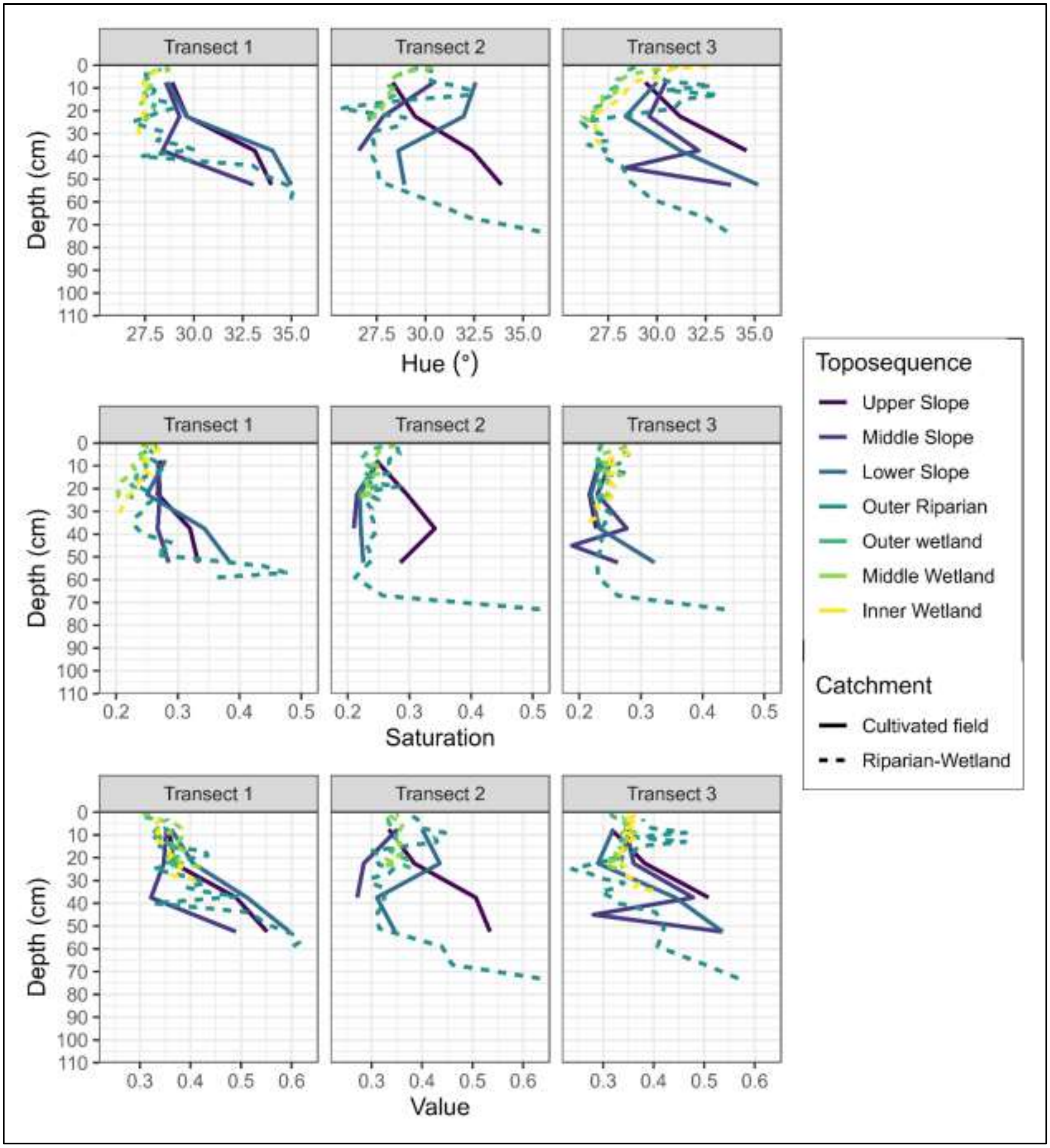

B18. Depth characterization of Munsell colour attributes of hue (e.g., colour itself), saturation (e.g., colour brilliance) and value (e.g., lightness/darkness) for different toposequence position within one wetland catchment (WetlandMCN1) in Bigstone's Creek, Alberta. Munsell colour attributes have been used for quantitative descriptions of soil colour.

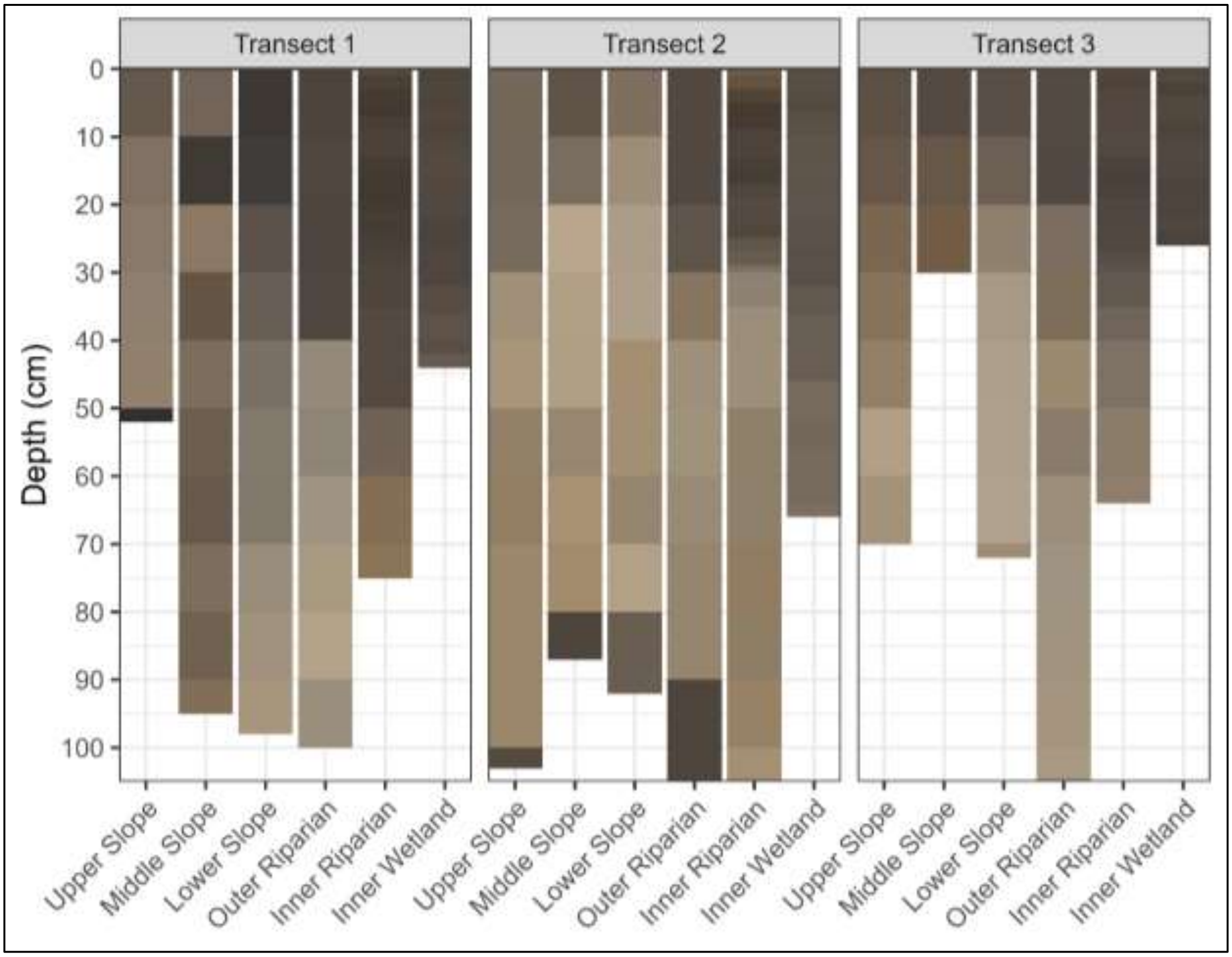

B19. Depth characterization of hexadecimal codes using combination of RGB coefficients (i.e., Red, Green and Blue) for different toposequence position within one wetland catchment (WetlandA) in Broughton's Creek, Manitoba. RGB colour space has been used for qualitative descriptions of soil colour.

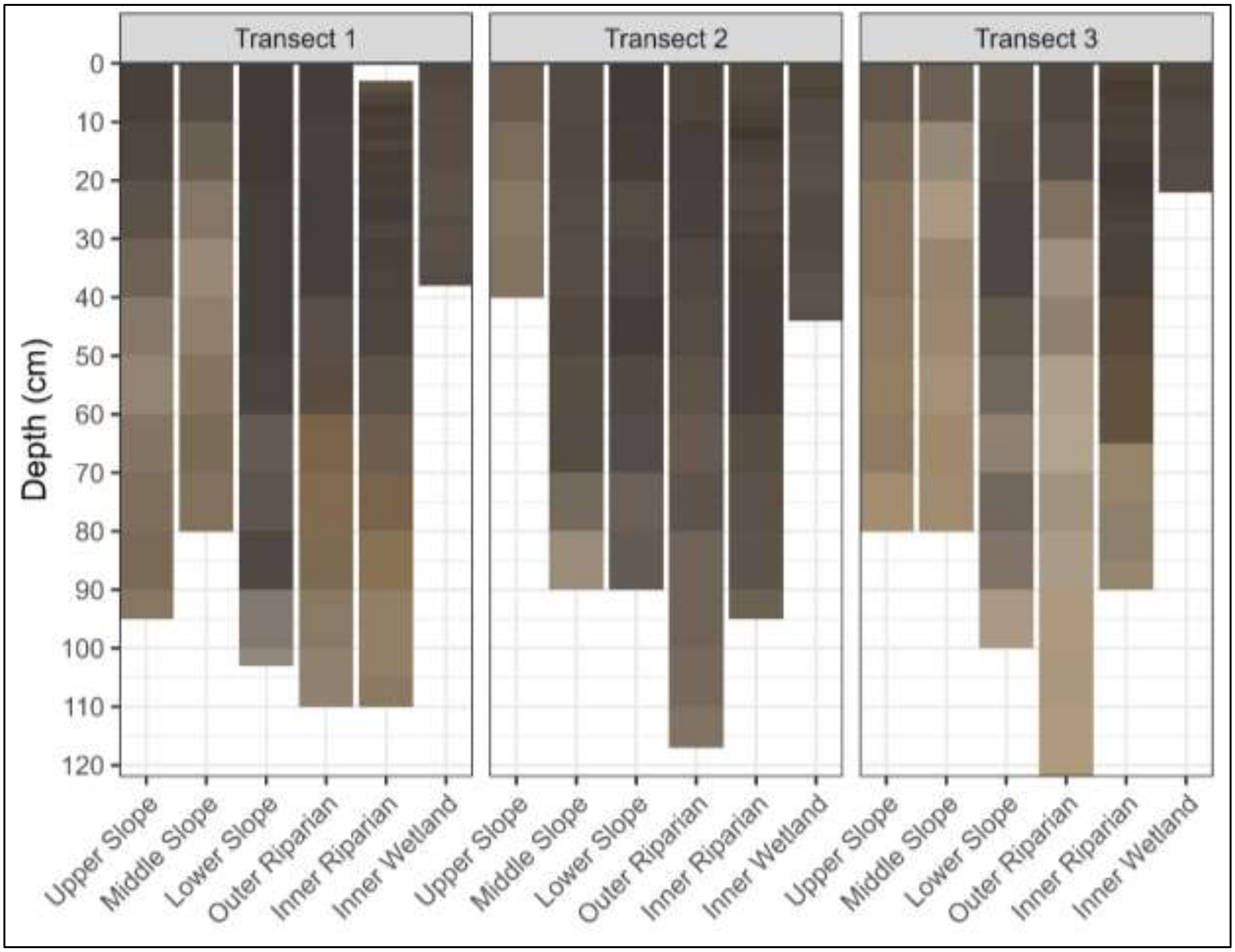

B20. Depth characterization of hexadecimal codes using combination of RGB coefficients (i.e., Red, Green and Blue) for different toposequence position within one wetland catchment (WetlandJ) in Broughton's Creek, Manitoba. RGB colour space has been used for qualitative descriptions of soil colour.

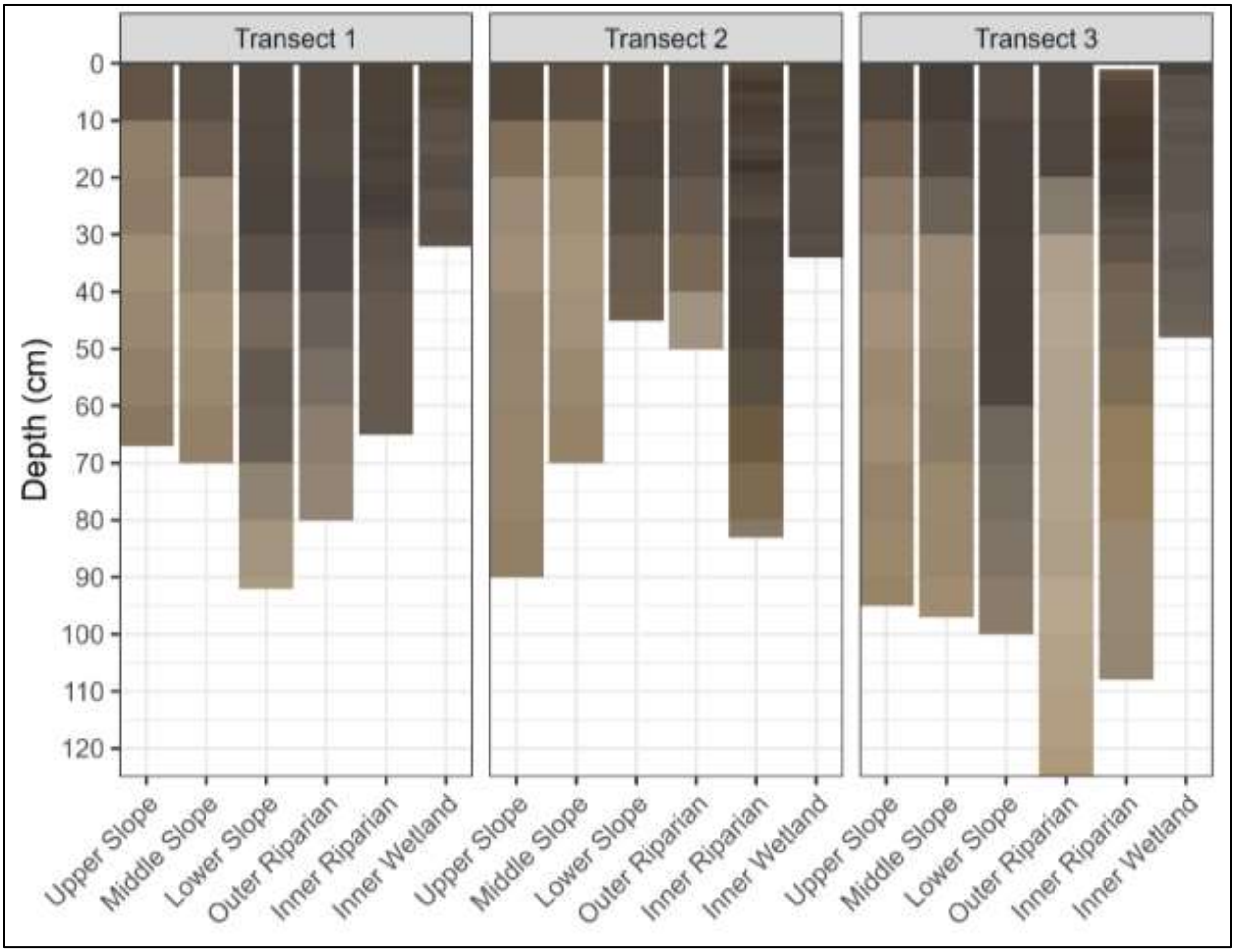

B21. Depth characterization of hexadecimal codes using combination of RGB coefficients (i.e., Red, Green and Blue) for different toposequence position within one wetland catchment (WetlandK) in Broughton's Creek, Manitoba. RGB colour space has been used for qualitative descriptions of soil colour.

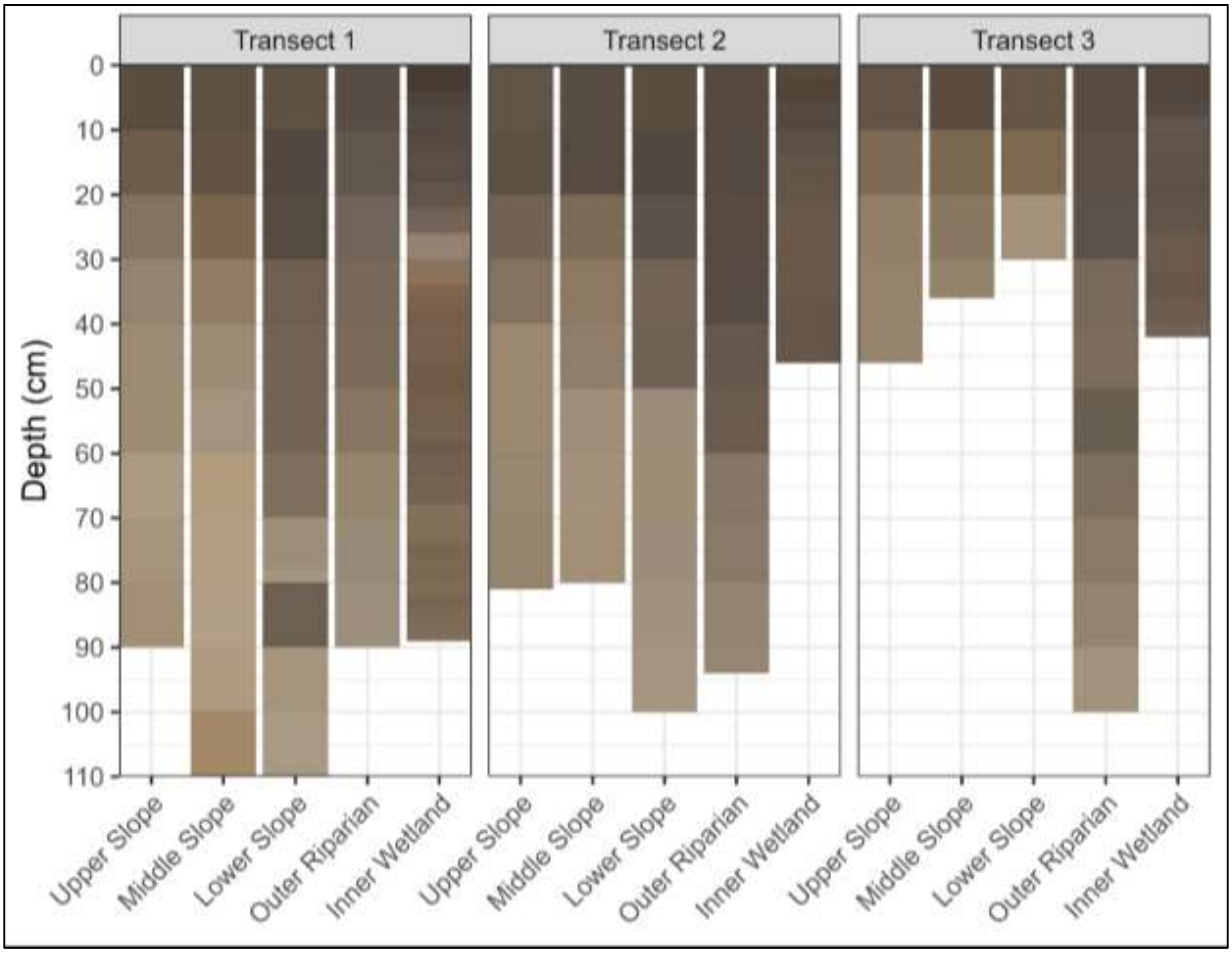

B22. Depth characterization of hexadecimal codes using combination of RGB coefficients (i.e., Red, Green and Blue) for different toposequence position within one wetland catchment (WetlandX) in Broughton's Creek, Manitoba. RGB colour space has been used for qualitative descriptions of soil colour.

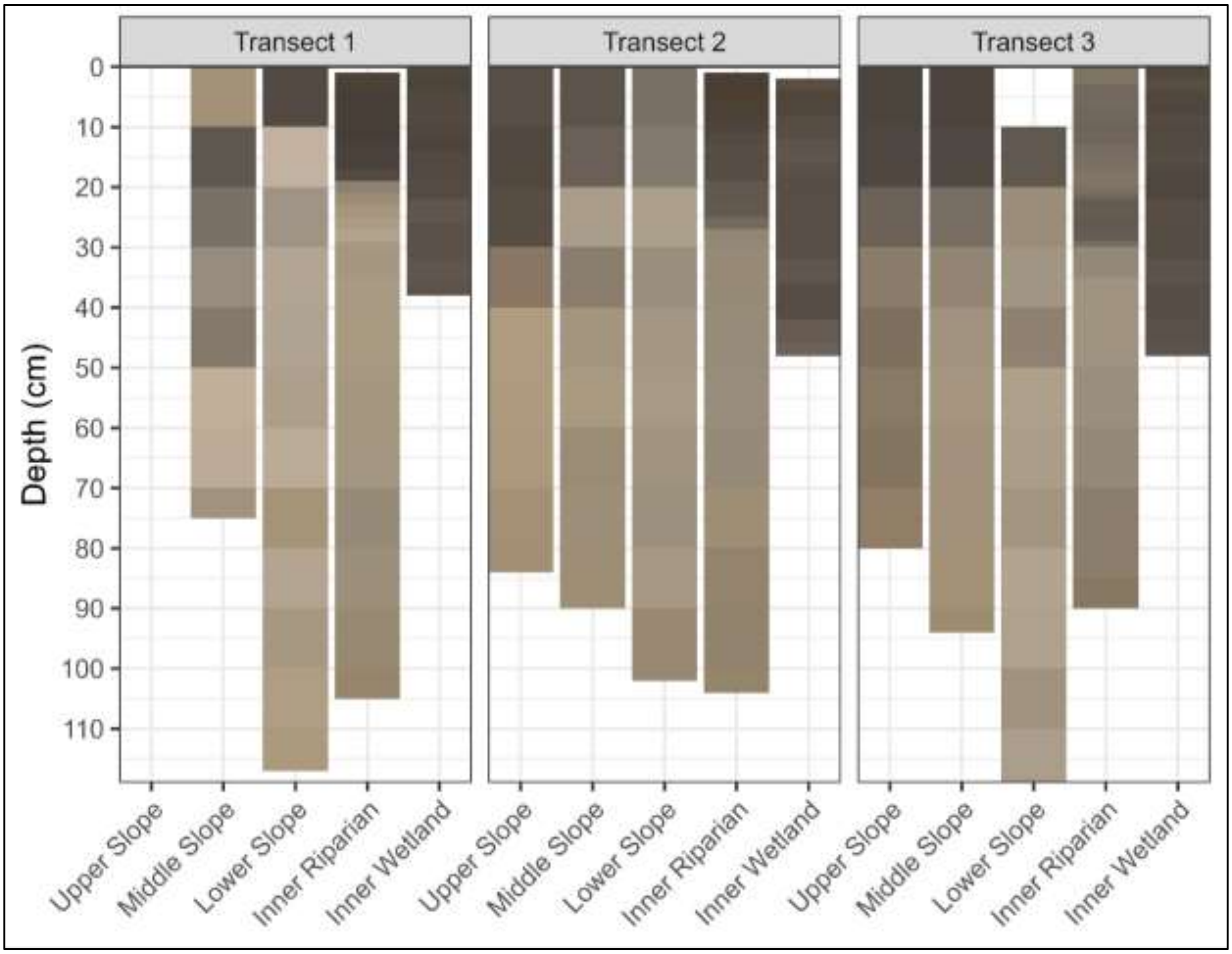

B23. Depth characterization of hexadecimal codes using combination of RGB coefficients (i.e., Red, Green and Blue) for different toposequence position within one wetland catchment (WetlandE- Native Prairie) in Broughton's Creek, Manitoba. RGB colour space has been used for qualitative descriptions of soil colour.

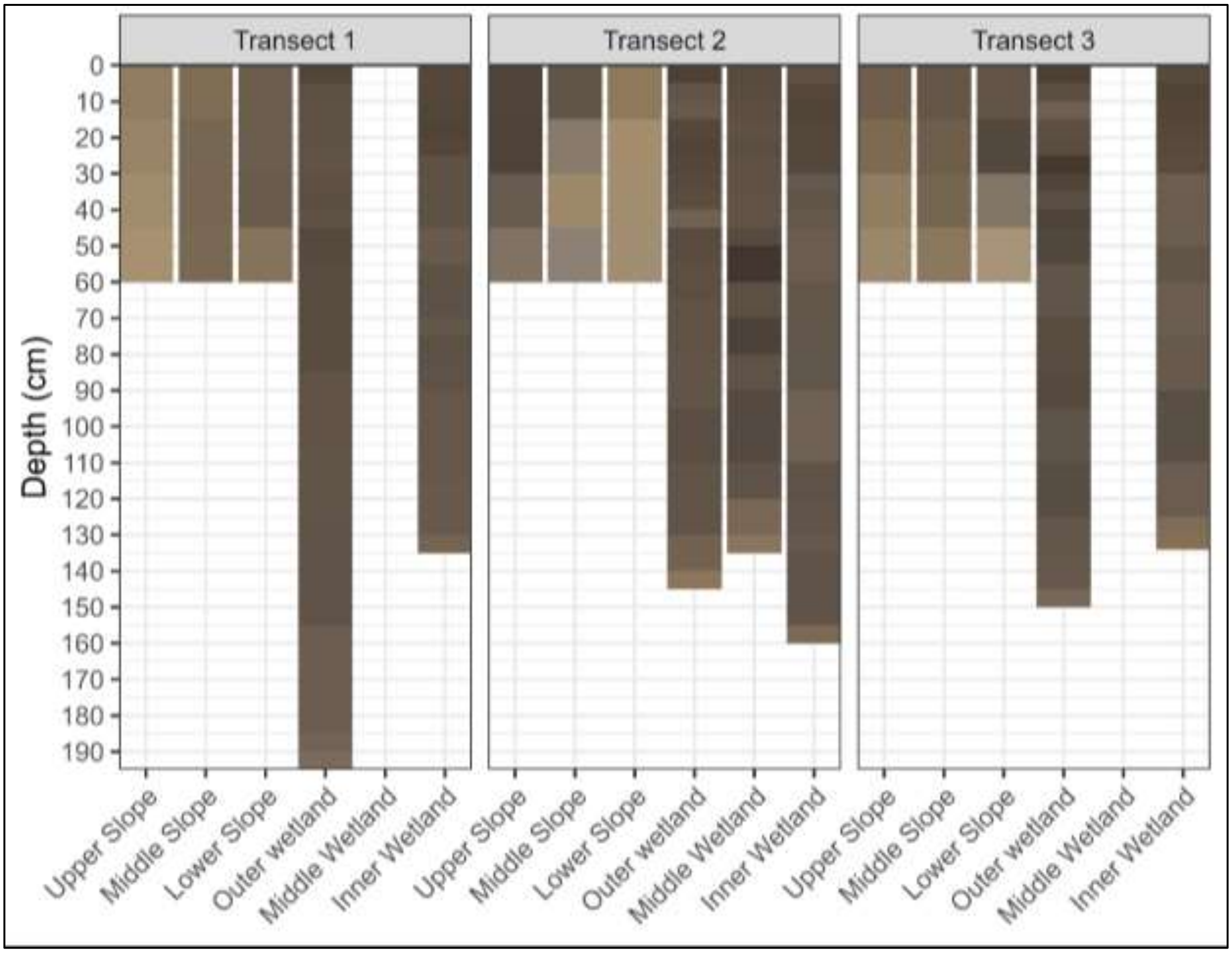

B24. Depth characterization of hexadecimal colour codes using combination of RGB coefficients (i.e., Red, Green and Blue) for different toposequence position within one wetland catchment (WetlandINT1) in Bigstone's Creek, Alberta. RGB colour space has been used for qualitative descriptions of soil colour.

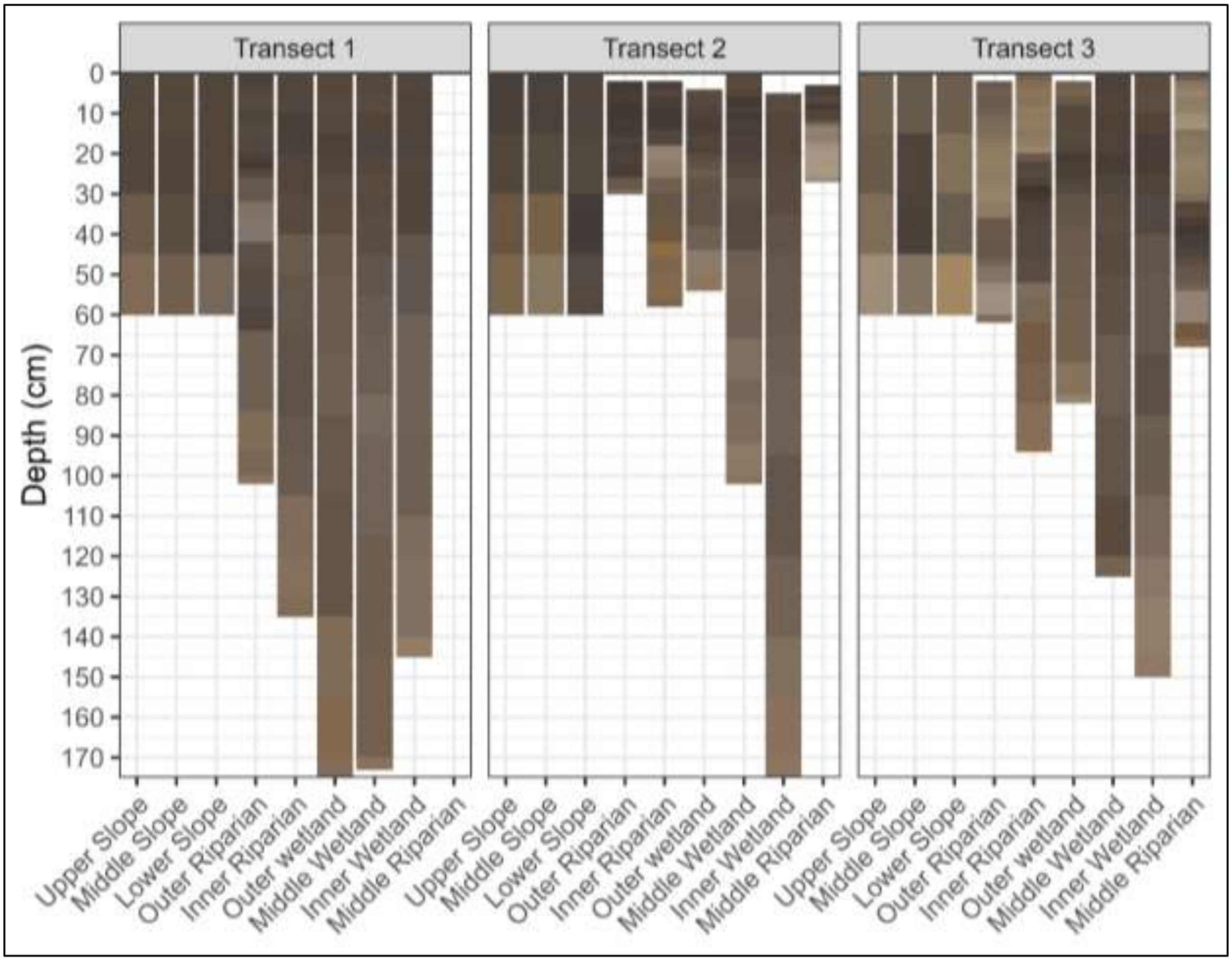

B25. Depth characterization of hexadecimal colour codes using combination of RGB coefficients (i.e., Red, Green and Blue) for different toposequence position within one wetland catchment (WetlandOZM1) in Bigstone's Creek, Alberta. RGB colour space has been used for qualitative descriptions of soil colour.

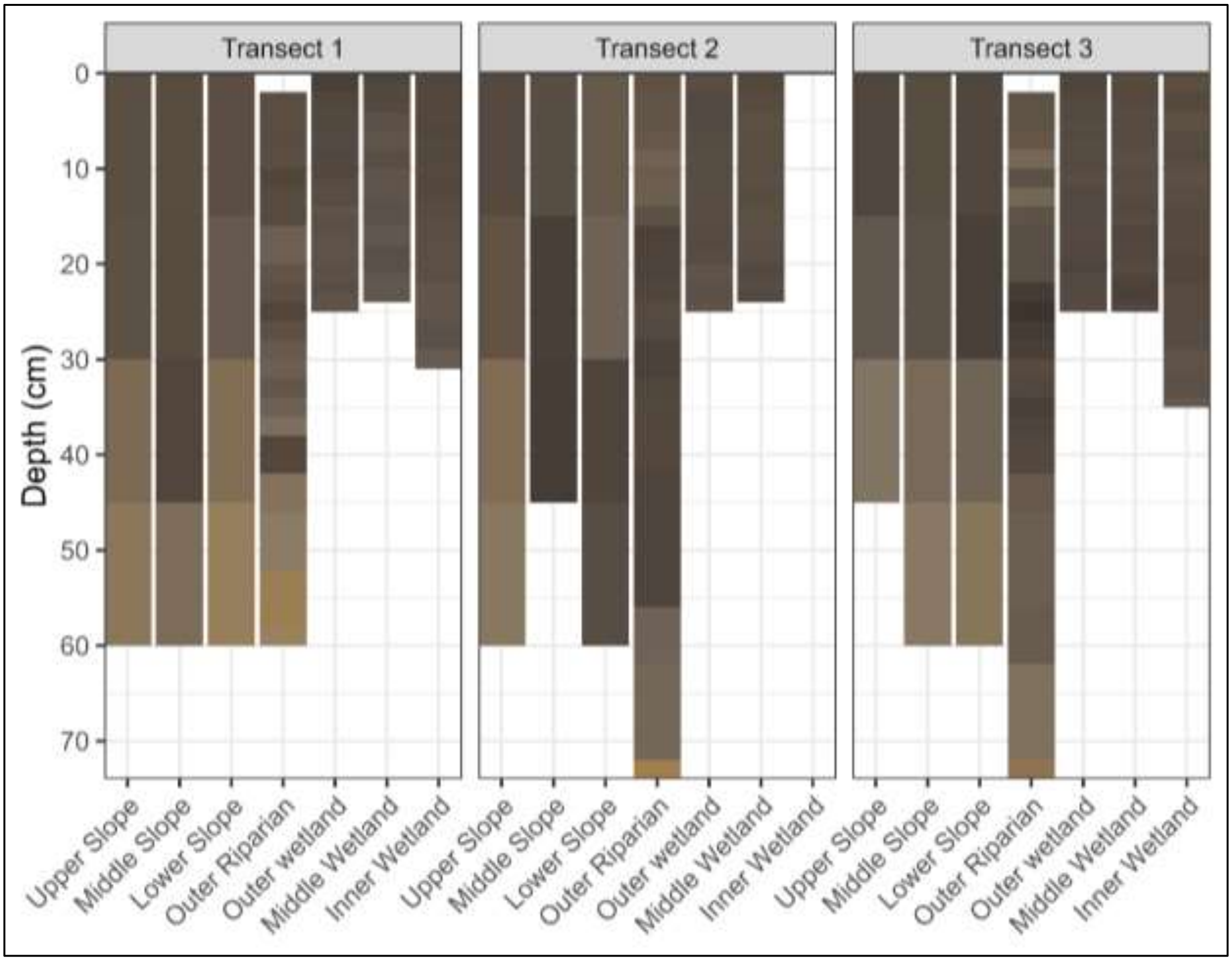

B26. Depth characterization of hexadecimal colour codes using combination of RGB coefficients (i.e., Red, Green and Blue) for different toposequence position within one wetland catchment (WetlandMCN1) in Bigstone's Creek, Alberta. RGB colour space has been used for qualitative descriptions of soil colour.